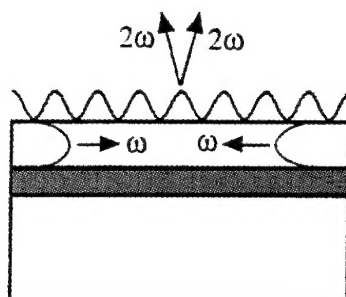




Materials for Nonlinear Optics



Capri, Italy, 8-12 July 1997

Organized by:



Università di Roma "La Sapienza"
Dipartimento di Energetica

Sponsored by:



European Commission
Università degli Studi di Roma "La Sapienza"
Dipartimento di Energetica
United States Air Force European Office of
Aerospace Research and Development
United States Office of Naval Research Europe
Fondazione Ugo Bordononi (FUB)
National Group of Quantum Electronics and
Plasma Physics of CNR (GNEQP)
Istituto Nazionale di Fisica della Materia (INFM)
Italian Society of Optics and Photonics (SIOF)
dB Electronics Instruments
Newport Microcontrole Italia
Proteo and SXST

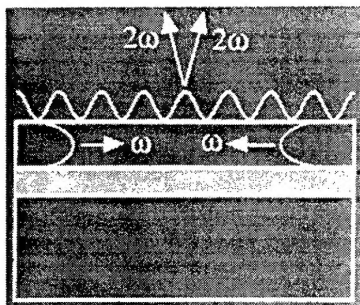
DISTRIBUTION STATEMENT A

Approved for public release;
Distribution Unlimited

REPORT DOCUMENTATION PAGE			Form Approved OMB No. 0704-0188	
Public reporting burden for this collection of information is estimated to average 1 hour per response, including the time for reviewing instructions, searching existing data sources, gathering and maintaining the data needed, and completing and reviewing the collection of information. Send comments regarding this burden estimate or any other aspect of this collection of information, including suggestions for reducing this burden to Washington Headquarters Services, Directorate for Information Operations and Reports, 1215 Jefferson Davis Highway, Suite 1204, Arlington, VA 22202-4302, and to the Office of Management and Budget, Paperwork Reduction Project (0704-0188), Washington, DC 20503.				
1. AGENCY USE ONLY (Leave blank)		2. REPORT DATE 23 July 1997		3. REPORT TYPE AND DATES COVERED Conference Proceedings
4. TITLE AND SUBTITLE Materials for Nonlinear Optics Conference			5. FUNDING NUMBERS F6170897W0109	
6. AUTHOR(S) Conference Committee				
7. PERFORMING ORGANIZATION NAME(S) AND ADDRESS(ES) Laboratory for Physics and Electronic Materials CEN Saclay Gif-sur-Yvette Cedex 91191 France			8. PERFORMING ORGANIZATION REPORT NUMBER N/A	
9. SPONSORING/MONITORING AGENCY NAME(S) AND ADDRESS(ES) EOARD PSC 802 BOX 14 FPO 09499-0200			10. SPONSORING/MONITORING AGENCY REPORT NUMBER CSP 97-1045	
11. SUPPLEMENTARY NOTES				
12a. DISTRIBUTION/AVAILABILITY STATEMENT Approved for public release; distribution is unlimited.			12b. DISTRIBUTION CODE A	
13. ABSTRACT (Maximum 200 words) The Final Proceedings for Materials for Nonlinear Optics, 8 July 1997 - 12 July 1997 The Topics covered include: Organic and inorganic single crystals; photorefractive polymers and crystals; theory of optical nonlinearities; molecular engineering; electro-optic polymers; liquid crystalline materials; magnetic materials; nanostructures.				
14. SUBJECT TERMS Non-linear Optics, Non-linear Optical Materials			15. NUMBER OF PAGES 197	
			16. PRICE CODE N/A	
17. SECURITY CLASSIFICATION OF REPORT UNCLASSIFIED	18. SECURITY CLASSIFICATION OF THIS PAGE UNCLASSIFIED	19. SECURITY CLASSIFICATION OF ABSTRACT UNCLASSIFIED	20. LIMITATION OF ABSTRACT UL	



Materials for Nonlinear Optics



Capri, Italy, 8-12 July 1997

Organized by:



Università di Roma "La Sapienza"
Dipartimento di Energetica

Sponsored by:



European Commission
Università degli Studi di Roma "La Sapienza"
Dipartimento di Energetica
United States Air Force European Office of
Aerospace Research and Development
United States Office of Naval Research Europe
Fondazione Ugo Bordon (FUB)
National Group of Quantum Electronics and
Plasma Physics of CNR (GNRQP)
Istituto Nazionale di Fisica della Materia (INFM)
Italian Society of Optics and Photonics (SIOF)
dB Electronics Instruments
Newport Microcontrole Italia
Proteo and SXST

19970814 050

NON LINEAR OPTICS

EOS TOPICAL MEETINGS

1. 8th Journées d'Etudes sur les Fonctions Optiques dans l'Ordinateur

8-9 September 1992 in Paris, France. Chair : P. Chavel.
Organised by SFO and EOS.

2. Microlens Arrays

13-14 May 1993 in Teddington, U.K. Chair : M. Hutley.
Organised by the Optical Group of the Institute of Physics (IOP).
Sponsors : the Royal Photographical Society and IEE.

3. Non-Conventional Optical Imaging Elements

14-17 September 1993 in Rydzyna (or Wroclaw), Poland. Chair : J. Nowak.
Sponsored by EOS.

4. Optical Metrology and Nanotechnology

27-30 March 1994 in Engelberg, Switzerland. Chair : Dr. K. Knop.
Organised by Paul Scherrer Institute. Sponsored by EOS, DGaO, SGOEM.

5. Microlens Arrays

11-12 May 1995 in Teddington, United Kingdom. Chair : Prof. M.C. Hutley.
organised by EOS and IOP.

6. Optics and Information

11emes Journees d'Etudes sur les Fonctions Optiques dans l'Ordinateur
23-27 October 1995 in Mulhouse, France. Chair : Dr. Philippe Refregier.
Organised by EOS and SFO. Sponsored by OSA and SPIE.

7. Nonlinear Optical Materials

14-18 January 1996 in Val Thorens, France. Chair : Dr. F. Kajzar.
Organised by EOS and SFO.

8. Near Field Optics

9-11 May 1995 in Brno, Czechia. Chair : Prof. P. Tomanek.
Organised by EOS and Technical Univ. of Brno, Czech Slovak Society for Photonics.

9. Free-Space Micro-Optical Systems

31 March - 3 April 1996 in Engelberg, Switzerland. Chair : Dr. Karl Knop.
Organised by EOS and PSI Zurich. Co-sponsored by SGOEM and DGaO

10. Advances in Acousto-Optics

6-7 June 1996 in Issy-Les-Moulineaux, France. Chair : Dr. Jacques Sapriel.
organised by the CNET, the SFO and the EOS. Sponsored by the DGA/DRET.

Back issue of digest for these former EOS Topical meetings
can be requested at the EOS Main Office :

EOS - c/o Françoise Chavel - BP 147 - 91403 ORSAY cedex - France

Phone : +33 1 69 35 87 20 - Fax : +33 1 69 85 35 65 - e-mail : francoise.chavel@iota.u-psud.fr

EOSTM/4 juillet 96



11th Topical Meeting of the European Optical Society

MATERIALS FOR NONLINEAR OPTICS

Capri (Italy)- July 8th-12th 1997

Organized
by



Università degli Studi di Roma "La Sapienza"
Dipartimento di Energetica

Sponsored
by



Co-Sponsored by

European Commission
Università degli Studi di Roma "La Sapienza"
Dipartimento di Energetica
United States Air Force European Office of Aerospace Research and Development
United States Office of Naval Research Europe
Fondazione Ugo Bordon (FUB)
National Group of Quantum Electronics and Plasma Physics of CNR (GNEQP)
Istituto Nazionale di Fisica della Materia (INFN)
The Italian Society of Optics and Photonics (SIOF)
dB Electronic Instruments
Newport Microcontrolle Italia
Proteo and SXST

Organizing Committee

Mario Bertolotti	Francois Kajzar	Francesco Michelotti
<i>Conference Chair</i>	<i>Program Chair</i>	<i>Secretaries</i>

Scientific Program Committee

V.Agranovich, Russian Academy of Sciences, Moscow, Russia.
F.Agullo-Lopez, Universidad Autonoma de Madrid, Madrid, Spain.
A.A.Andriesh, Academy of Sciences of Moldova, Kishinev, Moldova.
J.Y.Bigot, University of Strasbourg, Strasbourg, France.
W.Blau, Trinity College, Dublin, Ireland.
D.Bloor, University of Durham, Durham, United Kingdom.
A.Carenco, France Telecom-CNET, Bagneux, France.
H.A.Ferwerda, University of Groningen, The Netherlands.
C.Flytzanis, Ecole Polytechnique, Palaiseau, France.
P.Günter, Swiss Federal Institute of Technology, Zurich, Switzerland.
G. Guekos, Swiss Federal Institute of Technology, Zurich, Switzerland.
J.P.Huignard, Thomson-CSF, Orsay, France.
P.Lambeck, University of Twente, The Netherlands.
Y.Levy, Institut d'Optique Theorique et Appliquee, Orsay, France.
A.Miller, University of St.Andrews, United Kingdom.
J.Mlynek, University of Konstanz, Konstanz, Germany.
A.Miniewicz, Technical University of Wroclaw, Wroclaw, Poland.
M.Soskin, Ukrainian Academy of Sciences, Kiev, Ukraine.
B.S.Wherrett, Heriot-Watt University, Edimburgh, United Kingdom.
G.Zerbi, Politecnico di Milano, Milano, Italy.
L.Zanotti, MASPEC of CNR, Parma, Italy.
J.Zyss, France Telecom-CNET, Bagneux, France.

PROGRAMME

Tuesday, July 8th 1997

h14.00-15.00 **WELCOME BUFFET**

h15.30-15.30 **WELCOME ADDRESS**

- 15.30-16.00 F.Kajzar (*invited*), **Recent Advances in polymeric thin films orientation techniques**, CEA-DEIN/SPE, France.
- 16.00-16.30 V.Agranovich (*invited*), **Hybrid Frenkel-Wannier-Mott excitons at interface and in microcavity**, Institute of Spectroscopy - Russian Academy of Sciences, Moscow, Russia.
- 16.30-17.00 B.S.Wherrett (*invited*), **Materials for optical information processing**, Heriot-Watt University Physics Department, Edinburgh, Great Britain.
- 17.00-17.20 Ch.Bosshard^a, U.Gubler^a, P.Kaatz^b, W.Mazerant^b, P.Günter^b, **Optical third harmonic generation: cascaded second order nonlinearities in KNbO₃**, (a) Institute of Quantum Electronic- ETH Honggerberg, Zurich, Switzerland, (b) Department of Physics, University of Nevada Las Vegas, USA.
- 17.20-17.20 M.Brambilla^a, W.J.Firth^b, A.Lord^b, L.A.Lugiato^a, F.Prati^a, L.Spinelli^a, G.Tissoni^a, **Optical bullet holes in semiconductor microcavities**, (a) Università di Milano - Dipartimento di Fisica, Milano, Italy, (b) University of Strathclyde - Department of Physics, Glasgow, Scotland.
- 17.40-18.00 J.Trull, J.Martorell, R.Vilaseca, **Phase matching in photonic crystals with quadratic nonlinearities**, Universitat Politècnica de Catalunya- Departament de Física i Enginyeria Nuclear, Terrassa, Spain.
- 18.00-18.20 **COFFEE BREAK**
- 18.15-18.40 Y.Koike (*invited*), **High-speed photonics polymer and its applications**, Keio University Fac. of Science and Technology, Japan.
- 18.40-19.00 G.P.Banfi^a, P.K.Datta^a, V.Degiorgio^a, G.Donelli^a, D.Fortusini^a, J.N.Sherwood^b, **Frequency conversion through cascaded second-order nonlinearities in the NPP organic crystal**, (a) Università di Pavia - Dipartimento di Ingegneria Elettronica, Pavia, Italy, (b) University of Strathclyde - Department of Pure and Applied Chemistry, Glasgow, Scotland.
- 19.00-19.20 E.Raita and A.Kamshilin, **Nonlinear optical effects in photorefractive Bi₁₂TiO₂₀ crystals with internal surface reflections**, University of Joensuu - Vaisala Laboratory, Department of Physics, Joensuu, Finland.
- 19.20-19.40 A.Samoc, M.Samoc, B.Luther-Davies, **Nonlinear optical and waveguiding properties of poly-(p-phenylenevinylene)-poly-(1-vinyl-2-pyrrolidone)(PPV-PVP) blends**, Australian National University, Canberra, Australia.
- 19.40-20.00 F.Girardin, S.Pajarola, and G.Guckos, **Nonlinear parameters of bulk InGaAsP photonic devices**, IQE - Swiss Federal Institute of Technology, Zurich, Switzerland.

Wednesday, July 9th 1997

- 8.30-8.55 M.Carrascosa and F.Agullo-Lopez (*invited*), **Photorefractive processes in H:LiNbO₃**, Dept. de Física de Materiales C-IV, Universidad Autonoma de Madrid, Spain.
- 8.55-9.20 J.P.Huignard, H.Rajbenbach, A.Brignon (*invited*), **Photorefractive nonlinear optics: materials and application to information processing and laser beam control**, Laboratoire Central des Recherches - Thomson CSF, France.
- 9.20-9.45 M.Soskin (*invited*), **Materials for nonlinear singular optics**, Ukrainian Academy of Sciences Institute of Physics, Ukraine.
- 9.45-10.05 M.Kaczmarek^a, R.W.Eason^a, G.Maatz^a, M.H.Garrett^b, I.Mnushkina^c, **Photorefractive properties of infrared sensitive Rhodium doped BaTiO₃ processed in different conditions**, (a) University of Southampton-Optoelectronics Research Centre, Great Britain, (b) Nonlinear Photonics, Morgan Hill, USA, (c) Deltronic Crystal Industries, N. J., USA.
- 10.05-10.25 **COFFEE BREAK**
- 10.25-10.50 J.N.Sherwood (*invited*), **The Growth, Perfection and Structural Properties of Organic Electro-Optic Materials**, Univ. Strathclyde Dept. Pure and Applied Chemistry, Great Britain.

- 10.50-11.15 B.Boulanger, J.P.Fève, and G.Marnier (*invited*), **Nonlinear optical properties of KTP and its arsenate isomorphs: KTA, RTA, and CTA**, Laboratoire de Physique du Solide de l'Université de Bourgogne, France.
- 11.15-11.40 R.Urschel, G.Anstett, U.Bäder, A.Borsutzky, and R.Wallenstein (*invited*), **Noncollinear phase matching in nonlinear crystals: New prospects for pulsed optical parametric oscillators**, Universität Kaiserslautern Fachbereich Physik, Germany.
- 11.40-12.00 M.May^a, S.Debrus^a, J.Venturini^a, J.Baran^{b,c}, H.Ratajczak^{b,c,d}, **Second order nonlinear optical properties of Na₂SeO₄.H₂ScO₃.H₂O**, (a) Université Pierre et Marie Curie - Laboratoire d'Optique des Solides, Jussieu Paris, France, (b) Polish Academy of Sciences - Institute of Low Temperature and Structure Research, Wroclaw, Poland, (c) Institute of Chemistry, Wroclaw University, Poland, (d) Centre Scientifique de l'Académie Polonaise des Sciences, Paris, France.

12.00-17.00 **LUNCH BREAK**

- 17.00-17.25 A.Miniewicz (*invited*), **Liquid crystals as materials for real-time holographic optical devices**, Tech. Univ. Wroclaw Inst. of Phys. and Theor. Chemistry, Poland.
- 17.25-17.50 E.Santamato, G.Abbate, P.Maddalena, L.Marrucci, D.Paparo, E.Massera (*invited*), **Optical Kerr-like response of dye-doped nematics**, Univ. Napoli "Federico II" Dip. Scienze Fisiche, Italy.
- h17.50-18.10 M.Lindgren^a, Per-Otto Arntzen^b, J.Lindström^c, J.Örtengren^d, U.W.Gedde^d, A.Hult^d, F.Sahlén^d, M.Trolsås^d, D.Hermann^e, L.Komitov^e, S.T.Lagerwal^e, P.Rudquist^e, B.Stebler^e, **Analysis of electro-optic effects and SHG of pyroelectric liquid crystalline polymers - Simulations and experimental results**, IFM-Chemical Physics, Linköping University, Sweden, (b) National Defence Research Establishment, Division of Laser systems, Linköping, Sweden, (c) National Defence Research Establishment, Division of Material Research, Linköping, Sweden, (c) Royal Institute of Technology - Department of Polymer Technology, Stockholm, Sweden, (d) Chalmers University of Technology - Physics Department, Göteborg, Sweden.

18.10-18.35 **COFFEE BREAK**

- 18.35-19.00 A.Levenson (*invited*), **Quantum nonlinear optics in artificially phase-matched materials**, Centre National d'Etudes des Telecommunications, Bagneux, France.
- 19.00-19.20 G.D'Aguanno, C.Sibilia, E.Fazio, M.Bertolotti, **All-optical modulation in a type II perfect phase-matched SHG under quasi-static approximation**, Università di Roma "La Sapienza"-Dipartimento di Energetica, Italy.
- 19.20-19.40 M.Del Zoppo, C.Castiglioni, M.C.Rumi, and G.Zerbi, **How to use structural data from vibrational spectroscopy to obtain information on the NLO response of organic materials.**, Politecnico di Milano - Dipartimento di Chimica Industriale ed Ingegneria Chimica, Italy.
- h19.40-20.00 E.Borsella^a, E.Cattaruzza^a, G.De Marchi^a, F.Gonella^a, G.Mattei^a, P.Mazzoldi^a, S.Cestaro^a, G.Battaglin^b, R.Polloni^b, A.Quaranta^c, R.F.Haglund^d, **New methodologies for metal quantum-dot glass waveguides preparation**, (a) Università di Padova - Dipartimento di Fisica, Italy, (b) Università di Venezia - Dipartimento di Chimica Fisica, Italy, (c) Università di Trento - Dipartimento di Ingegneria dei Materiali, Italy

h20.00-21.30 **DINNER BREAK**

h21.30-23.00 **POSTER SESSION 1**

Thursday, July 10th 1997

- 8.30-8.55 S.Brasselet and J.Zyss (*invited*), **Optically induced multipolar micropatterning of nonlinear polymer films: from molecular to photonic engineering**, Centre National d'Etudes des Telecommunications, FRANCE.
- 8.55-9.20 M.Kryszewski (*invited*), **Thin anisotropic poly-porphyrin films with potential application in nonlinear optics**, Polish Acad.of Sciences Centre of Mol. and Macromol. Studies, Poland.
- 9.20-9.45 K.Sasaki (*invited*), **Dye doped active waveguides and optical fibers**, Keio University Faculty of Science and Technology, Japan.
- 9.45-10.05 I.Liakatas, M.S.Wong, Ch.Bosshard, P.Günter, **Nonlinear optical chromophores based on multi-donor substituted 4-nitrophenylhydrazones**, Institute of Quantum Electronics - ETH Honggerberg, Zurich, Switzerland

10.05-10.25 **COFFEE BREAK**

- 10.25-10.50 T.Wada, Y.Zhang, T.Isoshima, H.Sasabe (*invited*), **Hyper-structured molecules containing carbazole moieties for photorefractive application**, Frontier Research Program RIKEN, Japan.
- 10.50-11.15 J.P.Boilot^a, J.Biteau^a, F.Chaput^a, G.Counio^a, T.Gacoin^a, A.Brun^b, M.Canva^b, B.Darracq^b, Y.Lévy^b (*invited*), **Organic-inorganic solids by sol-gel and optical applications**, (a) Ecole Polytechnique, France, (b) Institut d'Optique Théorique et Appliquée, Université d'Orsay-Paris, France.
- 11.15-11.40 A.Montenaro^(a), P.P.Lottici^(b), D.Wouters^(c), G.Gnappi^(d), C.Sibilia^(e) (*invited*), **Optical properties of ferroelectric**, (a) Univ. Parma-Istituto di Strutturistica Chimica, Parma, Italy; (b) Univ.Parma-Dip.Fisica, Parma, Italy; (c) IMEC, Leuven, Belgium, (d) CO.RI.VE., Parma, Italy; (e) Univ.Roma 1-Dip.Energetica, Roma, Italy.
- 11.40-12.00 T.Zabulon, T.Brotin, R.Anémian, C.Andraud, A.Collet, S.Brasselet, I.Ledoux, J.Zyss, **Rod and octupolar polyenovanillins for nonlinear optics**, ENS-Lyon Stereochimie et Interactions moléculaires, France.

12.00-17.00 LUNCH BREAK

- 17.00-17.25 C.Taliani^(a), R.Zamboni^(a), R.Marks^(a), M.Muccini^(a), R.Mahrt^(b) (*invited*), **UHV grown C₆₀/sexithienyl multilayers**, (a) Istituto di Spettroscopia Molecolare C.N.R., Bologna, Italy; Phillips Univ., Marburg, Germany.
- 17.25-17.50 A.Bräuer^(a), T.Gabler^(b), R.Waldhäusl^(a), U.Bartuch^(b), H.H.Hörhold^(b), F.Michelotti^(c) (*invited*), **Nonresonant n₂ and TPA coefficient measurement in polymer waveguides by different measurement techniques**, (a) Fraunhofer Inst. for Appl. Optics and Prec. Engineering, Jena, Germany; (b) Friedrich-Schiller Univ., Jena, Germany; Univ.Roma 1-Dip.Energetica, Roma, Italy.
- 17.50-18.10 W.Wenseleers^a, A.W.Gerbrandij^a, E.Goovaerts^a, M.H.Garcia^b, M.P.Robalo^b, J.C.Rodrigues^b, P.Mendes^b, **Large first hyperpolarizabilities of eta5-monocyclopentadienyl-metal complexes measured by Hyper-Rayleigh-Scattering**, (a) University of Antwerp - Physics Department, Belgium, (b) Instituto Superior Técnico - Centro de Química Estrutural, Lisboa, Portugal.

18.10-18.35 COFFEE BREAK

- 18.35-19.00 F.Michelotti (*invited*), **Relaxation dynamics in poled polymers**, Univ. di Roma "La Sapienza" Dipartimento di Energetica, Italy.
- 19.00-19.20 G.Vitrant^a, X.Grégoire^a, H.Rezig^b, P.A.Chollet^c, F.Kajzar^c, **Photoinduced birefringence in thin azo-dye doped polymer film**, (a) LEMO-ENSEERG, Grenoble, France, (b) L.S.Telecoms, Tunis, Tunisia, (c) DEIN/SPE-CEA/LETI, Gif sur Yvette, France.
- 19.20-19.40 J.Muller, A.Fort, M.Barzoukas, **Importance of the polarizability's anisotropy of donor-acceptor chromophores in the properties of the low-Tg photorefractive polymers**, IPCMS Group d'Optique Non Linéaire et d'Optoélectronique, Strasbourg, France.
- 19.40-20.00 P.A.Blanche^a, P.C.Lemaire^a, C.Maertens^b, P.Dubois^b, R.Jérôme^b, **Photoinduced birefringence and diffraction efficiency versus temperature for various azo dye doped or linked polymers**, (a) Centre Spatial de Liège - Université de Liège, Belgium, (b) Université de Liège - Laboratoire de Chimie Macromoléculaire et des Matériaux Organiques, Belgium.

h20.00-21.30 DINNER BREAK

21.30-23.00 POSTER SESSION 2

Friday, July 11th 1997

- 8.30-8.55 J.Hulliger, P.J.Langley, A.Quintel, P.Rechsteiner (*invited*), **Channel-Type inclusion lattices of Perhydrotriphenylene: a new route to orientation-confined nonlinear optical molecules**, Univ. Bern Inst. für Anorg. Analyt. und Physikalische Chemie, Switzerland.
- 8.55-9.20 C.Sirtori (*invited*), **Quantum cascade lasers**, AT&T Bell Labs - Murray Hill, NJ, USA.
- 9.20-9.45 J.P.Dowling (*invited*), **Spontaneous emission and nonlinear effects in photonic band gap materials**, Weapons Sciences Directorate AMSMI-RD-WS-ST, Alabama USA.

9.45-10.05 A. Adinolfi, F. Minerva, M.C. Netti, R. Tommasi, M. Lepore, I.M. Catalano, **Linear and nonlinear optical absorption in Zn_{1-x}Cd_xSe/ZnSe multi-quantum-wells**, Università di Bari - Dipartimento di Fisica, Italy.

10.05-10.25 **COFFEE BREAK**

10.25-10.50 V. Berger, X. Marcadet and J. Nagle (*invited*), **Microcavities for NLO**, Laboratoire Central des Recherches / Thomson CSF, France.

10.50-11.15 A. Mecozzi (*invited*), **Four-wave mixing in semiconductor optical amplifiers for spectroscopy and device applications**, Fondazione Ugo Bordoni, Italy.

11.15-11.40 K. Rustagi (*invited*), **Polarization changing optical nonlinearities in semiconductor doped glasses**, Laser program Centre for Advanced Technology, India.

11.40-12.00 G. Ventruti^a, L. Chiavarone^a, M. Lugarà^a, V. Spagnolo^a, M. Ferrara^a, G.C. Righini^b, **Investigation of finite size effects in CdS doped sol-gel thin films by optical absorption and micro-Raman spectroscopy**, (a) Università di Bari - Dipartimento Interateneo di Fisica, Italy, (b) IROE-CNR, Firenze, Italy.

12.00-17.00 **LUNCH BREAK**

17.00-17.25 H. Kurz (*invited*), **Nonlinear optics in semiconductors and multiquantum wells**, Institute of Semiconductor Electronics, Aachen, Germany.

17.25-17.50 J. S. Aitchison^(a), C. J. Hamilton^(a), M. W. Street^(a), N. D. Whitbread^(a), D. C. Hutchings^(a), J. H. Marsh^(a), G. T. Kennedy^(b) and W. Sibbett^(b) (*invited*), **Control of the second and third order nonlinearities in GaAs/AlGaAs multiple quantum wells**, (a) University of Glasgow, Dept. of Electronics and Electr. Eng., (b) Department of Physics and Astronomy, University of St. Andrews, United Kingdom.

17.50-18.10 A. Fiore, V. Berger, E. Rosencher, N. Laurent, J. Nagle, **Selectively oxidized GaAs/AlAs heterostructures: a material with huge artificial birefringence (Dn=0.22) for phase-matched nonlinear frequency conversion**, Thomson CSF Laboratoire - Central de Recherches Groupe de Physique, Orsay, France.

18.10-18.35 **COFFEE BREAK**

18.35-19.00 A.A. Andriesh and V. Chumash (*invited*), **Nonlinear optical properties of amorphous chalcogenide semiconductors**, Center of Optoelectronics - Acad. of Sciences of Moldova, Moldova.

19.00-19.20 C. Razzetti^a, S. Romani^a, F. Bissoli^a, S. Bini^a, M. Zha^b, **Evaluation of some first and second order optical constants of monomethyl urea from as grown crystals**, (a) Università di Parma - Dipartimento di Fisica, Italy, (b) MASPEC - CNR, Parma, Italy.

19.20-19.40 J. Callaghan and W. Blau, **Nonlinear optical properties of neat and metal substituted fullerenes**, Trinity College Dublin - Physics Department, Ireland.

19.40-20.00 A. Le Garrec, M. Bucchia, M. Stehlé, **Nonlinear optical spectrometer**, SOPRA, Bois-Colombes, France.

20.00- **CONFERENCE DINNER**

Saturday, July 12th 1997

8.30-8.55 A.P. Piskarskas (*invited*), **New trends in parametric light amplification and generation**, Vilnius University Laser Research Center, Lithuania.

8.55-9.20 C. Sibilìa, P. Masciulli, M. Bertolotti (*invited*), **Optical properties of quasiperiodic (self similar) structures**, Univ. di Roma "La Sapienza" Dipartimento di Energetica, Italy.

9.20-9.45 I. Gravè (*invited*), **MQW structures for Nonlinear Optics**, Univ. of Pittsburgh Dept of Electrical Engineering, USA.

9.45-10.05 A. Berzanskis, K.H. Feller, **Pulsed squeezing in dispersive parametric interaction**, Technical University of Jena - Faculty of Physics and Medical Engineering, Germany.

10.05-10.25 **COFFEE BREAK**

10.25-10.50 G.P. Banfi, V. Degiorgio, D. Fortusini (*invited*), **Two-photon absorption measurements through ultrashort pulses**, Università di Pavia Dip. Ingegneria Elettronica, Italy.

10.50-11.15 F. Laurell (*invited*), **Quasi-phase matched structures for NLO applications**, Royal Institute of Technology Department of Physics II, Sweden.

- 11.15-11.40 S.Delysse, J.M.Nunzi, P.Raimond, **Two-photon absorption in non-centrosymmetric dyes**, DEIN/SPE CEA - Saclay, Gif sur Yvette, France.
- 11.40-12.00 J.McAleese, C.McQuade, D.B.Sheen, J.N.Sherwood, W.Qingwu, **Evolution of structure and morphology in vapour deposited films of some organic nonlinear optical materials**, University of Strathclyde - Department of Pure and Applied Chemistry, United Kingdom.
- 12.00-12.20 V.E.Gruzdev, M.N.Libenson, **Nonlinear effects induced by nonabsorbing micro-inclusions in transparent optical medium**, S.I.Vavilov State Optical Institute, St. Petersburg, Russia.

Wednesday 07/09/1997 - Poster SESSION 1

- P-1** P.Lefin, C.Fiorini, J. Nunzi, **The photoinduced translation diffusion of azobenzene -dyes in polymer matrices**, LETI (CEA - Technologies Avancées) DEIN-SPE, Gif sur Yvette, France
- P-2** T.Zabulon^a, R.Anémian^a, C.Andreaud^a, T.Brotin^a, A.Collet^a, S.Brassellet^b, I.Ledoux^b, J.Zyss^b, **Theoretical and experimental first-order hyperpolarizabilities of octupolar polyenes**, (a) Ecole Normale Supérieure de Lyon, Stéréochimie et interactions moléculaires, France, (b) Centre national d'études des télécommunications, France Télécom, Bagneaux, France
- P-3** I.V.Kityk^a, B. Sahraoui^b, X.Nguyen Phu^b, M.Sallé^c and G.Rivoire^b, **Nonlinear optical spectra of tetrathiafulvalene**, (a) Pedagogical University - Physics Institute, Czestochowa, Poland, (b) Université d'Angers - Laboratoire POMA, Faculté des Sciences, France, (c) Université d'Angers -Laboratoire IMMO, France
- P-4** R.E.Martin^a, U.Gubler^b, R.R.Tykwinski^a, C.Boudon^c, C.Bosshard^b, J.P.Gisselbrecht^c, P.Günter^b, M.Gross^c, and F.Diederich^a, **Structure-property relationships in polytriacylenes: effective conjugation length, influence of lateral conjugation, and donor/acceptor substitution**, (a) ETH-Laboratorium für Organische Chemie, Zurich, Switzerland, (b) ETH-Institut für Quantenelektronik, Zurich, Switzerland, (c) Université Louis Pasteur-Laboratoire d'Electrochimie, Strasbourg, France
- P-5** A. Tamulis^a, E.Stumbrys^b, L.M.Balevicius^b, J.Tamulienė^a, A. Tamulis^c, **Design of basic elements of digital and postdigital computers based on quantum mechanical investigation of fullerene and photoactive molecules**, (a) Institute of Theoretical Physics and Astronomy, Vilnius, Lithuania, (b) Vilnius University - Faculty of Physics, Lithuania, (c) Vilnius University - Faculty of Natural Sciences, Lithuania.
- P-6** A.El Osman, M.Dumont, **Dynamics of Molecular Orientation in Dye-Doped Polymers**, Institut d'Optique Theorique et Appliquée, Orsay, France
- P-7** G.Abbate^a, L.De Stefano^a, P.Mormile^b, L.Petti^b, G.C.Righini^c, L.Sirieto^c, **Light propagation in a dye-doped liquid crystal planar waveguide**, (a) Istituto di Cibernetica del CNR, Arco Felice, Italy, (b) CNR Istituto di Cibernetica, Arco Felice, Italy, (c) IROE-CNR, Firenze, Italy
- P-8** Y.Okada-Shudo^a, F.Kajzar^a, C.D.Merritt^b, and Z.H.Kafafi^b, **Nonlinear optical properties of multilayered structures and composites of C60 with electron donors**, (a) Centre d'Etudes de Saclay, Gif sur Yvette, France, (b) US Naval Research Laboratory, Washington, USA
- P-9** K.H.Feller^a, R.Gadonas^b, E.Gaizauskas^b, H.Glaeske^a, A.Pugzlys^b, **Application of J-aggregates as materials for optical switching**, (a) Technical University Jena - Faculty of Physics and Medical Engineering, Germany, (b) Vilnius University-Laser Research Center, Lithuania
- P-10** K.Shirai^a, M.Matsuoka^a, J.Y.Jaung^b, and K.Fukunishi^b, **Aminovinylidicyanopyrazines as new NLO chromophores with large b values and their self-assembling**, (a) Kyoto Women's University, Japan, (b) Kyoto Institute of Technology, Japan.
- P-11** M.Matsuoka, J.Y.Jaung, and K.Fukunishi, **Pyrazinophthalocyanines as new NLO chromophores and their molecular stacking**, Kyoto Women's University, Japan, (b) Kyoto Institute of Technology, Japan.
- P-12** E.Mulazzi, **Photoinduced infrared absorption spectra of conducting polymers**, Università di Milano - Dipartimento di Fisica, Italy
- P-13** P.Wojcicehowski, J.Ulanski, **Thermal stability of anisotropic LC polymer networks - The role of molecular relaxations**, Technical University of Lodz - Institute of Polymers, Poland
- P-14** M.Barzoukas^a, J.Muller^a, A.Fort^a, V.Alain^b, M.Blanchard-Desce^b, **Quadratic hyperpolarizability of donor-acceptor polyenes: a theoretical and experimental investigation**, (a) GONLO Institut de Physique et Chimie des Matériaux de Strasbourg, France, (b) Ecole Normale Supérieure -Département de Chimie, Paris, France
- P-15** S.Sottini^a, D.Grando^a, L.Palchetti^a, E.Giorgetti^a, R.Ricceri^b, G.Gabrielli^b, **A waveguide electro-optic modulator based on a DCANP Langmuir-Blodgett film**, (a) CNR-IROE, Firenze, Italy, (b) Università di Firenze -Dipartimento di Chimica, Italy

- P-16** G.Boudebs, M.Chis, A.Monteil, **Nonlinear image processor for third order susceptibility measurements and contrast increasing in the image plane**, Université d'Angers - Faculté des Sciences, France
- P-17** E.Campani^a, G.Gorini^a, M.Nencioli^a, G.Masetti^b, **Second harmonic generation from azobenzene derivatives in acrylic polymeric matrices**, (a) Università di Pisa - Dipartimento di Fisica, Italy, (b) CNR-Istituto di Biofisica, Pisa, Italy
- P-18** B.Sahraoui^a, G.Rivoire^a, M.Sallé^b, A.Gorgues^b, **Third order nonlinear optical properties of various families of tetrathiafulvalenes derivatives**, (a) Université d'Angers - Laboratoire POMA, France, (b) Université d'Angers-Laboratoire d'Ingénierie Moléculaire Matériaux Organiques, France
- P-19** N.V.Kamanina^a and N.A.Vasilenko^b, **Obtaining a compromise between high resolution, sensitivity and speed in the liquid-crystal spatial light modulator with a polyimide photosensitive layer**, (a) Vavilov State Optical Institute, St. Petersburg, Russia, (b) Karpov Research Physical Chemical Institute, Moscow, Russia.
- P-20** Withdrawn.
- P-21** Withdrawn.
- P-22** Withdrawn.
- P-23** U.Gubler^a, R.E.Martin^b, Ch.Bosshard^a, R.R.Tykwinski^b, P.Günter^a, F.Diederich^b, **Influence of conjugation length expansion and substitution on the second-order hyperpolarizability gamma of oligotriacetylenes**, (a) ETH Honggerberg - Institute of Quantum Electronic, Zurich, Switzerland, (b) Laboratory of Organic Chemistry- Institute of Quantum Electronic, Zurich, Switzerland.
- P-24** I.Liakatas, M.S.Wong, Ch.Bosshard, M.Bösch, P.Günter, **Novel zwitterionic chromophores for electro-optic polymers**, ETH Honggerberg - Institute of Quantum Electronic, Zurich, Switzerland
- P-25** V.V.Danilov and N.V.Kamanina, **Investigations of an optical analog of the Borrmann effect in resonant liquid-crystal media**, Vavilov State Optical Institute, St. Petersburg, Russia
- P-26** A.Boyle and W.Blau, **Polymeric nonlinear optical waveguides for all-optical switching at telecommunication wavelengths**, Trinity College Dublin - Physics Department, Ireland
- P-27** A.Davey, O.O'Connor, E.Bourdin, W.Blau, **Poly(Arylene Ethynylene) copolymers : a model study in molecular engineering for photonic devices**, Trinity College Dublin - Physics Department, Ireland
- P-28** G.Rojo, F.Agullo-Lopez, B.del Rey, T.Torres, **Second harmonic generation from subphthalocyanines films**, Universidad Autonoma de Madrid - Dep. Fisica de Mat. C-IV, Spain
- P-29** N.V.Kamanina and V.N.Kidalov, **Peculiarities of the interaction between human erythrocytes and liquid crystal matrix in their mixture**, Vavilov State Optical Institute, St. Petersburg, Russia
- P-30** D.De Feo^a, S.De Nicola^b, P.Ferraro^c, A.Finizio^b, P.Maddalena^a, G.Pierattini^b, **A new interferometric technique for the characterization of optical nonlinearities in nematic liquid crystals**, Università di Napoli - Dipartimento di Scienze Fisiche, Italy, (b) CNR-Istituto di Cibernetica, Arco Felice, Italy, (c) Istituto Professionale di Stato per l'Industria e l'Artigianato "G.L.Bernini", Napoli, Italy

Thursday 07/10/1997 Poster SESSION 2

- P-31** R.Alexandrescu^a, I.Morjan^a, I.Voicu^a, F.Huisken^b, **Iron-based thin films and nanoparticles produced by laser-induced CVD**, National Institute of Laser, Bucharest, Romania, (b) Max Planck Institut, Göttingen, Germany
- P-32** A.Kazlauskas, B.Ullrich, T.Kobayashi, **Interconnection between electronics and photonics by the application of bistability in luminescence in thin CdS and ZnSe films**, (a) Vilnius University, Institute of Material Science and Applied Research, Lithuania, (b) Department of Physics, University of Tokyo, Japan
- P-33** E.Frins^{a,b}, H.Schmitzer^a, W.Dultz^c, **Nonlinear phenomena in interferometry on the basis of the optical Berry-phases**, (a) Universität Frankfurt, Germany, (b) Universidad Montevideo, Uruguay, (c) Deutsche Telekom, Darmstadt, Germany.
- P-34** M.Fontana, M.Aillierie, F.Abdi, and K.Chah, **Role of intrinsic and extrinsic defects on electro-optic properties of LiNbO₃**, MOPS-CLOES, Université de Metz et Supélec, France.
- P-35** H.Schmitzer^a and W.Dultz, **Nonlinear optical properties of Mercury-(I)-Chloride**, (a) Universität Regensburg-Facultät für Physik, Germany, (b) Deutsche Telekom, Darmstadt, Germany.
- P-36** M. Lamy de la Chapelle^a, S.Lefrant^a, C.Journet^b, W.Maser^b, P.Bernier^b, A.Loiseau^c, **Characterization of bundles of single-walled carbon nanotubes produced by the electric arc technique**, (a) IMN - Université de Nantes, France, (b) GDPC-Université de Montpellier II, France, (c) ONERA - Lab. Phys. Solide, France

- P-37** I.Kasik, V.Matejec, J.Kanka, D.Berkova, **Fabrication and properties of materials for Er³⁺ doped Yb³⁺ sensitized high - power lasers**, Academy of Science of the Czech Republic - Institute of Radio Engineering and Electronics, Praha, Czech Republic.
- P-38** J.A.Kapoutsis^a, E.I.Kamitsos^a, I.P.Culeac^a, M.S.Iovu^b, **Infrared reflectance investigation of xSb₂S₃(1-x)As₂S₃ glasses**, (a) National Hellenic Research Foundation - Theoretical and Physical Chemistry Institute, Athens, Greece, (b) centre of Optoelectronics of the Institute of Applied Physics, Chisinau, Moldova
- P-39** A.Majchrowski, **Crystal growth of NLO borates**, Institute of Technical Physics WAT, Warsaw, Poland.
- P-40** A.Scacco^a, U.M.Grassano^b, G.Baldacchini^c, R.M.Monteverdi^c, S.Boiko^d, G.Tarasov^d, **Bistable optical excitation of FA(Li) centers in cubic crystals of alkali-halides**, (a) Università di Roma Tor Vergata - Dipartimento di Fisica, Italy, (b) Università di Roma "La Sapienza" - Dipartimento di Fisica, Italy, (c) ENEA C.R. Frascati, Italy, (d) Academy of Sciences of Ukraine - Institute of semiconductor Physics, Kiev, Ukraine.
- P-41** E.Serrano^a, M.P.Y.Desmulliez^b, H.Inbar^a, B.S.Wherrett^a, **Design, evaluation and optimization of MQW binary-phase modulators**, (a) Heriot-Watt University - Department of Physics, Great Britain, (b) Heriot-Watt University - Department of Computing and Electrical Engineering, Edinburgh, Great Britain.
- P-42** S.Monneret, F.Flory, **Nonlinear refractive index modification in dielectric waveguides**, LOSCM, ENSPM, Marseille, France.
- P-43** Y.D.Yannopoulos^a, E.I.Kamitsos^a, H.Jain^b, **Structure of potassium germanate glasses by vibrational spectroscopy**, (a) National Hellenic Research Foundation - Theoretical and Physical Chemistry Institute, Athens, Greece, (b) Lehigh University - Department of Material Science and Engineering, Bethlehem, USA.
- P-44** C.Baratto^a, P.P.Lottici^a, G. Antonioli^a, G. Gnappi^b, A. Montenero^c, M. Guarneri^c, T. Besagni^d, **Sol Gel preparation and characterization of alpha-Fe₂O₃ films**, (a) Università di Parma- Dipartimento di Fisica, Italy, (b) CORIVE, Parma, Italy, (c) Università di Parma- Dipartimento di Chimica, Italy, (d) MASPEC-CNR, Parma, Italy.
- P-45** E.Brambilla^a, F.Castelli^a, L.A.Lugiato^a, I.Abram^b, **Effect of exciton dephasing in a semiconductor microcavity**, (a) Università di Milano - Dipartimento di Fisica, Italy, (b) CNET, France.
- P-46** M.C.Netti^a, R.Tommasi^{a,b}, M.Lepore^c, I.M.Catalano^a, A.Vinattieri^d, M.Colucci^d, I.Suemune^e, **Picosecond relaxation dynamics of localized excitons in ZnSe/ZnS_xSe_{1-x} strained-layer superlattices**, (a) Università di Bari-Dipartimento di Fisica, Italy, (b) Università di Bari- Istituto di Fisica Medica, Italy, (c) Università di Napoli "Federico II" - Dipartimento di Fisica, Italy (d) LENS, Firenze, Italy, (e) Hokkaido University-Research Institute for Electronic Sciences, Sapporo, Japan.
- P-47** R.Calvani, R.Caponi, D.Roccato, **Nonlinear refractive index measurement of dispersion shifted fibres from the maximum frequency extent of SPM spectra**, CSELT S.p.A., Torino, Italy.
- P-48** M.Zha, M.Ardoino, L.Zanotti, **Solution growth of L-Alanine as a material for nonlinear optical applications**, MASPEC-CNR, Parma, Italy.
- P-49** M.Zha, M.Ardoino, L.Zanotti, **Studies on solution growth of large monomethylurea single crystals**, MASPEC-CNR, Parma, Italy.
- P-50** M.Bertolotti^(a), E.Fazio^(a), F.Garzia^(a), G.Lanciani^(a), C.Sibilia^(a), M.Suriano^(a), M.Zitelli^(a), G.C.Righini^(b), **Spatial optical solitons in a BK7 glass planar waveguide**, Univ.Roma "La Sapienza"-Dip.Energetica, Roma, Italy, (b) CNR-IROE, Firenze, Italy.
- P-51** L.Guilbert, J.P.Salvestrini, M.D.Fontana, **Electrooptical properties of hydrogen-bonded selenates**, C.L.O.E.S., Université de Metz-Supelec - Laboratoire de Matériaux Optiques à Propriétés Spécifiques, France.
- P-52** B.Sahraoui^a, W.Bala^b, G.Glowacki^b, **Third order nonlinear optical properties of Zn_{1-x}MgxSe crystals**, Université d'Angers - Laboratoire POMA, France, (b) N.Copernicus University-Institute of Physics, Torun, Poland.
- P-53** D.Truchado, G.Rojo, F.Agullo-Lopez, **Free electron model for the polarizabilities of nanosystems**, Universidad Autonoma de Madrid - Dept. Fisica de Materiales C-IV, Spain.
- P-54** A.Meffleh, S.Brunet, S.Benet, **Linear electro-optic measurements in Nd:MgO:LiNbO₃ and LiNbO₃ single crystals**, Université de Perpignan CNRS-IMR Groupe Physique des Matériaux-Métrologie, France.
- P-55** Q.Zou, **Analytical modeling of the transient effects during two-wave mixing in thin photorefractive crystals**, Institut National des Télécommunications, France.
- P-56** J.Rams, J.Olivares, J.M.Cabrera, **High index jump proton exchanged waveguides in z-cut LiNbO₃ with undergraded nonlinear optical coefficients**, Universidad Autonoma de Madrid - Dept. Fisica de Materiales C-IV, Spain.
- P-57** P.Zverev, **Nonlinearity of lithium fluoride crystals with F₂ - color centers**, General Physics Institute, Moscow, Russia.

- P-58** P. Zverev, T.T.Basiev, **Stimulated Raman scattering in solid state materials**, General Physics Institute, Moscow, Russia.
- P-59** A.Napoli, **Single atom manipulation of localized electromagnetic modes in one-dimensional photonic crystals**, Università di Palermo - Istituto di Fisica, Palermo, Italy.
- P-60** V.I.Kovalev, **The cubic nonlinear optical response of matter: dispersion and achievable values of parameters**, Lebedev Physics Institute, Moscow, Russia.
- P-61** O.Kh.Khasanov, T.V.Smirnova, O.M.Fedotova, **Frequency stability and selection in semiconductor lasers by phase-conjugate optical feedback**, Solid State & Semiconductor Physics Institute, Minsk, Belarus.
- P-62** O.Kh.Khasanov, T.V.Smirnova, O.M.Fedotova, **Multiple photon echo generation in optically dense crystals**, Solid State & Semiconductor Physics Institute, Minsk, Belarus.

Authors' Index

Abbate G.	34,114	Brasselet S.	45,56,104	Fiorini C.	103
Abdi F.	50	Brignon A.	21	Firth W.J.	6
Abram I.	167	Brotin T.	56,104	Flory F.	163
Adinolfi A.	72	Brun A.	53	Fontana M.	150,179
Agranovich V.M.	2	Brunet S.	183	Fort A.	65
Aguillo Lopez F.	20,142,182	Bucchia M.	89	Fortusini D.	12,96
Aillerie M.	150	Cabrera J.M.	187	Frins E.	149
Aitchinson J.S.	81	Callaghan J.	88	Fukunishi K.	119,121
Alain V.	126	Calvani R.	171	Gabler T.	59
Alexandrescu R.	146	Campani E.	131	Gacoin T.	53
Andraud C.	56,104	Canva M.	53	Gadonas R.	117
Andriesh A.	84	Caponi R.	171	Gaizauskas E.	117
Anémian R.	56,104	Carrascosa M.	20	Garcia M.H.	61
Anstett G.	30	Castelli F.	167	Garrett M.H.	24
Antonioli G.	166	Castiglioni C.	41	Garzia F.	177
Ardoino M.	173,175	Catalano I.M.	72,169	Gedde U.W.	37
Arntzen P.O.	37	Cattaruzza E.	43	Gerbrandij A.W.	61
Bäder U.	30	Cestaro S.	43	Giorgetti E.	127
Bala W.	180	Chah K.	150	Girardin F.	18
Baldacchini G.	159	Chaput F.	53	Gisselbrecht J.P.	108
Balevicius L.M.	110	Chiavarone L.	77	Glaeske H.	117
Banfi G.P.	12,96	Chis M.	128	Glowacki G.	180
Baran J.	31	Chollet P.A.	63	Gnappi G.	55,166
Baratto C.	166	Chumash V.	84	Gonella F.	43
Bartkiewicz S.	33	Collet A.	56,104	Goovaerts E.	61
Bartuch U.	59	Colocci M.	169	Gorgues A.	132
Barzoukas M.	65,126	Counio G.	53	Gorini G.	131
Basiev T.T.	191	Culeac I.P.	156	Grando D.	127
Battaglin G.	43	D.Aguanno G.	39	Grassano U.M.	159
Benet S.	183	Danilov V.V.	139	Gravé I.	92
Berkova D.	154	Darracq B.	53	Grégoire X.	63
Berger V.	74,82	Datta P.K.	12	Gross M.	108
Bernier P.	152	Davey A.	141	Gruzdev V.E.	102
Bertolotti M.	39,91,177	Debrus S.	31	Guarnieri M.	166
Berzanskis A.	94	De Feo D.	144	Gubler U.	4,108,135
Besagni T.	166	Degiorgio V.	12,96	Guekos G.	18
Bindra K.S.	76	del Rey B.	142	Günter P.	4,49,108,135,137
Bini S.	86	Del Zoppo M.	41	Guilbert L.	179
Bissoli F.	86	De Nicola S.	144	Haglund Jr R.F.	43
Biteau J.	53	Delysse S.	98	Hamilton C.J.	81
Blanchard-Desce M.	126	De Marchi G.	43	Herrman D.	37
Blanche P.A.	66	Desmulliez M.P.Y.	161	Hörhold H.H.	59
Blau W.J.	88,140,141	De Stefano L.	114	Huignard J.P.	21
Bösch M.	137	Donelli G.	12	Hulliger J.	68
Boiko S.	159	Dowling J.P.	71	Hult A.	37
Boilot J.P.	53	Driederich F.	108,135	Hutchings D.C.	81
Borsella E.	43	Dubois P.	66	Inbar H.	161
Borsutzky A.	30	Dultz W.	149,151	Isoshima T.	51
Bosshard Ch.	4,49,108,135,137	Dumont M.	112	Iovu M.S.	156
Boudebs G.	128	Eason R.W.	24	Jain H.	165
Bourdin E.	141	El Osman A.	112	Januszek A.	33
Buodon C.	108	Fazio E.	39,177	Jaung J.Y.	119,121
Boulanger B.	28	Fedotova O.M.	196,197	Jérôme R.	66
Boyle A.	140	Feller K.H.	94,117	Journet C.	152
Bräuer A.	59	Ferrara M.	77	Kaatz P.	4
Brambilla M.	6,167	Ferraro P.	144	Kaczmarek M.	24
		Fève J.P.	28	Kafafi Z.H.	116
		Finizio A.	144	Kajzar F.	1,63,116
		Fiore A.	82	Kamanina N.V.	134,139,143

Kamitsos E.I.	156,165	Mazerant W.	4	Rosencher E.	82
Kamshilin A.	14	Mazzoldi P.	43	Rudquist P.	37
Kanka J.	154	Mc Aleese J.	100	Rumi M.C.	41
Kapoutsis J.A.	156	Mc Quade C.	100	Rustagi K.C.	76
Kasic I.	154	Mecozzi A.	75	Sahlén F.	37
Kazlauskas A.	148	Mefleh A.	183	Sahraoui B.	106,132,180
Kennedy G.T.	81	Mendez P.	61	Sallé M.	106,132
Khasanov O.Kh.	196,197	Merritt C.D.	116	Salvestrini J.P.	179
Kidalov V.N.	143	Michelotti F.	59,62	Samoc A.	16
Kityk I.V.	106	Minerva F.	72	Samok M.	16
Kobayashi T.	148	Miniewicz A.	33	Santamato E.	34
Koike Y.	10	Mnushkina I.	24	Sasabe H.	51
Komitov L.	37	Monneret S.	163	Sasaki K.	48
Kovalev V.I.	194	Monteil A.	128	Scacco A.	159
Kryszewsky M.	47	Montenero A.	55,166	Schmitzer H.	149,151
Kurz H.	79	Monteriali R.M.	159	Serrano E.	161
Lagerwall S.	37	Morjan I.	146	Sheen D.B.	100
Lamy de la Chapelle M.	152	Mormile P.	114	Sherwood J.N.	26,100
Lanciani G.	177	Muccini M.	58	Shing Wong M.	49,137
Langley P.J.	68	Mulazzi E.	123	Shirai K.	119
Laurell F.	97	Muller J.	65,126	Sibbett W.	81
Laurent N.	82	Nagle J.	74,82	Sibilia C.	39,55,91,177
Ledoux I.	56,104	Napoli A.	193	Sirleto L.	114
Lefin P.	103	Nencioli M.	131	Sirtori C.	70
Lefrant S.	152	Netti M.C.	72,169	Smirnova T.V.	196,197
Le Garrec A.	89	Nguyen Phu X.	106	Soskin M.S.	23
Lemaire P.C.	66	Nunzi J.M.	98,103	Sottini S.	129
Lepore M.	72,169	Oak S.M.	76	Spagnolo V.	77
Levenson A.	38	O'Connor O.	141	Spinelli L.	6
Lévy Y.	53	Okada-Shudo Y.	116	Stebler B.	37
Liakatas I.	49,137	Olivares J.	187	Stehlé M.	89
Libenson M.N.	102	Örtegren J.	37	Street M.W.	81
Lindström J.	37	Pajarola S.	18	Stumbrys E.	110
Lindgren M.	37	Palchetti L.	127	Suemone I.	169
Loiseau A.	152	Paparo D.	34	Suriano M.	177
Lord A.	6	Parka J.	33	Taliani C.	58
Lottici P.P.	55,166	Petti L.	114	Tamuliene J.	110
Lugarà M.	77	Pierattini G.	144	Tamulis A.	110
Lugiato L.A.	6,167	Piskarskas A.P.	90	Tamulis A.	110
Luther Davies B.	16	Polloni R.	43	Tarasov G.	159
Maatz G.	24	Prati F.	6	Tissoni G.	6
Maddalena P.	34,144	Pugzlys A.	117	Tommasi R.	72,169
Maertens C.	66	Quaranta A.	43	Torres T.	142
Mahrt R.	58	Quintel A.	68	Toussaere E.	62
Majchrowski A.	157	Raimond P.	98	Trollsås M.	37
Marcadet X.	74	Raita E.	14	Truchado D.	182
Marks R.	58	Rajbenbach H.	21	Trull J.	8
Marnier G.	28	Rams J.	187	Tykwinski	108,135
Marrucci L.	34	Ratajczak H.	31	Ulanski J.	124
Marsh J.H.	81	Razzetti C.	86	Ullrich B.	148
Martin R.	108,135	Rechsteiner P.	68	Urschel R.	30
Martorell J.	8	Rezig H.	63	Vasilenko N.A.	134
Masciulli P.	91	Righini G.C.	77,114,177	Vasnetsov M.V.	23
Maser W.	152	Rivoire G.	106,132	Ventruti G.	77
Massera E.	34	Robalo M.P.	61	Venturini J.	31
Matejec V.	152	Roccatò D.	171	Vilaseca R.	8
Matsuoka M.	119,121	Rodrigues J.C.	61	Vinattieri A.	169
Mattei G.	43	Rojo G.	142,182	Vitrant G.	63
May M.	31	Romani S.	86	Voicu I.	146

Wada T.	51
Waldhäusl R.	59
Wallenstein R.	30
Wang Qingwu	100
Wenseleers W.	61
Wherrett B.S.	3,161
Whitbread N.D.	81
Wojciechowski P.	124
Wouters D.	55
Yiannopoulos Y.D.	165
Zabulon T.	56,104
Zamboni R.	58
Zanotti L.	173,175
Zerbi G.	41
Zha M.	86,173,175
Zhang Y.	51
Zitelli M.	177
Zou Q.	185
Zverev P.G.	189,191
Zyss J.	45,56,104

RECENT ADVANCES IN POLYMERIC THIN FILMS ORIENTATION TECHNIQUES

F. Kajzar

LETI(CEA - Technologies Avancées)

DEIN/SPE, CEA/Saclay, 91191 Gif-sur-Yvette Cedex, France

For a large class of practical applications implying second order nonlinear optical effects one needs macroscopically noncentrosymmetric materials. In particular the targeted applications include: frequency doubling, electro-optic modulation, frequency conversion and photorefractive effect. Composite polymeric materials have emerged to be an interesting class of materials for this kind of applications. They are inexpensive and can be easily processed into good optical quality thin films. These materials are also characterized by an ultrafast, THz response time. However, the quantity of interest, which is the macroscopic second order nonlinear optical susceptibility, depends on the polar order through the following, well known relation:

$$\chi^{(2)}(-\omega_3; \omega_1, \omega_2) = NF \langle \beta(-\omega_3; \omega_1, \omega_2) \rangle$$

where N is number density of NLO active molecules, F is the local field correction and β is the molecular first hyperpolarizability, and the brackets denote its orientational average. Optimization of the macroscopic susceptibility $\chi^{(2)}$ is possible not only by increasing the β value through molecular engineering or number density N but also by an increase in orientational order. The active chromophore orientation is obtained by a static field, photoassisted or all optical poling process. Different aspects of poling kinetics using different poling processes will be reviewed and discussed. In particular, the conjunction of static and optical fields leads to new interesting reorientational processes which may find practical applications. Also the influence of molecular environment on the kinetics of poling as well as the relaxation processes will be discussed.

HYBRID FRENKEL-WANNIER-MOTT EXCITONS AT INTERFACE AND IN MICROCAVITY

V.M.Agranovich, Institute of Spectroscopy, Troitsk, Moscow obl.
142092 Russia

We investigate unusual optical properties of exciton states at the interface of organic and inorganic quantum wells(QW) when the energy of 2D Frenkel exciton in the organic QW is near that of the 2D Wannier exciton in the inorganic semiconductor QW. We show that the coupling between QWs (Coulomb dipole-dipole) is responsible for the appearance of hybrid states with unusual linear and nonlinear optical properties. We investigate also the resonance phenomena in microcavity where coupling between QWs appears due to exchange of cavity photons even when QWs are separated by a distance of the order of the optical wavelength. We demonstrate that the new hybrid states in microcavity can be tailored to engineer the enhancement of exciton fluorescence efficiency and relaxation processes.

Materials for optical information processing

B.S.Wherrett

Heriot-Watt University - Physics Department
Edinburgh, Great Britain

Summary not available at time of printing.

Optical Third-Harmonic Generation: Cascaded Second-Order Nonlinearities in KNbO₃

Ch. Bosshard*, U. Gubler*, P. Kaatz#, W. Mazerant*, and P. Günter*

*Nonlinear Optics Laboratory, Institute of Quantum Electronics, ETH-Hönggerberg,
CH-8093, Zürich, Switzerland

#Department of Physics, University of Nevada Las Vegas,
Las Vegas NV 89154-4002, USA

Cascading is a process where lower-order effects are combined to contribute to a higher-order nonlinear process. Recently the potential of cascading for all-optical switching was realized and large nonlinear phase shifts due to cascading (second-harmonic generation (SHG) and difference-frequency mixing (DFM)) were observed in several materials [1].

Cascading also occurs in third-harmonic generation [1]. In this process a fundamental wave at frequency ω produces a wave at frequency 3ω ($\omega + \omega + \omega = 3\omega$). In noncentrosymmetric materials also sum-frequency mixing ($\omega_1 + \omega_2 = \omega_3$) and second-harmonic generation ($\omega + \omega = 2\omega$) are allowed. The two latter processes can be used to also obtain a wave at frequency 3ω as well: We first generate an intermediate field at frequency 2ω through second-harmonic generation. This field can interact with the fundamental wave through sum-frequency mixing ($2\omega + \omega = 3\omega$) to generate a field at frequency 3ω itself.

When applied to third-harmonic generation, cascading can be used for the absolute determination of the third-order nonlinearity $\chi^{(3)}$ since it often is a self-calibrating process [2]. This means the following: From a theoretical fit of an experimental third-harmonic generation Maker-fringe curve of a crystal that shows cascaded processes (Fig.1) one can directly obtain the ratio, $\chi^{(3)} / (\chi^{(2)})^2$. Therefore, if the values of $\chi^{(2)}$ are known, the value of $\chi^{(3)}$ can be determined. A subsequent comparison with a reference material, e.g. fused silica then yields $\chi^{(3)}$ of that material.

We have extended already existing work for the following reasons: (i) The reference value of $\chi^{(2)}$ of quartz (previously used) has considerably changed over the last 15 years (from 0.5pm/V down to 0.3pm/V at $\lambda=1064\text{nm}$ [3]). (ii) The ratio of $\chi^{(3)} / (\chi^{(2)})^2$ is not very well determined for crystalline quartz since $\chi^{(2)}$ of quartz is rather small. In the meantime high-quality crystals of KNbO₃ are available. KNbO₃ has much larger nonlinear optical susceptibilities $\chi^{(2)}$ with respect to its $\chi^{(3)}$ values and therefore allows a more precise determination of the ratio $\chi^{(3)} / (\chi^{(2)})^2$. (iii) It is of considerable interest to know the dispersion of $\chi^{(3)}$, on the one hand to get a reliable standard for the dispersion of $\chi^{(3)}$, on the other hand to get a better theoretical understanding of the dispersion behaviour in inorganic (and organic) materials. (iv) In addition, it is of fundamental interest to compare the third-order susceptibilities of KNbO₃ with the nonpolar KTaO₃. Both materials are ferroelectric perovskite (ABO₃) compounds. Whereas KTaO₃ has cubic symmetry at room temperature, KNbO₃ is only cubic

at high temperatures and transforms with decreasing temperature through the tetragonal phase to the orthorhombic phase at room temperature.

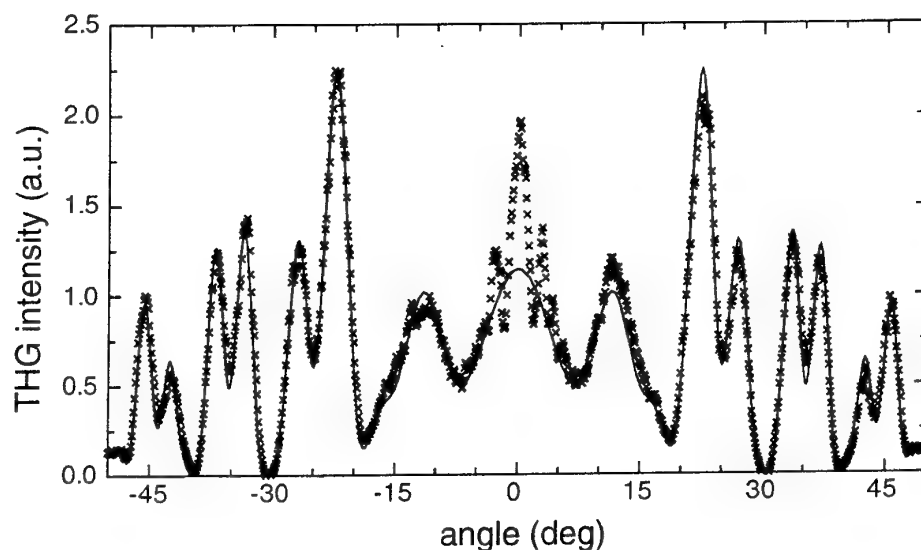


Fig.1 Example of a Maker-fringe curve showing cascading in third-harmonic generation in KNbO₃ (a-plate) at $\lambda=1907\text{nm}$. The interference pattern is due to a combination of $\chi_{3333}^{(3)}(-3\omega, \omega, \omega, \omega)$ and $\chi_{333}^{(2)}(-3\omega, 2\omega, \omega) \cdot \chi_{333}^{(2)}(-2\omega, \omega, \omega)$.

We will present experimental results based on cascading in third-harmonic generation at different wavelengths in KNbO₃ and α -quartz and present a new reliable reference value for fused silica. The effect of local-field cascading on our experiments will be discussed and the dispersion relations for $\chi^{(3)}$ KNbO₃, KTaO₃, α -quartz, and fused silica will be interpreted in terms of the currently used models (such as Miller's rule [4,5]).

References:

- [1] G. I. Stegeman, M. Sheik-Bahae, E. Van Stryland, and G. Assanto, Opt. Lett. **18**, 13 (1993).
- [2] G. R. Meredith, Phys. Rev. B **24**, 5522 (1981).
- [3] R.C. Eckardt, H. Masuda, Y.X. Fan, and R.L. Byer, IEEE J. Quant. Electron. **26**, 922 (1990).
- [4] R. C. Miller, Appl. Phys. Lett. **5**, 17 (1964).
- [5] J. J. Wynne, Phys. Rev. **178**, 1295 (1969).

OPTICAL BULLET HOLES IN SEMICONDUCTOR MICROCAVITIES

M. Brambilla¹, W. J. Firth², A. Lord², L. A. Lugiato¹, F. Prati¹, L. Spinelli¹,
G. Tissoni¹

¹ *Istituto Nazionale di Fisica per la Materia, Dipartimento di Fisica, Via Celoria 16, Milano, Italy.*

² *Department of Physics, University of Strathclyde, 107 Rottenrow, G4 0NG Glasgow, Scotland.*

Abstract

Two recent papers [1, 2] have shown the possibility of controlling the formation, the interaction, the localization and the erasure of spatial optical solitons (SS) in passive nonlinear resonators driven by a coherent plane wave field. The idea is of considering the transverse planes, orthogonal to the propagation direction of the beam as a blackboard on which light dots can be written and erased at any desired location. The SS are generated by shining localized address pulses, which locally create a bleached area that persists after the passage of the pulse, hence the name of 'optical bullet holes' (OBH), also used for this kind of spatial solitons [1].

The results of [1, 2] pave the way to the realisation of an optical memory array of individually addressable OBH, with 2^N coexisting states for an array of N solitons (*i.e.* $\sqrt{N} \times \sqrt{N}$).

This picture was obtained from a two-level model for a passive (*i.e.* inversionless) material which works under purely absorptive conditions, in absence of any refractive effect. Spatial solitons in an organic material, under conditions corresponding to the saturable absorber model analysed in [1, 2], have been recently experimentally observed at PTB in Braunschweig [3]. In the opposite situation of pure refraction, we have also analysed a model where the material is described as a Kerr medium, and shown that SS can be generated also in that case, even if in a smaller parametric domain [4].

The two-level absorptive model and the Kerr medium model are paradigmatic in nonlinear optics, however they are not adequate to describe the case of a semiconductor material, which is the one of interest for the prospective applications of these ideas. Such a case requires studying a set of equations which is intrinsically much more complex than the absorptive or Kerr medium models, for two reasons. First, the two latter models consist in a single partial differential equation for the complex field envelope, while in a semiconductor the field equation must be coupled with a carrier equation. The second is that it is essential to include carrier diffusion, which tends to disfavour the stability of OBH. This implies that also the equation

for the material becomes a partial differential equation, a difficulty that does not arise in any two-level model.

Precisely, we formulated and analysed two models for a semiconductor material in a resonant microcavity. The first corresponds to the 'passive' case that the material has no population inversion, and is a MQW with an exciton nonlinearity which is modeled as a Lorentzian line. The second corresponds to the 'active' case of population inversion induced by an injected current. The configuration is basically that of a driven broad-area VCSEL with the gain arising from free carriers; however, the values of the current are such that the VCSEL is below threshold in absence of driving field.

The partial differential equations are numerically integrated in space and time by means of split-step techniques. The results have been checked by the technique developed in [1], which allows to calculate the stationary OBH bypassing dynamical transients, and has been appropriately generalised to tackle the more complex structure of the equations met in the semiconductor case.

The data collected in this way lead to a rather clearcut picture for the appearance of OBH and their control in semiconductor systems. Most importantly the parametric domains, where SS exist, are sizably extended and accessible to the experimental realization. In the active case (VCSEL) the OBH arise under conditions of self-focusing and are quite robust against carrier diffusion. In the passive case robust OBH can emerge even under conditions of self-defocusing, because the waveguiding effect provided by saturation [the guidance arising from the (negative) loss profile] is still able to overcome the antiguiding action of self-defocusing.

The analysis of the process of writing and erasing solitons by means of narrow laser pulses has revealed that solitons can be erased even when the address pulse is not aimed exactly, *i.e.* the system is able to self-accomodate errors in the position of the pulse.

The results of our theoretical and numerical investigations lead to conclude that the realisation of an array of spatial solitons using semiconductor materials is feasible. By appropriate selection of the operative conditions, both the active and the passive case present promising perspectives to reach this objective.

Acknowledgements

Work in the framework of the ESPRIT Long Term Research Project PASS (Spatial Soliton Array Processor).

References

- [1] W. J. Firth and A. J. Scroggie, *Phys. Rev. Lett.*, **76**, 1623 (1996).
- [2] M. Brambilla, L. A. Lugiato and M. Stefani, *Europhys. Lett.* **34**, 109 (1996).
- [3] C. O. Weiss *et al.*, report of the PASS project.
- [4] W. J. Firth and A. Lord, *J. Mod. Opt.*, **43**, 1071 (1996).

Phase Matching in Photonic Crystals with Quadratic Nonlinearities

by

J. Trull, Jordi Martorell, and R. Vilaseca

Departament de Física i Enginyeria Nuclear, Universitat Politècnica de Catalunya,

08222 Terrassa (Barcelona), Spain.

Tel.: 34-3-739 8137, E-mail: Vilaseca@fen.upc.es

Materials with a three dimensional periodic distribution of the dielectric constant, or photonic band gaps, have been proposed as a class of materials where it will be possible to control the properties of the radiative matter integrated within them.¹ In particular, alteration of the nonlinear interaction within a photonic crystal has been considered for the development of new optoelectronic devices or to enhance the nonlinear interaction to fabricate materials suitable for second harmonic (SH) generation.² The experimental work presented in this paper shows that the nonlinear interaction responsible for generation of SH light in a crystal made of polystyrene spheres coated with a nonlinear molecule is localized at the surface of each sphere. In such crystals the generated SH light is phase matched with the incident fundamental light by the bending of the photon dispersion curve at the boundary of the forbidden zone or Bragg reflection band of the corresponding set of crystalline planes. In our experiments we have measured the SH intensity generated in reflection from several crystals made with a different concentration of $0.115\ \mu\text{m}$ spheres, upon incidence of a 35 ps pulse of less than 5 mJ at the wavelength of 1064 nm. As the concentration of spheres is reduced the space between spheres increases, and consequently for a given frequency of the generated SH light the Bragg condition is satisfied at a larger angle. The maximum generated SH intensity (where phase matching occurs) is shown in figure 1 (as solid dots) for five

crystals fabricate with a decreasing concentration of spheres as the angle for the phase matching configuration increases. In a theoretical model developed we have considered each crystalline plane responsible for the generation of SH light as a sheet of dielectric material covered with a layer of nonlinear molecules in each side of the sheet. The molecules from one layer are oriented in a direction that is opposite to the direction of the molecules from the other layer. After a numerical calculation of the SH intensity reflected by the (111) planes of the fcc lattice, shown as a solid line in figure 1, we have found a very good agreement with the experimental results.

¹ E. Yablonovitch, Phys. Rev. Lett. **58**, 2059 (1987), Jordi Martorell and N. M. Lawandy, Phys. Rev. Lett. **65**, 1877 (1990).

² Jordi Martorell, R. Vilaseca, and R. Corbalán, to appear in Appl. Phys. Lett.

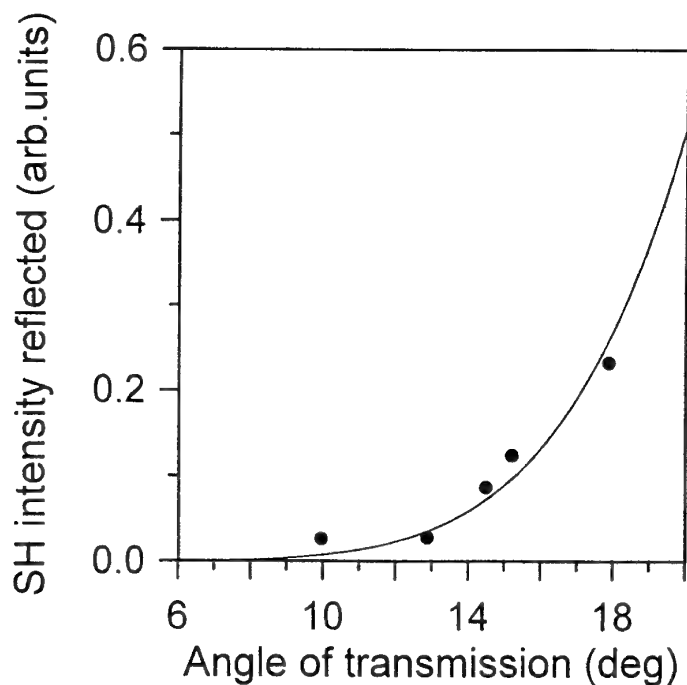


Figure 1. Reflected SH intensity as a function of the angle of transmission for five crystals with different concentrations of $0.115 \mu\text{m}$ latex spheres. The dots correspond to the experimental data points while the line corresponds to the theoretical prediction.

High-speed Photonics Polymer and Its Application

Yasuhiro Koike

Faculty of Science and Technology, Keio University / Kanagawa Academy of Science and Technology
3-14-1, Hiyoshi, Kohoku-ku, Yokohama, 223 / 1-1-1, Fukuura, Kanazawa-ku, Yokohama, 236

1. Graded-Index POF for Data Communication

For recent several years, research activities of the POF have been focused on the high-speed data communication in LAN, interconnection, premises area, etc.

A needed fiber length in premises area or in buildings may be up to several hundred meters. Even considering the lowest ATM of 156 Mb/s for such a distance, the SI POF can not be adopted due to limitation of the modal dispersion. Recently 622 Mb/s data rate has been also required for CATV and clear moving pictures. The GI POF will be very useful for such purposes in which existing wire cables or low NA SI POF can not be utilized. We have reported that a 2.5 Gb/s 100 m transmission using LD at 0.65- μ m wavelength was succeeded by the poly methyl methacrylate (PMMA) base GI POF.^{1,2} In this paper, we also show the possibility of high speed transmission by the perfluorinated (PF) polymer base GI POF for longer distance up to a few kilometers. The relationship between the required bit rate and distance is shown in Fig. 1 for various wire and fiber cables.

2. Trial of High-Speed Data Transmission

Optimization of the refractive index profile of the GI POF should be the key technology in order to minimize the modal dispersion. The possible bit rate in GI POF link was theoretically calculated considering both modal and material dispersions by using WKB method.^{3,4} Figure 2 shows the relation between the possible bit rate and refractive index profile of the GI POF which was approximated by the index exponent g in the power law of the equation

$$n(r) = n_1 \left[1 - \left(\frac{r}{a} \right)^g \Delta \right], \quad (1)$$

$$\Delta = \frac{n_1^2 - n_2^2}{2n_1^2} \approx \frac{n_1 - n_2}{n_1}. \quad (2)$$

Here, n_1 and n_2 are refractive-indices at center axis and cladding of the fiber respectively, a is radius of the core, and Δ is relative difference of the refractive-index. The light source was assumed to be an LD with 2-nm spectral width.

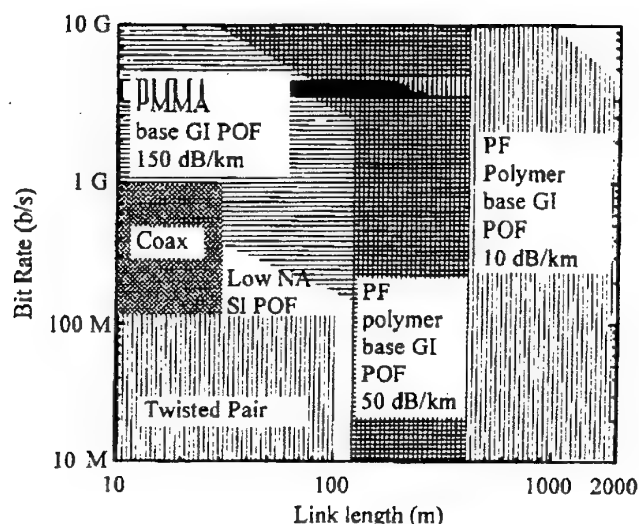


Fig. 1 Possible bit rate versus link length.

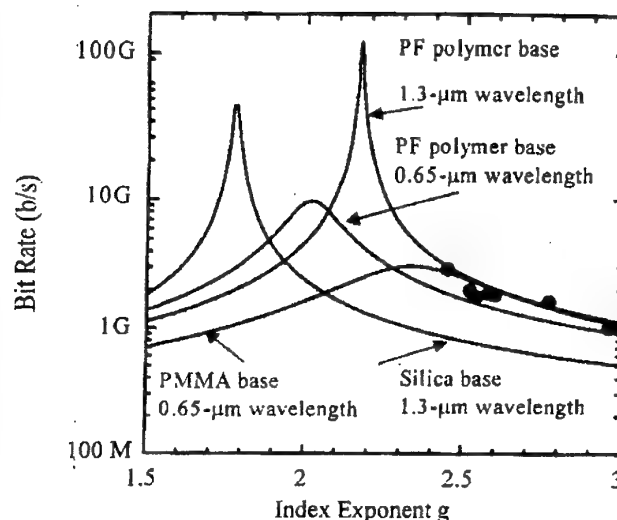


Fig. 2 Relation between index exponent of GI POF and bit rate in 100-m link. ●: Experimental value

It should be noted that the bit rate in PMMA base GI POF link is limited to less than 4 Gb/s even when the index profile is optimum because of the large material dispersion⁴. In the case of the PMMA base GI POF, its refractive index profile can be controlled to have desired index exponent g by the interfacial-gel polymerization technique.¹ Experimental results of data transmission are plotted in Fig.2. A good agreement between the experimental values and theoretical curve was observed. Therefore, when the index profile is optimum in the PF polymer base GI POF (index exponent g should be 2.17), more than 10 Gb/s transmission in 1 km link can be expected.

References

1. Y. Koike, T. Ishigure, E. Nihei, *IEEE J. Lightwave Technol.*, **13**, 1475 (1995)
2. T. Ishigure, E. Nihei, S. Yamazaki, K. Kobayashi, and Y. Koike, *Electron. Lett.*, **31**, 467 (1995)
3. J. W. Fleming, *J. Am. Ceram. Soc.*, **59**, 503 (1976)
4. T. Ishigure, E. Nihei, and Y. Koike, *Appl. Opt.*, **35**, 2048 (1996)

Frequency conversion through cascaded second-order nonlinearities in the NPP organic crystal

G.P. Banfi, P.K. Datta, V. Degiorgio, G. Donelli, D. Fortusini

Dipartimento di Elettronica - Università di Pavia, Via Ferrata 1, 27100 Pavia, Italy

tel. (+39) 382 505208, fax (+39) 382 422583; e-mail: degiorgio@ipvsp4.unipv.it

J.N. Sherwood, Department of Pure and Applied Chemistry, University of Strathclyde, Glasgow, UK

In this paper we describe an experiment of frequency conversion through two cascaded second-order processes [1] in an organic crystal of N-(4-nitrophenyl)-(L)-prolinol (NPP).

The most attractive feature of NPP is its large usable quadratic nonlinearity. The growth and linear/nonlinear optical properties of NPP are described in Refs. 2-5. The large birefringence of NPP in the xz plane allows a wide phase-matching range and even non-critical phase-matching at 1.15 μm , but it decreases the angular acceptance.

Our sample is 3mm-thick along the normal to the cleavage plane (101). One side of the cleavage plane is left as grown while the other face is mildly polished. Actually the polishing decreased the quality of the surface which scatters more than the unpolished face.

We first investigated the quality of our crystal against the published data through second harmonic generation experiments, by using as a source an optical parametric oscillator (OPO). The OPO, pumped by a frequency-doubled mode-locked Nd:YAG laser, generates 30 ps pulses and is tunable from 0.8 to 1.3 μm . Our data on the wavelength dependence of the phase matching angle are in good agreement with the results of Ref. 2, while they show some discrepancy with the predictions based on the Sellmeier equations using the coefficients given in Ref. 3 (Fig 1). We also found that the dielectric z axis is not exactly perpendicular to the cleavage plane, but it forms an angle of about 2° with the cleavage face normal.

In the frequency conversion experiment two collinear beams at frequencies ω_a and ω_b interact to give an output beam at frequency $\omega_c = 2\omega_a - \omega_b$. The physical process consists of second-harmonic generation of the pump beam ω_a , followed by difference frequency generation $2\omega_a - \omega_b$. The overall effect can be described as a third-order process with an "effective $\chi^{(3)}$ " that for NPP is expected to be of the order of $10^{-16} \text{ m}^2 \text{ V}^{-2}$.

Pump and probe pulses are generated by two OPOs, both pumped by the second harmonic of the Nd:YAG laser. We chose the pump wavelength λ_a equal to 1.15 μm , in order to obtain non-critical phase-matching for SHG. The probe wavelength λ_b needs to be close enough to λ_a

to keep the phase mismatch for the overall process as small as possible, so we chose $\lambda_b=1.16 \mu\text{m}$. The generated signal is then at $\lambda_c=1.14 \mu\text{m}$.

Our preliminary data show a conversion efficiency from λ_b to λ_c of about 20%, using a peak intensity for the pump pulse of 30 MW/cm^2 . This efficiency is significantly higher than our former result on MBA-NP [1], but it is still below the value one might expect from the high nonlinearity of NPP. Experiments are in progress in order to determine more accurately the dependence of the conversion efficiency on pump intensity and on wavelength.

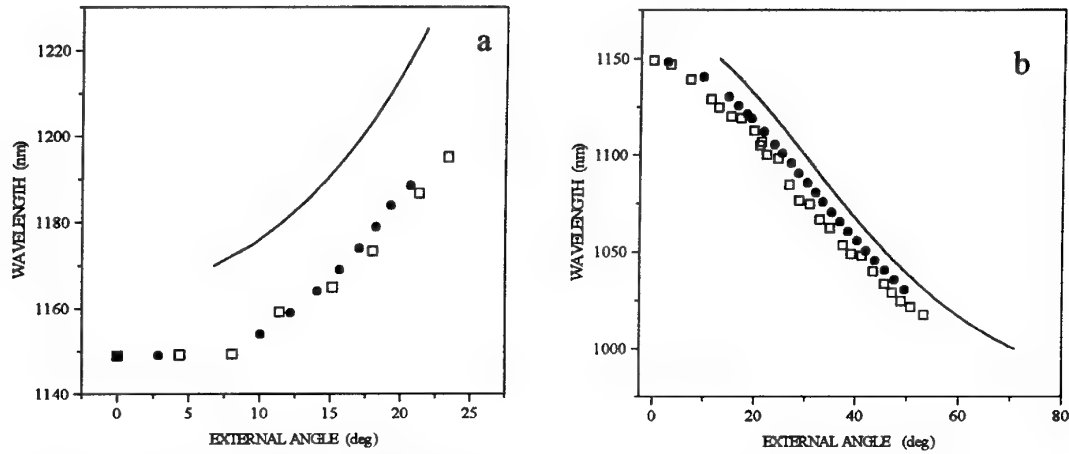


Fig. 1: dependence of the external type I phase-matching angle on wavelength;
a) generation in xz plane **b)** generation in yz plane.
 ●: our data; □: experimental data from Ref. 2; Lines: calculated data according to Ref. 3.

References

- 1) S. Nitti et al., Optics Commun. **106**, 263 (1994).
- 2) I. Ledoux et al, J. Opt. Soc. Am. B **4**, 987, (1987).
- 3) I. Ledoux et al, Optics Commun. **80**, 149, (1990).
- 4) S. X. Dou, et al, J. Opt. Soc. Am. B **10**, 1708, (1993).
- 5) B. Y. Shekunov et al, J. Phys. Chem. **99**, 7130, (1995).

Nonlinear optical effects in photorefractive $\text{Bi}_{12}\text{TiO}_{20}$ crystals with internal surface reflections

Erik Raita and Alexei A. Kamshilin

Väisälä Laboratory, Department of Physics, University of Joensuu,

Po Box 111, FIN-80101, Joensuu, Finland

Phone: +358-13-2513235; Fax: +358-13-2513290; E-mail: raita@cc.joensuu.fi

Thin and long (fiberlike) $\text{Bi}_{12}\text{TiO}_{20}$ (BTO) crystals have been intensively investigated for a few years since the experimental demonstration of the efficient double phase conjugation of mutually incoherent beams in such a crystal.¹ BTO samples, which have a length of about 10-mm and a rectangular cross-section of about 1mm^2 , have been initially proposed as a model for better understanding of the processes that would happen in a real fiber geometry. However, besides some superficial advantages over conventionally used bulk crystals, such as higher energy densities and longer interaction length, the single crystal fiberlike samples showed up some new optical phenomenons. This fact allows one to consider fiberlike crystals as a separate, advanced group of photorefractive materials. Indeed, all these new nonlinear effects including wide angular-band recording of efficient mutually-pumped phase-conjugators (MPPCs)¹, anomalously fast photorefractive response², highly efficient coherent amplification of weak optical signals³, phase coupling of laser-diodes⁴ etc. become possible because of the internal surface reflections, which are specific for fiberlike geometry.

In this report we present a review over the recent experimental results that we have obtained using fiberlike BTO crystals grown in our laboratory in Joensuu. The crystal-growth equipment developed at our department allows us to produce samples by using either the Laser Heated Pedestal Growth (LHPG) technique or the Czochralsky method. The presentation contains the recently published results as well as some new unpublished material. It shows that photorefractive devices based on fiberlike crystals are faster and more efficient compared with the bulk-crystal-based ones.

It is known that the efficient beam coupling in sillenite BSO-type crystals is only possible when an external electric field is applied to a sample. The theory says, the stronger field is applied, the higher coupling coefficient, but the slower response.⁵ This causes problems with bulk crystals because one needs to make a big change in external voltage to change a little the amplitude of applied field. Controlling the coupling efficiency of thinner fiberlike samples is much easier. Moreover, it turned out that the bulk-crystal theory is no longer valid for the crystals with the internal surface reflections since all the processes are affected by the nonlinear interaction of internally reflected scattering and the

incident light. After being internally reflected the scattered fanning beams interfere with the incident light and get self-diffracted on this new dynamic grating back towards the side surface. Finally, the light is self-confined near that surface generating a photorefractive surface waves.⁶

Up to now, the slow response of currently available photorefractive materials has been the main problem for their practical implementation. However, it may be overcome by exploiting the energy of the optical surface waves. It was shown that as much as 95% of the incident energy can be transferred to the surface waves.³ Such a remarkable energy concentration accelerates the photorefractive interaction between the light waves. Thus, the response time of the fanning effect diminishes significantly when the scattering is accompanied by the surface waves generation.⁶ We have used that fact to construct the fast MPPC, whose operating speed is 5 ms at its fastest and the response time is adjustable by changing the external voltage⁷. To the best of our knowledge, this is the fastest MPPC observed in photorefractive crystals under the cw pumping. Another way to exploit that energy is to use the surface waves as an energy source for the coherent amplification of weak signal beams. As high amplification gain as 16,000 has been obtained by coupling the signal beam and the photorefractive surface wave in the crystal measuring 0.8 mm x 3.0 mm x 20.0 mm.³

References:

- ¹ A. A. Kamshilin, R. Ravattinen, H. Tuovinen, T. Jaaskelainen, and V. V. Prokofiev, *Opt. Commun.* **103**, 221 (1993).
- ² A. A. Kamshilin, E. Raita, V. V. Prokofiev, and T. Jaaskelainen, *Appl. Phys. Lett.* **67**, 3242 (1995).
- ³ A. V. Khomenko, A. Garcia-Weidner, and A. A. Kamshilin, *Opt. Lett.* **21**, 1014 (1996).
- ⁴ A. A. Kamshilin, T. Jaaskelainen, V. V. Spirin, L. Y. Khriachtchev, R. Onodera, and Y. Ishii, "Laser-diodes injection locking with a double phase-conjugate mirror in photorefractive Bi₁₂TiO₂₀ fiberlike crystal under external alternating voltage," to be published in *J. Opt. Soc. Am. B*.
- ⁵ S. I. Stepanov and M. P. Petrov, *Opt. Commun.* **53**, 292 (1985).
- ⁶ A. A. Kamshilin, E. Raita, and A. V. Khomenko, *J. Opt. Soc. Am. B* **13**, 2536 (1996).
- ⁷ E. Raita, A. A. Kamshilin, V. V. Prokofiev, and T. Jaaskelainen, "Fast mutually pumped phase conjugation using transient photorefractive coupling", to be published in *Appl. Phys. Lett.*

Nonlinear optical and waveguiding properties of poly(*p*-phenylenevinylene) - poly(1-vinyl-2-pyrrolidone) (PPV-PVP) blends .

Anna Samoc, Marek Samoc and Barry Luther-Davies

Laser Physics Centre, Research School of Physical Sciences and Engineering
Australian Photonics Corporate Research Centre
The Australian National University, Canberra ACT 0200, Australia

This contribution addresses the problem of the availability of highly nonlinear third-order materials for all-optical switching in planar waveguides. π -conjugated polymers show large third-order nonlinearities in the femtosecond range. For example, the nonlinear figures of merit for poly(*p*-phenylenevinylene) (PPV) at 800 nm appear to be quite favourable : n_2 reaching $1 \times 10^{-11} \text{ cm}^2/\text{W}$, two-photon absorption losses $\beta=80 \text{ cm/GW}$ or less, the two-photon merit factor $T=\beta\lambda/n_2$ can be lower than unity [1]. The linear and nonlinear optical properties of PPV prepared by the precursor route depend strongly on the degree of conjugation achieved during conversion of the precursor polymer [2].

We present results of characterisation of a new optically nonlinear polymer system containing poly(*p*-phenylenevinylene) (PPV) and poly(1-vinyl-2-pyrrolidone) (PVP) abbreviated as PPV-PVP composite. Blends of PPV and PVP combine the excellent optical wave-guiding behaviour of polyvinylpyrrolidone with high third-order nonlinearity of poly(*p*-phenylenevinylene). A reduction of the band-gap and an enhancement of the fs nonlinear refractive index at 800 nm was observed in the films containing a low content of PPV.

The research was carried out on thin films prepared by spin-coating of solutions of the PPV precursor polymer mixed with a required amount of polyvinylpyrrolidone in a common solvent, subsequently converted to the composite at elevated temperatures in vacuum. The films were characterised with absorption spectra and refractive index measurements prior to the measurements of n_2 with degenerate four wave mixing at 800 nm.

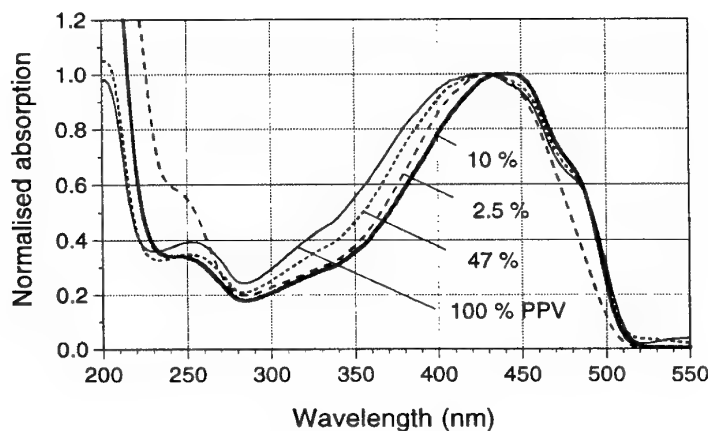


Figure 1. Absorption spectra of films of PPV-PVP composites converted at 150 °C.

We found a remarkable influence of the environment on properties of PPV in PPV-PVP composites. Figure 1 shows an enhancement of optical properties of PPV in the composites: the bathochromic shift and narrowing of the main absorption band in the less concentrated samples. This indicates that better conjugated structures can be built in the diluted system. The absorption coefficients increased with increasing concentration of PPV in a nonlinear way, see Figure 2a. The nonlinear refractive index followed a similar, saturation-like dependence as shown in Figure 2b. It tends

to saturate at higher PPV contents.

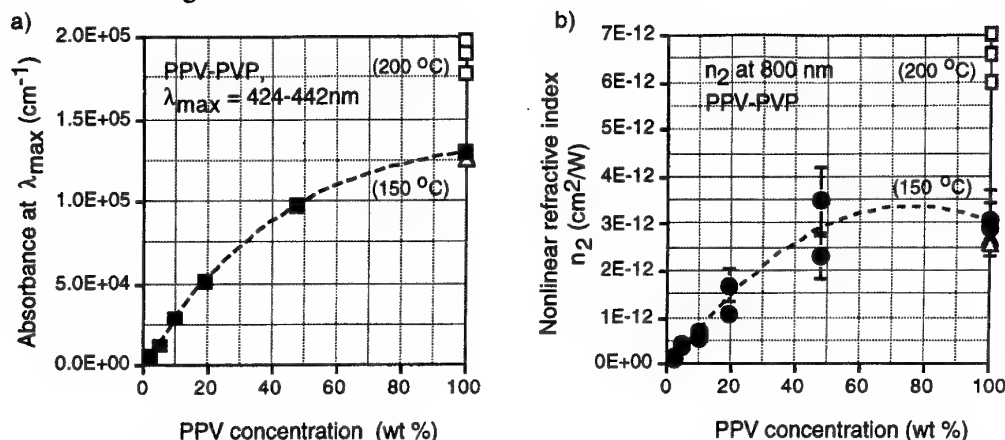


Figure 2. Maximum absorption (Figure 2a) and fs nonlinear refractive indices (Figure 2b) in the films of PPV-PVP composites converted at 150 °C for 2+3 hours and in several samples of neat PPV converted at 200 °C for 1+2 hours, all in vacuum.

PPV-PVP films are birefringent, indicating anisotropic ordering of rigid-rod PPV molecules. TE and TM refractive indices of the films of composites depend on PPV concentration and the temperature of conversion, as shown in Figure 3.

Our focus has been to obtain low loss PPV waveguides. The linear optical losses in the neat PPV waveguides are high. On the other hand, PVP films exhibit excellent waveguiding. Total losses measured at 632.8 nm and 810 nm in films of PPV-PVP composites were anisotropic and wavelength dependent. They increased with the PPV concentration and depended on the temperature used for the film conversion as in the examples shown in Figure 4.

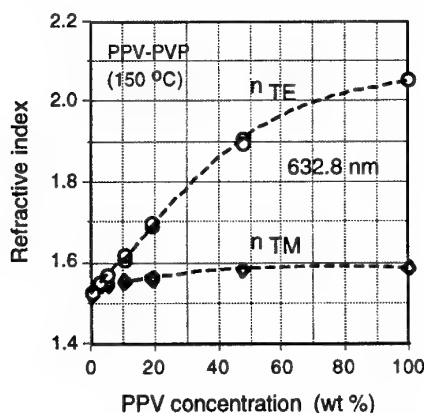


Figure 3. Anisotropy of refractive indices in the films of PPV-PVP blends converted at 150 °C for 2+3 hours in vacuum.

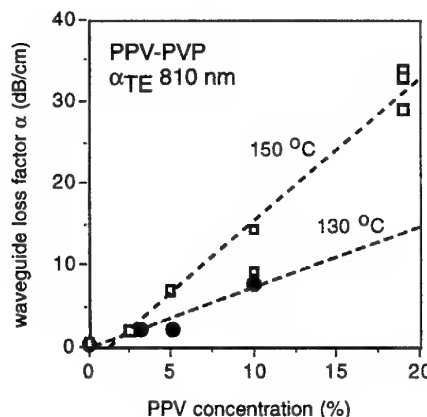


Figure 4. Waveguide total losses in PPV-PVP films depend on the content of PPV and temperature of conversion.

The origin of optical losses in PPV composites will be discussed.

1. A. Samoc, M. Samoc, M. Woodruff and B. Luther-Davies, Tuning the properties of poly(*p*-phenylenevinylene) for use in all-optical switching. *Optics Letters*, **20**, 1241 (1995).
2. A. Samoc, M. Samoc, B. Luther-Davies and M. Woodruff, Poly(*p*-phenylenevinylene) - an attractive material for photonics applications. Chapter in: *Electrical and Optical Polymers*. ed. by D.L. Wise, D.J. Trantolo and G.E. Wnek, World Scientific, in press.

Nonlinear parameters of bulk InGaAsP photonic devices

François Girardin, Stephan Pajarola and Georg Guekos

Institute for Quantum Electronics, Swiss Federal Institute for Technology, CH-8093 Zurich, Switzerland.
email: girardin@iqe.ethz.ch

It is now well known that nonlinearities in semiconductor material may limit the high-speed dynamics of associated active devices. The underlying physical effects, however, can be used for specific functions such as optical bistability and wave-mixing. Among the various parameters introduced in the modelling to describe the nonlinear behavior the phase-amplitude coupling factor α , and the gain suppression coefficient ϵ play an important role. In this contribution we report on measurement results of these two parameters in bulk InGaAsP/InP optical amplifiers and lasers. The studied devices are ridge waveguide structures designed for being polarization insensitive in the operation wavelength range around 1.55 μm .

The phase-amplitude coupling factor α is defined as the ratio of the real to the imaginary part of the susceptibility. This leads to both FM and AM modulation of the optical field when modulating the injection current. It has been shown that the ratio $\frac{\beta}{m}$ of the FM to AM modulation index can be expressed as [1]:

$$\left| \frac{\beta}{m} \right| = \frac{|\alpha|}{2} \sqrt{1 + \left(\frac{\Omega_c}{\Omega} \right)^2}, \text{ where } \Omega_c = \frac{\epsilon S}{\tau_p}. \quad (1)$$

Here, Ω is the modulation frequency and Ω_c the corner frequency, S is the photon density and τ_p the photon lifetime. From the measurement of $\frac{\beta}{m}$ for different modulation frequencies, the parameters α and ϵ can be derived. At high modulation frequencies ($\Omega \gg \Omega_c$) expression (1) simplifies to $|\alpha| = 2|\beta/m|$. In the setup, the laser output is fed into an interferometer containing an acousto-optic modulator and a delay line and is analyzed on a spectrum analyzer. In the frame of this work two semiconductor optical amplifiers (SOA) of different length and an external cavity laser (ECL) fabricated in our group were investigated.

SOA: The FM and AM responses have been measured separately at the frequency of 5 GHz; the interferometer has been used to measure β . The index m has been measured by monitoring the optical power with an oscilloscope. The injected CW currents are 200 and 650 mA for the 500 and 1500 μm long device, respectively. As can be seen in Figure 1, α increases with wavelength as it has been theoretically calculated [2]. On the other hand, the obtained values (around 6 and 12 at gain peak) are high compared to theoretical calculations in bulk InGaAsP materials [2]. Moreover an increase of α with the length of the device has been found. This can be due to a higher population inversion in the long device where the ridge is narrower than in the other. The influence of the strong non-uniformities present in the long devices may lead to an increase of the effective α [3]. The most popular models for active semiconductor devices are derived from the density matrix formalism; rate equations are calculated for the different quantities [4]. In most of the cases α is considered as a constant [5]. In the case of SOA modelling, and particularly for wavelength conversion where the considered wavelength range is very large, this point becomes critical. Moreover in wavelength conversion by four-wave mixing in SOAs α is one of the key parameters.

ECL: A 500 μm long device, one facet AR-coated, was used in an external cavity configuration [6]. The technique employed for the determination of β/m is based on the one described in [7]. The data from measurements for different injection currents were separately fitted to the expression (1). Fig. 2 shows the derived gain saturation coefficient, ϵ for different power levels. The obtained values are in the upper range of those reported in the literature [8]. An unexpected [9] increase of ϵ for output powers over 2.3 mW is observed. This behavior cannot be explained by taking only the spectral hole-burning into account. An analysis of the other sources of gain suppression, such as carrier heating, may give an explanation of this behavior. Those points will be addressed in the presentation. This suggests that the influence of gain saturation cannot be neglected even for moderate power levels of a few mW.

Conclusion: We have measured an unusual behavior of two important nonlinear parameters, the phase-amplitude coupling factor and the gain suppression coefficient in 1.55 μm bulk InGaAsP/InP devices.

These measurements suggest that a precise modelling required for the development of new devices should include the nonlinear effects in a more accurate form as the usual one.

REFERENCES

- [1] M. Osinski and J. Buus, "Linewidth broadening factor in semiconductor lasers : an overview", *IEEE J. Quantum Electron.*, **23**, 9-28, 1987.
- [2] W.W. Chow, S.W. Koch, and M. Sargent III, *Semiconductor-laser physics*, chap. 5, Springer-Verlag, 1994.
- [3] F. Girardin, G-H. Duan, and P. Gallion, "Linewidth rebroadening due to nonlinear gain and index induced by carrier heating in strained quantum-well", *IEEE Photon. Technol. Lett.*, **8**, 334-336, 1996.
- [4] G. P. Agrawal and N. K. Dutta, *Long wavelength semiconductor lasers*, Van Nostrand Reinhold, New York, 1986.
- [5] A. Mecozzi, "Analytical theory of four-wave mixing in semiconductor amplifiers", *Opt. Lett.*, **19**, 892-894, 1994.
- [6] S. Pajarola, G. Guekos, and J. Mørk, "Optical generation of millimeter-waves using a dual polarization emission external cavity diode laser", *PTL*, **8**, 157-159, 1996.
- [7] H.I. Mandelberg, R.D. Grober, and P.A. McGrath, "Frequency and amplitude modulation in extended cavity diode lasers", in *OFC/IOOC'87*, number WC4, 1987.
- [8] J. Huang and L.W. Casperson, "Gain and saturation in semiconductor lasers", *Opt. and Quantum Elec.*, **25**, 369-390, 1993.
- [9] H. Li, "RF-modulation measurement of linewidth enhancement factor and nonlinear gain of vertical-cavity surface-emitting lasers", *IEEE Photon. Technol. Lett.*, **8**, 1594-1596, 1996.

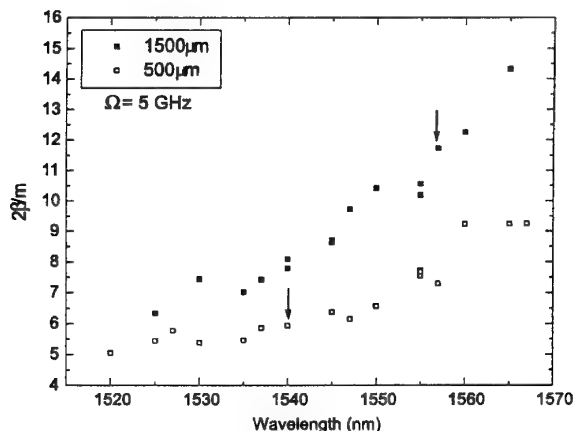


Fig. 1. $2\beta/m$ versus wavelength for two different SOAs. The arrows denote the gain peak of the SOAs.

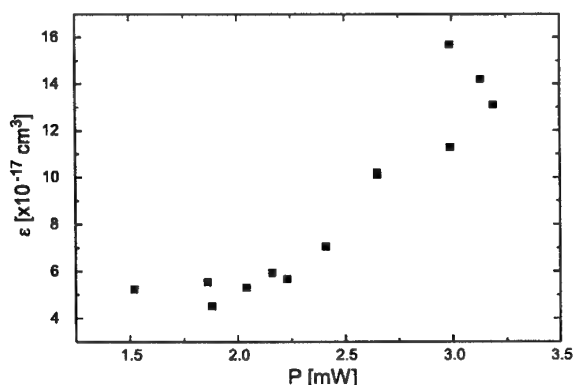


Fig. 2. Gain suppression coefficient as a function of the emitted power of the external cavity laser diode.

PHOTOREFRACTIVE PROCESSES IN H:LiNbO₃

M. Carrascosa and F. Agulló-López

Dept. Física de Materiales, Universidad Autónoma de Madrid
Cantoblanco, 28049 Madrid

Most LiNbO₃ crystals contain an appreciable amount of H doping. This contents can be easily enhanced by heating the crystal in a water vapor atmosphere or under a hydrogen flow¹. It is now well recognized that these protons have a strong influence on photorefractive (PR) recording and erasure processes and are dramatically relevant at high temperatures (100- 300 °C). In particular, protons can be used to fix or stabilize the recorded electronic holograms versus subsequent illumination by neutralizing or screening the electronic space-charge field². This process is very relevant for permanent storage applications where a very large number of read-outs have to be performed without erasing the recorded information.

In this communication the experimental and theoretical situation concerning the photorefractive kinetics in H:LiNbO₃ will be reviewed. First, the available information on the various physical and transport parameters for this material will be critically evaluated. Then, rate equations involving both electrons and protons, previously worked out by Carrascosa and Agulló-López³, will be reformulated in a simpler nomenclature. The following relevant physical situations have been then discussed within that model:

a) Grating recording at high temperature (i.e. grating fixing). In particular, the dependence of the steady-state space-charge field on temperature and grating vector has been worked out. Coupling gain and noise reduction effects will be, then, analyzed in the light of recent experimental work.

b) Kinetics of grating developing with homogeneous illumination at RT. The role of the various physical parameters will be discussed. Moreover, the problem of the life-time of the developed gratings in the dark will be addressed.

c) A new method of selective developing using a sinusoidal illumination pattern will be proposed and discussed. Its advantages with regard to the standard homogeneous illumination will be remarked.

Finally, the limitations of the used model and some suggestions for future work will be put forward.

REFERENCES

1. J.M.Cabrera, J.Olivares, M.Carrascosa, J.Rams, R.Müller and E.Dieguez, Adv. Phys.45,349 (1996).
2. A.S.Kewitsch, A.Yariv and M.Segev, in *Photorefractive effects and materials*, D.D.Nolte de., Kluwer Academic Publishers. Boston, 1995, pp.173-216.
3. M.Carrascosa and F.Agulló-López, J.Opt.Soc.Am.B7,2317 (1990).

**PHOTOREFRACTIVE NONLINEAR OPTICS :
MATERIALS AND APPLICATION TO INFORMATION PROCESSING AND
LASER BEAM CONTROL**

J-P. Huignard, H. Rajbenbach, A. Brignon

Thomson-CSF, Laboratoire Central de Recherches
Domaine de Corbeville,
91404 Orsay Cedex (France)

Summary

Photorefractive crystals are a particular class of nonlinear materials which are of great interest for several applications in coherent optics. First, the material exhibits a photoinduced index modulation when illuminating with CW or pulsed laser light ; second, the process involves the formation of a space charge field : the mechanism has no threshold effect and the response time scales as the inverse of the incident beam intensity on the crystal. Today a large variety of crystal now exist and have been used for laboratory experiments in the visible and in the near Infrared with both ferroelectric oxydes and semiconductors. We will emphasize in this talk recent results achieved with materials like Rh-BaTiO₃⁽¹⁻²⁻³⁾ and Sn₂P₂S₆⁽⁴⁾ which operate at the Nd-YAG laser wavelength $\lambda = 1.06 \mu\text{m}$. Gain coefficients, respectively $\Gamma \approx 10 \text{ cm}^{-1}$ for BaTiO₃ and $\Gamma = 5 \text{ cm}^{-1}$ for SPS are now obtained with high power CW lasers. Other specific characteristics of these crystals will be reviewed and compared gain and response time for CW and pulse operation, spatial frequency response, probe beam amplification versus input pump intensity. We present recent results achieved at TH-CSF / LCR with an infrared sensitive crystals Rh-BaTiO₃ applied to the phase conjugation of a Q-switched Nd-YAG-MOPA configuration operating at $\lambda = 1.06 \mu\text{m}$ ⁽⁵⁾. Because of the high gain of this crystal we operate in the self pumped geometry thus allowing to demonstrate a compact and all solid state phase conjugate laser. We achieve a phase conjugate reflectivity of 32 % (55 % in CW) with good fidelity and response time of several minutes. In this experiment, a maximum output energy of 65 mJ for an input energy of 25 μJ is measured using a four-pass arrangement in the amplifier. Alternatively, we also present two-wave coupling in Rh-BaTiO₃ to clean up the beam of CW Nd-YAG lasers : the clean signal beam is amplified without bearing any phase information from the strongly aberrated pump beam. Beside their application to laser beam control, photorefractive crystals also open attractive perspectives for parallel information processing of 2D analog images⁽⁶⁾. We illustrate these capabilities in a compact optical correlator which operates in the visible ($\lambda = 530 \text{ nm}$) in a joint Fourier transform configuration with a

photorefractive BSO crystal. The capabilities of this processor for performing pattern recognition at several thousand correlations per second are discussed and presented.

To conclude, the field of photorefractive nonlinear optics continues to progress and very significant new results have been recently demonstrated. Growing better materials with optimized dopant concentration is still one of the major objective for the research labs in particular for operation in the infrared wavelengths ($\lambda = 0.8 \mu\text{m}$ to $1.5 \mu\text{m}$). Also, there is now as strong interest for applications to phase conjugation and clean-up of pulsed or CW lasers : Photorefractive materials open attractive features for the realization of solid state near IR lasers which may operate at high average powers.

References :

1. M. Kaczmarek and R.W. Eason, Opt. Lett. **20**, 1850 (1995).
2. A. Brignon, J-P. Huignard, M. H. Garrett and I. Mnushkina, Opt. Lett. **22**, 215 (1996).
3. N. Huot, J. M. C. Jonathan, G. Pauliat, D. Rytz and G. Roosen, Opt. Comm. **135**, 133 (1997).
4. S. G. Odulov, A. N. Shumelyuk, G. A. Brost and K. M. Magde, Appl. Phys. Lett. **69**, 3665 (1996).
5. A. Brignon, J-P. Huignard, M. H. Garrett and I. Mnushkina, to be published in Opt. Lett. **22**, (1st April, 1997).
6. H. Rajbenbach et al., Proc. SPIE, 2752-214 (1996).

Materials for Nonlinear Singular Optics

M.S.Soskin and M.V.Vasnetsov
Institute of Physics, National Academy of Sciences of Ukraine
Prospect Nauki 46, Kiev-22, 252650 Ukraine

Singular optics is a new branch of modern optics studying phase singularities of light waves. Light interaction with nonlinear media causes phase distortions which create phase defects on an initially smooth wavefront, thus producing "optical vortices". Physical background and review of main results in nonlinear singular optics are presented. The requirements to materials for nonlinear singular optics are discussed.

Photorefractive properties of infrared sensitive rhodium doped BaTiO₃ processed in different conditions

M. Kaczmarek, R.W. Eason, G. Maatz
Optoelectronics Research Centre
University of Southampton
United Kingdom

M.H. Garrett
Nonlinear Photonics, Morgan Hill, CA
U.S.A.

I. Mnushkina
Deltronic Crystal Industries, N. J.
U. S. A.

Rhodium doped BaTiO₃ has interesting photorefractive properties which enable us to observe high phase conjugate reflectivities [1,2] and signal amplification [3] both in the visible and the near-infrared. The aim of current investigations of Rh:BaTiO₃ is to determine both the optimum dopant concentration, and processing conditions to improve the performance and the speed of this photorefractive crystal above 1 μm [4]. We have investigated lightly doped with rhodium (400 ppm) BaTiO₃, annealed in different conditions.

The three Rh:BaTiO₃ crystals we studied - as-grown, annealed in oxygen and annealed in air - came from the same boule and were post-processed separately. Firstly, we measured the actual concentration of rhodium in our samples via mass spectroscopy. The results showed that there was only 2-4 ppm of rhodium in crystals grown from the 400 ppm of rhodium in the melt. This gives a 0.005-0.01 segregation coefficient. For comparison, we performed mass spectroscopy on our original blue, rhodium doped BaTiO₃ [1,3] and measured approximately 14 ppm of rhodium in this crystal. These results indicate that only very little of this purposely added dopant ends up in the crystal and the rest of the rhodium is most likely alloying with the crucible. In spite of that, changes in the photorefractive performance of Rh:BaTiO₃, versus nominally undoped BaTiO₃ are quite pronounced. Hence, it is important to investigate further the presence and importance of other dopants and impurities, as well as the significance of secondary centres, the topic which is still not well researched.

Secondly, we compared absorption spectra of our three samples. In general, the as-grown sample and the annealed in oxygen sample had very similar spectrum, while the absorption of the crystal annealed in air was much lower. For example, in the visible (645 nm), the as-grown sample had $\alpha=1.43\text{ cm}^{-1}$, the annealed in oxygen crystal was 1.36 cm^{-1} , and the annealed in air sample had only 0.34 cm^{-1} . This difference in absorption comes from different concentration of oxygen fixed during annealing. The oxygen annealed sample was processed in pure oxygen and then quenched to fix the oxygen concentration. This oxidising atmosphere would increase the relative number of Rh⁴⁺ (versus Rh³⁺). Annealing in air, at 1000°C, provides much lower oxygen concentration and effectively reduces the crystal. As a result, the absorption decreases [4] and, if conditions are right, the effective number of traps increases.

We continued studies of absorption of Rh:BaTiO₃ crystals by investigating the effect of light intensity on the magnitude of absorption. Change (induced transparency or induced absorption) usually indicates the presence of secondary photorefractive centres. Measuring this effect in 400 ppm Rh:BaTiO₃ crystals showed that the induced change is very small (less than 0.1 cm^{-1} at 647 nm and less than 0.2 cm^{-1} at 514.5 nm). This result is quite different from the one we obtained earlier from the original blue Rh:BaTiO₃ which showed pronounced light-induced transparency at visible wavelengths ($\Delta\alpha=0.9\text{ cm}^{-1}$ at 647 nm) and light-induced absorption in the near-infrared.

The photorefractive performance of 400 ppm crystals was also investigated via self-pumped phase conjugation. The reflectivity of self-pumped phase conjugation reached 50% at 514.5 nm crystal and was

stable, unlike in the original blue Rh:BaTiO₃. However, this promising magnitude of reflectivity could only be achieved at the peak absorption (514 nm) and no phase conjugation was observed above 750 nm. High reflectivities (up to 76% in the near-infrared) achieved in the original blue Rh:BaTiO₃ would suggest that having a higher rhodium concentration, and hence a higher absorption, is essential for efficient SPPC. However, so far, it is not clear that higher SPPC reflectivities are simply proportional to dopant concentration, especially as the problem of writing a SPPC grating and providing an optimum feedback to form such a grating is not a straightforward.

We also used two-beam coupling method to compare the three samples of Rh:BaTiO₃. The annealed in oxygen sample showed some finite beam coupling at 514.5 nm, smaller than the as-grown sample. However, no significant coupling was observed at near-infrared wavelengths. The annealed in air sample proved to be quite interesting, as processing seemed to reduce the crystals in such a way that it showed very little coupling. One could speculate that annealing could have brought the crystal close to the compensation point. The as-grown crystal responded the best at wavelengths from visible to the near-infrared. Efficient coupling (14.9 cm⁻¹ at 514.5 nm) was observed in the visible, and also at the near-infrared (10.2 cm⁻¹ at 800 nm). However, the considerable gain achieved at 1 μ m (6.8 cm⁻¹) is particularly interesting (Table 1) and promising, especially when taking into account the very low absorption at this wavelength. In fact, the original blue Rh:BaTiO₃ also showed high coupling at 1.06 μ m, despite low absorption. This raises the possibility of achieving finite beam coupling at the important communication wavelengths of 1.3 and 1.5 μ m [5].

Table 1

Crystal	original blue Rh:BaTiO ₃	as-grown 400 ppm Rh:BaTiO ₃
Wavelength	1064 nm	1000 nm
Coupling coefficient	11.2 cm ⁻¹	6.8 cm ⁻¹
Absorption coefficient	0.06 cm ⁻¹	0.05 cm ⁻¹

The results of our experiments 400 ppm Rh:BaTiO₃ crystals confirm earlier findings by Wechsler et al. [4] which showed that reducing a crystal improves the strength of its photorefractive effect. We have decided to investigate the possibility of changing further the reduction ratio and increasing the speed of photorefractive response via ion-implantation. Implantation with high energy hydrogen ions produces planar photorefractive waveguides. Photorefractive properties of these waveguides are different than that of a bulk material, and the photorefractive response time is shorter due to high intensity of light confined in a waveguide. We have implanted the annealed in air sample, aiming to modify its photorefractive properties, hopefully moving away from the compensation point state to more reduced conditions. The initial measurements, however, showed no significant improvement in beam coupling efficiency after ion-implantation. We intend to pursue this project further, implanting the annealed in air crystal with higher doses of hydrogen ions.

We also plan to investigate the ability for efficient beam coupling of 400 ppm Rh:BaTiO₃ further in the infrared and study other, more heavily doped with rhodium, BaTiO₃ crystals. Furthermore, the experimental evidence of efficient coupling, observed in the range of wavelengths where the crystals' absorption was negligible, requires a suitable model.

References

- [1] G. W. Ross, P. Hribek, R. W. Eason, M. H. Garrett, D. Rytz, *Opt. Comm.* **101**, 60 (1993).
- [2] B. A. Wechsler, M. B. Klein, C. C. Nelson, R. N. Schwartz, *Opt. Lett.* **19**, 536 (1994).
- [3] M. Kaczmarek, R. W. Eason, *Opt. Lett.* **20**, 1850 (1995).
- [4] B. A. Wechsler, G. D. Bacher, C. C. Nelson, M. B. Klein, S. MacCormack, J. Feinberg, *Nonlinear Optics Conference, Hawaii, July 1996*.
- [5] M. Horowitz, B. Fischer, Y. Barad, Y. Silverberg, *Conference on Lasers and Electro-Optics CLEO'96, Anaheim, May 1996, paper CFA7*.

The Growth, Perfection and Structural Properties of Organic Electro-Optic Crystals

John N Sherwood,
Department of Pure and Applied Chemistry,
University of Strathclyde,
Glasgow, G1 1XL,
Scotland, UK

The realisation that the basis of the non-linear optical properties of molecular systems lies in the properties and structure of the molecules has led to the design of a wide range of materials, some of which show superlative performance. Despite this attraction no organic crystalline solid has found regular application in operational devices. The principal reason for this is that, in general, the quality of materials produced routinely is low. Due to this and their mechanical nature, organic materials are believed to be less suitable for device preparation than are inorganic materials. Added to this is the belief that they are less amenable to preparation in other formats, e.g. thin films than their inorganic counterparts.

In later years our studies of the preparation of these materials have been directed both towards the solution of these problems and to a better understanding of the relationships between optical properties and structural behaviour.

Structural Perfection

The principal problem in obtaining high structural and hence optical perfection are the high supersaturations needed to produce reasonable sized crystals in short time periods. These lead to the regular development of inclusions in the sample no matter what technique is used for their preparation. The situation is made worse by the anisotropy of growth characteristic of these highly polar materials. This can lead to zero growth in some directions under conditions which would give good quality growth in others.

Such problems can only be overcome through careful kinetic assessment of the growth process to define growth conditions for which the best growth can occur.

Through such studies, single crystal specimens of bulk and thin film crystals can be prepared of high structural and optical perfection.

Mechanical Strength

The low mechanical strength of these materials is the next major limiting factor to their use. This can manifest itself in two ways:

1. The structural integrity of the material and its amenability to cutting and polishing.
2. The resistance of the material to damage from interaction with the incident radiation beam.

To improve the first, it is essential to develop a design capability which increases the inter-molecular forces in the system whilst maintaining both the non centro-symmetric nature of the crystal and its efficiency. The often used method of increasing the degree of inter-molecular hydrogen bonding is unlikely to achieve this. Most of the more efficient systems are considerably hydrogen bonded anyway and even those which are highly so, e.g. urea, are still soft and low melting.

A more subtle approach is needed for altering the shape and packing of the molecules to yield a more compact and strongly bonded structure. To define the basic rules of such changes we have investigated the "adjustment" of the substituents of a chosen material, MBANP. We have succeeded in producing related materials of similar or greater efficiency but considerably higher melting and of a much greater hardness. The changes point to ways in which other molecules may be similarly re-configured. It is interesting to note that another improvement is that such materials become more easily and perfectly crystallised.

The radiation hardness of organic materials is known to be high but variable due no doubt to the perfection achievable. Damage thresholds greater than GW/cm^2 are regularly quoted. Our studies of this phenomenon in high quality crystals reveal that this is defined by two factors; provided that one remains outside of the absorption edge; the mechanical nature of the material and the anisotropy of thermal expansion and thermal conductance. Assessment of these properties and their relationship to molecular and crystal structure again show how improved molecular design can lead to improved performance.

**Nonlinear optical properties of KTP
and its arsenate isomorphs KTA, RTA and CTA**

B. Boulanger, J.P. Fève and G. Marnier

Laboratoire de Physique de l'Université de Bourgogne, UPRESA-CNRS 5027

UFR des Sciences et Techniques, BP 400, 21011 DIJON Cedex

KTiOPO₄ (KTP) is an efficient nonlinear optical material used in numerous laser devices. In particular KTP is a privileged crystal for Second Harmonic Generation (SHG) of 1.064 μm Nd:YAG lasers because this interaction is phase-matched in a direction with a small walk-off angle, $\rho = 0.27^\circ$, a non negligible figure of merit, $d_{\text{eff}}^2/n^3 = 1 \text{ pm}^2\text{V}^{-2}$ [1], and a very weak absorption, around $1\%\text{cm}^{-1}$ at 0.532 μm and $0.1\%\text{cm}^{-1}$ at 1.064 μm [2]. That leads for example to the generation of about 100 W average power at 0.532 μm from a Q-switched Nd:YAG laser emitting 210 W at 1.064 μm (2.5 kHz, 30 ns) [3]. KTP is also phase-matched for sum- and difference-frequency mixing over a broad range, from 0.4 μm to 4 μm [4]. It is then an attractive crystal for Optical Parametric Amplification (OPA) and Oscillation (OPO), with for example the generation of 30 mJ at 1.58 μm , for eye-safe applications, from an angular non-critical OPO pumped at 1.064 μm (10Hz, 19.5 ns) [5].

The occurrence of a photo-chromic damage, called gray-track, limits the use of KTP in high power applications. Gray-tracking is essentially observed during 1.064 μm SHG, and it has been shown that it is only due to a non-linear absorption of the Second Harmonic beam, for peak intensity greater than 80MWcm^{-2} at 0.532 μm at 10 Hz [6]. Furthermore, the gray-tracking "threshold" peak intensity is a decreasing exponential function of the repetition rate of the laser, but the corresponding average intensity remains constant, around 16kWcm^{-2} [7].

KTP belongs to the non-centrosymmetric orthorhombic mm2 point group, with the space group Pna2₁. The origin of its quadratic non-linearity is attributed to the short Ti-O bonds ($\approx 1.74 \text{ \AA}$) in the strongly distorted TiO₆ octahedra [8]. KTP is one compound of the isostructural titanyl family MTiOXO₄. This structure is of prime interest in nonlinear optical materials engineering because it allows to keep quadratic nonlinear optical properties with the ability to modify the birefringence, and so to tune the phase-matching directions by substitution on the M or X sites [9]. The arsenate isomorphs (X \equiv As) are transparent until 5.3 μm instead of 4.5 μm for the phosphate compounds [10]. They are attractive for applications in the near infra-red, because their transparency is increased in comparison with the phosphate compounds which are less efficient above 3 μm because of a strong absorption.

KTiOAsO₄ (KTA), RbTiOAsO₄ (RTA), and the caesium compound CsTiOAsO₄ (CTA), which has been invented by us [11], are considered here. Each of these crystals covers entirely the 3 - 5 μm range by difference frequency mixing pumped in the visible range. 1.32 μm type II phase-matched SHG clearly shows that the arsenate compounds are complementary to each others. The figure of merit and the walk-off angle of KTA and CTA are ($1.23 \text{ pm}^2\text{V}^{-2}$, 2.35°) [12] and ($0.235 \text{ pm}^2\text{V}^{-2}$, 0.45°) [13] respectively. CTA gives a better SHG conversion

efficiency than KTA for strong focusing conditions: $w_0 < 14 \mu\text{m}$ for $L = 1\text{mm}$, $w_0 < 71 \mu\text{m}$ for $L = 5 \text{ mm}$ and $w_0 < 142 \mu\text{m}$ for $L = 10 \text{ mm}$ (w_0 is the $1/e^2$ beam waist radius and L is the crystal length); for larger beam radii, the aperture function does not compensate the nonlinearity which leads to a smaller efficiency for CTA. Then the choice of the most efficient crystal for a given interaction must take into account the pump beam geometry and the crystal volume of good optical quality which it is possible to grow. The study of RTA is currently performed in our laboratory by the sphere method for both phase-matching directions and quadratic nonlinear coefficients measurements. This method was initially devoted to phase-matching studies [1,14] and we have recently shown the ability of this method for the measurement of the absolute magnitude of the SHG effective coefficient with an accuracy of 10 % in a KTP crystal cut in a sphere [15].

KTP and its isomorphs have also electrooptical properties. They are used as Pockel's cell: for example, RTA has an half wave voltage of 2.7 kVcm^{-1} [16].

All these materials can be processed for waveguide optics by ion-exchange, K-Rb for example [17], or by Liquid Phase Epitaxy [18]. It is then possible to fabricate segmented waveguides for the Quasi-Phase-Matching [17].

- [1] B. Boulanger, J.P. Fève, G. Marnier, B. Menaert, X. Cabirol, P. Villeval and C. Bonnin, J. Opt. Soc. Am. B/Vol.11, No.5, pp750-757 (1994).
- [2] J. Mangin, A. Khodjaoui and G. Marnier, Phys. Stat. Sol. (a)120, pp111-120 (1990).
- [3] S. Velsko, C. Ebberts, B. Comaskey, G. Albrecht and S. Mitchell, ASSL, AME2-1, pp63-65 (1994).
- [4] J.D. Bierlein and H. Vanherzeele, J. Opt. Soc. Am. B/Vol. 6, No. 4, pp622-633 (1989).
- [5] G.A. Grabon, W.L. Moon, G. Witt and L. Jones, SPIE, vol.2145, pp299-308 (1994).
- [6] B. Boulanger, M.M. Fejer, R. Blachman and P.F. Bordui, Appl. Phys. Lett. 65 (19), pp2401-2403 (1994).
- [7] J.P. Fève, B. Boulanger, G. Marnier and H. Albrecht, Appl. Phys. Lett. 70 (3), pp1-3 (1997)
- [8] N.K. Hansen, J. Protas and G. Marnier, C. R. Acad. Sci. Paris 307(II), pp475 (1988).
- [9] L.T. Cheng and J.D. Bierlein, SPIE, vol. 1863, pp43-53 (1993).
- [10] J. Mangin, G. Marnier, B. Boulanger and B. Menaert, Institute of Physics Conference Series N°.103, Part 1, pp65-67. Bristol: Institute of Physics (1989).
- [11] G. Marnier, B. Boulanger and B. Menaert, J. Phys. : Condens. Matter 1, pp5509-5513 (1989).
- [12] B. Boulanger, G. Marnier, B. Menaert, X. Cabirol, J.P. Fève, C. Bonnin and P. Villeval, Mol. Cryst. Lid. Cryst. Sci. Technol. - Sec. B: Nonlinear Optics, vol. 4, pp133-142 (1993).
- [13] B. Boulanger, J.P. Fève, G. Marnier, G.M. Loiacono, D.N. Loiacono and C. Bonnin, IEEE J. Quantum Electron, to appear in 1997.
- [14] G. Marnier and B. Boulanger, Optics Commun., vol. 72, n° 3-4, pp139-143 (1989)
- [15] B. Boulanger, J.P. Fève, G. Marnier, C. Bonnin, P. Villeval and J.J. Zondy, J. Opt. Soc. Am. B, to appear in 1997.
- [16] R.A. Stolzenberger, D.N. Loiacono and J. Rottenberg, CLEO'94, CFF2, p415 (1994).
- [17] F. Laurell, J.B. Brown and J.D. Bierlein, Appl. Phys. Lett. 60(9), pp1064-1066 (1992).
- [18] G. Marnier, French patent n° 2609976 (1986) and US patent n° 4746396 (1988).

Noncollinear phase matching in nonlinear crystals: New prospects for pulsed optical parametric oscillators

R. Urschel, G. Anstett, U. Bäder, A. Borsutzky, and R. Wallenstein

Fachbereich Physik, Universität Kaiserslautern, 67653 Kaiserslautern, Germany

Abstract

Noncollinear phase matching in nonlinear crystals offers a variety of advantages for the design and the performance of pulsed optical parametric oscillators. We report on the influence of noncollinear phase matching on the bandwidth, the tunability, the conversion efficiency and the beam profile of Nd:YAG laser pumped ns OPOs. New advantageous aspects like adjustable bandwidth (in the range of 0.1 nm - 30 nm), homogeneous spatial beam profile (almost TEM₀₀) and improved conversion efficiencies (by up to a factor of 5) predicted by numerical simulations are confirmed by experimental investigations.

Second - Order Nonlinear Optical Properties of $\text{Na}_2\text{SeO}_4 \cdot \text{H}_2\text{SeO}_3 \cdot \text{H}_2\text{O}$ Crystal

Marie May^a, Solange Debrus^a, Julien Venturini^a, Jan Baran^{b,c} and Henryk Ratajczak^{b,c,d}

^a*Laboratoire d'Optique des Solides, Boîte Courrier 80, Université Pierre et Marie Curie, 4 Place Jussieu 75252 - Paris cedex 05, France*

^b*Institute of Low Temperature and Structure research, Polish Academy of Sciences, 50-950 Wrocław 2, P.O. Box 937, Poland*

^c*Institute of Chemistry, Wrocław University, 50-383 Wrocław, Joliot-Curie 14, Poland*

^d*Centre Scientifique de l'Académie Polonaise des Sciences, 74 rue Lauriston, 75116-Paris, France*

$\text{Na}_2\text{SeO}_4 \cdot \text{H}_2\text{SeO}_3 \cdot \text{H}_2\text{O}$ are transparent orthorhombic (class group mm2) crystals which exhibit interesting second order nonlinear optical properties in the blue region. We report here a linear and nonlinear theoretical investigation of their optical properties and an experimental demonstration at $\lambda_{\omega} = 871.6$ nm.

The $\text{Na}_2\text{SeO}_4 \cdot \text{H}_2\text{SeO}_3 \cdot \text{H}_2\text{O}$ crystal is built of sodium cations, selenate anions, molecules of selenious acid and water. The Na^+ cations occupy general positions whereas the SeO_4^{2-} anions, water and H_2SeO_3 molecules lie in the symmetry planes perpendicular to the a axis [1]. The selenate anions and selenous acid molecules form infinite chains along the a axis through hydrogen bonds, with an O...O distance of 2.622(15) Å. Water molecules of C_s symmetry are attached to the selenious acid molecules by weak hydrogen bonds with an O...O distance of 2.957(25) Å. Large single crystals of high optical and mechanical quality were grown by slow evaporation at 300 K of an aqueous solution containing Na_2SeO_4 and H_2SeO_3 in a 1:1 stoichiometric ratio.

In such a symmetry, the dielectric principal axes (X,Y and Z) are parallel to the orthorhombic axes. The three refractive indices $n_x(=n_a)$, $n_y(=n_b)$ and $n_z(=n_c)$ were measured for some wavelengths of visible spectrum and fitted by a single-pole Sellmeier equation. Between 400 nm and 1100 nm, we have $n_x > n_y > n_z$. The effect of walk-off was demonstrated to be negligible whatever the internal angle is, for any propagation direction lying in a principal dielectric plane.

Linear transmission spectra have been recorded with polarizations along the three dielectric axes. For each polarization, the crystal transparency over the visible spectrum is high (more than 80 %).

In an mm2 structure there remains only five nonzero tensorial components, namely d_{15} , d_{24} , d_{31} , d_{32} and d_{33} in the contracted notation. Assuming that Kleinman's relations apply in the transparency domain of the crystal, the tensor reduces to 3 nonzero coefficients : $d_{31}(= d_{15})$, $d_{32}(= d_{24})$ and d_{33} .

The d_{31} Maker fringes have been measured with input polarization parallel to X axis and output polarization lying in YZ plane. In the same way, the d_{33} Maker fringes have been measured with input and output polarizations parallel to Z axis. Finally, it is demonstrated that the nonlinear coefficients are twice the d_{11} quartz coefficient at $\lambda_{\omega} = 871.6$ nm.

Type I and type II SHG phase-matching in the main dielectric planes were calculated from the deduced Sellmeier coefficients. Concerning the type I phase-matching it occurs in the three following configurations : i) \mathbf{E}^{ω} is parallel to Y axis and propagates in ZX plane ; $\mathbf{E}^{2\omega}$ lies in ZX plane. ii) \mathbf{E}^{ω} propagates in XY plane and lies in this plane ; $\mathbf{E}^{2\omega}$ is parallel to Z axis. iii) \mathbf{E}^{ω} propagates in the YZ plane and is parallel to X axis ; $\mathbf{E}^{2\omega}$ lies in YZ plane. Type II phase-matching occurs in one single configuration : the ω electric field propagates in the ZX plane and the 2ω electric field is polarized parallel to Y axis.

Type I phase-matching second harmonic generation was experimentally demonstrated at 871.6 nm. The incident ω vibration is parallel to X axis and the 2ω wave is polarized in the YZ plane. The measured phase-matching external angle is 24.1° corresponding to an internal angle θ_{PM}^{ω} of 14.8° . The computed value from Sellmeier coefficient is 14.6° corresponding to an external angle of 23.8° . The angular-acceptance-length product is 7.5 mrad.cm. This value is less than that of KTP (20 mrad.cm) at 1064 nm [2] but higher than that of BBO (1 mrad.cm).

References

- [1] J. Baran, T. Lis, M. Marchewka and H. Ratajczak, J. Mol. Struct., 250 (1991) 13.
- [2] H. Yamamoto, S. Funato, T. Sugiyama, R.E. Jonhson, R.A. Norwood, J. Jung, T. Kinoshita and K. Sasaki, J. Opt. Soc. Am., B13 (1996) 837.

LIQUID CRYSTALS AS MATERIALS FOR REAL-TIME HOLOGRAPHIC OPTICAL DEVICES

A. Miniewicz

Janusz Parka*, Stanisław Bartkiewicz, Adam Januszko

*Institute of Physical and Theoretical Chemistry, Technical University of Wrocław,
Wrocław, Poland*

**Institute of Technical Physics, Military University of Technology, Warsaw, Poland*

Tremendous effort in developing optical signal processing methods resulted that optical systems become to be competitive with alternate data processing technologies. This was possible due to developments in 3-D optical storage materials coupled with recent developments of liquid-crystal display (2-D input device) and solid-state detector array (2-D output device) technologies. As holographic techniques are widely used in the optical systems architecture the important role is played by photosensitive materials able to show capabilities of dynamic hologram recording and erasing. They are used in the real-time holographic optical devices serving as optical processors, light amplifiers, special filters, etc. and are the key elements in devices allowing for pattern recognition, associative memory or moving object extraction. Up to now, mostly inorganic photorefractive crystals and also polymeric photorefractive materials, were studied and exploited in that respect.

We report on a novel class of materials - liquid crystal (LC) systems giving a promise of replacing the classic photorefractives in some applications. We describe several mechanisms occurring in liquid crystals which can be used for reversible or permanent holographic storage. Emphasis is put on the dye-doped LC systems. Information carrying interference light intensity pattern is mapped in a non-linear optical liquid crystal in the form of spatial effective index of refraction changes. Obtained in this way phase holograms can be read with the same or another laser source. One of the most efficient mechanism converting light intensity pattern into a refractive index modulation occurs via charge carrier photogeneration and current flow modulating externally applied electric field and subsequent local reorientation of long molecular axes [1]. The effectiveness of this process depends on specific design of LC panel as well as on physicochemical and optical parameters of a LC itself. From our extensive studies of dynamic holography in the dye-doped LCs [2] we are able to formulate some rules helpful in designing of an efficient optically addressed spatial light modulator (OASLM). Recently we demonstrated characteristics of transmissive optically addressed spatial light modulator manufactured on the basis of a nematic LC mixture doped with 1,4-dibuthylamino 9,10-anthraquinone dye and showing $\eta = 20\%$ diffraction efficiency under external dc voltage of only ~ 10 V. Dynamic hologram recording/erasing was possible at a relatively high speed of 500 cycles per second. Observed dynamic characteristics coupled with a low operating voltage and proved long time fatigue-less performance of the modulator make it interesting for many real-time holographic applications.

References

- [1] Khoo I.C., *Optics Lett.* **20**, 2137-2139 (1995)
- [2] Miniewicz A., Bartkiewicz S., Januszko A. and Parka J., in *Photoactive Organic Materials Science and Applications*, eds. F. Kajzar, V.M. Agranovich and C.Y.-C. Lee, *NATO ASI Series*, vol. 9, Kluwer Academic Publishers, Dordrecht, 1996, pp. 487-500

Optical Kerr-like response of Dye-Doped Nematics

E. Santamato, G. Abbate, P. Maddalena, L. Marrucci, D. Paparo,
E. Massera

INFN, Dipartimento di Scienze Fisiche, Università di Napoli, Pad. 20,
Mostra d'Oltremare, 80125, Napoli, Italy

Abstract

We present our most recent results on laser-induced optical reorientation in mixtures made by adding small amounts of organic dyes to nematic liquid crystals. The optical reorientation process is biased by the molecular interaction between dye and nematic host, so that the reorientation is dramatically enhanced. The addition of suitable dye may also reverse the sign of the observed optical Kerr effect, providing a simple way to obtain highly nonlinear defocusing material.

The laser-induced optical reorientation in nematic liquid crystals[1, 2] was extensively studied in the last two decades[3], because the resulting optical Kerr-like nonlinearity is huge and may be of great interest for applications. It was observed recently that the optical reorientation process may be enhanced over two orders of magnitude, when small amounts of absorbing dye are added to the pure nematic host[6]. A similar dye-induced enhancement of the optical Kerr response was also observed in the isotropic phase[7]. The enhancement effect is remarkable, because all other macroscopic properties of the material (except the light absorption coefficient) remain almost unchanged after having the dye added to the nematic. In particular, the material time constants remain unchanged (the same as the pure material) in despite of the enormous increase of the nonlinear optical response. Also the sign of the optical Kerr coefficient may be reversed by adding a suitable dye, changing the material from focusing to defocusing. The effect is wavelength dependent, so that the sample may be focusing at some wavelength and defocusing at another wavelength.

In this work we present some comparative experiments about the enhancement of the optical reorientation in several dye-nematic mixtures, obtained by changing both the guest and the host material. The experimental data are then compared with a phenomenological model, that although less detailed than the one already reported[8], permits to obtain substantially equivalent results in a simpler way. We studied both anthraquinone and azo dyes, observing quite similar effects. The results presented in this work, however, refer to anthraquinone dyes only, because azo dyes, unlike anthraquinone dyes, are known to undergo *cis-trans* photoisomerization, when illuminated by green light. Photoisomerization changing the dye molecular conformation may well

lead to a reorientation of the nematic host proportional to the incident laser intensity. But, quite surprisingly, anthraquinone dyes, whose molecular conformation is very stable, produce a much larger enhancement of the optical reorientation in the nematic, despite of the small amount of dye (a few percent) present in the mixture. In the anthraquinone dyes, the molecular conformation remains unchanged, and only the electronic state is affected by the photon absorption. The enhancement effect is expected to be quite general and was indeed observed in the majority of dye-nematic mixtures. We studied 11 dyes in five different nematic hosts (5CB, MBBA, E7, E63, 3010) and only one dye showed zero torque enhancement, within the experimental errors[9]. Moreover, we found both positive and negative enhancement factors. We ascribe the changing in sign of the observed optical nonlinearity to the reversing in sign of the difference $\Delta u = u_e - u_g$, between the interaction energies of the dye molecules in their excited and ground state. A simple model is presented that, although neglecting the molecular diffusion and the dye saturation, is enough to understand the main features of the molecular mechanism underlying the phenomenon. A merit figure, characteristic of the guest-host molecular interaction only, was also devised. The model presented here can be seen as the low diffusion limit of a much more complicated statistical model already appeared in the literature[8]. The enhancement effect was found to be strongly dependent on the host, and it is very large when the liquid crystal host has strong polar groups, as CN, in its side chain. The corresponding change of Δu is to be ascribed to the (electronic or protonic) intramolecular charge redistribution and not to a conformational transitions, at least for anthraquinone dye. Some aspects of the phenomenon, as for example the wavelength dependence of the merit figure of AQ2 in E63 host, is not yet well understood. We hope however that the results presented here may be of some help in suggesting a way to make guest-host systems exhibiting a very high amplification of the optical torque. Having such materials could be very interesting for nonlinear optics applications, because the increase of the nonlinear response is not accompanied here by a corresponding decreasing in the response time.

References

- [1] B. Ya. Zel'dovich, N. F. Pilipetskij, A. V. Sukhov, and N. V. Tabiryan, *JEPT Lett.*, **32**, 263 (1980).
- [2] S. D. Durbin, S. M. Arakelian, and Y. R. Shen, *Phys. Rev. Lett.*, **47**, 1411 (1981).

- [3] For recent reviews on the subject, see, for example, I. C. Khoo and S. T. Wu, *Optics and nonlinear optics of liquid crystals*, Series in Nonlinear Optics, World Scientific, Singapore, 1993.
- [4] M. Tamburrini, E. Ciaramella, and E. Santamato, *Mol. Cryst. Liq. Cryst.*, **241**, 205 (1994).
- [5] L. Marrucci, G. Abbate, S. Ferraiuolo, P. Maddalena, E. Santamato, *Mol. Cryst. Liq. Cryst.*, **237**, 39 (1993).
- [6] I. Jánossy and T. Kósa. *Opt. Lett.*, **17**, 1183 (1992).
- [7] D. Paparo, L. Marrucci, G. Abbate, E. Santamato, M. Kreuzer, P. Lehnert, T. Vogeler, *Phys. Rev. Lett.*, **78**, 38 (1997).
- [8] I. Jánossy, *Phys. Rev. E*, **49**, 4 (1994).
- [9] G. Abbate, G. Arnone, A. Lauria, P. Maddalena, L. Marrucci, D. Paparo, and E. Santamato, *Novel Optical Materials and Applications*, Edited by I. C. Khoo, F. Simoni, and C. Umeton, John Wiley & Sons, p. 133, 1997.

The Role of Optical Nonlinearities in the Generation of Localized Photons

Roger Andrews

Department of Materials Science and Metallurgy
University of Cambridge
Pembroke St.
Cambridge CB2 3QZ

In this paper we present a microscopic model to describe the generation of entangled pair photons from non-linear crystals. A complete quantum-mechanical calculation of second-order non-linear susceptibilities is presented and their importance in describing the pair photon amplitude is highlighted. The localizability property of single photons is then discussed within the framework of the model.

Analysis of electro-optic effects and SHG of Pyroelectric Liquid Crystalline Polymers - Simulations and experimental results.

Mikael Lindgren

IFM-Chemical Physics, Linköping University, S-581 83 Linköping, Sweden

Per-Otto Arntzen

National Defense Research Establishment, Division of Laser Systems, P.O. Box, S-581 11 Linköping, Sweden

Jan Lindström

National Defense Research Establishment, Division of Materials Research, S-172 90 Sundbyberg, Sweden

Jonas Örtengren, Ulf W. Gedde, Anders Hult, Fredrik Sahlén, Mikael Trollsås

Department of Polymer Technology, Royal Institute of Technology, S-100 44, Stockholm, Sweden

David Hermann, Lechezar Komitov, Sven T. Lagerwall, Per Rudquist, Bengt Stebler

Physics Department, Chalmers University of Technology, S-412 96 Göteborg, Sweden

Abstract

A new numerical method to calculate the transmission and reflection coefficients of anisotropic multilayered thin films has been developed. The theory was implemented in a Matlab computer program where the boundary and eigenmodes of refraction were solved by a numerical matrix manipulations containing all six field components simultaneously. The method allows a large number of adjacent thin layers possessing arbitrary anisotropy of the dielectric constant. The method is extended to allow quadratic nonlinear optical effects, and it is shown how electro-optic effects and second harmonic generation in arbitrary anisotropic systems can be modeled. Experimental data of ferroelectric liquid crystal systems and novel pyroelectric liquid crystal polymers (PLCP) based on binary mixtures of two monomers which exhibit a smectic C* phase; **A2c**: 4''-{(R)-(-)-2-[(10-acryloyloxy)decyl]oxy}-3-nitrophenyl 4-4'-[(11-acryloyloxy)undecyloxy]phenyl}benzoate, **A1b**: 4''-{(R)-(+)-2-octyloxy}-3''-nitro phenyl 4-(4'-[(11-acryloyloxy)undecyloxy]phenyl) benzoate, were compared with simulations. Both liquid crystal monomers have an NO₂ function to enhance the nonlinear optical properties, and one of the monomers, **A2c**, enables polymerisation to a cross-linked polymer. The d_{16} - and d_{23} -coefficients were found to be in the range 0.65 - 0.8 pm/V.

**Quantum nonlinear optics in
artificially phase-matched materials**

Ariel Levenson

FRANCE TELECOM / CNET / PAB, Laboratoire de Bagneux

B.P. 107, F-92225 Bagneux Cedex - France

phone: (33 1) 42 31 75 36

e-mail: levenson@bagneux.cnet.fr

During the last 10 years impressive experimental demonstrations have brought quantum optics to a certain maturity. These demonstrations spans right from fundamental to more "applied" aspects and have given rise to a wide variety of results, to cite but a few examples: the squeezing of quantum noise of CW and pulsed lasers, the repeated quantum non demolition measurement of a quantum state and the noiseless distribution of an optical information. At the very heart of these progress is nonlinear optics and particularly second order optical parametric interactions.

The quantitative evolution of performance was, however, slower than the expected since the very beginning. This is mainly due to the numerous parasitic effects that usually degrade the photon statistics. Among of them are residual absorption, modal mixing, unwanted nonlinear effects, ...

In this talk I will attempt to give some insight on why artificially phase matched materials are expected to boost quantum optics in the near future. I will in particular discuss QPM LiNbO₃ as an example of mature material, but will also consider more prospective approaches such as QPM silica fibres and artificially phase-matched semiconductor microcavities.

All-optical modulation in a type II perfect phase-matched SHG under quasi-static approximation.

G. D'Aguanno, C. Sibilia, E. Fazio, and M. Bertolotti

Dipartimento di Energetica, Università di Roma, Via A. Scarpa 14,
00161 Roma, Italy GNEQP of CNR and INFM, Italy

Recently interest in second order-nonlinearities has been grown because of the possibility of using this nonlinearities in all-optical devices, e.g., nonlinear Mach-Zender interferometers, nonlinear direction couplers [1] and optical transistor [2]. In particular an experimental demonstration of a KTP all-optical transistor action in a type II SHG under unbalanced input intensity and perfect phase matched conditions has been reported in ref.[3].

In this work we report a theoretical study of a type II SHG under perfect phase matching in order to analytically clarify the various phenomena, in particular the all-optical modulation occurring when the interaction takes place with unbalanced input intensities. In particular we point out that when the SHG take place at perfect phase matching no nonlinear phase change of the interacting fields is possible, as commonly claimed [4], but only an amplitude modulation of the interacting fields driven by the input intensity ratio as it results from a rigorous analytical treatment of the coupled differential equations for the second order interactions [5,6].

If the spectral bandwidth of the pulses is small compared to their central frequency, the three interacting fields may be assumed quasi-monochromatic. Moreover under quasi-static approximation when the input pulses propagate, the solutions for the quadratic interaction at perfect phase matching ($\Delta q=0$) are the following [6]:

$$\bar{E}_1(z, t) = \bar{e}_1 f_1(t) \sqrt{\frac{8\pi}{cn_1} I_1(z=0)} \left| \operatorname{cn} \left(4\omega \eta f_2(t) \sqrt{\frac{\pi}{cn_1 n_2 n_3} I_2(z=0)} z | m \right) \right| \cos(q_1 z + \Phi_{10} - \omega t) \quad (1.1)$$

$$\bar{E}_2(z, t) = \bar{e}_2 f_2(t) \sqrt{\frac{8\pi}{cn_2} I_2(z=0)} \operatorname{dn} \left(4\omega \eta f_2(t) \sqrt{\frac{\pi}{cn_1 n_2 n_3} I_2(z=0)} z | m \right) \cos(q_2 z + \Phi_{20} - \omega t) \quad (1.2)$$

$$\bar{E}_3(z, t) = \bar{e}_3 f_1(t) \sqrt{\frac{16\pi}{cn_3} I_1(z=0)} \left| \operatorname{sn} \left(4\omega \eta f_2(t) \sqrt{\frac{\pi}{cn_1 n_2 n_3} I_2(z=0)} z | m \right) \right| \cos(q_3 z + \Phi_{30} - 2\omega t) \quad (1.3)$$

where $m = \frac{f_1^2(t) I_1(z=0)}{f_2^2(t) I_2(z=0)}$ is the parameter of the elliptic functions, $f_j(t)$ ($j=1,2$) are the temporal

profiles of the "o" and "e" electric field pulses at the input of the nonlinear material surface (in general we have to consider $f_1(t) \neq f_2(t)$ in order to take into account of the possible temporal delay between the "o" and the "e" beam at the input of the nonlinear material surface) and $I_j(z=0)$ ($j=1,2$) is

the peak intensity of “o” and “e” pulses at the input. All the fields have no phase-modulation or phase changes but only amplitude-modulations which are described by the modules of the elliptic functions. These modules depend on the input pump-intensities ratio.

It is possible to demonstrate that eqs. (1) describe correctly the experimental results as reported for ex.in ref.[3] where the transmission of the fundamental frequency (FF) beam from a crystal is studied versus the input polarization angle α in a type II SHG. In fact from eqs.(1) the total normalized FF intensity is a time dependent function:

$$T_{FF}(z,t) = \frac{f_1^2(t) \sin^2 \alpha \operatorname{cn}^2 \left(4\omega \eta f_2(t) |\cos \alpha| \sqrt{\frac{\pi}{cn_1 n_2 n_3}} I_{PUMP} z \left| \frac{f_1^2(t)}{f_2^2(t)} \tan^2 \alpha \right| \right) + f_2^2(t) \cos^2 \alpha \operatorname{dn}^2 \left(4\omega \eta f_2(t) |\cos \alpha| \sqrt{\frac{\pi}{cn_1 n_2 n_3}} I_{PUMP} z \left| \frac{f_1^2(t)}{f_2^2(t)} \tan^2 \alpha \right| \right)}{f_1^2(t) \sin^2 \alpha + f_2^2(t) \cos^2 \alpha} \quad (2)$$

which fit very well the experimental results reported in ref. [3].

References

- [1] G. Assanto, G.I. Stegeman, M. Sheik-Bahae, and E. W. Van Stryland, *Appl. Phys. Lett.* **62**, 1323 (1993)
- [2] P. St. J. Russel, *Electron. Lett.* **29**, 1228 (1993)
- [3] G. Assanto, Z. Wang, D.J. Hagan, and E.W. Van Stryland, *Appl. Phys. Lett.* **67**, 2120 (1995)
- [4] A. Belostotsky, A.S. Leonov, and A.V. Maleshko, *Opt. Lett.*, **19**, 856, (1994)
- [5] G. D’Aguanno, C. Sibilis, E. Fazio M. Bertolotti and E. Ferrari, Submitted for publication on *Journ. of Mod. Opt.*
- [6] G. D’Aguanno, C. Sibilis, E. Fazio M. Bertolotti, , Submitted for publication on *Opt. Comm.*

HOW TO USE STRUCTURAL DATA FROM VIBRATIONAL SPECTROSCOPY TO OBTAIN INFORMATION ON THE N.L.O. RESPONSE OF ORGANIC MATERIALS

M. Del Zoppo, C. Castiglioni, M.C. Rumi and G. Zerbi

Dept. of Industrial Chemistry, Politecnico di Milano, P. L. da Vinci, 32, 20133 Milano (Italy)

Vibrational spectroscopy has been used to obtain reliable determinations of molecular optical nonlinearities of polyconjugated organic materials. The "vibrational method" has been assessed with a careful study of various push-pull systems (1,2). Also the solvent dependent n.l.o. behaviour has been accounted for (3).

Very recently this approach has been applied to the case of more complex systems. Especially interesting are the results obtained for 2D systems (e.g. Rylenes, Acenes etc.) (4). Up to now the method has been used only for solutions; more recently it has been extended also for the determination of the molecular hyperpolarizabilities in the solid state. (5)

The basis on which the vibrational method relies is the close relationship between the electronic properties and peculiar structural parameters (6). It has been shown that the electronic properties are coupled to variations of the nuclear geometry through particular modifications of the structure of the CC backbone. The vibrational spectrum, both in frequency and intensity, on its turn is heavily affected by such structural modifications. This can be proven theoretically, by properly displacing the nuclear geometry and then calculating on one hand the modification of the electronic properties and on the other the modification of the vibrational spectra (7).

From this analysis it turns out that vibrational intensities are particularly rich in informations. As a consequence the spectral pattern can be used to infer first of all informations on the molecular

structure as function of the molecular surroundings. This kind of information is not readily accessible with other techniques. Moreover it is possible to derive the modifications induced on the n.l.o. behaviour.

It becomes hence possible to use the vibrational spectra not only to obtain a measure of the optical nonlinearities but also as a tool to guide the search for new materials in the context of a material engineering approach.

- (1) C. Castiglioni, M. Del Zoppo, P. Zuliani and G. Zerbi, *Synth. Metals*, **74**, 171 (1995); P. Zuliani, M. Del Zoppo, C. Castiglioni, G. Zerbi, C. Andraud, A. Collet, *J. Phys. Chem.*, **99**, 1624 (1995)
- (2) M. Del Zoppo, C. Castiglioni, P. Zuliani, G. Zerbi, *Adv. Materials*, **8**, 345 (1996)
- (3) P. Zuliani, M. Del Zoppo, C. Castiglioni, G. Zerbi, S.R. Marder, W.J. Perry, *J. Chem. Phys.*, **103**, 9935 (1995)
- (4) M. C. Rumi, G. Zerbi, K. Mullen, M. Rehan, *J. Chem. Phys.*, in press
- (5) G. Brambilla, Thesis in Engineering (1996)
- (6) C. Castiglioni, M. Del Zoppo, G. Zerbi, *Phys Rev.B*, **53**, 13319 (1996)
- (7) C. Castiglioni, M. Del Zoppo, V. Gerola, G. Zerbi, *J. Opt. Soc. B*, submitted

NEW METHODOLOGIES FOR METAL QUANTUM-DOT GLASS WAVEGUIDES PREPARATION

E. Borsella^{1,*}, E. Cattaruzza¹, G. De Marchi¹, F. Gonella¹, G. Mattei¹, P. Mazzoldi¹, S. Cestaro¹,
G. Battaglin², R. Polloni², A. Quaranta³, R. F. Haglund Jr.⁴

¹INFM, Dipartimento di Fisica, Università di Padova, via Marzolo 8, 35131 Padova, Italy.

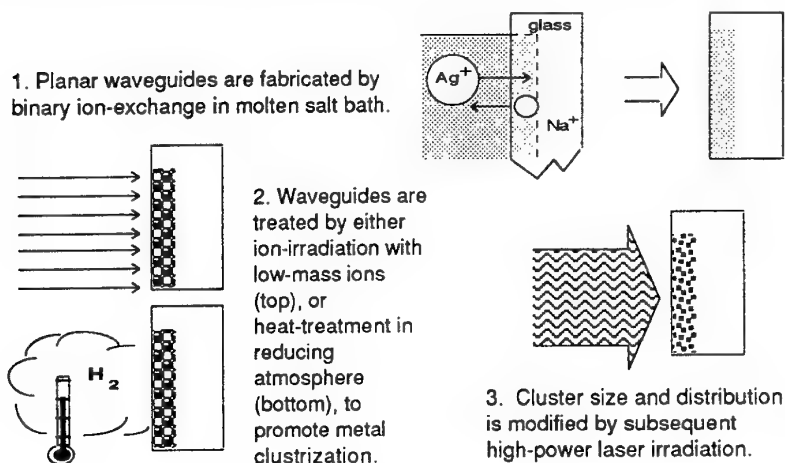
*permanent address: ENEA, Dip. INN/FIS-SPET, Frascati, Roma, Italy.

²INFM, Dip. di Chimica-Fisica, Univ. di Venezia, Calle Larga S. Marta 2137, 30123 Venezia, Italy

³INFM Padova and Dip. di Ing. dei Materiali, Università di Trento, via Mesiano 77, 38050 Trento, Italy

⁴Department of Physics and Astronomy, Vanderbilt University, Nashville, Tennessee 37235, USA

Metal quantum-dot composites (MQDC) glasses [1] are formed by small metal clusters embedded in glass matrices. In the last few years, much attention has been dedicated to the development of new methodologies for the fabrication of these materials, since metal clusters in the nanometer range of size have been shown to greatly enhance the nonlinear optical response of the host material, due to dielectric and quantum confinement effects [2]. In particular, metal nanocluster-doped glasses exhibit an enhanced third-order susceptibility [3], whose real part is related to the intensity-dependent refractive index. Nonlinear switching devices can be based on optical waveguide structures which provide strong beam confinement in prescribed patterns. In these devices, the intensity of an optical signal is used as the parameter that causes switching between two output channels, thus performing logic operations. The technological interest is strengthened by the general interest in strongly quantum-confined electronic systems which exhibit several effects deriving from the increased electronic density of states near the conduction-band edges. Moreover, it should be mentioned the compatibility of the glass with silicon-based electronic materials.



Novel sequential methodologies [4-6] are used to prepare silver and copper colloidal glass waveguides, following multi-step processes as sketched in fig. 1: soda-lime glass slides [7] are first ion-exchanged in molten baths of either silver or copper salts. As the temperature is risen, interdiffusion takes place between the transition metals of the bath, that penetrate into the glass, and the alkali ions of the glass, that outcome to dilute the bath. In this way, graded-index optical waveguides are created several microns thick. Different experiments were

performed on ion-exchanged samples. Some waveguides were irradiated by low-mass ions at energies varying from 20 keV to 2 MeV [5,8]. Other waveguides were heat-treated in H_2 atmosphere for several hours and temperatures in the range 120°C to 250°C [9]. With both these methodologies, metal aggregation in nanoclusters is promoted.

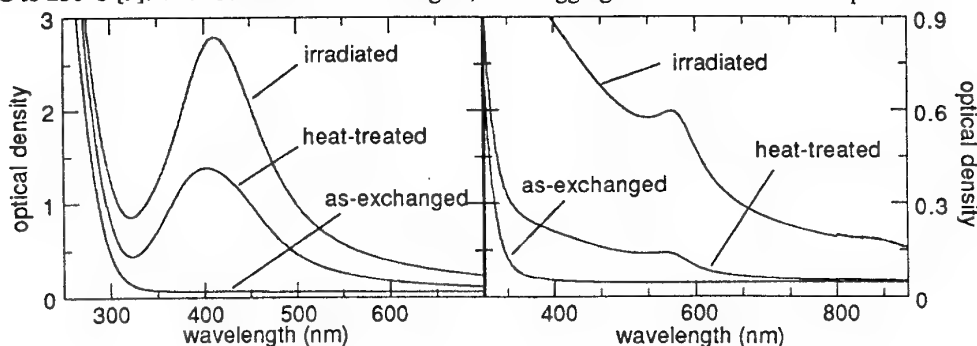
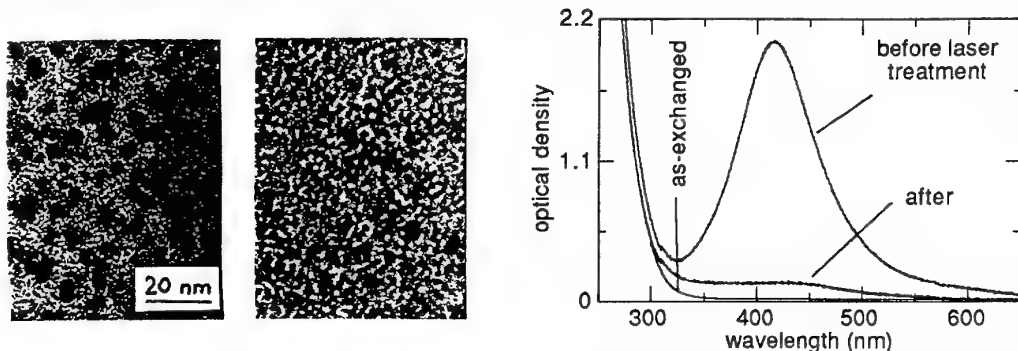


Figure 2 shows the optical absorption spectra of silver- and copper-doped waveguides, before and after irradiation with helium beams in the MeV energy range and before and after heat-treatments in H_2 atmosphere. Surface plasmon resonance (SPR) peaks are evident in both cases, indicating the presence of metallic clusters with radii of a few nanometers. The irradiation effect is actually to promote the cluster formation, related to radiation-enhanced diffusion of silver. The different role played by the preparation parameters (temperature, bath type and processing time for the ion-exchange, and current, fluence, temperature and type of ion for the ion-irradiation step) is expected to allow the development of a fabrication protocol with effective cluster formation control. In the case of heat-treated samples, the hydrogen permeation and ion-exchange between hydrogen and sodium are steps of the annealing process. By these methodologies, samples with n_2 values up to $10^{-13} \text{ m}^2/\text{W}$ have been obtained, that are at least comparable with values obtained from MQDC prepared by more assessed methods, or from semiconductor-doped glasses.

As a third step, cluster size distribution is further modified by means of high power laser irradiation [6]. The main advantages of this sequential method is the possibility of tailoring cluster formation within waveguiding layers, selecting very small clusters (a few nanometers in diameter) for which the absorption cross section is extremely low. Laser irradiation is performed with single pulses of a Nd:YAG laser at either $\lambda=1064 \text{ nm}$ or $\lambda=532 \text{ nm}$, and energy densities below $1 \text{ J}/\text{cm}^2$, with a pulse duration of 10 ns. The presence of small clusters even after the laser treatment was detected by Transmission Electron Microscopy (TEM) analysis, as shown in fig. 3. TEM bright-field cross-sectional views are shown of a sample, ion-exchanged in a molten $\text{AgNO}_3:\text{NaNO}_3$ bath at 320°C for 15 minutes, and subsequently irradiated with $5 \times 10^{16} \text{ He}^+/\text{cm}^2$ at 100 keV, before (left) and after (right) laser beam irradiation. Laser-irradiated samples exhibit a reduction of the cluster size, with a corresponding increase in the number of clusters. Fig. 3 (right) shows the attenuation of the SPR peak following the laser-irradiation, due to the decrease of the clusters size.



The potential of the presented methods lies in the possibility of controlling the clusters growth and their size distribution (and so their optical response) through the variation of the preparation parameters. Moreover, these sequential methodologies allow in principle to design channel waveguides along prescribed patterns, with obvious application in the integrated-optical device preparation.

- [1] P. Mazzoldi, G. W. Arnold, G. Battaglin, F. Gonella and R. F. Haglund, Jr., *J. Nonlin. Opt. Phys. Mater.* **5** (1996) 285.
- [2] C. Flytzanis, F. Hache, M. C. Klein, D. Ricard and Ph. Roussignol, *Progr. Opt.* **29** (1991) 323.
- [3] U. Kreibig and M. Vollmer, *Optical Properties of Metal Clusters* (Berlin, Springer 1995).
- [4] G. Battaglin, G. De Marchi, F. Gonella, E. J. Knystautas, P. Mazzoldi and C. Meneghini *J. Non-Cryst. Solids* **196** (1996) 79.
- [5] F. Garrido, F. Caccavale, F. Gonella and A. Quaranta, *J. Europ. Opt. Soc. A: Pure Appl. Opt.* **4** (1995) 771.
- [6] F. Gonella, G. Mattei, P. Mazzoldi, E. Cattaruzza, G. W. Arnold, G. Battaglin, P. Calvelli, R. Polloni, R. Bertonecello and R. F. Haglund, Jr., *Appl. Phys. Lett.* **69** (1996) 3101.
- [7] F. Gonella, A. Quaranta, A. Sambo, F. Caccavale and I. Mansour, *Opt. Mater.* **5** (1996) 321.
- [8] F. Gonella, E.J. Knystautas, G. Mattei, P. Mazzoldi, C. Meneghini, E. Cattaruzza, F. Garrido and D.H. Osborne, Jr., *Nucl. Instr. Meth. B* (1997) in press.
- [9] G. De Marchi, F. Caccavale, F. Gonella, G. Mattei, P. Mazzoldi, G. Battaglin and A. Quaranta, *Appl. Phys. A* **63** (1996) 403.

OPTICALLY INDUCED MULTIPOLAR MICROPATTERNING OF NONLINEAR POLYMER FILMS: FROM MOLECULAR TO PHOTONIC ENGINEERING

Sophie BRASSELET and Joseph ZYSS

France Telecom - CNET

Departement d'Electronique Quantique et Moléculaire

196 av. H. Ravera

92225 BAGNEUX, FRANCE

The development of electrooptic polymers now stands at the onset of technological fruition as a result of almost two decades of intense molecular engineering studies and of the more recent maturing of semiconductor compatible integrated optics fabrication processes. Nevertheless, the full potential of organic systems for nonlinear optics and related applications may not have been fully exploited so-far within the paradigmatic orientational scheme of a dipolar *molecular diode* structure coupled with an externally applied poling electric field at thermal equilibrium¹. In particular, such a configuration makes it difficult to implement (quasi)-phase matched gratings for (cascaded) quadratic NLO, guarantee polarization independent telecom device behaviour or engineer other propagative (e.g. soliton generation) or QED (e.g. microcavity) configurations. A different approach, whereby all-optical photoinduced processes are called-upon instead of thermally equilibrated ones and traditional 1-D systems are traded for more general 3-D multipolar molecules (e.g. octupolar, dipolar or a combination of these) opens-up new possibilities to address these issues. It permits indeed to micropattern a controlled $\chi^{(2)}$ spatial (or pixellised) distribution whereby the magnitude and ratios of macroscopic tensorial coefficients are balanced at will by phase and ellipsometric adjustment of the writing beams².

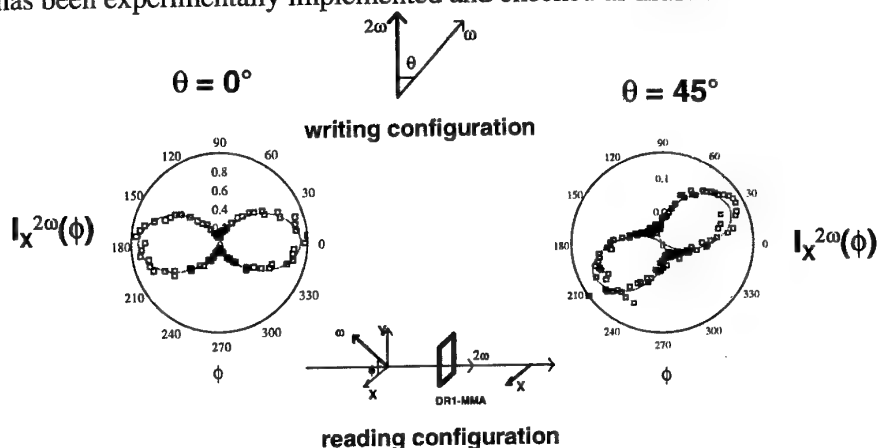
From a conceptual point of view, this approach is based on the recognition of the parallelism and coupling rules of the irreducible multipolar rotational spectra of both rank 3 write field and β tensors. Indeed, the three-photon transition probability as well as the resulting $\chi^{(2)}$ tensor can be expressed as:

$$\chi^{(2)} = N \sum_{J=1,3} \frac{1}{2J+1} \|\beta^J\|^2 E^J$$

where J labels the rotational components (J=1 for the dipole J=3 for the octupole, J=0 and 2 being eventually added to the summation in the case of resonant processes), $E = E^{2\omega^*} \otimes E^\omega \otimes E^\omega$ representing the *write* field tensor and β the quadratic molecular hyperpolarizability scaling, within a resonant two level *write* scheme, with the underlying joint one- and two-photon absorption cross-section.

This expression evidences the possibility to monitor and control the magnitude and moreover the irreducible rotational spectrum and nonlinear anisotropy of the $\chi^{(2)}$ tensor

distribution by playing on the write field tensor via its irreducible E^J coefficients. This approach has been experimentally implemented and checked as illustrated below.



The irreducible spectrum of E tensor can be fully spanned for all J 's ranging from 0 to 3 by varying the polarizations of the incoming ω and 2ω write beams. The figure above corresponds to a "scissor"-like configuration whereby both write fields are linearly polarized at an intermediary angle θ which can be continuously varied. The $\chi^{(2)}$ pattern is then read by SHG with an incoming linearly polarized beam at a variable polarization angle ϕ . Purely octupolar (resp. dipolar) configurations have been used, based on co-(resp. counter-) clockwise circular polarizations at ω and 2ω , the more general intermediate case corresponding to a circular ω and elliptic 2ω beam. We have shown in particular that a polarization independent $\chi^{(2)}$ structure can be shaped by use of an octupolar write configuration shining a quasi 1-D DR1 guest-host polymer film. This apparently "orthogonal" and hence forbidden coupling is in fact made possible by the recognition that 1-D systems (e.g. a β tensor ultimately reduced to a single β_{xxx} coefficient along the main molecular axis) still provide a significant $J=3$ component. Purely algebraic considerations show indeed that, in such case, $\|\beta^{J=3}\| = \sqrt{2/3}\|\beta^{J=1}\| = \sqrt{2/5}\beta_{xxx}$, octupolar molecules remaining of course ideally tailored candidates for such a scheme with $\|\beta^{J=3}\| = \beta_{xxx}$.

Finally we conclude with the rather provocative, however theoretically grounded statement that whereas a non-zero $\beta^{J=3}$ component is perfectly compatible with a cancelled $\beta^{J=1}$ component (such is precisely the definition of nonlinear octupoles), the opposite is not true. Cancellation of $\beta^{J=3}$ entails cancellation of $\beta^{J=1}$, and hence of the full β , which, strictly speaking, questions the very existence of nonlinear dipoles!

- (1) I. Ledoux and J. Zyss, in *Novel Optical Materials and Applications*, I.C. Khoo, F. Simoni and C. Umeton Ed., Chapter I, pp. 1-48, 1997
- (2) S. Brasselet and J. Zyss, "multipolar molecules and multipolar fields: probing and controlling the tensorial nature of nonlinear molecular media", to be published in *J. Opt. Soc. Am. B* (1997, feature issue on *Organic and Polymeric Nonlinear Optical Materials*)

Thin chemically anisotropic polyporphyrin films with potential application in non-linear optics

M. Kryszewski

Center for Molecular and Macromolecular Studies
Polish Academy of Sciences; 90-363 Lodz; Poland

Polymer Physics Department, Polymer institute
The Technical university of Lodz; 90-924 Lodz, Poland

Porphyrins have been only occasionally incorporated into polymers either as pendant groups on standard polymers, or less commonly as integrated components of the main chain polymeric structure. Their major application was to obtain systems to develop devices for solar energy conversion, in which the linked porphyrins serve as an array of light-harvesting and electron transfer units.

Following our studies on anisotropic polymer films, we have investigated the interfacial polymerization of porphyrins bearing functional groups (e.g. amine or acid chloride and/or carbonyl and hydroxyl groups) which leads to thin films which have an asymmetry of functional groups at the surfaces. The phase transfer polymerization was carried out using e.g. tetra(p-chlorocarbonyl)porphyrin in chloroform with tetra(p-hydroxyphenyl)porphyrin in aqueous base. Similarly to the literature data (1) we have established that these films display a chemical structural asymmetry in that sense that opposite surfaces show distinctive differences in the type of unreacted functional groups. We have investigated the structure and the growth mechanism of these asymmetric films as well as penetration of polar asymmetric molecules. It appears that the inclusion of such polarized asymmetric molecules enhances the prospect of non-centrosymmetric arrangements.

When illuminated by steady-state broad band light these films develop directional photopotentials whereby film surface with the acid surface develops more negative potential. Photoinduced charge separation involves electron transfer towards the acid surface of the film increasing the asymmetric polarity of these films.

Poly(porphyrin)s with optically active inclusions offer the advantage of great chemical, thermal and environmental stabilities.

1) W. Li and C.W. Wamser, *Langmuir* **11** (1995) 4061

The financial support of KBN under the Grant 3 TO9B/164/08p01

Dye doped active waveguides and optical fibers

K.Sasaki

Keio University Faculty of Science and Technology
Japan

Summary not available at time of printing.

Nonlinear Optical Chromophores Based on Multi-Donor Substituted 4-Nitrophenylhydrazones

Ilias Liakatas, Man Shing Wong, Christian Bosshard and Peter Günter
Nonlinear Optics Laboratory, Institute of Quantum Electronics, ETH-Hönggerberg,
CH-8093, Zürich, Switzerland

Organic materials have drawn considerable attention during the last few years due to their high performance with regard to linear electro-optic and nonlinear optical effects.[1] A large number of nonlinear optical molecules developed for crystal formation, incorporation into polymers or formation of Langmuir-Blodgett films have been synthesized and characterized with respect to both their microscopic and macroscopic nonlinear optical properties by many research groups. To be a highly efficient material, the constituted molecules need to exhibit large second-order molecular hyperpolarizabilities as well as align non-centrosymmetrically in such an orientation that the molecular contribution can be maximized in the bulk or film.

We have been investigating nonlinear optical molecules for organic crystals[2] and electro-optic polymers.[3] Such molecules are generally made of a highly extended π -conjugated core bearing electron donor-acceptor pair at the ends. However, for the formation of crystals very few molecules can be favourably packed and developed into useful nonlinear optical materials.

One of our approaches is to use a non-rod-shaped π -conjugated hydrazone backbone as a highly extended π -conjugated core which shows a high preference for non-centrosymmetric packing and improves the crystal properties relative to the classical counterparts.[4, 5] One of the successful examples in this class is 4-dimethylaminobenzaldehyde-4-nitrophenylhydrazone, DANPH, which was found to have the largest phase-matchable nonlinear optical coefficient $d_{12} = 270 \pm 50$ pm/V at $\lambda = 1.524$ μm up to now.[6]

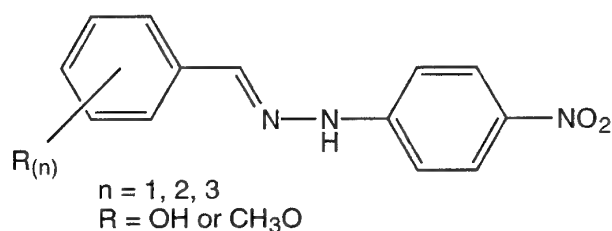


Fig.1 General formula of the substituted 4-Nitrophenylhydrazones

We will report on a new series of acentric 4-nitrophenylhydrazone derivatives which bear more than one hydroxy or methoxy donating group (Fig.1). Their molecular and nonlinear optical properties were characterized with semi-empirical calculations and hyper-Rayleigh scattering, HRS. The AM1 semi-empirical calculations were initially used to study the ground state molecular properties of these hydrazones. HRS measurements were performed in 1,4-dioxane using the Stokes line ($\lambda = 1.542$ μm) of a methane Raman cell pumped by a Nd:YAG nanosecond laser operating at $\lambda = 1.064$ μm . This wavelength allows the determination of the first-order hyperpolarizabilities β of the new compounds away from the absorption of these molecules. The HRS as well as Kurtz and Perry

powder test results of several compounds showed second-order nonlinearities and second harmonic powder signals comparable to that of DANPH. Compounds and results will be presented and discussed.

One of these new molecules (3,4-dihydroxybenzaldehyde-4-nitrophenylhydrazone, **3,4-DHNPH**) exhibited excellent crystal properties and crystals with a size up to 5 mm could be easily obtained by slow evaporation. Differential scanning calorimetry and thermal gravimetric analysis showed that these crystals have high melting and decomposition temperatures. Their crystal structure derived from x-ray analysis showed a robust hydrogen-bonded three-dimensional crystal packing. The polar direction of the acentric layers form an angle of about 20° with the polar crystallographic a-axis (Fig.2), which is an optimized chromophoric configuration for electro-optic effects.

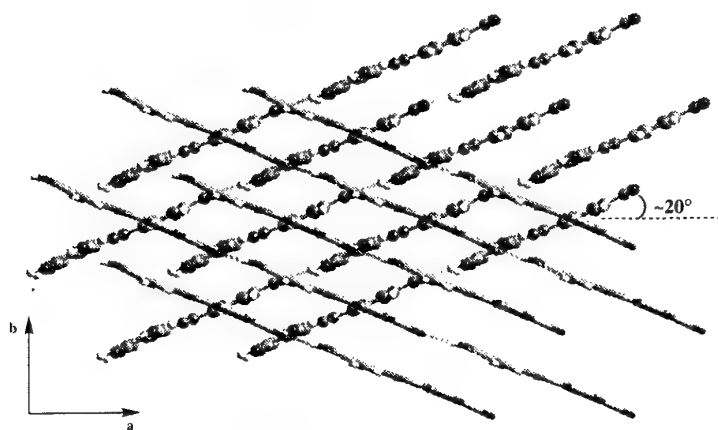


Fig. 2 The relative arrangement of two acentric layers of **3,4-DHNPH**.

Acknowledgments: We acknowledge Prof. V. Gramlich for the x-ray analysis of **3,4-DHNPH** and the Swiss National Science foundation for financial support.

References:

- [1] C. Bosshard, K. Sutter, P. Prêtre, J. Hulliger, M. Flörsheimer, P. Kaatz, and P. Günter, *Organic Nonlinear Optical Materials*, vol. 1. Amsterdam: Gordon and Breach Science Publishers, 1995.
- [2] M. S. Wong, C. Bosshard, and P. Günter, "Engineering of Polar Molecular Crystals with Optimized Chromophoric Orientation for Nonlinear Optics," *Ferroelectrics*, 1997, in print.
- [3] I. Liakatas, M. S. Wong, C. Bosshard, M. Ehrensperger, and P. Günter, "Stilbazolium Based Zwitterionic Chromophores for Electro-optic Polymers," *Ferroelectrics*, 1997, in print.
- [4] C. Serbutoviez, C. Bosshard, G. Knöpfle, P. Wyss, P. Prêtre, P. Günter, K. Schenk, E. Solari, and G. Chapuis, "Hydrazone Derivatives, an Efficient Class of Crystalline Materials for Nonlinear Optics," *Chem. Mater.*, vol. 7, pp. 1198-1206, 1995.
- [5] M. S. Wong, U. Meier, F. Pan, C. Bosshard, V. Gramlich, and P. Günter, "Five-membered Heteroaromatic Hydrazone Derivatives for Second-order Nonlinear Optics," *Adv. Mater.*, vol. 8, pp. 416-420, 1996.
- [6] S. Follonier, C. Bosshard, G. Knöpfle, U. Meier, C. Serbutoviez, F. Pan, and P. Günter, "A New Nonlinear Optical Organic Crystal: 4-Dimethylaminobenzaldehyde-4-nitrophenylhydrazone (DANPH)," *J. Opt. Soc. Am. B*, vol. 14, 1997.

Hyper-Structured Molecules Containing Carbazole Moieties for Photorefractive Application

Tatsuo Wada, Yadong Zhang, Takashi Isoshima and Hiroyuki Sasabe
Frontier Research Program, The Institute of Physical and Chemical Research (RIKEN)
2-1 Hirosawa, Wako, Saitama 351-01, JAPAN

and
CREST (Core Research for Evolutional Science and Technology), JST
1-4-25 Mejiro, Toshima-ku, Tokyo 171, JAPAN

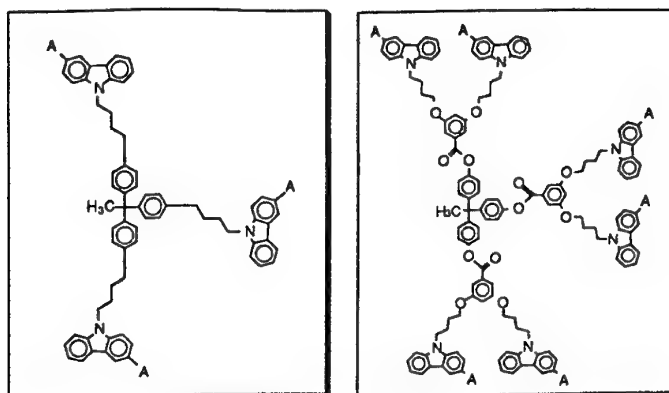
Abstract

In the future optical information processing technologies, the physics of photorefractive effect gives attractive clues to the development of self-diffraction, phase conjugation, dynamic holography, holographic memory, optical image amplification, adaptive optical processors and so forth¹⁾. The basic nature of photorefractive effect is simply described by an interaction between optical interference patterns and photoexcited charge carriers generated in the material which exhibits the second-order optical nonlinearity (Pockels effect)²⁾. Therefore the requirement for photorefractive materials is to have both photoconductive properties and Pockels effect at the same time. Typical photorefractive materials developed in the past are ABO₃ perovskite crystals such as BaTiO₃ and KNbO₃, and organic multi-component systems such as charge-transfer (CT) complex crystals and poled polymers³⁾. These poled polymers consist of three components: the first is a nonlinear optically active chromophore to provide an electro-optic response, the second is a hole transporting molecule and the third is a photosensitizer which exhibits photoconductive properties. Although these multi-component systems have good film-forming properties, they have multistep carrier hopping processes which reduce the carrier mobility due to various traps. In order to create effective space charge modulation, efficient photocarrier generation and large drift mobilities are two of key factors which should be addressed. There is a limitation of the maximum concentration of chromophores due to the phase separation in multi-component systems, which leads to the reduction of optical quality. Therefore the multifunctional chromophores with both photoconductive and electro-optic properties, so called 'monolithic' photorefractive molecules should be developed⁴⁾. In this paper, we will describe our approach to design and synthesize these molecular systems, that is, topologically well defined hyper-structured molecules with carbazole moieties for photorefractive application.

Carbazole compounds are well-known to exhibit good hole transporting properties and their photocarrier generation efficiency can be sensitized by formation of charge transfer complexes. Recently we synthesized a cyclic carbazole oligomer as well as head-to-tail carbazole dimers, trimers and main-chain polymers, carbazole dendrimers and conjugated trimers as a multifunctional chromophore⁴⁾. Carbazole oligomers can be considered as a perfectly defined structure. Carbazole dendrimers form a solid film by spin coating, which can then be poled at elevated temperatures to achieve alignment required for an electro-optic response⁵⁾. We obtained efficient photorefractive effects using conjugated carbazole trimers. Electric field-induced alignment and thermal relaxation of hyper-structured molecules can be controlled by the molecular-level tuning of the size, shape, surface chemistry and topology.

In the hyper-structured molecular systems such as carbazole dendrimers and conjugated trimers we can expect molecular level controls of size, shape, surface chemistry, topology and flexibility better than point-like molecule. The carbazole starburst oligomers have a film-forming property and show a glass-transition behavior. Values of glass transition temperature (T_g) were controlled by the length of spacer, the number of carbazole rings and acceptor groups. Amorphous molecular solid films could be prepared without supporting matrix by spin-coating from the solution. These thin films were poled above T_g to achieve the non-centrosymmetric alignment of molecular dipoles required for an electro-optic response.

The values of the second-order nonlinear optical coefficients (d_{ij}) changed depending on the acceptor groups. The relation between chemical structures and d_{ij} values of dendrimers were shown in Figure 1. Although the optimal poling was not achieved, large d_{ij} values (ca. 50 pm/V) were obtained due to the high density of nonlinear optical chromophores.



Nonlinear Optical Susceptibility

A	d_{33} (pm/V)	d_{31} (pm/V)
-CHO	6.9	5.0
-NO ₂	30.8	12.5
-CH ₂ C(CN) ₂	49.6	41.4

Figure 1. Second-order nonlinear susceptibilities in dendrimer films.

Photoconductive properties of these dendrimer systems were examined by means of a xerographic discharge technique. It is clearly confirmed that these molecular systems have multifunctional properties, *i.e.*, both photoconductivity and second-order nonlinear optical responses. The photorefractive phase shift measurement indicated that the induced index grating is shifted by 90° with respect to the absorption grating.

We constructed a two beam coupling setup using a piezo-translator and four-wave mixing setup for full characterization of photorefractivity. By using a four-wave mixing setup the optical image reconstruction of distorted images due to phase conjugation has been demonstrated. The multiple holographs can be stored in 150mm thick photorefractive medium through angular-encoded method and each image can be read out at respective angle.

References

- 1) M. E. Orczyk and P. N. Prasad, *Photonics Sci. News*, **1**, 3 (1995).
- 2) G. C. Valley and M. B. Klein, *Optical Eng.*, **22**, 704 (1983).
- 3) S. Ducharme, J. C. Scott, R.J. Twieg and W. E. Moerner, *Phys. Rev. Lett.*, **66**, 1846 (1991).
- 4) T. Wada, Y. Zhang, L. Wang and H. Sasabe, *Mol. Cryst. Liq. Cryst.*, **280**, 71 (1996).
- 5) Y. Zhang, L. Wang, T. Wada and H. Sasabe, *Macromolecules*, **29**, 1569 (1996).

Organic-inorganic solids by sol-gel and optical applications

J.-P. Boilot, J. Biteau, F. Chaput, G. Counio, T. Gacoin

Groupe de Chimie du Solide, Physique de la Matière Condensée, URA CNRS 1254 D,
Ecole Polytechnique, 91128 Palaiseau Cedex, FRANCE

A. Brun, M. Canva, B. Darracq, Y. Lévy

Institut d'Optique Théorique et Appliquée, UA CNRS 14,
Bât. 503, Université d'Orsay-Paris XI, B.P. 147, 91403 Orsay Cedex, FRANCE

The sol-gel process is now well-known as a synthetic route for the preparation of glasses. The first stage is a room temperature polymerization of a suitable monomer leading to a porous and amorphous material (xerogel). The second stage is the closure of pores at several hundred degrees to form the final glass. We concentrate on the porous materials prepared at the first stage which can be obtained in any desired shape, including thin films, and are able to trap organic molecules or clusters.

The polymerization is initiated by adding water to a solution of alkoxide in ethanol. Concerning silicon alkoxide precursors (such as the tetraethoxysilane $\text{Si}(\text{OEt})_4$ or TEOS), the chemical conditions are generally chosen in such a way that nearly complete hydrolysis occurs in a few minutes. This allows to realize separately the condensation with the formation of siloxane bridges $[\equiv\text{Si}-\text{O}-\text{Si}\equiv]$ between the hydrolyzed species $[\equiv\text{Si}-\text{OH}]$. Thus, from a quantitative analysis of NMR, X-ray scattering, and viscoelasticity data, we have shown that the condensation can be split into different parts. The first steps of the condensation consist in a progressive assembling of small organized units. This is followed by a reaction limited cluster aggregation phase which gives rise to fractal aggregates of dimension 2.1 and a typical size of 5-10 nm. Gelation is then considered as the percolation of fractal clusters resulting from the aggregation phase. Consequently, due to the growth of fractal clusters, gels turn into porous materials known as xerogels after a conventional drying in air at 20-60 °C.

The basic idea to prepare molecule and nanocrystals doped-xerogels is simple: it consists in adding a solution of the desired dopant to the initial polymerizing system and stopping the process at the xerogel stage. However, if we concentrate on the preparation of materials for optical applications, the poor chemical and mechanical properties of these porous xerogels make it difficult to use them. For instance, the brittleness of these exotic materials is well-known to be a major problem for the obtention of monoliths.

We have largely improved the properties of the xerogels in the last years and developed a new class of materials: the dense xerogels. This was performed both by modifying the synthetic procedures and by using organofunctional silicon alkoxides. Modified alkoxide precursors $\text{RSi}(\text{OEt})_3$ where R is a non-hydrolysed hydrophobic group, such as methyl, vinyl and amyltriethoxysilane (noted MTEOS, VTEOS and ATEOS) lead to organic - inorganic hybrid matrices. The permanent organic group decreases the mechanical tensions during the drying process. Functionalized alkoxides $\text{F-R}'\text{-Si}(\text{OEt})_3$ where F is a chemical function such as amino or isocyanate group and R' an alkyl spacer, allow to covalently graft active organic and

biological molecules on the xerogel matrix to avoid a phase separation and consequently to increase the concentration of the guest molecules.

Due to the improvement of the mechanical properties, the dense xerogels can be polished (one nanometer in surface roughness), and consequently, the optical quality is perfect (transmission coefficient of 92% at 633 nm for a cylindrical sample of 1 cm in thickness). Due to the closed porosity of the xerogels, molecular species are definitely trapped and consequently well protected against the chemical and the photochemical degradation.

Besides, we have shown that the diversity of the alkoxide type precursors allows to modify the properties of the doped-xerogels by changing the nature and the intensity of chemical and steric interactions between the optically active guest system and the solid host matrix. A large variety of materials have been then developed for optical and optoelectronic applications :

- By using hybrid organic-inorganic matrix, the electron - phonon coupling is reduced. This preserves the chemical identity of the guest molecule and improves its photostability. In comparison with solutions or inorganic matrices, the efficiency and the lifetime of tunable dye lasers and the photoluminescence of semiconducting nanoparticles are improved.

- By using polar inorganic matrix, strong dipolar interactions can take place between the guest molecule and the host inorganic matrix. For instance, hydrogen bond interactions stabilize a local anisotropy induced by optical field leading to optical memory. They can also stabilize polar metastable species such as the zwitterionic open form of the spiro-oxazine giving a reverse photochromism. Acido-basic exchange stabilizes the cis form during the photoisomerization of azo dyes, leading to an adjustable index change which allows to write gratings and channel waveguides.

- By covalent grafting, one can limit the degree of freedom of the active molecules and leads to polyfunctional systems. Anchoring of the guest system tends to reduce the width of the homogeneous absorption band of porphyrins, allowing the persistent spectral hole burning above 100K. Finally, the covalent grafting stabilizes the orientation anisotropy induced by static electric field. This allows to prepare materials with large quadratic nonlinearities for frequency-doubling applications and also photorefractive materials for holographic image storage.

Optical properties of ferroelectrics

A. Montenero^(a), P.P. Lottici^(b), D. Wouters^(c), G. Gnappi^(d), C. Sibilio^(e)

(a) Dip. Chimica Gen. Univ. di Parma

(b) Dip. Fisica Univ. di Parma,

(c) IMEC, Leuven, Belgium

(d) CO.R.I.VE. Parma

(e) Dip. Energetica Univ. di Roma La Sapienza

Ferroelectric materials play a big role on Electronics, but the possibility to use them also in Optoelectronic is a big challenge for everyone involved in this field.

These materials could be made by long organic molecules, FLCs (ferroelectric polymers) or by inorganic oxides as the PLZT ($\text{Pb}(\text{La})\text{Zr}_x\text{Ti}(1-x)\text{O}_3$). Both of them have some peculiarities and a short review of the preparation methods is presented.

In the case of ferroelectrics obtained by oxides a technique relatively new as sol-gel seems to give very good results specially for what concerns the thin films. But also in this case the chemical procedure is not easy and composition defects cause a change in the electrical and optical properties.

Rod and Octupolar Polyenovanillins for Nonlinear Optics

Thomas Zabulon^a, Thierry Brotin^a, Rémi Anémian^a, Chantal Andraud^a, André Collet^a,

Sophie Brasselet^b, Isabelle Ledoux^b, Joseph Zyss^b.

^aÉcole normale supérieure de Lyon, Stéréochimie et Interactions moléculaires, 69364 Lyon cedex 07, France.

^bCentre National d'Étude des Télécommunications, France Télécom, Bagneux, France.

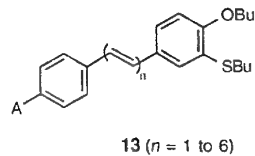
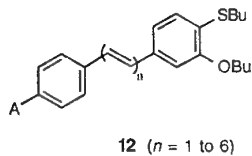
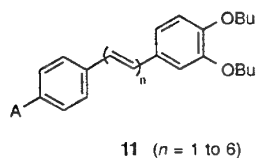
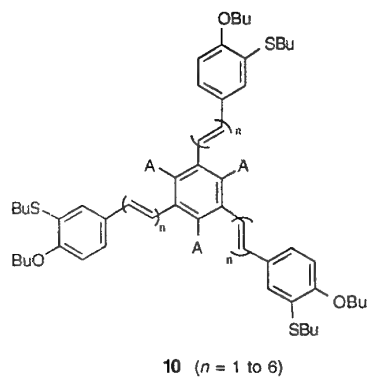
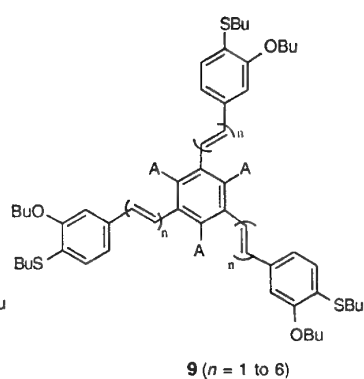
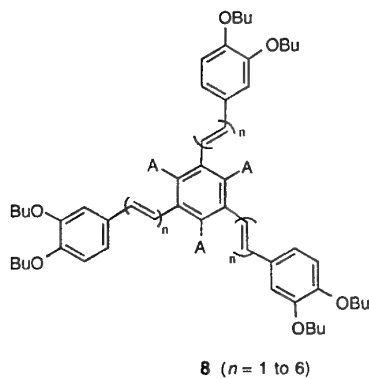
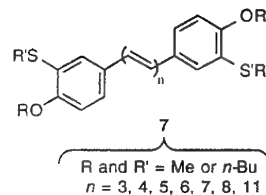
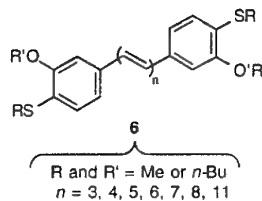
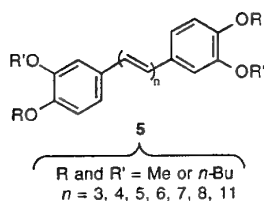
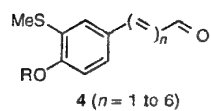
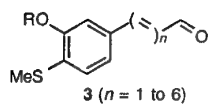
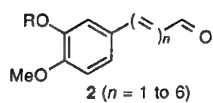
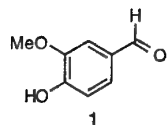
The interest in nonlinear optics of push-pull polyenovanillins **2-4**, a family of polyenes deriving of vanillin **1** has been already demonstrated¹. These molecules were used for the synthesis of the symmetrical donor-donor polyenes **5-7** and octupoles **8-10**.

We describe the hyperpolarizability properties of these two new families. The polyenes were synthesized by using a straightforward Wittig-Horner polyvinylolation ; in all cases the structure of the obtained isomer was assigned by 500 MHz ¹H-NMR and could be confirmed for some molecules by single crystal X-ray crystallography.

The UV-VIS absorption and fluorescence spectra of these polyenes were recorded and interpreted in the light of CNDO/S calculation which allowed the identification of the different transitions. For symmetric polyenes **5-7**, large γ values were obtained from EFISH measurements ($\gamma_{1,34} = 11 \times 10^{-33}$ esu for molecules **5** and **6** with $n = 11$) with an exponential increase of the second-order hyperpolarizability with the conjugation length m (defined as $m = n + 4$).

For octupolar systems **8-10**, the modulus of β ($\|\beta\|$) were studied by CNDO/S calculations as a function of the number of double bonds n and the relation $\beta \propto n^\alpha$ was predicted as in the case of their rod equivalent **11-13**. Furthermore, the significant contribution of the octupolar component to β was shown with an improved transparency-efficiency trade-off. These theoretical results were confirmed by experimental data obtained from HRLS measurements on series **8** and **11**.

¹ Andraud, C.; Brotin, T.; Garcia, C.; Pellé, F.; Goldner, P.; Bigot, B.; Collet, A. *J. Am. Chem. Soc.* **1994**, *116*, 2094-2102 ; Brotin, T.; Andraud, C.; Ledoux, I.; Brasselet, S.; Zyss, J.; Perrin, M.; Thozet, A.; Collet, A. *Chem. Mater.* **1996**, *8*, 890-906.



A = CHO or H

UHV GROWN C₆₀/SEXITHIENYL MULTILAYERS

Carlo Taliani, Roberto Zamboni, Robert Marks, Michele Muccini
Istituto di Spettroscopia Molecolare CNR, Via Gobetti 101, 40129 Bologna, Italy
and
Rainer Mahrt.
Phillips Universitaet, Fach Phys. Chem., Marburg

A large attention has been devoted to the study of electron transfer in C₆₀/conjugated polymer composites but a detailed understanding of the basic processes is still debated. We will report on the UHV growth and characterization of multilayers of C₆₀/sexithienyl oligomer where the layers are defined at monolayer resolution with the aim to study the physics of the electron transfer process in a well-defined model system. The optical properties and the electronic structure is studied by means of absorption and photoluminescence spectroscopy. No evidence of a ground state charge-transfer state is obtained. On the other hand a new non-radiative channel opens up in multilayer compared with the separate independent films as it is shown by the dynamics of photoexcitations studied by means of transient spectroscopy. The non-linear optical susceptibility has been investigated by third harmonic generation.

presenting and contact author: , , phone: +39-51-6398531, Fax +39-51-6398539,
E-mail taliani@area.bo.cnr.it.

Nonresonant n_2 and TPA coefficient measurement in polymer waveguides by different measurement techniques

A. Bräuer*, T. Gabler°, R. Waldhäusl*, U. Bartuch°, H.-H. Hörhold°, F. Michelotti

**Fraunhofer Institut für Angewandte Optik und Feinmechanik
Schillerstr. 1, 07745 Jena, Germany*

°Friedrich-Schiller-Universität, Max-Wien-Pl. 1, 07743 Jena, Germany

Universita di Roma 1- Dip. Energetica - V.A. Scarpa, 16 I-00161 Roma, Italy

In the last few years great attention has been devoted to the study of non-resonant third order optical nonlinearities of conjugated polymers in the near infrared spectral region. The relatively high nonlinear coefficient, the processability and hybridization feasibility make such materials good candidates for photonic devices fabrication. Many π -conjugated polymers, however, have difficulties in forming stable, low loss waveguides. Thus, there are only a few reports on nonlinear optical measurements in waveguides [1].

The family of the substituted poly(phenylene-vinylene) (PPV) does not show this drawback. Substituents like mono-phenyl (MP-PPV), di-phenyl (DP-PPV) and di-phenoxy (DPOP-PPV), as well as DP-PPV/DP-PFV-copolymer result in low loss PPV waveguides (< 1 dB/cm) which are extremely stable against pulsed optical intensity (up to 16 GW/cm^2) with 9 kHz repetition rate. These materials are very good model substances for demonstration of opto-optical switching devices, because high nonlinear phase shifts can be induced.

Before designing nonlinear optical switching waveguide devices, the linear and, especially, the nonlinear optical parameters, like the nonlinear refractive index parameter n_2 and the two photon absorption coefficient α_2 and their dispersion have to be measured in order to figure out the wavelength with the highest possible n_2/α_2 ratio. Two experimental methods were explored, a semi-integrated Mach-Zehnder interferometer (MZI) [2] and spectral broadening measurements [3].

In comparison to normally used external MZIs where only one arm is a channel waveguide, in the "semi-integrated" MZI the two arms consist of neighbouring strip waveguides, similarly to a fully integrated MZI. The experimental arrangement is based on the customary set-up for end-face coupling by a microscope objective. A half wedge glass plate is put in front of the input objective. The half wedge plate splits the expanded beam of the Ti-Sapphire-Laser into two parts with slightly different propagation directions. Thus, after passing the input microscope objective, the laser light is concentrated in two focal points. The advantage of such a set-up compared to an external interferometer is a much better stability and therefore a better accuracy. Drift effects caused by temperature changes and mechanical instabilities of all optical elements have nearly equal influence on both beams in the interferometer and, thus, do not lead to an additional shift in the interference pattern. Phase shifts of about 0.05π can be detected. Because of the small optical-path-length-difference it is possible to work without an additional delay line in the ps-regime. The two spots, that are brought to interference have automatically the same spot size, so that it is very easy to get a stable interference pattern on the CCD camera.

The results of the nonlinear refractive index n_2 measurements are displayed in Fig. 1. More than one measurement point for the same material at a certain wavelength indicate that we made measurements on different waveguides. For DPOP-PPV n_2 is in the order of $1 \times 10^{-14} \text{ cm}^2/\text{W}$ and for RCo 52 it is about $2 \times 10^{-14} \text{ cm}^2/\text{W}$ in the whole investigated wavelength region between 880 nm and 990 nm. The n_2 -values for DP-PPV / DP-PFV-copolymers (RCo 52) are about a factor of two larger than those of DPOP-PPV. This corresponds qualitatively to predicted scaling laws. In particular, n_2 should increase as the absorption maximum λ_{max} is shifted to longer wavelength and

as the linear absorption coefficient at λ_{\max} and the anisotropy of the refractive indices are increased. This is correct for our materials.

Values of α_2 as a function of wavelength are plotted in Fig. 2. α_2 is a decreasing function of wavelength over the measured range.

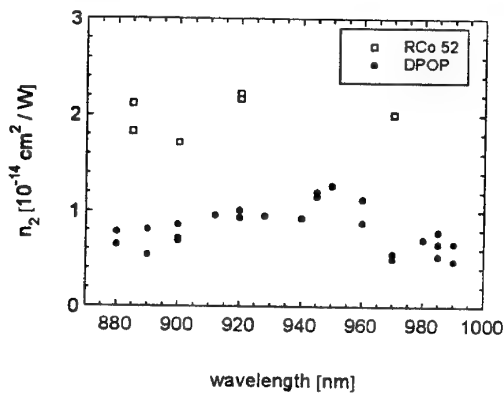


Fig. 1: n_2 dispersion of two different PPV

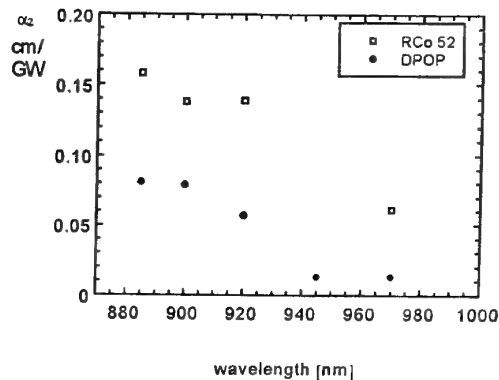


Fig. 2: α_2 dispersion

For the spectral broadening measurements, the light was injected in the quasi TE_0 mode of the channel waveguide by end fire coupling through a microscope objective. The spectrum of the transmitted light was measured by coupling the output end facet of the waveguide to the input of a spectrum analyser. The incident peak powers were measured in front of the waveguide

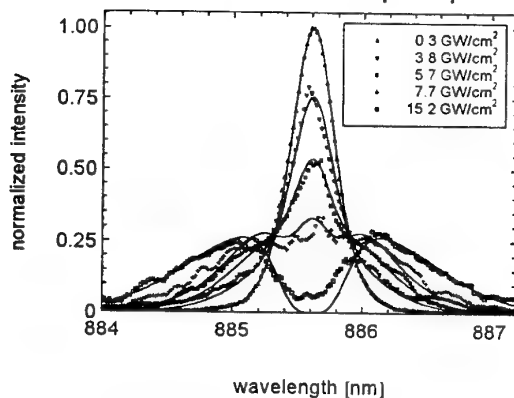


Fig. 3: Measured (markers) and calculated (lines) normalized frequency spectras for several different incoupled peak powers

and the incoupled peak powers were calculated with the coupling efficiency, that was estimated in the linear loss measurements. In Fig. 3 we show the spectrum of the transmitted beam for several incoupled peak intensities. In the low power regime the spectrum is corresponding to the one predicted for the pulse duration used and the temporal shape. Data obtained for increasing incoupled peak intensities show a broadening of the spectrum itself and the appearance of the first central minimum, corresponding to a maximum nonlinear phase shift of about 1.5π (length of waveguide 0.8 cm). The observed spectral pulse broadening is rather symmetric, indicating that the nonlinear refractive index change respond to the input pulse instantaneously.

In RCo 52-PPV, the first experimental observation of spatial solitons in a polymer waveguide was obtained [4]. To obtain a deeper understanding of the experimental results numerical simulations were carried out of the spatial- temporal objects under investigation. The numerical simulations agree quite well with the experimental findings.

- [1] M. Asobe, I. Yokohama, T. Kaino, S. Tomaru, T. Kurihara, Appl. Phys. Lett. **67**, 891 (1995)
- [2] Th. Gabler, R. Waldhäusl, A. Bräuer, U. Bartuch, R. Stockmann, H.-H. Hörhold, Optics. Comm. **137** (1997) 31-36
- [3] Th. Gabler, R. Waldhäusl, A. Bräuer, F. Michelotti, H.-H. Hörhold, U. Bartuch, Appl. Phys. Lett. (1997)
- [4] U. Bartuch, U. Peschel, Th. Gabler, R. Waldhäusl, H.-H. Hörhold Optics. Comm. **134** (1997) 49-54

Large First Hyperpolarisabilities of η^5 -monocyclopentadienyl-metal Complexes Measured by Hyper-Rayleigh Scattering.

W. Wenseleers, A.W. Gerbrandij[†] and E. Goovaerts

Physics Department, University of Antwerp-UIA, Universiteitsplein 1, B-2610 Antwerp, Belgium

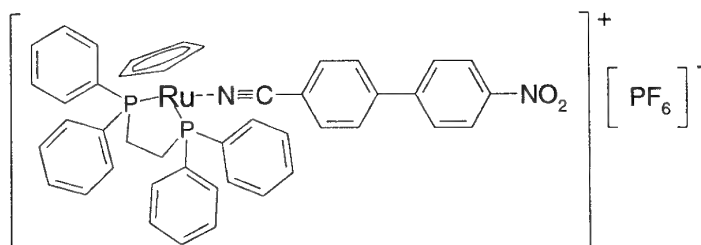
M.H. Garcia, M.P. Robalo, J.C. Rodrigues and P. Mendes

Centro de Quimica Estrutural, Instituto Superior Técnico, Avenida Rovisco Pais, 1096 Lisboa Codex, Portugal

Faculdade de Ciências, R. Ernesto de Vasconcelos, Ed. C1, 1700 Lisboa, Portugal

Abstract

During the last decade, organometallic compounds have received considerable attention for their interesting nonlinear-optical properties^{1,2}, mainly due to the strong charge transfer transitions (metal to ligand or ligand to metal) that typically occur in these compounds. We studied a series of ionic η^5 -monocyclopentadienyl-metal compounds (metal = Co, Ni, Ru, or Fe) possessing *p*-substituted benzonitrile ligands³ (see figure) by hyper-Rayleigh scattering in liquid solution⁴ at the fundamental wavelength of 1.064 μm (laser pulses of 70ps width, 2kHz repetition rate, and 20-25 μJ energy). The fact that in these compounds the metal center is in the plane of the conjugated ligand is expected to improve the NLO properties.² Furthermore, the orthogonal π and π^* orbitals of the $\text{C}\equiv\text{N}$ group have the right symmetry to interact with the *d* orbitals of the metal, favoring π -interactions. The metal was systematically varied to explore complexes in which the organometallic fragment acts as an acceptor group (metal = Co, Ni), as well as ones in which the metal is used as a donor (Ni, Ru, Fe). Complexes with organometallic fragments as acceptor groups were found to possess rather small hyperpolarisabilities, in the same order of magnitude as those of the free nitrile ligands. For Ru and Fe complexes however, very high first hyperpolarisabilities were measured, up to 360×10^{-30} esu. The high β -values are attributed to π -back-donation resulting in an extension of the conjugated π -system from the organometallic fragment - acting as a donor group - via the nitrile to the acceptor group NO_2 .



1. M.H.L. Green, S.R. Marder, M.E. Thompson, J.A. Bandy, D. Bloor, P.V. Kolinsky and R.J. Jones, *Nature*, **330** (1987), 360.
2. J.C. Calabrese, L.-T. Cheng, J.C. Green, S.R. Marder, and W. Tam, *J. Am. Chem. Soc.*, **113** (1991), 7227-7232.
3. A.R. Dias, M.H. Garcia, M.P. Robalo, M.L.H. Green, K.K. Lai, A.J. Pulham, S.M. Kuebler, and G. Balavoine, *J. Organomet. Chem.*, **453** (1993), 241-247.
A.R. Dias, M.H. Garcia, J.C. Rodrigues, M.L.H. Green, and S.M. Kuebler, *J. Organomet. Chem.*, **475** (1994), 241-245.
4. K. Clays, A. Persoons, *Phys. Rev. Letts.*, **66** (1991), 2980-2983.

[†] On leave from Gorlaeus Laboratories, University of Leiden, The Netherlands.

Relaxation dynamics in poled polymers

F. Michelotti^(a) and E. Toussaere^(b)

(a) Università degli Studi di Roma "La Sapienza"
Dipartimento di Energetica
INFM and GNEQP of CNR
Roma, Italy

(b) FRANCE TELECOM
Centre National d'Etudes des Telecommunications
Bagneux, France

A review of our recent experimental and theoretical results on poling of side-chain copolymers, either in a dc or pulsed electric field, is presented. A technique for the in-situ measurement of the electro-optic coefficient is described. Experimental results, obtained for Disperse Red 1 side-chain PMMA and its crosslinkable variant Red Acid Magly, show Williams-Watts-Kohlrausch isothermal relaxation of the 2nd order response and Vogel-Fulcher-Tamann-Hesse temperature dependence of the relaxation time constant, above glass transition T_g . On the theoretical side, the growth of the macroscopic 2nd order nonlinear optical (NLO) properties of side-chain and crosslinkable copolymer species, under application of a periodic electric poling field, is modelled. Rotational diffusion of diazo-dye dipoles, in the presence of crosslinking sites randomly distributed in the copolymer matrix, is discussed. The influence of the poling field frequency and of the density of crosslinking sites on the asymptotic 2nd order NLO properties is shown. Numerical results are compared with experimental ones, for two cited copolymers, showing a good agreement. The model can be used in order to optimize the copolymer parameters, in order to maximize the final 2nd order NLO properties.

Photoinduced birefringence in thin azo-dye doped polymer film.

G. Vitrant¹, X. Grégoire¹, H. Rezig², P.A. Chollet³ and F. Kajzar³.

1 LEMO-ENSERG, BP257, 38016 Grenoble, France.

2 L.S. Telecoms, ENIT, BP37, TUNIS 1002, Tunisia.

3 DEIN/SPE - CEA/LETI, 91191 Gif sur Yvette, France.

Photosensitive organic polymers have potential wide-range applications especially for hologram and more generally image recording. Great interest is specially put on reversible mechanisms such as photoanisotropic processes, photochromic transformations or photochemical reactions for making re-writable recording media^[1]. We believe that such phenomena may also found some applications for the optical control of waveguide devices such as switches or polarizers which justify the current detailed investigation of thin film behavior.

In this communication we report on recent results of experimentally observed photoinduced birefringence in thin-films of PMMA functionalized with DR1. It was recently pointed out by Rochon et al^[2] that such thin films can be used to record re-writable waveguide grating couplers. The origin of the grating was found to be in a change of the film thickness in the illuminated parts with respect to the unilluminated ones, rather than in a change of the refractive index of the material.

We have done pump-probe time resolved experiments in order to separate the contributions of the thickness and anisotropy changes which are produced under illumination. This is carried out recording simultaneously the time evolution of the 2 TE modes and of the 2 TM modes which are supported by the planar waveguide depicted Fig.1. Low intensity cw He-Ne laser is used as the probe at the wavelength 632.8 nm. The waveguide is made by the spin-coating deposition of a polymer film of thickness $e=635\mu\text{m}$ on a silica substrate in which a grating coupler has been previously etched. From the changes of the effective indices of the 4 guided modes, we were able to accurately deduce the changes in the thickness (Δe) and in the principal refractive indices Δn_x , Δn_y , Δn_z . These are new results which extend currently published ones^[3] and will permit a more detailed analysis of the film behavior.

As an example, we have plotted on Fig. 2, results obtained using a z-polarized incident pump with an irradiance of $4\text{mW}/\text{cm}^2$ only. The pump beam is coming from an Ar+ laser at the wavelength 514 nm which is sent perpendicular to the plane of the waveguide. Each plot consist of 4 successive pump-on/pump-off cycles which are particularly visible on the Δn_z graph. The duration of each of the 8 periods is approximately 100 seconds. The records start with a pump-on period during which we observe a strong increase of the thickness and a strong decrease of the indices n_y and n_z which only partially recovers in the next rest period as well as in the following cycles. Other experiments show totally reversible writing-erasing cycles under alternatively z and y polarised pumps which are very promising for waveguide switching applications.

The characteristics of the phenomena are being currently experimentally analysed in more details and tentative analysis in terms of photo-induced isomerisation and orientation is in progress. Conclusions will be presented at the conference

- 1 VA. Barachevsky, RA Lessard and WF Frank "Photoinduced effects in organic thin films. Polymers in optics: physics, chemistry and applications", Crit. rev. of opt. sci. and tech, 63, pp. 2-24 (1996).
- 2 P. Rochon, E. Batalla and A. Natansohn "Optically induced surface gratings on azoaromatic polymer films," Appl. Phys. Lett. 66, p. 136, (1995).
- 3 P. Rochon, J. Gosselin, A. Natansohn and S. Xie, "Optically induced and erased birefringence and dichroism in azoaromatic polymers", Appl. Phys. Lett. 60, p. 4, (1992).

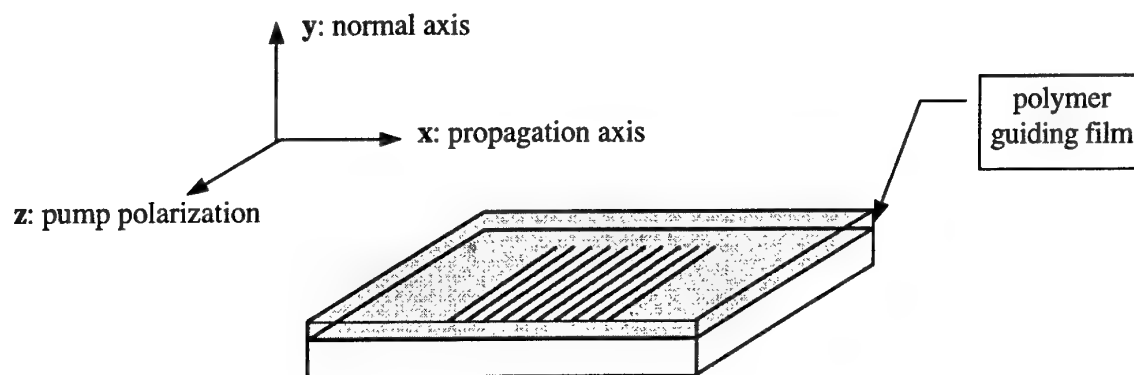


Figure 1: Sketch of the waveguide geometry using an input grating coupler.

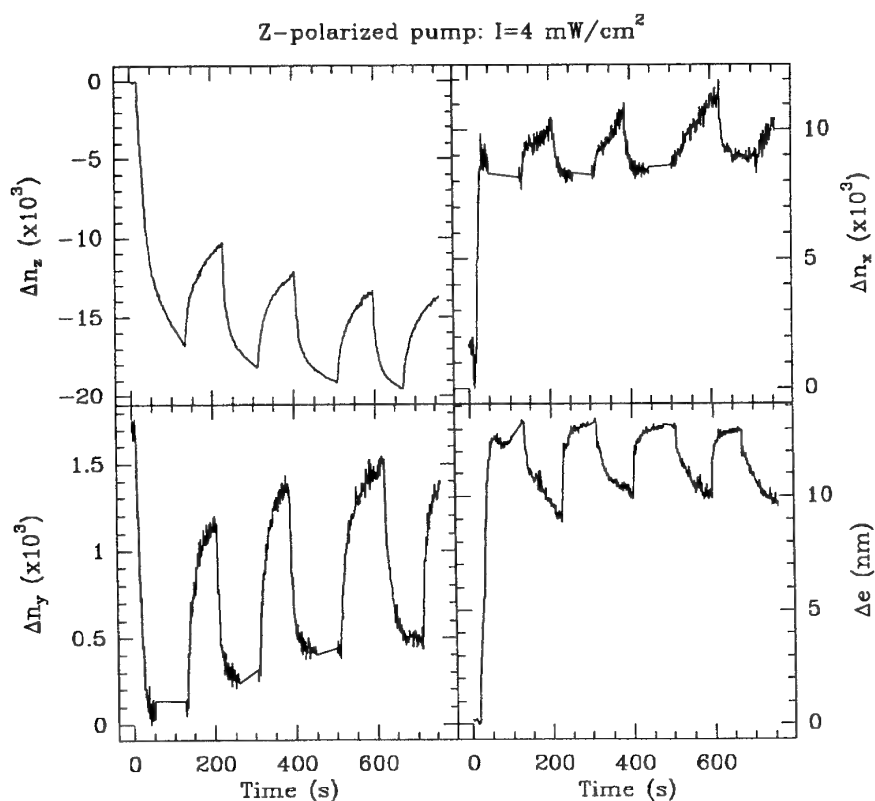


Figure 2: Measurements of optically induced anisotropy and thickness changes.

Importance of the polarizability anisotropy of donor-acceptor chromophores in the properties of low- T_g photorefractive polymers.

J. Muller, A. Fort, M. Barzoukas

*Institut de Physique et Chimie des Matériaux de Strasbourg, Groupe d'Optique
Nonlinéaire et d'Optoélectronique, UMR 046, 23 rue du Loess, 67037 Strasbourg,
France*

Photorefractive polymers (PP) having low glass transition temperatures (T_g) are being extensively studied due to their potential applications. The modulation of the refractive index, induced by illumination of PP films with a light intensity pattern, combines two different mechanisms: photoconduction and electrooptic effect. This last effect is generated by doping PP with donor-acceptor chromophores having large quadratic hyperpolarizabilities β and by partially orienting their ground-state dipoles μ_g with an electric field. Actually, it has been shown in these low- T_g materials in which molecules are free to move at room temperature, that the refractive index change is enhanced by orientational birefringence that overmatches the electrooptic contribution. This orientational birefringence is induced by the anisotropy $\Delta\alpha$ of the chromophores linear polarizability.

We describe a special experimental set-up we have developed, based on the transmission ellipsometry technique, that measures the product $\mu_g^2 \Delta\alpha$ of chromophores in solution. Furthermore, we have combined this technique with ground-state dipole moment measurements and with electric-field-induced-second-harmonic (EFISH) generation measurements to determine all the important parameters (μ_g , $\Delta\alpha$, β) contributing to the refractive index change in low- T_g PP. Consequently, this approach can be highly useful to screen the properties of various donor-acceptor chromophores before fabricating doped PP films. Finally, we present results obtained on different donor-acceptor chromophores and show how these results can be used to optimize the photorefractive response of low- T_g PP.

Photoinduced birefringence and diffraction efficiency versus temperature for various azo dye doped or linked polymers.

Pierre-Alexandre Blanche, Philippe C. Lemaire

Centre Spatial de Liège - Université de Liège

Parc Scientifique du Sart Tilman, Avenue du Pré-Aily

4031 ANGLEUR (LIEGE) - BELGIUM

phone : +32-4-3676668, fax : +32-4-3675613, E-Mail : pablanche@ulg.ac.be

Christophe Maertens, Philippe Dubois, Robert Jérôme

Laboratoire de Chimie Macromoléculaire et des Matériaux Organiques

Université de Liège, Sart Tilman (B6), 4000 LIEGE - BELGIUM

phone : +32-4-3663565 fax : +32-4-3663497

ABSTRACT

Because of the potential applications in photonics of organic systems, studies are presently focusing on polymers that reversibly change their refractive index according to illumination. Photoinduced birefringence and "true" photorefractive phenomena lead both to refractive index modulation, but reach it by two different ways. Photoinduced birefringence arises by molecular orientation with respect to the light polarization and photorefractivity by space-charge grating and electro-optic modulation. However, in organic compounds, these two effects seem not to be so far: it has appeared that photorefractivity can be enhanced by molecular orientation in the space-charge field [1] and that the same azo dye molecule can exhibit electro-optic effect and birefringence [2].

Recently, in order to better understand the microscopic effects in both phenomena, we have studied the polymer matrix PVK (Poly(N-vinylcarbazole)) doped with azo dye molecules DMNPAA (2,5-dimethyl-4-(p-nitrophenylazo)anisole) and ECZ (N-ethylcarbazole) which act as a plasticizer. We have used this compound because it has been proved that it is a good photorefractive polymer if a small amount (1 weight percent) of 2,4,7-trinitro-9-fluorenone (TNF) is added [3] and it can be used for photoinduced birefringence experiments [2]. By this study, we have pointed out the role of the temperature on the photo-induced birefringence and on the diffraction efficiency coming from the molecular photo-orientation [4-6]. Theoretical models have been proposed in order to describe the molecular behaviour according to the temperature. In these models some parameters can be correlated with microscopic quantities like the free volume of the polymer or the orientation efficiency of the chromophores.

In this paper, we present the influence of glass transition temperature and the link between the polymer and the chromophore on the photoinduced birefringence versus temperature. Indeed, these parameters influence the free volume of the polymer and the ability, for the chromophore molecules, to reorient themselves into the polarized laser beam. Comparison between experimental results and theoretical models are presented.

On the basis of the same copolymer matrix "PCn": [n(N-carbazolyl)undecyl methacrylate] where n is 6 or 11, and [2,5-dimethylphenyl-[(4-nitrophenyl)azo]-phenoxy alkylmethacrylate], we have chemically linked the chromophore DMNPAA by different ways. Thus, the alkyl group linking the DMNPAA molecules to the copolymer can be changed between hexyl (6 carbons) and undecyl (11 carbons). The DMNPAA can also be added without any chemical bound, by simply blending it with the polymer.

For the experiments according to the glass transition temperature (T_g), we have used the PVK:DMNPAA:ECZ compound where the concentration of the plasticizer (ECZ) varies. By this way, the T_g can be modulated between 10°C to 70°C and the other parameters remain constant.

These experiments, coupled to our models, allow to refine the understand of the photoinduced orientation of the azo dye molecules, and the different factors influencing it. This permits to improve the different figures of merit in order to develop a better medium for holographic recording.

1. W.E. Moerner, S.M. Silence, F. Hache, G.C. Bjorklund, Journal of the Optical Society of America B, Vol.11, n°2, 320-330, (1994).
2. P.-A. Blanche, Ph.C. Lemaire, C. Maertens, P. Dubois, R. Jérôme, to be published in Optics Communication.
3. K. Meerholz, B.L. Volodin, Sandalphon, B. Kippelen, N. Perghambaran, Nature, Vol.371, 6 October 1994.
4. P.-A. Blanche, Ph.C. Lemaire, C. Maertens, P. Dubois, R. Jérôme, proceeding of the 5th conference on polymer characterization "POLYCHAR-5", Denton, Texas USA, January 1997.
5. P.-A. Blanche, Ph.C. Lemaire, C. Maertens, P. Dubois, R. Jérôme, submitted to Polymer Engineering and Science.
6. P.-A. Blanche, Ph.C. Lemaire, C. Maertens, P. Dubois, R. Jérôme, to be presented to the JSAP/OSA Topical Meeting on "Photorefractive materials effects and devices", Chiba, Japan, June 1997.

Channel-Type Inclusion Lattices of Perhydrotriphenylene : a New Route to Orientation-Confined Nonlinear Optical Molecules

J. Hulliger, P. J. Langley, A. Quintel, P. Rechsteiner

Department of Chemistry and Biochemistry, University of Berne

Freiestr. 3, 3012-Berne, Switzerland

fax ++41 31 631 3993, e-mail hulliger@IAC.unibe.ch

A supramolecular approach demonstrates that linearly shaped NLO building blocks exhibit parallel alignment when co-crystallized with perhydrotriphenylene (PHTP). In the case of D,A-disubstituted guest molecules, materials exhibiting macroscopic polar properties were obtained with a success rate of nearly 95%.

The design of molecular materials exhibiting optimum linear *electro-optic* (EO) or *third order nonlinear optic* (NLO) properties requires that molecular building blocks possessing high β_{zzz} or γ_{zzzz} values undergo a parallel packing in the solid state. Despite the report of the syntheses of a large number of molecular systems with NLO properties, there are only a few EO materials for which crystal packing results in a nearly parallel alignment of the β_{zzz} -axes.

Recently, Ramamurthy et al. [1] and Eaton et al. [2] reviewed the tailoring of the solid state, the optical and NLO properties of some *channel-type inclusion lattices*. Channel-type inclusion lattices formed by PHTP and typical NLO molecules open up a promising route towards efficient organic EO crystals [3]: formation of PHTP-NLO systems yielded materials exhibiting macroscopic polar properties in close to 95% of present synthetic attempts (over 30 cases). Although a host component such as PHTP will reduce the density of dipoles when compared to single component NLO materials, the *supramolecular approach* is particularly of interest in the case of NLO molecules whose native crystals are centrosymmetric (close to 75% of known examples) or exhibit a non-parallel alignment of dipoles (over 95% of known examples).

Besides the achievement of parallel packing and a surprisingly high yield of polar materials, there are other important advantages of using a dilute but crystalline material (in the PHTP-guest system, NLO molecules are separated by an inter-channel distance of ~ 14 Å): photochemical degradation of NLO components is topochemically restricted to an interaction of donor (D) and acceptor (A) groups only; and due to the absence of an efficient intermolecular π -interaction, no bathochromic shift is to be expected.

Thus far, only an optimization of the EO effect has been addressed. However, design of *organic photorefractive materials* [4] comes to the conclusion that channel-type inclusion lattices would be optimum if photoconduction along individual channels could be achieved.

Racemic all-*trans*-PHTP is known to form continuous channel-type inclusion lattices with a variety of guest molecules and polymers. The solid state of PHTP-guest is built up by stacked PHTP molecules leaving space for hexagonal or orthorhombically/monoclinically distorted channels filled by oblong guest molecules. X-ray analysis revealed that guest molecules undergo close packing along the channels and in some cases hydrogen bonding or polarization induced functional group interaction is observed. This implies that dilution of the dipoles is restricted to two dimensions only (molar ratio PHTP:NLO = 2:1, with respect to 2-D honeycomb packing). Axial protons of PHTP moieties provide a nearly uniform and non-polar van der Waals potential of the channel wall, and are therefore suited to accommodating the less polar part of the van der Waals surface of dipolar guest molecules whose lateral dimensions do not exceed an average channel diameter of ~ 5 Å. Diffuse scattering phenomena observed on rotating X-ray crystal photographs of PHTP-NLO indicate a lateral disorder of parallel dipolar strings extending along different channels.

In order to provide guidelines to the design of NLO frames required to be included, we have explored the inclusion capacity of the PHTP host compound with respect to representative π -conjugated molecular frames [3] attached to commonly used D and/or A substituents. As a result of a broad study comprising of more than 50 different systems, we can conclude that a variety of structural elements discussed in ref. [3] represent valuable choices. Although we could demonstrate that these inclusion lattices show polar properties, we have to discuss the real structure i.e. the domain structure of the materials. Theoretical models and experimental work on the formation of 180° domain states will be presented as well.

[1] V. Ramamurthy, D. F. Eaton, *Chem. Mater.*, **6**, 1128-1136 (1994). [2] D. F. Eaton, A. G. Anderson, W. Tam, Y. Wang, *J. Am. Chem. Soc.*, **109**, 1886-1888 (1987); W. Tam, D. F. Eaton, J. C. Calabrese, I. D. Williams, Y. Wang, A. G. Anderson, *Chem. Mater.* **1**, 128-140 (1989). [3] J. Hulliger, O. König, R. Hoss, *Adv. Mater.*, **7**, 719-721 (1995); R. Hoss, O. König, V. Kramer-Hoss, U. Berger, P. Rogin, J. Hulliger, *Angew. Chem. Int. Ed. Engl.*, **35**, 1664-1666 (1996); O. König, U. Berger, J. Hulliger, *Proc. SPIE Vol. 2852*, Nonlinear Optical Properties of Organic Materials IX (Ed.: G.R. Moehlmann), 23-31, 1996; O. König, J. Hulliger, *Nonlinear Optics* (1996), in press. [4] J. Hulliger, O. König, P. Rogin, P. Rechsteiner, A. Quintel (Ritzi), P. J. Langley, *SPIE Proc. Vol. 2850*, Organic Photorefractive Materials and Xerographic Photoreceptors (Ed.: S. Ducharme), 54-62, 1996.

The quantum cascade laser: a unipolar semiconductor laser for the mid-infrared

Carlo Sirtori

Thomson-CSF, Laboratoire Centrale de Recherches, 91404 Orsay, France

Quantum cascade (QC) lasers are unipolar semiconductor lasers based on electronic intersubband transitions. These transitions connect states of the same band (conduction or valence) arising from size quantization in quantum wells and as such depend on the shape of the envelope functions of the initial and final state of the transition. By judicious control of the quantum well widths and the tunneling barrier thickness one can conceive artificial potentials such that energy level separations, dipole matrix elements, lifetimes and scattering times are dependent on the characteristic potential design.

The laser consists of many stages in series of coupled quantum wells which, under a strong electric field, originate a potential stair case where electrons streaming down, sequentially emit photons at the steps and as such this light source is not based on the radiative recombination of electrons and holes like in conventional laser diodes. Each stage consists of two parts: the "active region" where photons are generated and the "injector / relaxation" region. The latter is a digitally graded superlattice which plays the role of injector on one end of the active region and that of collector on the other. After the emission of photons, electrons proceed into the injector, thermalize and finally enter into the next active region. In this way during their path across the quantum structure they are "recycled" a number of times equal to the total number of stages.

Using InGaAs/InAlAs material system, grown lattice matched on InP, different quantum cascade lasers have been fabricated with wavelengths spanning from 4.2 to 11.5 μm . Pulsed operation at and above room temperature has been achieved in the whole spectral range demonstrating the first room temperature semiconductor laser at these wavelengths. A specific set of devices designed to enhance the performance at high temperature have delivered more than 200 mW peak power at 300 K at 5 μm wavelength. After a general description of the laser performance, new designs and results of structures for two colour lasers and for electrical tuning of wavelength will be presented.

Spontaneous emission and nonlinear effects in photonic band gap materials

J.P.Dowling

Weapons Sciences Directorate AMSMI-RD-WS-ST
Alabama USA.

Summary not available at time of printing.

Linear and Nonlinear Optical Absorption in $\text{Zn}_{1-x}\text{Cd}_x\text{Se}/\text{ZnSe}$ Multi-Quantum Wells

A. Adinolfi, F. Minerva, M. C. Netti, R. Tommasi, * M. Lepore and I. M. Catalano
Dipartimento di Fisica e Istituto Nazionale per la Fisica della Materia, Università di Bari,
via Amendola 173, I-70126 Bari, Italy

Interest in optical devices in the visible spectrum has motivated the exploration of several modulated structures involving zinc chalcogenides and their alloys.

$\text{Zn}_{1-x}\text{Cd}_x\text{Se}/\text{ZnSe}$ MQW's exhibit stable excitons at room temperature and a reduced exciton-phonon coupling, promising to be good candidates for the development of coherent emitters in the blue-green spectral region.

We performed a detailed investigation of the excitonic properties of $\text{Zn}_{1-x}\text{Cd}_x\text{Se}/\text{ZnSe}$ MQW's with different cadmium concentration by means of one- and two-photon absorption photoluminescence excitation (OPA-PLE, TPA-PLE) spectroscopy.

The different parity selection rules governing the one- and two-photon absorption processes allowed us to selectively probe the fundamental and excited excitonic states (OPA allowed 1s and TPA allowed 2p) associated with the $n = 1, 2$ subbands. Moreover TPA spectroscopy permitted also to investigate the excitonic property dependence on the exciting field polarization vector ($\vec{\epsilon}$) with respect to the carriers confinement direction (z).

We report here representative low-temperature emission spectra for the sample with a 26% cadmium content and a well width of 3 nm. In Fig. 1 we show PL and OPA-PLE spectra and in Fig. 2 TPA spectra for both exciting configurations.

The comparison between experiments and theoretical prediction, when strain is taken into account [1,2], allowed us to single out a well defined set of band parameters and to gauge the band-offsets in these heterostructures.

Thanks to the evident band edge in the TPA spectrum measured in the $\vec{\epsilon} \perp z$ configuration, it has been possible to measure the binding energies of the $n = 1, 2$ TPA allowed excitons. Furthermore we obtain the first clear experimental evidence of $n = 2$ light-hole excitons even if they are weakly bound only by Coulomb interaction.

Acknowledgements

The authors wish to acknowledge A. Franciosi, L. Sorba, and L. Vanzetti from Laboratorio Tecnologie Avanzate Superfici e Catalisi dell'Istituto Nazionale per la Fisica della Materia, for providing the samples.

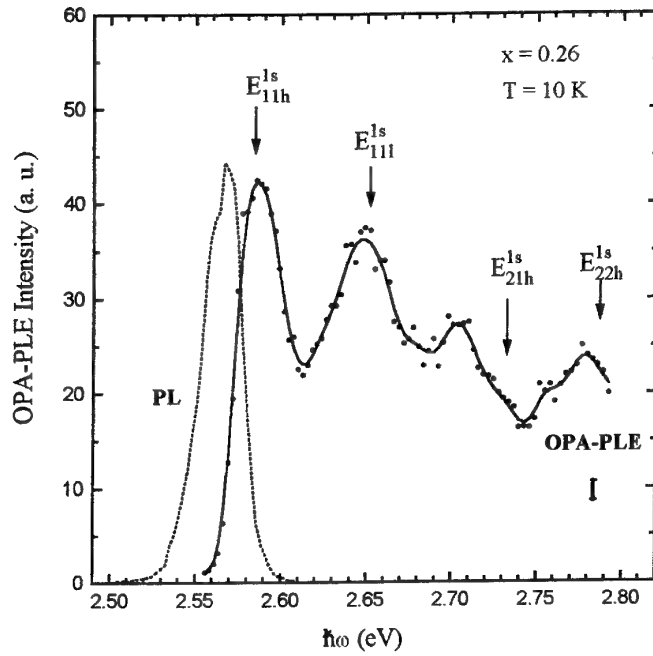


Fig. 1. PL and OPA-PLE spectra from $\text{Zn}_{1-x}\text{Cd}_x\text{Se}/\text{ZnSe}$ multiple quantum wells with $x = 0.26$ at $T = 10$ K. The arrows mark the positions of the theoretical excitonic transition energies.

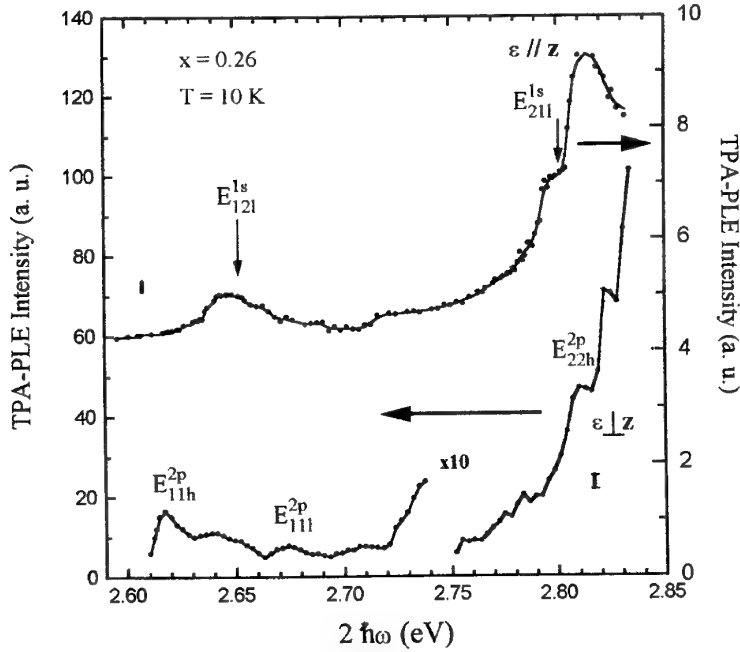


Fig. 2. Two-photon absorption photoluminescence excitation (TPA-PLE) spectra from $\text{Zn}_{1-x}\text{Cd}_x\text{Se}/\text{ZnSe}$ multiple quantum wells with $x = 0.26$ at $T = 10$ K obtained in the $\varepsilon \perp z$ and $\varepsilon // z$ electric field polarization configurations. The arrows mark the positions of the theoretical excitonic transition energies.

(*) Permanent address: Istituto di Fisica Medica, Università di Bari, via Amendola 173, I-70126 Bari, Italy

[1] H. S. Cho, P. R. Prucnal, Phys. Rev. B, **36**, 3237 (1987)

[2] V. Pellegrini et al., Phys. Rev. B, **51**, 5171 (1995)

Microcavities for Non Linear Optics.

V. Berger, X. Marcadet and J. Nagle,

THOMSON CSF Laboratoire Central de Recherches, Domaine de Corbeville, 91400 ORSAY FRANCE.

Tel: 33 1 69 33 90 84, email:berger@lcr.thomson.fr

Frequency conversion in monolithic semiconductor microcavities is theoretically investigated. Semiconductors like GaAs are highly interesting for frequency conversion because of their high second order non linear coefficient. However, since those materials are not birefringent, the problem of phase matching has to be solved.

In the first part, second harmonic generation in a doubly resonant monolithic cavity is studied. Intracavity phase matching is investigated. It is shown that both the double resonance condition and the phase matching condition for the two counter propagating second harmonic intracavity waves can be satisfied with a cavity length equal to the coherence length of the non linear process, and with well designed mirror phases. For that purpose, metallic mirrors are well suited, but multilayer mirrors acting exactly as metallic mirrors, as far as the second harmonic generation process is concerned, are preferable. Such "pseudo metallic" multilayers dielectric mirrors are presented. The possibility of maintaining the double resonance with only one tuning parameter is also investigated. This point is very important since two tuning parameters are not practical in a realistic device.

In the second part, difference frequency generation in a GaAs microcavity is proposed. This scheme can be used to generate mid IR frequencies with two near IR pump sources. Both pumps are resonant with two longitudinal modes of the wide microcavity, and the Bragg mirrors are transparent for the mid IR. For this normal incidence non linear process, it is then necessary to grow a (111) GaAs microcavity. Whereas microcavities of finesses up to several thousands have been demonstrated on (100) GaAs, this kind of thick layers growth on (111) orientation is much more difficult. This is illustrated by preliminary experimental results.

Four-wave mixing in semiconductor optical amplifiers.

Antonio Mecozzi
Fondazione Ugo Bordoni
Via B.Castiglione, 59 00142 Roma ITALY

We will review recent four-wave mixing experiments in semiconductor optical amplifiers, including experiments where a recently proposed technique permits the use of femtosecond pump and probe pulses for investigating the optical nonlinearities of waveguide devices. These experiments may provide informations on the coherence properties of the ultrafast nonlinear response of an active semiconductor device to an optical pulse excitation.

Polarization Changing nonlinearities in Semiconductor doped Glasses

K.C.Rustagi,K.S.Bindra and S.M.Oak
Centre for Advanced Technology,Indore 452013,India

In the picosecond regime, resonant optical nonlinearities in semiconductor doped glasses are quite well understood in the band filling model. In the simplest such model, the change in dielectric function induced by the laser is isotropic and is not expected to contribute to Optical Kerr Effect. We report here our results on OKE just below and just above the band edge. The measured signal corresponds to a nonlinear susceptibility comparable to the intensity dependent refractive index and shows strong increase across the band edge. The response time and fall time are both faster than our laser pulse (20 ps). Possible mechanism of this nonlinearity are discussed.

"Investigation of finite size effects in CdS doped sol-gel thin films by optical absorption and micro-Raman spectroscopy".

G.Ventrucci, L.Chiavarone, M.Lugarà, V.Spagnolo, M.Ferrara, G.C.Righini*

Dipartimento Interateneo di Fisica - Unità INFM - Bari (Italy).

*IROE-CNR - Firenze (Italy).

In the last few years II-VI semiconductor nanocrystals embedded in glass matrix have received considerable attention due to their novel properties and promising applications as short-response-time non linear optical devices. For non-linear optical applications, it is important to study thin films of the active material due to their wave-guiding behaviour.

One of the most promising techniques used in growing thin films is the sol-gel process already widely involved in industrial processes for devices production due to a good stoichiometric control, good homogeneity of the film structure and low sintering temperature. This last feature avoids several inconveniences of classical methods such as oxidation and coalescence at high temperature.

In order to investigate quantum confinement effects and some correlations between growth conditions and optical properties in CdS doped sol-gel thin films, we performed micro-Raman and linear absorption spectroscopy measurements.

CdS doped sol-gels were prepared by hydrolysis and condensation polymerization of organic precursor. Thin films were then prepared by dip-coating the gel onto silica substrates. In order to obtain films with the same thickness ($\sim 0.4\mu\text{m}$), slow withdrawal from the gel was carried by properly adjusting the speed of the motor.

Absorption and Raman spectra gave us experimental evidence of quantum size effects in these samples. The absorption edges were blue-shifted, compared with bulk CdS crystal, due to the carrier confinement. In particular, the MRIII sample showed a shoulder relative to the excitonic transition from the highest hole subband to the lowest electron subband (fig. 1a).

The localization of the phonon wave function causes the relaxation of the $q=0$ selection rule in the first-order Raman scattering which, in turn, results, for materials with a negative phonon dispersion, in a red-shift of the peak position and a low-frequency asymmetric broadening of the Raman bands (1,2). These effects were observed in our samples (Fig. 1b - MRIII sample). The smaller the crystal dimensions, the stronger the finite size effects, i. e. the red-shift of the peak position is a decreasing function of the nanocrystals mean radius. This behavior allowed to assess the mean radius of the samples and analyze its dependence on the molar ratio (M) of Cadmium precursor to the capping agent in the starting gel solution (Fig.2).

Besides, a combination of micro-Raman and absorption measurements gave us information about the crystal quality of CdS nanocrystals and the scattering centre density as a function of the concentration of Cadmium precursor.

The linear absorption was measured as a function of temperature in order to study the phonon-electron interaction in these nanostructures.

Figure 3 shows the shift of the first absorption peak as a function of temperature for MR III sample. The experimental value of dE_G/dT of the band gap energy is $dE_G/dT = -2.4 \cdot 10^{-4} \text{ eV K}^{-1}$ in the range 70-300K. It is smaller than the CdS bulk value, $dE_G/dT = -4.1 \cdot 10^{-4} \text{ eV K}^{-1}$, due to an increase of the excitons - LO phonon interactions with confinement (3).

References

- [1] H.Richter, Z.P.Wang and L.Levy, Solid State Commun. 39,625 (1981).
- [2] I.H.Campbell and P.M.Fauchet, Solid State Commun. 58, 739 (1986).
- [3] S.Nomura, T.Kobayashi, Phys.Rev.B45(3), 1305 (1992).

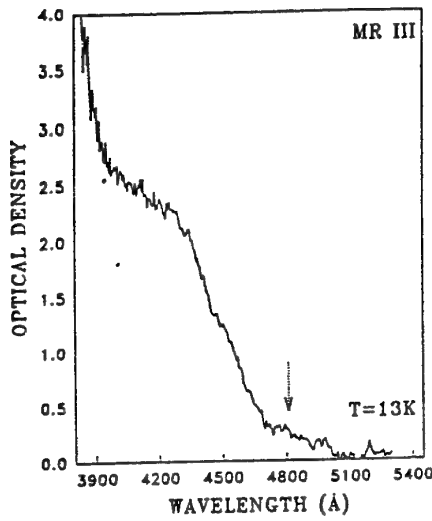


FIG. 1A

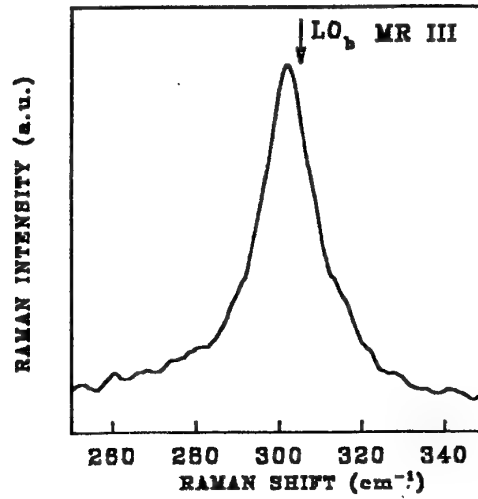


FIG. 1B

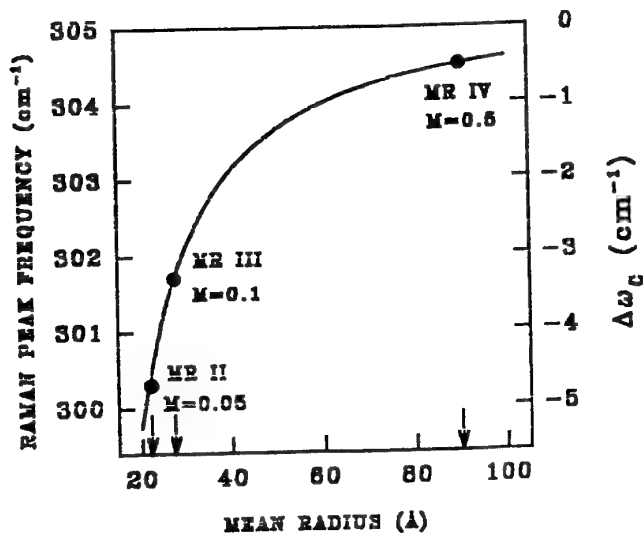


FIG. 2

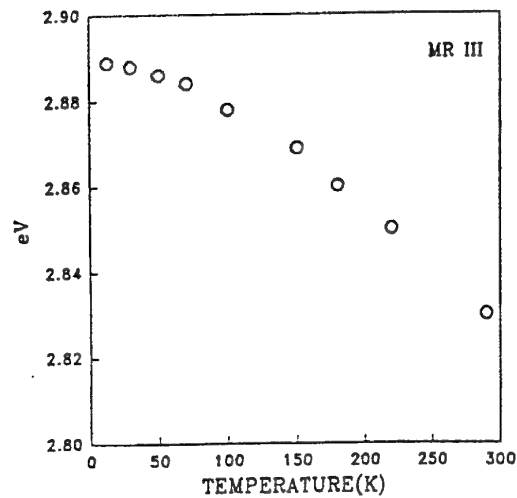


FIG. 3

Nonlinear Optics in Semiconductors and Multiquantum Wells

Heinrich Kurz

Institut für Halbleitertechnik, RWTH Aachen, Sommerfeldstr. 24, D-52056 Aachen,

Tel. +49-241-807890, FAX +49-241-8888 246, e-mail: kurz@iht-ii.rwth-aachen.de

Semiconductors and semiconductor heterostructures allow to tailor nonlinear optical properties of matter in a well defined way concerning the desired wavelength, speed, and the strength of the nonlinearity. Especially the confinement of electrons and holes in quantum wells allows to fabricate structures exhibiting enhanced nonlinear optical effects associated with excitonic transitions. By applying femtosecond spectroscopy, it has been made possible to study the coherent and incoherent properties of these systems with a high temporal resolution, thus gaining detailed insight into the processes involved into the interactions of photons, electrons and the crystal lattice.

One of the most important interactions determining the response of semiconducting devices is carrier-phonon interaction via the Fröhlich interaction. At room temperature, where the thermal occupation of LO phonons is high, the ultrafast nonlinear response at the lowest exciton transition is strongly affected by the rapid thermal dissociation of excitons. A detailed analysis of the nonlinear transmission change associated with these transitions exhibits the importance of phonon-assisted transitions within the valence band structure.

Of particular importance for the development of THz devices are the coherent properties of semiconductors prepared by the excitation of several electronic eigenstates with an ultrashort laser pulse. In semiconductor superlattices, coherent wavepacket oscillations, denoted as Bloch oscillations, are observed up to room temperature and frequencies ranging from 200 GHz up to 10 THz. In this system, LO-phonon scattering of electronic distributions plays an important role concerning the phase coherence of Bloch oscillations.

Beside the above discussed quantum confined systems, a very attractive candidate for ultrafast devices for the generation of THz radiation, nonlinear switches, and as photorefractive medium is low-temperature grown GaAs (LT GaAs). This materials is grown by MBE at temperatures of approx. 200°C leading to the growth of non-stoichiometric material with excess As in the order of a few percent. After high temperature annealing, most of the excess As precipitates into arsenic clusters. The annealed material exhibits a carrier lifetime in the sub-picosecond regime based on the trapping of carriers at point/defects and/or As clusters. We observe a strong ultrafast optical nonlinearity in this bulk material close beneath the band gap, which is comparable to the nonlinearities obtained in quantum confined systems. We attribute this observation to the presence of shallow bound states associated with potential fluctuations.

Control of the second and third order nonlinearities in GaAs/AlGaAs multiple quantum wells

J. S. Aitchison*, C. J. Hamilton*, M. W. Street*, N. D. Whitbread*, D. C. Hutchings*, J. H. Marsh*, G. T. Kennedy† and W. Sibbett†.

* Department of Electronics and Electrical Engineering, University of Glasgow, Glasgow. G12 8QQ UK.

† Department of Physics and Astronomy, University of St. Andrews, St. Andrews, Fife, KY16 9SS

We report on the use of impurity free vacancy disordering techniques to control the nonlinear optical properties of GaAs/AlGaAs multiple quantum wells. This process results in a shift in the position of the absorption edge to higher energy and has been used to modify the second and third order nonlinear coefficients. We have observed a reduction of ~50% in the value of n_2 for a band gap shift of around 40 nm. This change arises due to the combined effects of increasing the band gap and increasing the detuning. The process can also result in a modulation on the magnitude of the $\chi^{(2)}$ coefficient and provides a potential mechanism for realising quasi-phase matched structures.

**SELECTIVELY OXIDIZED GaAs/AlAs HETEROSTRUCTURES: A
MATERIAL WITH HUGE ARTIFICIAL BIREFRINGENCE ($\Delta n = 0.22$) FOR
PHASE-MATCHED NONLINEAR FREQUENCY CONVERSION**

A. Fiore, V. Berger, E. Rosencher, N. Laurent and J. Nagle

Laboratoire Central de Recherches - THOMSON-CSF

Domaine de Corbeville - 91404 Orsay (France)

We demonstrate the use of AlAs selective lateral oxidation¹ to realize huge birefringence GaAs/(Al-oxide) heterostructures. The form birefringence² available in these high-index contrast multilayer waveguides can be used to phase match nonlinear frequency conversion. Both difference frequency generation of mid-infrared radiation from near-infrared sources and frequency conversion around 1.5 μm can be phase-matched³.

Birefringence is measured⁴ by monitoring the second harmonic (SH) fringes created along the guide by the nonlinear interaction of counterpropagating TE and TM modes (Fig. 1 (a)). Fig. 1(b) shows the SH fringe pattern imaged on the surface of a waveguide containing a single 100 nm AlAs layer between a GaAs core and an AlGaAs cladding, before (upper part) and after (lower part) oxidation. From the measured fringe period we deduce that birefringence is enhanced from $\Delta n(\text{UNOX})=0.017$ to $\Delta n(\text{OX})=0.038$ due to oxidation. We then measured the birefringence in a waveguide composed of a five-layer 270 nm $\text{Al}_{0.1}\text{Ga}_{0.9}\text{As}$ / 25 nm Al-oxide heterostructure embedded between two Al-oxide cladding layers. Fig. 2 shows the far-field image of the surface-emitted SH from the waveguide surface, before and after oxidation. The corresponding measured birefringences are: $\Delta n(\text{UNOX})=0.013$ and $\Delta n(\text{OX})=0.22$. The birefringence in the oxidized waveguide is sufficient to phase match difference frequency generation of 5 μm radiation from two ≈ 0.9 μm sources.

¹ A. R. Sugg, J. N. Holonyak, J. E. Baker, F. A. Fish, and J. M. Dallesasse, *Appl. Phys. Lett.* **58**, 1199 (1991).

² J. P. v. d. Ziel, *Appl. Phys. Lett.* **26**, 60 (1975).

³ A. Fiore, V. Berger, E. Rosencher, N. Laurent, S. Theilmann, N. Vodjdani, and J. Nagle, *Appl. Phys. Lett.* **68**, 1320 (1996).

⁴ D. Vakhshoori, M. C. Wu, and S. Wang, *Appl. Phys. Lett.* **52**, 422 (1988).

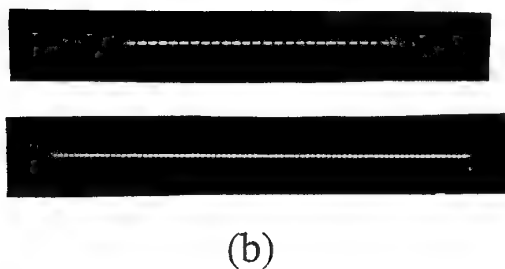
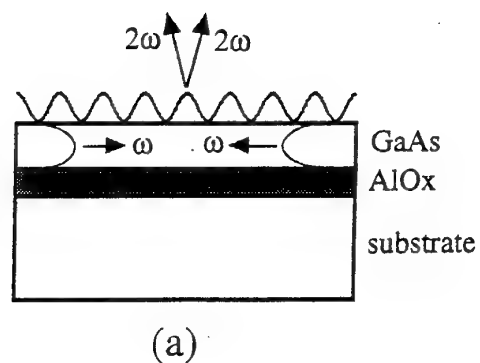


Fig. 1: (a) Schematics of surface-emitting second harmonic generation in GaAs/AlAs oxidized waveguides. (b) CCD near-field images of the second harmonic surface-emitted from single-layer unoxidized (upper part) and (lower part) oxidized waveguides. The YAG pump beam propagates along the axis of the SH pattern.

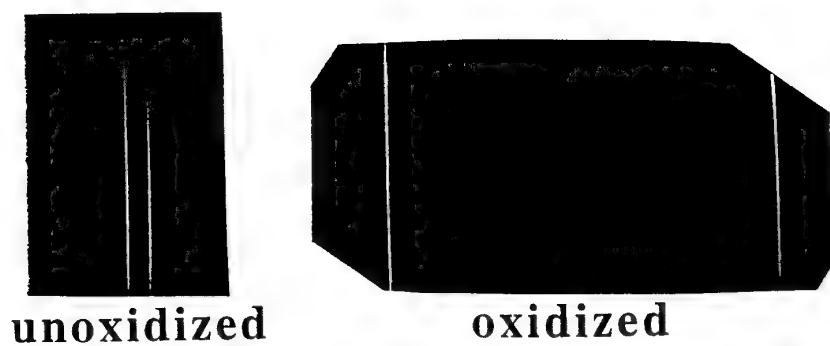


Fig. 2: CCD far-field images of the second harmonic surface emitted from a GaAs/AlAs multilayer unoxidized and oxidized waveguides.

NONLINEAR OPTICAL PROPERTIES OF AMORPHOUS CHALCOGENIDE SEMICONDUCTORS

A. Andriesh and V. Chumash

Center of Optoelectronics, I. A. P., Academy of Sciences of Moldova
Academiei St. 1, Chisinau, 2028, MOLDOVA

The linear and nonlinear photoinduced optical phenomena in chalcogenide glasses (ChG) have recently been extensively studied using thin films, planar waveguides and optical fibers. Many of linear phenomena are described in terms of the model with carrier multiple trapping on the localized states. In the same time there exist photoinduced phenomena leading to nonlinear behavior of optical constants which require to involve other physical models of explanation.

In this paper the peculiarities of the nonlinear interaction of laser pulses with the ChG (As_2S_3 , As_2Se_3 , AsSe , GeSe_2 , $\text{As}_{22}\text{S}_{33}\text{Ge}_{45}$) are studied, showing that these glasses are an interesting material for high speed optoelectronics. Attention is primary given to those nonlinear phenomena that are characteristic of the amorphous semiconductors, and, as a rule, have no analogous in crystalline phase. The physical mechanisms, which can contribute to the nonlinear light absorption in ChG under pulsed excitation, are critically reviewed and a model of the physics of the nonlinear interaction of strong light with amorphous semiconductor, taking into account the light interaction with nonequilibrium phonons and localized vibrational excitations, is considered for the explanation of the experimental results. The photoinduced phenomena could be used in a range of optical components for optical and optoelectronics devices. ChG are attractive candidates for the fabrication of holographic and discrete optical recording media, as well as, for all-optical passive and active devices in the same medium. In recent years a variety of both passive (fibers, planar waveguides, lenses, gratings) and active (nonlinear devices based on Fabry-Perot interference, optical bistability and optical hysteresis) elements have been demonstrated [1-3].

It is shown that increasing the incident light intensity over some threshold value (I_t) leads to a nonlinear light transmission by the ChG films [1-5]. As a result of the nonlinear light absorption a change of the time profile of the laser pulses was recorded, which leads to hysteresis-like dependencies of the output light intensity (passed through the sample) on the corresponding value of the input. The photoinduced increase of the ChG light absorption coefficient has a reversible character, i.e. the medium fully restores to its initial transmission state after the ending of the laser pulse, and if the same place of the sample is irradiated with another laser pulse the effect can be completely repeated.

The main peculiarities of the nonlinear laser transmission in ChG thin films are the following: a nonlinear increase of the light absorption coefficient; a nonlinear refractive index change, whose magnitude depends strongly on the excitation intensity; the threshold character of the nonlinear transmission; the change of the time profile of the laser pulses, leading to a hysteresis transmission dependence; the characteristic time constants of the sample photoinduced darkening, which does not exceed the laser pulse duration; the independence of the nonlinear transmission character on the light beam diameter, on the film thickness, and on the substrate material; the weak dependence from the laser pulse wavelength; the successive step character of restoration of light transmission initial state; the full restoration of light transmission initial state in a microsecond time interval; the temperature behavior of the parameters of the nonlinear interaction (the invariance of the light intensity threshold values and of the transient time into the nonlinear light absorption state); the independence on the photostructural transformations.

The different viewpoints of the physical mechanisms that can explain the peculiarities of the nonlinear light absorption in ChG are discussed briefly in [1-6]. Experimentally was demonstrated that it is impossible to explain the laser pulse nonlinear transmission by the homogeneous heating of the ChG films [1-5]. This impossibility was demonstrated by femtosecond spectroscopy measurements also [6].

Laser pulses with $\sim 1,5$ J energy were used, which can not provide a substantial heating during probe excitation with 100 fs pulses at 300 K.

A distinctive peculiarity of the amorphous semiconductors is the presence of a high ($10^{16} - 10^{19} \text{ cm}^{-3}$) density of the localized states in the optical band gap [2]. As a rule, in the literature the light absorption peculiarities in the ChG transparent region are connected with carrier occupation and redistribution on these states. However, the laser pulse nonlinear absorption at ChG interband excitation, presented in this work, cannot be explained on the basis of the occupancy and redistribution of the carriers on the localized states with their next excitation in the conduction band. It is conditioned by the fact that the probability of the transitions "localized state-band" is some orders lower than the interband optical transitions probability and, it is rather difficult to experimentally distinguish such a low contribution to the absorption (at the same light wavelength) from the interband absorption [1-5]. The direct experiment, which additionally confirms the impossibility of application of the model based on the occupancy and redistribution of the carriers on the localized states with their next excitation in the conduction band, is the measurement of nonlinear laser pulse absorption in a-Si:H films [7-9]. In spite of difference between spectrum of the localized states in the band gap of the a-Si:H and of the chalcogenide glasses, the peculiarities of the laser pulse nonlinear absorption in a-Si:H films (measured in the similar excitation conditions) qualitatively are the same as in the case of chalcogenide glasses.

The temperature behavior of the linear and nonlinear optical absorption in ChG and a-Si:H films points to the important role which phonons play in the process of the interband light absorption. The peculiarities of nonlinear light absorption can be understood in the framework of the model of the nonlinear interaction of powerful light with ChG, taking into account the light interaction with nonequilibrium phonons and localized vibrational excitations. In order to demonstrate the adequacy of the proposed model, an additional experiment was performed. The main point of this model is the localization of vibrational excitations. The peculiarities of the laser pulse absorption in films of amorphous and crystalline (without localization possibilities) As_2S_3 films were measured in the similar excitation conditions, and no dependence of pulse absorption in crystalline As_2S_3 from the pulse intensity was revealed.

In conclusions, the nonlinear interaction of laser pulses with ChG and a-Si:H films have been investigated, which can be explained by the model taking into account the interaction with nonequilibrium phonons and localized vibrational modes. This model and the model with carrier multiple trapping on the localized states may explain the most peculiarities of interaction of light with amorphous materials.

1. V. Chumash, I. Cojocaru, E. Fazio, F. Michelotti, M. Bertolotti. Progress in Optics, **36**, pp. 1-47, 1996.
2. M. Popescu, A. Andries, V. Ciumas, M. Iovu, S. Sutov D. Tiuleanu. Fizica Sticlelor Calcogenice, Ed. Stiintifica, Bucuresti & I. E. P. Stiinta, Chisinau, 1996, 486 pag.
3. M. Bertolotti, V. Chumash, E. Fazio, A. Ferrari, C. Sibilis, J. Appl. Phys., **74**, pp. 3024-3027, 1993.
4. A. M. Andriesh, N. A. Enaki, I. A. Cojocaru, N. D. Ostafeichuk, P. G. Cherbari, V. N. Chumash, Sov. J.T.F. Lett., **14**, pp. 1985-1989, 1988.
5. A. M. Andriesh, O. I. Bogdan, N. A. Enaki, I. A. Cojocaru, V. N. Chumash, Buletin Ross. Acad. Sci., Phys. Ser., **56**, pp. 96-109, 1992.
6. E. Fazio, D. Hulin, V. Chumash, F. Michelotti, A. M. Andriesh and M. Bertolotti, J. Non.-Cryst. Solids, **168**, pp. 213-222, 1993.
7. G. N. Bostan, I. A. Cojocari, E. Carbunescu, V. N. Ciumas, Buletin Academy of Sciences of Moldova, Physics&Technics, **2**, pp. 60-63, 1992.
8. A. Andriesh, V. Chumash, E. Carbunescu, I. Cojocaru, G. Bostan. Romanian Journal of Physics, **38**, No. 9&10, pp. 897-902, 1993.
9. V. Chumash, I. Cojocaru, G. Bostan, G. De Cesare, S. La Monica, G. Maiello, A. Ferrari. "Optical Diagnostics of Materials and Devices for Opto-, Micro- and Quantum Electronics- OPTDIM'95", SPIE Proceedings, Kiev, **2648**, pp. 23-28, 1995.

EVALUATION OF SOME FIRST AND SECOND ORDER OPTICAL CONSTANTS OF MONOMETHYL UREA FROM AS GROWN CRYSTALS.

C. Razzetti, S. Romani, F. Bissoli , S. Bini

Physics Department, University of Parma

M. Zha

MASPEC CNR Institute, Parma

Monomethylurea (NMU) single crystals have been grown in MASPEC Institute and Strathclyde University, Glasgow, in an effort to investigate new organic materials suitable for nonlinear optical applications in the visible-UV region of the spectrum. In this report we summarize the results, in some cases preliminary, of some optical characterisations performed on single crystals grown in MASPEC by the constant-volume decreasing-temperature solution growth method.

Thanks to the favourable crystal morphology and to the satisfactory optical quality of the samples it was thought possible to evaluate the dispersion of the indexes of refraction and at least one of the elements of the **d** and **r** tensors from as grown crystals by developing suitable, or adapting existing, experimental techniques.

Major effort was devoted to implement a reflectometric method, based on the collection and fitting of the R_{pp} element of the general reflectance matrix, able to work on one single natural face of the crystals and to give the three indexes of refraction pertinent to the orthorhombic biaxial structure of NMU. This has been reasonably accomplished by varying the azimuthal orientation of the sample with respect to the incidence plane. Details of the experimental layout and fitting

procedure will be given, together with the calibration results on well defined isotropic and uniaxial reference samples. By using three different source wavelengths a Sellmeier's interpolation of the data was performed and used in subsequent nonlinear characterisations

A double modulation polarimeter, whose details will be given, was then employed to evaluate, with some approximations which will be discussed, the low frequency electrooptical coefficient r_{56} at two wavelengths. The obtained values are around 1 pm/V and decrease with decreasing wavelength.

Phase matched second harmonic generation from Nd:YAG fundamental was then used to evaluate the d_{14} shg coefficient, using Type II interaction with pump beam propagating nearly normal to one natural face of the crystal. The value found is around 1 pm/V. Details of the layout and procedures will be given.

From the overall results it seems that the optical characterisation of crystals of favourable morphology can be obtained from as grown specimens: the accuracy and the sensitivity of the methods employed are, at the state, satisfactory and however liable to implementation.

Discrepancies with results obtained by Strathclyde University by more classical methods will be discussed.

Other qualitative comments on problems affecting the material at the present state of the art of the growth technology will be added, with main emphasis on thermal loading effects on tuning curves and bulk damage.

NONLINEAR OPTICAL PROPERTIES OF NEAT AND METAL SUBSTITUTED FULLERENES

Joseph Callaghan and Werner J. Blau
Physics Department, Trinity College Dublin, Dublin 2, Ireland

The third order nonlinear optical properties of C_{60} , C_{70} and Pt and Pd derivatives of these were investigated by picosecond optical phase conjugation at 1064 nm and 532 nm. The magnitudes of the nonlinearities obtained did not differ appreciably from one another and the second order hyperpolarisabilities were of order $9 \times 10^{-47} \text{ m}^5/\text{V}^2$. At 1064 nm the metal derivatives exhibited a larger nonlinearity than the intrinsic response from C_{60} , with C_{70} showing the largest response of the materials studied. At 532 nm a large acoustic response was found for all samples arising from laser induced phonon scattering.

Transient absorption and pump-probe studies confirm the location of the triplet states in both C_{60} and C_{70} and have determined the lifetime of the excited singlet state to be 1.2 ns and 0.6 ns, respectively. The metal derivatives possess dual component decays which were assigned as intersystem crossing and triplet decay with lifetimes of approx. 10 ps and 1.5 ns. The large decrease in these lifetimes can be explained with the Heavy Atom Effect.

Optical limiting experiments were carried out at 532 nm. From the intensity dependant transmission measurements, coupled with a population level kinetic study, excited state absorption cross sections and efficiencies for optical limiting were determined. Due to the high molecular symmetry, C_{60} possesses the highest limiting efficiency. Metal derivatives perform better than C_{70} , but less efficiently than C_{60} .

Non Linear Optical Spectrometer

Anne Le Garrec, Marc Bucchia, Marc Stehlé
SOPRA, 26 rue Pierre Joigneaux
92270 Bois-Colombes, FRANCE

SOPRA has contributed to laser based systems and analytical tools technology since the early 1980's. More recently, new organic material with nonlinear optical properties are synthesized and studied by Chemists and Physicists. NLO Spectrometer is a tool made for characterization of the NLO properties of these new materials.

The NLO Spectrometer has been designed to provide the researchers a complete integrated measuring system and characterize non linear optical and electro optical materials. It can measure the non-linear coefficients either of liquids or of solids, such as crystals and films.

For liquids, at molecular microscopic scale, the induced dipole moment p^{NLO} can be written by using the four first coefficients of the powers of electric applied field E .

$$p^{NLO} = \mu + \alpha E + \beta E^2 + \gamma E^3$$

where : μ : Permanent ground state dipole moment

α, β, γ : the first, second and third order polarisabilities of the studied molecule.

For $\mu * \beta$ product and γ determinations we use Electric Field Induced Second Harmonic Generation (EFISH) and Third Harmonic Generation (THG) methods which are performed using a wedge technique. By translating a wedged liquid cell perpendicularly to the fundamental laser beam, Maker-fringe amplitude oscillations of the generated harmonic signals are obtained. In the particular case of the determination of β the permanent dipole moment must be known. This μ determination is deduced from the measurements of dielectric constants and refractive indices of solutions with different concentrations by using the Guggenheim procedure. For α determination of solutes we use the Lorentz-Lorenz formula. This determination is reduced to calculation by using refractive index variation versus concentrations.

The NLO Liquid cell is consisting of a small angle wedge shaped cell with thick windows, where high voltage pulses are applied in synchronism with the laser pulses. The cell assembly is transversely moved by stepping motor, micro computer controlled.

The side advantages of NLO Spectrometer are its high throughput of NLO values, absolute units (in ESU and/or CGS), user friendly window TM software and the flexible modular approach.

NLO Spectrometer is made under common licence of CNET and CEA institutions. It benefits from scientific advice with Dr J. ZYSS and Dr F. KAJAR.

New trends in parametric light amplification and generation

A.P.Piskarskas

Vilnius University Laser Research Center
Lithuania.

Summary not available at time of printing.

OPTICAL PROPERTIES OF QUASIPERIODIC (SELF - SIMILAR) STRUCTURES

C. SIBILIA ,

*Dipartimento di Energetica, Università "La Sapienza" di Roma, Via Scarpa 14-16
Roma, 00161, Italy*

E-mail: sibilial@axrma.uniroma1.it

and

P.MASCIULLI , M. BERTOLOTTI

*Dipartimento di Energetica, Università "La Sapienza" di Roma, Via Scarpa 14-16
Roma, 00161, Italy*

E-mail: Bertolotti@axrma.uniroma1.it

The practical development of nonlinear optical devices is often hindered by the lack of materials with the proper combination of desirable properties such as a large nonlinear response , short response times and high damage thresholds. For this reason , much effort has been directed toward the development of materials possessing these properties . The most common approach for doing so is to search for synthesize new materials, but an alternative approach is to fabricate composites from one or more constituent materials.

During these last years much work has been performed in the direction of semiconductor microcrystals in a suitable matrix or in the direction of metal colloids, especially at frequencies near the surface plasmon resonance . Recently it has been demonstrated that a layered configuration of materials with high refractive index contrast can show an effective dielectric constant higher than the one of the basic materials ¹. This behavior modify also the nonlinear third order response of the composite with an interesting enhancement of the nonlinearity . All these results show that a suitable choice of the material " architecture" opens the way towards ideal materials for nonlinear optical devices.

The aim of this work is to study a suitable geometry of the layered system to improve the results recently presented for regular layered structure. In fact we study a fractal code to realize the layered structure, as the one described by a Cantor or a Fibonacci code.

Preliminary calculations show that a sensible enhancement of the nonlinear coefficient can be obtained .

References

- 1 R.J.Gehr, G.L.Fisher, R.W.Boyd, J.E.Sipe ,Phys. Rev.a 53, (1996) p.2796

Switching and control of electric field configurations along multi-quantum well structures

Ilan Gravé
Department of Electrical Engineering
University of Pittsburgh

The phenomenon of high-field domain formation and expansion along superlattice/multi quantum well systems has been observed with the first pioneering works on such structures; yet, only recently, it has been better understood and displayed in its full complexity, paving the way to possible applications. Experimentally it was usually observed by monitoring negative differential resistance oscillations in the electric characteristics (I-V curves) of the samples. It is due to the fact that a uniform field distribution becomes unstable with respect to the formation of high and low electric field domains. This can be described in transport terms as a field-induced breaking of the miniband conduction in superlattices, or a sequential resonant tunneling mechanism in multi-quantum well systems, involving alignment between ground subbands in adjacent wells in the low field region, and ground to excited subband alignment in the high field region. When increasing the applied field, one can observe the progressive inclusion of additional quantum well periods into the high field domain, at voltages correlated with the difference in subband energies and with the periods of the oscillations in the I-V characteristics.

Recently optical tools were used to probe, in a more direct way, the field distributions along such systems. These experiments can be performed using interband or intersubband spectroscopy. A rich configuration of electric domains can be achieved by energy diversification, i.e., quantum wells / superlattices possessing a large number of confined energy levels, or by spatial diversification, i.e., a number of different stacks of quantum wells arranged in series. These experiments showed that different electric domains can coexist under special bias conditions. Moreover, domains were shown not only to form and expand with increasing voltage, but also to spontaneously switch their distribution at specific applied voltage. This phenomenon was used to design and implement switching devices such as a multi-color switching-peak infrared detector. This type of nonlinear optical response can be in principle used for a number of applications. Additional experiments have shown that some interesting features of electric field distributions along low-dimensional systems can be designed and controlled to display desired properties. One example is the choice of nucleation site of the high field domain, sometimes in apparent contrast with the screening effect implicit in domain formation.

The behavior of electric field configurations along superlattices/multi-quantum well structures is strongly linked to the availability of free space charge. Heavy doping or strong illumination providing this charge will induce stable field configurations. A supply of charge less than needed may result in a spatial oscillation of space charge among different sites. The regime of lowest charge supply can produce transient field domains resulting in spontaneous current oscillations reminiscent of transferred electron devices and Gunn diodes; however the negative differential resistance driving the effect originates from low-dimensional transport properties rather than from bulk inter-valley transfer.

In addition to its importance for transport studies, the presence of space charge accumulation at definite sites along a superlattice/multi-quantum well system together with the presence of different field domains rise the possibility of spatial control, localization and/or modulation of optical nonlinear effects along such structures.

In this talk we will present our latest results including observation of high field domains involving alignment of extended-state subbands in shallow wells, and a study of nonuniform photoluminescence quenching due to the expansion of high field domains along a multi-quantum well region. Schemes for achieving all-optical switching of field configurations and space charge localization in such structures will be presented and discussed.

PULSED SQUEEZING IN DISPERSIVE PARAMETRIC INTERACTION

A. Beržanskis, K. -H. Feller

Technical University Jena, Faculty of Physics and Medical Engineering,

Tatzendpromenade 1b, D-07745 Jena, Germany

E-mail: audrius@stud.fh-jena.de

Quantum propagation of light pulses in a dispersive non-linear media is quite cumbersome. Some conceptual problems arise when the quantum theory is developed starting from the full Maxwell equations [1-6]. It is realised that for the quantum propagation of light fields the treatment with the modal Hamiltonian is not appropriate because it neglects the spatial propagation of the fields. Complicated description of interaction of a few waves in the quantum approach contrasts sharply with the simplicity of the classical approach. On the other hand, the phenomenological approach that consists in taking the classical equations and quantizing them was quite successful in analysing the experiments [2, 6-9]. Pulse propagation methods are well developed to deal with interaction of light pulses in classical non-linear optics. The methods are sufficiently accurate to describe a wide variety of diffractive, dispersive, and non-linear phenomenon. Making some approximations at a classical level simplifies drastically the quantization procedure [3].

In this paper we present analysis of degenerate parametric down-conversion and SH generation. Additionally, we study the case of large a phase mismatch for the harmonic generation, i.e. the case of cascaded $\chi^{(2)}$. The latter opportunity to generate squeezed light receives a great deal of attention these days [13-17]. We start from the general classical equations of motion. We write them in Hamiltonian form and perform the quantization of the system in the Fourier transform space. The approach can be used to derive equations both in time- and space-domain. In this way the equations take into account properly both dispersion and diffraction effects. The equations are received from a well defined Hamiltonian, thus, these are well-defined quantum operator equations. Generalisation to the spatio-temporal case is straightforward.

The quantum operator equations are highly non-linear and can barely be solved without making any approximation. Thus, we solve them by linearisation technique which was first developed to study squeezing in the Kerr media [8, 10, 11]. Recently the method was used to analyse the propagation of quantum fluctuations in travelling-wave second order non-linear processes [12-14, 16, 17]. The linearised equations are written for c-number functions, thus, they can be solved by standard numeric techniques.

Since a limit of CW case was analysed thoroughly elsewhere [2-6, 18, 19] we present the analysis of squeezing generation by means of short pulses. The use of pulses is of high interest in squeezing experiments while such pulses may be very intense and, thus, non-linear

effects may be large. We investigate the interaction of pulses with duration of the order of the inverse of the gain bandwidth of parametric generation and less. The dispersion and diffraction effects are very important in this case and they limit the performance of the device. Few papers can be mentioned which deal with pulsed parametric interactions in a dispersive non-linear medium. Such regime was discussed in [20] where the positive-P representation was used to generate stochastic equations of motion for c-number functions. Our approach gives the results which are consistent with those presented in [20]. On the other hand, the approach is more flexible while we deal with ordinary equations. In this way we are able to treat much wider class of the phenomena.

Pulsed regime has many new features which are absent in CW case. For instance the group velocity mismatch causes walk-off of the interacting pulses in the time domain and it may play crucial role in the squeezed light generation by short pulses. On the other hand, group velocity dispersion is responsible for the broadening of pulses, it causes a reduction of the pulse intensity what results the reduction of the squeezing level. The results of our numeric simulations show that the influence of these effects may be optimised by choosing proper phase modulation of the initial pulses.

Detection technique of the pulsed squeezed light is discussed in the paper. The measured quantum noise can be greatly reduced with the use of a time dependent local oscillator. An optical pulse has quite a complicated complex envelope after having passed through the dispersive non-linear medium. Thus a special preparation of a local oscillator pulse is necessary to reduce the measured noise.

Finally, to shed the light on our method we present a practical example, i.e. we present the squeezing spectra for a parametric frequency converter based on a BBO crystal. We show up the limitations for the squeezing generation which appear due to the group velocity mismatch and dispersion in the parametric down- and up-conversion. The set of parameters which optimise the performance of the device is discussed.

References

1. I. Abram, Phys. Rev. A 35, 4661 (1987).
2. C. M. Caves, D. D. Crouch, J. Opt. Soc. Am. B 4, 1535 (1987).
3. T. A. B. Kennedy, E. M. Wright, Phys. Rev. A 38, 212 (1988).
4. D. D. Crouch, Phys. Rev. A 38, 508 (1988).
5. P. D. Drummond, Phys. Rev. A 42, 6845 (1990).
6. B. Huttner, S. Serulnik, Y. Ben-Aryeh, Phys. Rev. A 42, 5594 (1990).
7. B. Yurke, P. Grangier, R. E. Slusher, M. J. Potasek, Phys. Rev. A 35, 3586 (1987).
8. M. J. Potasek, B. Yurke, Phys. Rev. A 35, 3974 (1987).
9. R.-D. Li, S.-K. Choi, C. Kim, P. Kumar, Phys. Rev. A 51, R3429 (1995).
10. Y. Lai, H. A. Haus, Phys. Rev. A 40, 844 (1989).
11. Y. Lai, H. A. Haus, J. Opt. Soc. Am. B 7, 386 (1990).
12. Z. Y. Ou, Phys. Rev. A 49, 2106 (1994).
13. R.-D. Li, P. Kumar, Phys. Rev. A 49, 2157 (1994); R.-D. Li, P. Kumar, J. Opt. Soc. Am. B 12, 2310, (1995).
14. A. Beržanskis, K.-H. Feller, A. Stabinis, Opt. Comm. 118, 438 (1995).
15. S. Schiller, G. Breitenbach, S. F. Pereira, R. Paschotta, A.G. White, J. Mlynek: San Jose, SPIE 2378, 91 (1995).
16. A. Beržanskis, K.-H. Feller, A. Stabinis, Appl. Phys. B 64, (1997) in press.
17. L. Noirie, P. Vidakovic, J. A. Levenson, 'Squeezing Due To Cascaded Second Order Nonlinearities in Quasi-Phase-Matched Media', to be published in J. Opt. Soc. Am. B (1996).
18. A. Beržanskis, R. Gadonas, G. Jonusauskas, A. Piskarskas, A. Stabinis, Lith. Phys. Journ. 6, 290 (1993); A. Beržanskis, R. Gadonas, G. Jonusauskas, A. Piskarskas, A. Stabinis, Laser Physics 4, 639 (1994).
19. M. I. Kolobov, I. V. Sokolov, Sov. Phys. JETP 69, 1097 (1989).
20. M. G. Raymer, P. D. Drummond, S. J. Carter, Opt. Lett. 16, 1189 (1991).

Two-photon absorption measurements through ultrashort pulses

G. P. Banfi ,V. Degiorgio, D. Fortusini,
Dipartimento di Elettronica, Università di Pavia, 27100 Pavia, Italy

Abstract

An experimental arrangement for fast and reliable measurements of the two-photon-absorption (TPA) coefficient β and its wavelength dispersion will be reported. The optical source is provided by a femtosecond travelling wave parametric generator which delivers broadly tunable pulses with sufficient energy, and then intensity, to detect the nonlinear absorption also in samples with a small βL , L being the sample thickness. The short time duration of the pulses minimizes the accumulation of the carriers excited by TPA which could otherwise produce a significant absorption on their own. To calibrate the set-up, use was made of second-order crystals, phase-matched for second harmonic generation, which mimic a two-photon absorber. Results of TPA measurements will be given with particular emphasis on TPA of semiconductor doped glasses. Example of TPA spectra of thin organic films will be also given.

Quasi-phasematched structures for nonlinear optical applications

Fredrik Laurell

Physics Department

Royal Institute of Technology, 100 44 Stockholm, Sweden

phone 46-8-7911327, fax 46-8-7896672, Fl@optics.kth.se

Periodically poled ferroelectrics are attractive for quasi-phasematched (QPM) nonlinear frequency conversion and we are presently seeing a rapid development of bulk and waveguide QPM materials around the world. The prime advantages with QPM is that the nonlinear interaction can be tailored for a noncritical phasematching at any wavelength and any polarization within the transparency range of the material. Furthermore, the strongest nonlinear tensor component can be utilized which can give an order of magnitude increase in the conversion efficiency compared to conventional birefringent phasematching (BPM).

Most of the work have been concentrated on periodically poled LiNbO_3 (PPLN) and excellent results have been obtained both for optical parametric oscillators (OPOs) and for frequency doubling of Nd:YAG lasers. However, the high poling voltage together with lateral spreading of the domains during poling presently limits the sample thickness to about 1 mm and make it difficult to pole very dense grating necessary for frequency doubling into the blue. There are also problems with PPLN when used at high power levels where multi-photon absorption sets in and leads to thermal lensing. Alternative materials that have been successfully periodically poled are LiTaO_3 and crystals from the KTP family. These can more easily be poled for blue light generation and the KTP family crystals can be poled to a thickness of several mm.

Periodically poled crystals could be used inside or outside the laser cavity. Intra-cavity frequency doubling for miniature lasers is usually associated with the so called "green problem". This is due to nonlinear mode coupling involved in the frequency doubling process. It is enhanced by polarization mode mixing appearing in Type II phasematching, which is the commonly used for green micro-lasers. The green problem is eliminated or greatly reduced by going to a QPM frequency doubling where a short crystal and a single polarization is utilized. Frequency doubling to the blue has for BPM primarily been restricted to materials with low nonlinear coefficients, or KNbO_3 which has been difficult to grow with sufficient quality in volumes. It is now possible to build blue lasers using QPM in established nonlinear materials. For OPOs several advantages exists with QPM, the polarization can be chosen as desired, walk-off can be eliminated, the tuning curves can be modified from broadband to narrow band and a much higher effective nonlinearity can be used. QPM can also be used in many other areas, electro-optic beam deflectors and modulators are two which could be of interest for miniature light sources.

Glass can also be periodically poled and a permanent nonlinearity ($> 1 \text{ pm/V}$) is then recorded into the surface of the glass. This is of potential interest for fiber and waveguide lasers.

This seminar will describe the principles and possibilities with QPM and its place in miniature diode pumped coherent light sources.

Two-Photon Absorption Spectroscopy of Non-Centrosymmetric Dyes

S.DELYSSE, J.M.NUNZI, P.RAIMOND

LETI (CEA-Techonologies Avancées), DEIN/SPE

CEA Saclay, 91191 Gif-sur-Yvette Cedex, France.

Two-photon absorption (TPA) spectroscopy of organic dyes is an attractive field for different purposes. TPA up-conversion lasing in dye doped polymers has recently been demonstrated [1]. The TPA limits switching efficiency of polymer waveguide devices [2]. TPA is an important photophysic issue in the field of two-photon laser microscopies [3]. However, TPA are apparently difficult to interpret in the case of non-centrosymmetric stilbene dyes [4].

We measured TPA spectra in the visible and near-infrared for an azo-dye (DR1) and a stilbene-dye (DBANS) using an improved Kerr gate experiment. The so-called, Kerr ellipsometry [5] consists in a pump-probe experiment with picosecond pulses. We induce a transient birefringence in a sample with a strong linear polarized electric field and we test induced anisotropy by sending a weak linear polarized electric field at 45° to the pump. This probe light is a continuum and permits spectroscopic measurement from 300 nm to 1400 nm. Kerr ellipsometry which is a high resolution method, detects small effects like TPA. We rotate a polarizer, after the sample, around signal minimum and we analyse ellipticity of the depolarized probe light. So, we study the state of polarisation instead of transmission through the Kerr gate. TPA spectroscopy is a coherent effect occurring with simultaneously absorption of pump and probe photons.

Figure 1 and 2 are plots of linear extinction coefficient ϵ and TPA coefficient β , defined as $\alpha = \alpha + 2\beta \cdot I$, where I is intensity energy (in $\text{GW} \cdot \text{cm}^{-2}$) and α is linear absorption coefficient (in cm^{-1}).

DR1 (fig. 1) and DBANS (fig.2) have similar molecular structures. They absorb in the same wavelength domain. Nevertheless, comparing one-photon absorption (OPA) and TPA spectra which are expected to have the same shape deduced from a two level model for non-centrosymmetric dyes, we noticed a difference of linewidths for the TPA than for the OPA peak. It appears impossible to explain this phenomenon using a two electronic levels model with inclusion of vibronic sub-structure [4]. We developed a three-levels model, taking account of all the transition momenta (μ_{ij}) between states and of all the dipolar momenta ($\Delta\mu_{ii} = \mu_{ii} - \mu_{00}$). As a result, expression of the third-order susceptibility is the sum of two terms : $(\mu_{01} + \Delta\mu_{01})^2 \cdot D(\omega - \omega_{01})$ and $(\mu_{02} + \Delta\mu_{02})^2 \cdot D(\omega - \omega_{02})$, where $D(\omega - \omega_{0i})$ is a resonant denominator between ground and excited states. The difference concerning stilbene-dye is due to competition between transition and dipole momenta, giving a constructive effect for the lowest energy transition and a destructive effect ($\mu_{0i} \cong -\Delta\mu_{0i}$) for the upper one. For DBANS, energy difference between excited states is $\Delta\omega \cong 0$. For DR1, $\Delta\omega$ may be greater than the linewidth, that is $\Delta\omega > 0.6 \text{ eV}$. Solvatochromism experiment confirm these results.

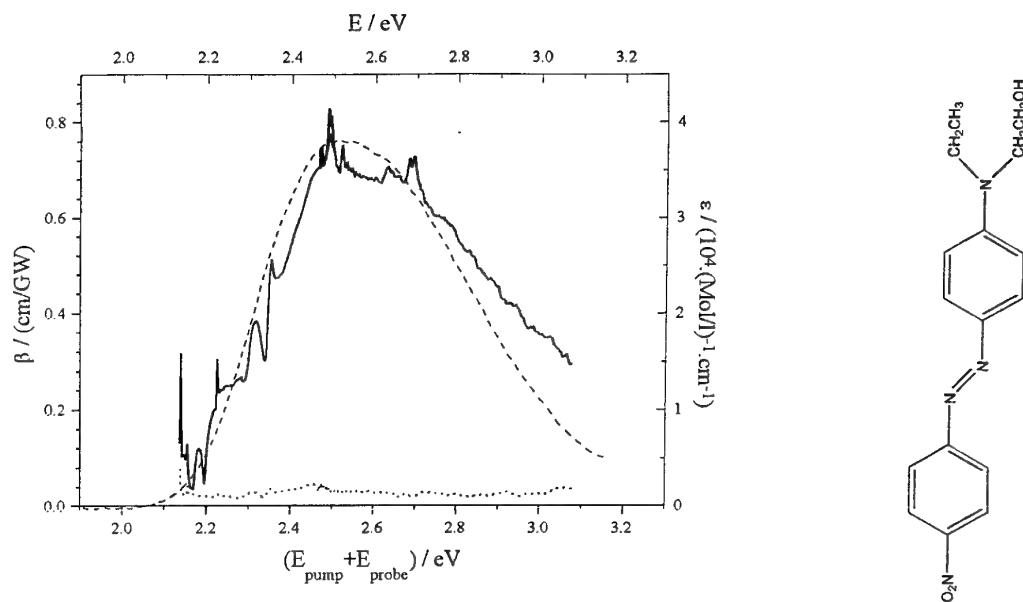


Fig. 1. Two-photon absorption coefficient β (solid curves) versus total energy pump+probe (bottom axis) induced in a 70 g/l solution of DR1 ($N=1.34 \times 10^{26} \text{ m}^{-3}$). The dashed curve represents the extinction coefficient ϵ of DR1 versus photon energy (top axis) measured with a spectrophotometer. Dotted curve is the standard deviation (error) of the TPA data.

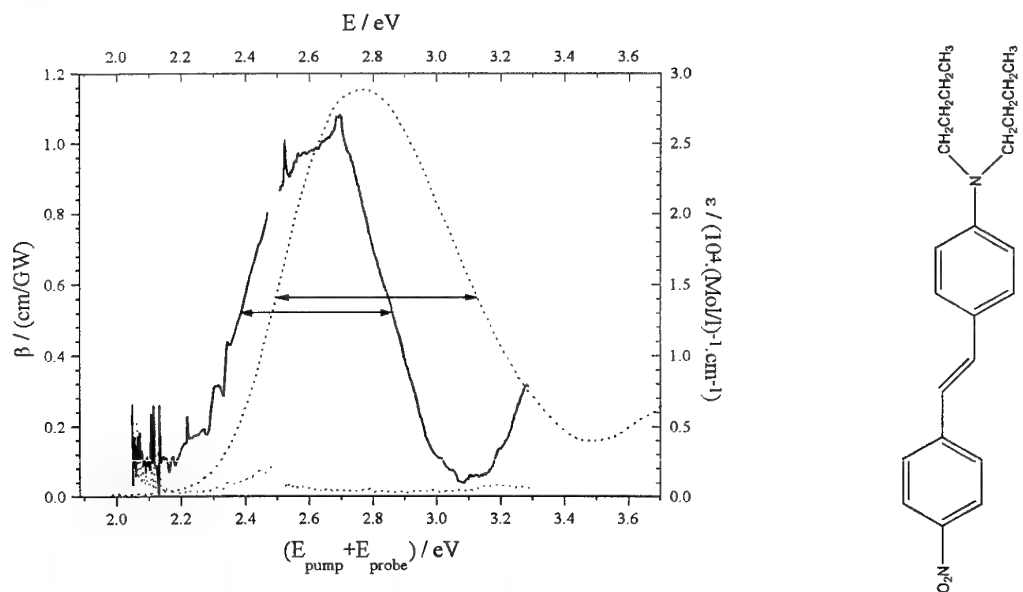


Fig. 2. Two-photon absorption coefficient β (solid curves) versus total energy pump+probe (bottom axis) induced in a 70 g/l solution of DBANS ($N=1.20 \times 10^{26} \text{ m}^{-3}$). The dashed curve represents the extinction coefficient ϵ of DBANS versus photon energy (top axis) measured with a spectrophotometer. Dotted curve is the standard deviation (error) of the TPA data.

- [1] A. Mukherjee, Appl. Phys. Lett. **62** (26), 3423-3425 (1993).
- [2] G.I. Stegeman et al, Photoactive organic materials, (Kluwers Academic Publishers, NATO ASI Series, Vol.9, 1996) pp.75-108.
- [3] C. Xu and W. Webb, J. Opt. Soc. Am. B **13** (3), 481-491 (1996).
- [4] J. Cornil et al, Photoactive organic materials, (Kluwers Academic Publishers, NATO ASI Series, Vol.9, 1996) pp.17-32.
- [5] N. Pfeffer, F. Charra, J.M. Nunzi, Opt. Lett. **16**, 24 (1991).

Evolution of structure and morphology in vapour deposited films of some organic non linear optical materials

J. McAleese, C. McQuade, D.B. Sheen, J.N. Sherwood and Wang Qingwu
Department of Pure and Applied Chemistry
University of Strathclyde, Glasgow G1 1XL, U.K.

Growing organic films by vapour deposition, for use in integrated optical devices for example, would be expected to have a number of advantages over melt growth, solution growth or Langmuir Blodgett methods. Impurity levels and film thickness can in principle be controlled precisely, and the technique being a 'dry' process adapts well with current electronic and optical fabrication technologies. Our belief that the method has potential is based on the demonstration by Hewig and Jain (1) that a vapour deposited film of p-chlorophenyl urea on glass acts as a waveguide to convert a TM_0^ω to a $TM_2^{2\omega}$ mode for a fundamental wavelength of 0.9 μm . The phase matching for SHG was clearly shown to be thickness dependent, being achieved at a thickness of 0.85 μm . However, the results highlighted a number of problems associated with structure and morphology which would have to be overcome if vapour deposited films were to find any serious practical applications. The most pernicious of these appeared to be the radiation losses associated with light scattering from the crystallite defects and boundaries of what was essentially a polycrystalline film. The question is therefore whether one can, through choice of substrate and control of deposition conditions, produce the desired structural and morphological requirements. Achieving such an aim clearly implies a more fundamental understanding of the mechanisms involved in organic film growth than is currently available.

To build up sufficient background information, we have been investigating the growth of thin films of the second order non linear optical materials 4-aminobenzophenone (ABP) and 4-(N,N-dimethylamino)-3-acetamidonitrobenzene (DAN) on a number of single crystal substrates, and assessing the structure and morphology of these films using a combination of techniques including optical microscopy, electron microscopy, X-ray diffraction and atomic force microscopy.

Films of 4-aminobenzophenone grown on a prebaked (200°C for 24 hrs) KCl (001) substrate at 30°C up to a thickness of five microns using a vapour flux of $2\text{--}7 \times 10^{13}$ molecules. $\text{cm}^{-2} \text{ s}^{-1}$ are polycrystalline, with epitaxial growth leading to an ordered bi-axial structure. An increase in crystallite size at the expense of crystallite numbers occurs continually as deposition progresses. The importance of molecular flux in the evolution of film morphology, as opposed just to increased thickness, is highlighted by the fact that thermal annealing alone does not lead to any morphological changes. A reduction in molecular flux and increase in substrate temperature also lead to increased crystallite size as a consequence of a lower primary nucleation rate. The form and habit of individual crystallites is comparable to that predicted by equilibrium form models suggesting that the film grows under near equilibrium conditions. Although during growth the film appears discontinuous, comprising of individual crystallites, atomic force microscopy reveals the presence of an underlying continuous

film which we believe to be essentially amorphous. The evolution of the morphology can be explained if under flux, this primary layer is maintained in a fluid or partially fluid condition and the major contribution to growth of the crystalline film is from this layer rather than directly from the vapour.

The growth of DAN on KCl (001) is significantly different from ABP, although the changes observed can be explained in a similar way. Crystalline films deposited on prebaked (200°C for 24 hrs) cleaved substrates using a flux of $\sim 8 \times 10^{13}$ molecules $\text{cm}^{-2} \text{s}^{-1}$ are found to be initially disordered. Continued deposition leads to reorganisation of the film which, if the substrate temperature is greater than 30°C, results in an epitaxial film comprising approximately $1 \mu\text{m} \times 1 \mu\text{m}$ crystallites in a bi-axial structure. This process does not occur through thermal annealing alone. Using a lower flux of $\sim 6 \times 10^{12}$ molecules $\text{cm}^{-2} \text{s}^{-1}$ to produce films $< 100\text{nm}$ thick again reveals that a continuous, possibly amorphous primary layer is present, and that the crystallites which make up the thicker film form either from this layer or on top of it. The recrystallisation and ripening which is clearly observed in the thicker films under continued molecular flux might again be explained by the presence of a fluid primary layer.

There are many examples in the literature of epitaxial growth of organic crystallites on various structured substrates. The question is how many of these grow, like ABP and DAN, in a way which involves an unstructured primary layer. Evidence has recently come to light that the electrical conductivity of vapour deposited Cu-phthalocyanine on glass undergoes an anomalous change during the early stages of growth at about 7nm thickness which, coupled with the observation of a break in the intensity of the 002 X-ray diffraction peak at the same thickness, led Matsushige et al.(2) to conclude that the film was initially amorphous, with the crystal clusters that constitute the final film growing from this layer. Sakamoto et al.(3) have observed similar effects with Raman scattering from nitrobenzene multilayers on Ni (111) at 150K and reached a similar conclusion regarding the presence of an amorphous layer which starts to recrystallise above a certain thickness. It is also of interest to note that Hewig and Jain in modelling their results suggest that a graded index model might be more appropriate than a step-index model for their p-chlorophenyl urea waveguides, which would result if the first few layers of the film were amorphous and that as deposition proceeded the film became more crystalline.

Such effects have important consequences regarding the optical properties of such films and clearly require more intensive investigation.

References

1. G.H. Hewig and K. Jain, *Optics Comm.*, 1983, **47**, 347.
2. S. Kawato, K. Hayashi, T. Horiuchi and K. Matsushige, *Mol. Cryst. Liq. Cryst.*, 1996, **280**, 247.
3. K. Sakamoto, G. Mizutani and S. Ushioda, *Surf. Sci.*, 1991, **259**, 79.

Nonlinear effects induced by nonabsorbing micro-inclusions in transparent optical medium

Vitali E. Gruzdev, Mikhail N. Libenson
S. I. Vavilov State Optical Institute
Birzhevaya Liniya 12, St. Petersburg 199034, RUSSIA
Tel.: (812) 218-02-31

E-mail: photphys@dost.beam.ifmo.ru libenson@beam.ifmo.ru

ABSTRACT

Nonabsorbing micro-inclusions appear in many optical materials [1]. They can result in some unusual nonlinear optical phenomena. The model presented in the paper describes abrupt local increasing of amplitude of high-power light field in transparent optical material. It is based on formation of unstable field structure in dielectric microsphere [2]. Possibility for field instability to arise is estimated making use of model of diffraction of high-amplitude plane wave on sphere which radius is about radiation wavelength. Field instability is shown to be threshold-like phenomenon. There are estimated threshold amplitude of incident wave and field amplification in microsphere.

We consider also a model in which small local enhancement of the field amplitude is initiated by low-absorbing spherical inclusion which size is less than radiation wavelength, so resonant field mode cannot be formed in the sphere. Bearing in mind nonlinear dependence of refractive index of the host material on light intensity we develop a model to describe "spreading" of initial defect up to size appropriate for the first resonant field mode to be formed. Increasing of refraction index due to nonlinear light-matter interaction and existence of high-Q eigenmodes of coated dielectric sphere [3,4] can both cause positive feedbacks and result in field instability in the medium [2]. Physical reason for the instability to develop is considered and shown to be connected with formation of positive feedback arising with light-induced formation of microsphere's eigenmodes. The models can be applied to analysis of some experimental data on optical breakdown of transparent dielectrics and thin films both impurity-induced and intrinsic.

REFERENCES

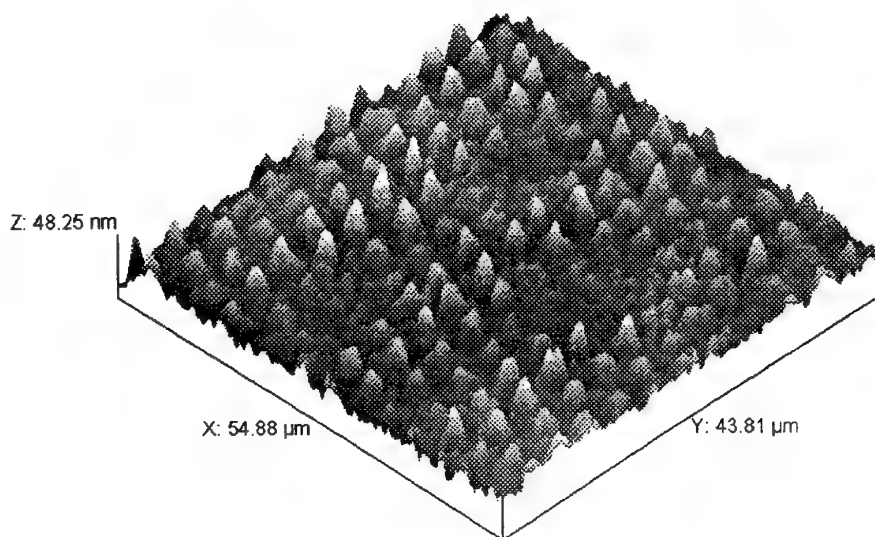
1. M.R.Kozlowski, R.Chow, "The role of defects in laser damage of multilayer coatings", Proc. SPIE v. 2114, pp. 640-649 (1993).
2. V.E.Gruzdev, M.N.Libenson, "Electrodynamic instability as a reason for bulk and surface optical damage of transparent media and thin films", Proc. SPIE, v.2714, pp.595-603 (1995).
3. A.B.Pluchino, "Surface waves and the radiative properties of micron-sized particles", Appl. Opt., v. 20, N 17, p. 2986 (1981).
4. T.Kaiser, S.Lange, and G.Schweiger, "Structural resonances in a coated sphere: investigation of the volume-averaged source function and resonance positions", Appl. Opt., v. 33, N 33, p. 7789 (1994).

The photoinduced translation diffusion of azobenzene-dyes in polymer matrices

Philippe Lefin, Céline Fiorini and Jean-Michel Nunzi

LETI (CEA - Technologies Avancées)
DEIN-SPE, Saclay, 91191 Gif sur Yvette, France
tel : (33) 1 69 08 68 12, fax : (33) 1 69 08 76 79, email : nunzi@cea.fr

Micrometer-amplitude holographic surface relief gratings are optically induced by resonant visible exposure in azobenzene dye-containing polymers.^{1,2} We propose a simple diffusion model accounting for the essential dynamic features of surface relief grating formation. Surface relief is interpreted as a concentration grating induced by dye migration along the exciting polarization direction, further to trans-cis isomerization. It accounts for intensity, polarization and grating pitch dependencies. Understanding of the process appears essential for holographic grating applications. It opens new perspectives associated with optically controlled anisotropic diffusion.



The Figure shows an inverted AFM profile of such grating recorded in a DR1 / PMMA blend, using the interferences from a 515 nm argon-ion laser through an array of collimated-holes.

1. D.Y. Kim, L. Li, J. Kumar and S.K Tripathy, *Appl. Phys. Lett.* **66** (1995) 1166.
2. P. Rochon, E. Batalla and A. Natansohn, *Appl. Phys. Lett.* **66** (1995)136.

Theoretical and experimental first-order hyperpolarizabilities of octupolar polyenes

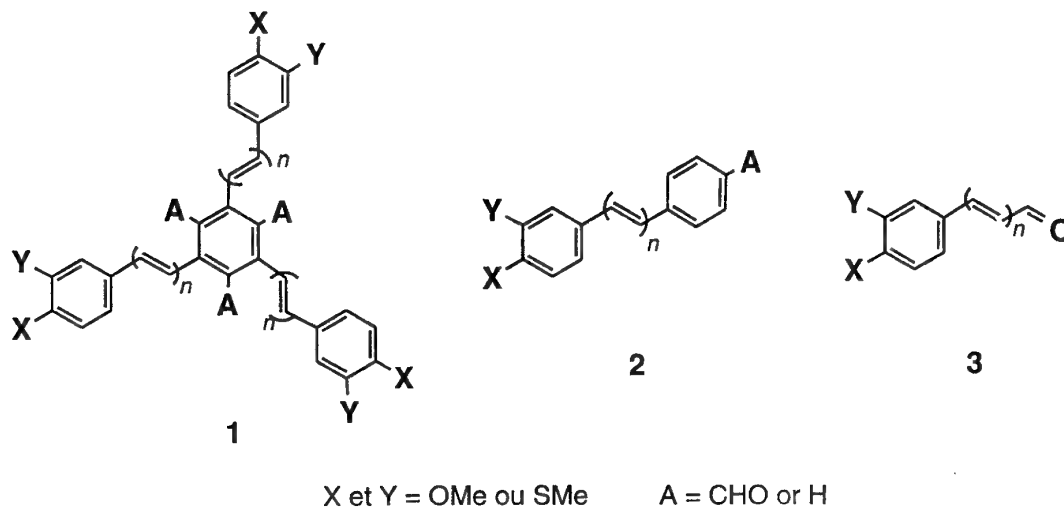
Thomas Zabulon^a, Rémi Anémian^a, Chantal Andraud^a, Thierry Brotin^a, André Collet^a,
Sophie Brasselet^b, Isabelle Ledoux^b, Joseph Zyss^b.

^aEcole normale supérieure de Lyon, Stéréochimie et interactions moléculaires, 69364 LYON Cedex 07, France.

^bCentre national d'étude des télécommunications, France Télécom, Bagnex, France

The classical dipolar approach for high hyperpolarizabilities has been recently revised ; the concept of octupolar molecules for large optical nonlinearities has been proposed¹ and demonstrated experimentally². The theory predicts, in spite of the cancellation of all the vectorial components (dipole moment, vectorial part of hyperpolarizability tensor β), an enhancement of the modulus of β due to non negligible off-diagonal components.

The purpose of this work was to check this theory in the case of the octupolar polyenes **1** in comparison with their rod equivalents **2**. These polyenes are polyenovanillines (molecules **3**) derivatives whose relevance in nonlinear optics, evidenced recently³, is a consequence of their high stability and their large hyperpolarizabilities.



¹ Zyss, J. *Nonl. Opt.* **1991**, 1, 3; Zyss, J. *J. Chem. Phys.* **1993**, 98, 6583; Zyss, J.; Ledoux, I. *Chem. Rev.* **1994**, 94, 77.

² Zyss, J.; Dhenaut, C.; Chau Van, T.; Ledoux, I. *Chem. Phys. Lett.* **1993**, 206, 409; Verbiest, T.; Clays, K.; Samyn, C.; Wolff, J.; Reinhoudt, D.; Persoons, A. *J. Am. Chem. Soc.* **1994**, 116, 9320.

³ Andraud, C.; Brotin, T.; Garcia, C.; Pellé, F.; Goldner, P.; Bigot, B.; Collet, A. *J. Am. Chem. Soc.* **1994**, 116, 2094. Brotin, T.; Andraud, C.; Ledoux, I.; Brasselet, S.; Zyss, J.; Perrin, M.; Thozet, A.; Collet, A. *Chem. Mater.* **1996**, 8, 890.

The modulus of β ($\|\beta\|$) has been studied as a function of the number of double bonds m (defined as $m = n + 4$ for **1** and **2**) and the relation $\|\beta\| \propto m^\alpha$ (where $\alpha \approx 1.5$) has been predicted, the same as the one in dipolar systems. Furthermore, the comparison of $\|\beta\|_o$ (octupolar case) and $\|\beta\|_r$ (rod equivalent) led systematically to the ratio $\frac{\|\beta\|_o}{\|\beta\|_r} \approx 1.5$ (Figure 1) with an improved transparency-efficiency trade-off (Figure 2), confirming the significant contribution of the octupolar component to the β value.

X = Y = OMe, A = CHO

1 : Octupole

2 : Rod equivalent

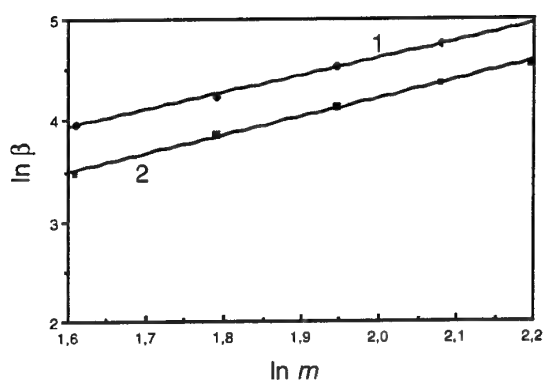


Figure 1

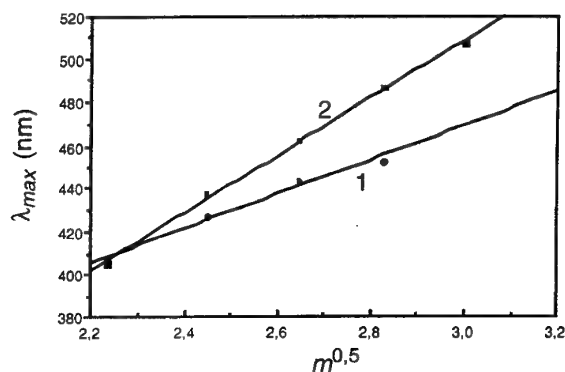
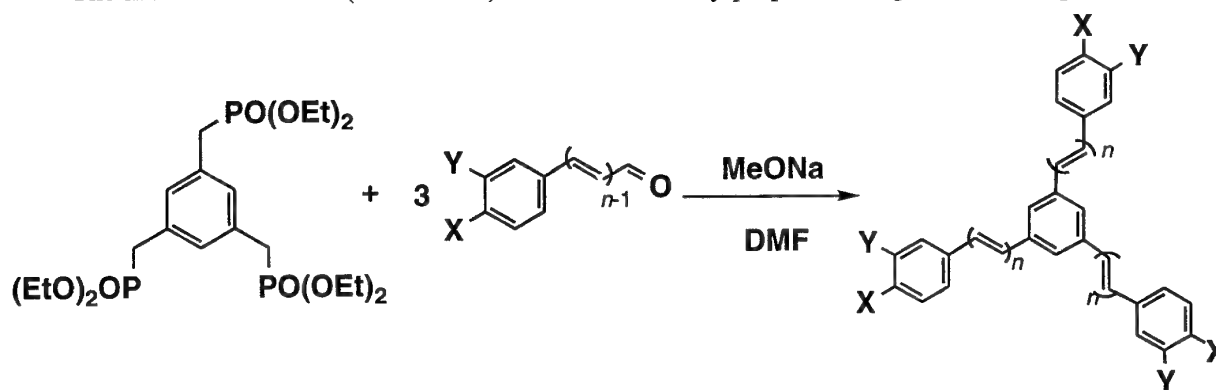


Figure 2

The molecules **1** and **2** (with A = H) have been recently prepared using the following route :



The UV-VIS absorption and fluorescence spectra of these molecules have been recorded and their nonlinear optical properties have been measured via the HRLS technique, and compared with the theoretical results.

NONLINEAR OPTICAL SPECTRA OF TETRATHIAFULVALENES

I.V. Kityk¹, B. Sahraoui², X.Nguyen Phu², M. Sallé and G.Rivoire²

¹ *Physics Institute, Pedagogical University, Al. Armii Krajowej 13/15,
42201 Częstochowa, Poland*

² *Laboratoire POMA, EP CNRS 130, Université d'Angers, 2, boulevard Lavoisier,
49045 Angers CEDEX 01, France*

³ *Laboratoire IMMO, EP CNRS 66, Université d'Angers, 2, boulevard Lavoisier,
49045 Angers CEDEX 01, France*

An increasing interest in materials for nonlinear optics has been recently observed. Such materials should exhibit large nonlinear optical susceptibilities with the change of the chemical contents. Their transparency, absorption or time-dependent response are equally important from the application point of view. The tetrathiafulvalene (TTF) derivatives could be suitable candidates for presenting such behaviour [1]. Their charge-transfer salts show usually remarkable conducting or even superconducting properties [2]. It was shown [1] that CO₂CH₃ groups (which are polar and electron withdrawing) involved in some of these molecules contribute to second-order optical hyperpolarizability. The hyperpolarizabilities are in particular about 10⁴ times greater than for CS₂ at the same wavelength of 532 nm.

In our previous work [3] we have measured the second-order hyperpolarizabilities using a degenerate four-wave mixing method. The main goal of present work is to reveal a connection between a given molecular structure and a tendency to change the nonlinear optical hyperpolarizabilities under influence of backside of the molecule modification.

First of all, we are interested in a possible influence of different molecular parameters (e.g., single or double bond length alterations, end-group substitution species and molecular symmetries) on the nonlinear hyperpolarizability.

Therefore, we have carried out a complex optimization of the molecular structural arrangement using the molecular dynamics approach. A main difference of our approach in comparison to traditional ones consists in taking into account many structural configurations and their mutual interactions. So, we have build the structural clusters with different values of optimized potential energy. We have afterwards performed a self-consistent calculations coming out from the local density functional procedure (LDF), iteration procedure with continuously varying values of the potential energy in a given molecular system. To introduce values of the partial molecular geometry contributions, we have renormalized them using weighting factors.

Second problem which appeared during the calculations consisted in necessity of taking into account intercluster couplings. To undergo this problem we have considered all the molecule as the superpositions of the dipole momentum which come both from the different parts of the same molecule and from the effective environmental molecule. It is a very difficult problem and we have performed the minimizations of corresponding energies approaching solely linear dipole couplings between the considered clusters. With the increasing of the coordination sphere radius we have continued the self-consistent procedure to obtain the convergence of the energy values within the 0.002 Ry. All the calculations were performed using *ab initio* methods. In the Hamiltonian of the corresponding secular equation we have added also the vibrational and electron-vibrational parts. We have

unambiguously shown that only the simultaneous accounting both of the electronic and vibrational parts as well as the interactions between them gives the results which are in good agreement with the experiment.

The cluster boundary conditions are very critical for these calculations since they are very sensitive to sample sizes. To avoid this complication, we have proposed a special procedure to prevent any potential jump on the boundaries.

To understand their contribution and a problem of quasi-phonon anharmonicity, we have included electrostatic operators of electron-vibronic interactions in a linear approximation. To calculate the Green functions, we have performed the summations over 1120 points within the effective „muffin-tin” sphere where the coordinates were determined from the lattice dynamics matrices for the quasi-phonons at 13450 points within the effective sphere. An influence of the neighbouring molecules was introduced by an effective local Lorentz field that effectively influences the scaling of eigenvalues and eigenvectors.

A Dyson equation was used with the introduced electron-vibronic perturbed potential, that takes into account the defect of charge and mass. A relation between real and imaginary parts of the Green function can be obtained using standard Kramers-Kronig dispersion relations which connect real and imaginary parts of response functions. Using the electron-vibration perturbation, we can essentially improve the obtained results.

To calculate final nonlinear optical susceptibilities, we have taken into account contributions of the intra- as well as cluster bonds.

Besides negligible deviations, a good correlation between the experimental and theoretical data should be pointed out.

A comparison of the experimental and theoretical data of absorption spectra (see Fig. 3) indicates their good agreement. The latter suggests a possibility to use this model as a basis for similar calculations in the case of photopolymers. Moreover, the present results give a useful tool for technologists to enhance the optical susceptibilities by substitution of the backbones by NH_2 or NH_3 groups.

REFERENCES:

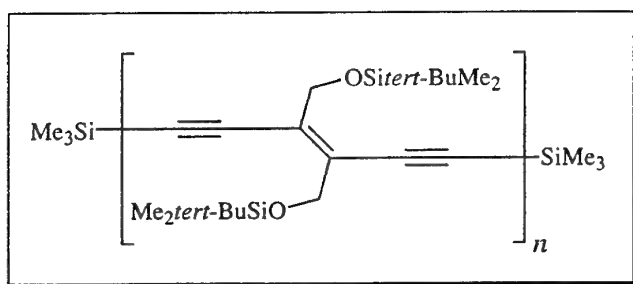
1. Sylla M., Zaremba J., Chevalier R., Rivoire G., Khanous and Gorgues A. 1993, *Synth.Metals*, V.59, p.111.
2. Ferraro J.R. and Williams J.M., 1987, *Introduction to Synthetic Electrical Conductors* (NY: Academic Press, 3. Williams J.M., Ferraro J.R., Thorn R.J., Carlson K.D., Geiser U., Wang H., Kini A.M. and Whangbo M.H., 1992, *Organic Supraconductors (Including Fullerenes), Synthesis, Structure, Properties and Theory* (Englewood Cliffs, New Jersey: Prentice-Hall.
3. B.Sahraoui, M.Sylla, J.P.Bourdin, G.Rivoire, J.Zaremba, J.Modern Optics, 1995, V.42, N 10, pp.2095-2107.

Structure-Property Relationships in Polytriacetylenes: Effective Conjugation Length, Influence of Lateral Conjugation, and Donor/Acceptor Substitution

Rainer E. Martin^a, Ulrich Gubler^b, R. R. Tykwinski^a, Corinne Boudon^c, Christian Bosshard^b, Jean-Paul Gisselbrecht^c, Peter Günter^b, Maurice Gross^c, and François Diederich^a

^aLaboratorium für Organische Chemie, ETH-Zentrum, Universitätsstr. 16, CH-8092 Zürich (Switzerland), Tel. +41-1-632 26 36, Fax +41-1-632 11 09, ^bInstitut für Quantenelektronik, ETH-Hönggerberg, CH-8093 Zürich (Switzerland) and ^cLaboratoire d'Electrochimie, Université Louis Pasteur, F-67008 Strasbourg Cedex (France).

Polytriacetylenes [PTAs, $-(C\equiv C-CR=CR-C\equiv C)_n-$]^[1] are the third linearly conjugated polymers with a non-aromatic all-carbon backbone in the progression which starts with polyacetylene $-(CR=CR)_n-$; PA] and polydiacetylene $-(C\equiv C-CR=CR)_n-$; PDA] and ultimately leads to carbyne $-(C\equiv C)_n-$. To explore structure-property relationships in PTAs, we have prepared a series of monodisperse oligomers ranging from monomer **1a**^[1,2] to hexamer **1f** by oxidative *Glaser-Hay* coupling of a *trans*-bis-deprotected *E*-1,5-hexadiyn-3-ene^[1,2] with the corresponding *trans*-mono-deprotected monomer unit, which acts as an end-capping reagent.



	<i>n</i>	length ^a [Å]
1a	1	9.6
1b	2	16.9
1c	3	24.2
1d	4	31.5
1e	5	38.8
1f	6	46.1

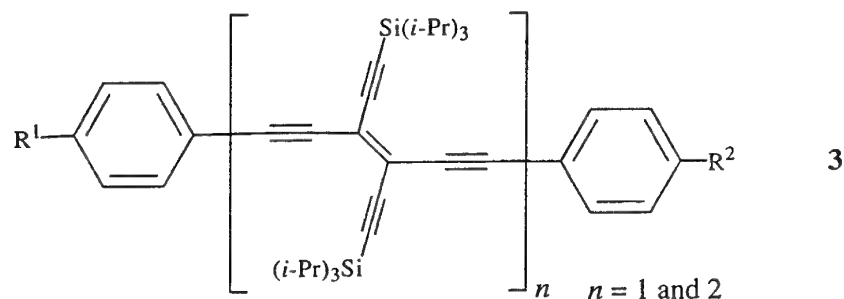
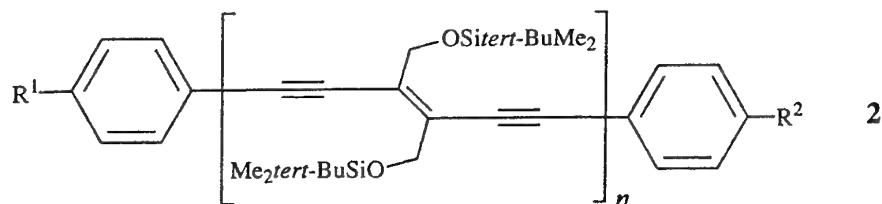
^ameasured from Si to Si

All compounds are stable towards exposure to light, air, and temperatures beyond their melting points and have been fully characterized; they are readily soluble in a wide range of solvents.

To estimate the effective conjugation length (L_d) in PTAs, the solution optical gap E_g was plotted as a function of $1/n$ for compounds **1a-f** and two polydisperse samples (22-mer and 31-mer)^[1]. These study revealed that the effective conjugation length was

reached in PTAs containing $n = 11 \pm 1$ monomer units, which corresponds to a total of 30 - 36 double and triple bonds and a rod length of 75 - 90 Å, respectively.

The non-resonant second-order molecular hyperpolarizability, γ , was measured for 1a-f via third harmonic generation (THG) in CHCl_3 solutions at $\lambda = 1.907 \mu\text{m}$. Plotting γ/n vs. n revealed a power law for γ with a fitted exponent $a = 2.5 \pm 0.1$. Together with the THG measurements of the polymer samples, a critical conjugation length of about 10 monomer units, in excellent agreement with the value obtained from UV/Vis spectroscopy, is obtained.



To evaluate the influence of donor/acceptor substituents and the effects of lateral conjugation paths in PTAs, we studied the two oligomer sets 2 and 3. We will report on the synthesis of these functionalized oligomers and show trends in the electrical (redox potentials) and optical (UV/Vis, NLO) properties as a function of substitution pattern and length.

- [1] M. Schreiber, J. Anthony, F. Diederich, M. E. Spahr, R. Nesper, M. Hubrich, F. Bommeli, L. Degiorgi, P. Wachter, P. Kaatz, C. Bosshard, P. Günter, M. Colussi, U. W. Suter, C. Boudon, J.-P. Gisselbrecht, M. Gross, *Adv. Mater.* **1994**, *6*, 786-790.
- [2] a) R. R. Tykwinski, M. Schreiber, R. Pérez Carlón, F. Diederich, V. Gramlich, *Helv. Chim. Acta* **1996**, *79*, 2249; b) J. Anthony, Dissertation, University of California, Los Angeles, 1993.

Design of Basic Elements of Digital and Postdigital Computers Based on Quantum Mechanical Investigation of Fullerene and Photoactive Molecules

A. Tamulis, E. Stumbrys*, L.M. Balevicius*, J. Tamuliene, A. Tamulis**

Institute of Theoretical Physics and Astronomy, A. Gostauto 12, 2600 Vilnius, Lithuania; Faxes: +(370-2)-225361, 224694; Phone: +(370-2)-620861; e-mail: TAMULIS@ITPA.LT

*Faculty of Physics, Vilnius University, Sauletekio al. 9, III rumai, 2054 Vilnius, Lithuania

**Faculty of Natural Sciences, Vilnius University, M.K. Ciurlionio 21/27, 2009 Vilnius, Lithuania

Quantum mechanical investigations of the stability of empty fullerene C_{20+2n} ($n = 0, 2, 3, \dots, 16$) molecule isomers with the highest symmetry and the corresponding endohedral fullerene cages with twenty eight encapsulated atoms: even valence – Be, C, O, Mg, Si, S, Zn, Ge, Se, Cd, Sn, Te, Hg, Pb and odd valence – H, N, F, Al, P, Cl, Ga, As, Br, In, Sb, Tl, Bi were performed using the point set group theory in the framework of semiempirical MOPAC-PM3 method [1].

The quantum mechanical investigations of fullerene C_{24} , C_{26} , C_{28} molecule conformers are performed in the framework of point set group theory and semiempirical PM3 configuration interaction, MNDO, AM1 and *ab initio* SCF/UHF methods. The main criterion of stability of calculated fullerene molecules we state the lowest total energy of various isomers and conformers that appears due to the Jahn-Teller distortion. The most stable occurs C_{24} D_6 symmetry conformation with term $1A_1$ and open shell C_{26} D_{3h} symmetry conformation with term $5A'_1$.

The stability and geometry of clathrates $C_{60} + CS_2$ were investigated by using PM3 and *ab initio* SCF/RHF methods. It were found two stationary points of these derivatives during geometry optimization procedure. The calculations of system consisting from two C_{60} and three CS_2 were investigated for the understanding the orthorhombic packing in above mentioned clathrates.

The quantum chemical calculations and investigations of the stability of twenty eight photoactive charge transfer supramolecules constructed from disc-like pentayne (pentakis(phenyle thynyl)phenyl) molecules with radicals $R = -OC_5H_{11}$, $-CH_3$, $-CF_3$, $-CN$ and seven organic electron acceptor molecules: TNF, TeNF, TCNQ, $TN_9(CN)_2F$, TCNB, TeClBQ, TeFTCNQ were performed using the MOPAC-PM3 method. All supramolecules have relatively small energetic gap, i. e. they are good electron donors and good electron acceptors at the same time. Therefore these supramolecules should be molecular photodiodes. Energies of formation are largest for supramolecules constructed from disc-like pentayne with $-CH_3$ radical and TeNF or $TN_9(CN)_2F$ molecules - 2.16 and 2.20 kcal/mol respectively. It was founded that: a) all investigated supramolecules: disc-like pentayne molecules::electron acceptor molecules are stable, possess dipole moments and are potential molecular photodiodes; b) the order of decreasing stability of the above mentioned supramolecules with various radicals is: $-CH_3 > -OC_5H_{11} > -CF_3 > -CN$; c) the order of decreasing stability of the supramolecules with various electron acceptor

molecules is: $\text{TeN9(CN)}_2\text{F} > \text{TeNF} > \text{TNF} > \text{TeFTCNQ} > \text{TCNQ} > \text{TCNB} > \text{TeCIBQ}$ [1].

Molecular implementation (MI) of two, three, four variable logic functions, summators of neuromolecular networks, cells of quantum cellular automata, devices of electronically genome regulation were designed based on results of quantum chemical calculations of electron donor, electron insulator, electron acceptor and fullerene molecules [1]. Complete set of sixteen MIs of two variable logic functions (for example: OR, AND, Implication, Equivalence, Difference, etc.) was designed and also proposed using MIs of two variable molecular logic function initial basic sets: {OR, AND, Negation} or {NOR} and, or {NAND}. We have described in more detail the designed MIs of: a) two variable logic functions OR, NOR, AND, NAND (two sets: one designed from planar molecules and another - from fullerene molecules), Converse Unitary Negation-1, Converse Unitary Negation-0, Unitary Negation-1, Unitary Negation-0, "0" and "1" Matrix Constants; b) three variable logic functions AND, NAND, OR, NOR analogs; c) four variable logic functions OR, NOR, AND, NAND analogs, d) molecular cell that simulates one of Life figures, e) summator of neuromolecular network that simulates sigmoidal behaviour of artificial neurone. This was done based on quantum chemical investigations of organic photo-induced electron donor molecules: a) carbazole, 3,6-dibromcarbazole, TeMePhDA, PhDA; b) electron acceptor molecules: TCNQ, TCNB, TeCIBQ, small empty and endohedral fullerene molecules: C₆₀, C₂₈, C₂₈H₄, C₂₄H₂, C₂₀, C₂₀H₆, A@C₆₀, A=Be, Zn, Cd and c) electron insulator molecules.

[1] Tamulis A., Stumbrys E., Tamulis V. and Tamuliene, J., "Quantum Mechanical Investigations of Photoactive Molecules, Supermolecules, Supramolecules and Design of Basic Elements Molecular Computers", in NATO ASI series, High Technology; Vol. 9, Ed. by F. Kajzar, V.M. Agranovich and C.Y.-C. Lee, "Photoactive Organic Materials: Science and Applications", June 25-30, 1995, Avignon, France, Kluwer Academic Publishers, Doderecht/Boston/London, 1996, p.p. 53-66.

Dynamics of Molecular Orientation in Dye-Doped Polymers.

Ahmad El Osman and Michel Dumont,

Institut d'Optique Théorique et Appliquée (Laboratoire associé au CNRS),
Bât.5O3, B.P.147, F-91403 ORSAY Cedex, France.

Tel: 33 (1) 69 35 87 53 Fax: 33 (1) 69 35 87 00

E-mail: Michel.Dumont@IOTA.u-psud.FR

In the past five years, we have demonstrated and studied Photo-Assisted Poling (PAP)[1] of polymeric films doped with photoisomerizable dye molecules (such as $\text{trans} \Rightarrow \text{cis}$ photoisomerization of azo-dyes, or spiropyran \Rightarrow photomerocyanine isomerization). In this process, successive photoisomerization and relaxation cycles, in presence of a DC electric field, allow the poling of the sample at room temperature and induce $\chi^{(2)}$ NLO properties. We have developed a dynamical model of PAP[2] which also describes Photo-Induced Anisotropy (PIA: birefringence and dichroism induced by optical pumping with a polarized resonant light beam) and All-Optical Poling (AOP: poling by coherent optical pumping with ω and 2ω light frequencies)[3].

This model has been successful for describing the general behavior of the three processes. Nevertheless the precise fitting of experimental curves is impossible because the theoretical model implies exponential relaxations (for mathematical solvability), while it is well known that all relaxation processes in polymeric materials are not exponential. Some interesting experiments have highlighted the non exponential relaxation of the orientation of photomerocyanine molecules in PMMA[4]: the instantaneous relaxation rate appears to be time dependent, after the pumping switch-off.

Several other parameters are not yet known, such as the rôle of back photoisomerization ($\text{cis} \Rightarrow \text{trans}$, for azo-dyes, or merocyanine \Rightarrow spiropyran). This process is included in the theory, but further experiments are in progress in order to improve the knowledge of the spectroscopic properties of the unstable photoisomer.

Our purpose is to summarize previous studies on optical ordering of anisotropic and polar chromophores and to present new results. In particular we are performing measurements of photoinduced dichroism, simultaneously on several wavelengths, in order to determine the evolution of the anisotropy in both isomeric states. From these measurements, it is possible to deduce the average rotation of molecules associated with photoisomerization and the angular mobility in each state. We expect also information on the transition dipole moment of the unstable state and on the quantum yield of back photoisomerization. We also use attenuated total reflection experiments for the measurement of photoinduced birefringence and of electrooptic properties of polymeric films.

All these studies are useful for the fundamental knowledge of dye-doped polymeric materials for applications to integrated optics and particularly for electrooptic modulation. They are also of interest for the new field of organic photorefractive materials, since it has been demonstrated that orientation of anisotropic molecules plays an important rôle in the index grating formation.

REFERENCES

1. Z. Sekkat and M. Dumont, Appl. Phys. B, **54**, 486 (1992) and Nonlinear Optics, **2**, 359 (1992).
2. M. Dumont, S. Hosotte, G. Froc and Z. Sekkat, SPIE proceedings, Vol. **2042**, Photopolymers and Application in Holography, Optical Data Storage, Optical sensors and Interconnects, p 2 (1993) and M. Dumont, G.Froc and S.Hosotte, Nonlinear Optics , **9**, 327 (1995)
3. M. Dumont, In : Photoactive Organic Molecules, Science and Applications, F.Kajzar Ed., Nato ASI Series Vol. 9, Kluwer Academic Publishers (1996), p 501, "*A Common Model for optical Ordering of Photoisomerizable Molecules*"
4. S. Hosotte and M. Dumont, Synthetic Metals, **81**, 125 (1996) and SPIE proceedings, Vol. **2852**, Nonlinear Optical Properties of Organic Materials IX, p 53 (1996).

Light propagation in a dye doped liquid crystal planar waveguide

G. Abbate¹, L. De Stefano¹, P. Mormile², L. Petti², G. C. Righini³, L. Sirleto³

1. *Dipartimento di Scienze Fisiche, Università di Napoli, Padiglione 20 Mostra d'Oltremare, I-80125 Napoli, Italy*
2. *Istituto di Cibernetica, C.N.R., Via Toiano 6, I-80072 Arco Felice (Napoli), Italy*
3. *IROE-CNR, Via Panciatichi 64, 50127 Firenze, Italy*

Abstract

Since 1990 it is known that mixtures of organic dyes and Liquid Crystals (LC) can broaden the application range of nonlinear optical effects based on LC materials. The dye dopant main feature is a great enhancement of the LC nonlinear optical response. The response coefficient, depending on various parameters, such as guest-host mixture, dye concentration, light wavelength, etc..., can be increased by a factor of the order of 100. In addition, this factor can be either positive or negative, thus giving rise to self-focusing and self-defocusing effects, respectively: the latter feature is particularly attractive in designing nonlinear optical devices, if we consider that pure LC materials can only exhibit nonlinearity of self-focusing type. This effect contributed to the renewed interest since 4-5 years on integrated optics applications of LC based devices, at least when fast responses are not required.

With the aim of a better understanding of the behaviour of such devices and their design optimisation we developed a double step theoretical model. First, we analysed the light propagation in a nonlinear and anisotropic waveguide, with a LC core; second, we extended the known modal matching technique in order to fully consider the anisotropy and nonlinearity of these media when they are coupled with other guiding structures. In particular, our model is suitable in the case of polarisation maintaining devices, in which pure TM or TE modes can propagate, and also in the case of hybrid polarisation modes, provided the optical axis remains in the plane of the waveguide. Owing to the optical behaviour of LC materials and to the great changes in refractive index that they can exhibit, the usual modal coupling method, which neglects reflected and radiative modes, is in no way exploitable for real design optimisation. Thus, in our model we considered the reflected modes arising at interfaces between different waveguides, and we proposed also a way to handle radiation modes.

By means of a powerful computing technique, we have numerically analysed the case of three coupled waveguides: two glass waveguides (linear and isotropic) as first and third sections and a dye-doped LC waveguide (LCWG) as a second section of the device. The LCWG is initially configured in a planar alignment of the molecular long axis, coinciding with the optical axis, and TM polarised light propagates through the device. Our results show that above a proper light power threshold, for a positive dye, a molecular reorientation is induced with a consequent nonlinear refractive index change. This threshold reorientation could be a first order transition with the consequent optical bistability loop, if the sample thickness is greater than a critical one ($2\text{ }\mu\text{m}$ in our simulations). The analysis of the field amplitude profile inside the LCWG shows that a self-confinement effect, due to the local increase of the refractive index in the centre of the waveguide core, can explain the bistability. It is worth noting that the power needed to observe the nonlinear effects, even for film thickness below $3\text{ }\mu\text{m}$, is well within the limits that we can achieve with a cw Ar^+ laser, and this is not the case for a pure LC material without the dye induced enhancement. Furthermore, in such a thin waveguide the scattering losses, which usually impose severe limitations to the practical realisation of LC-based guiding devices, are greatly reduced.

In order to experimentally study these effects, we designed and realised the previously analysed three-section guiding device. The structure used is a graded index bimodal glass waveguide, made by the ion exchange technique, with a basin dug into it by photolithography. Both the waveguide core and the basin were $3\text{ }\mu\text{m}$ deep, and the latter was filled with the LC. A TM polarised beam was injected in the device by prism coupling and decoupled in the same way. We observed the threshold occurrence for nonlinear effects. Above threshold, the nonlinear change of the field amplitude profile in the LCWG leads to a different coupling with the modes of the output waveguide. Thus, increasing the guided light power results in a mode exchange of the output power, which can be detected. The experimental data are in good agreement with the numerical results. Similar results were also obtained with the LCWG in homeotropical alignment and TE polarised input light.

Nonlinear optical properties of multilayered structures and composites of C₆₀ with electron donors

Y. Okada-Shudo^{a,*}, F. Kajzar^a, C. D. Merritt^b and Z. H. Kafafi^b

a) CEA, LETI - Technologies Avancees, DEIN/SPE/GCO, Centre d'Etudes de Saclay
91191 GIF SUR YVETTE CEDEX, France

b) US Naval Research Laboratory, Washington, D. C. 20375, USA

*) Present address: Tokyo University of Telecommunications, Tokyo, Japan

Abstract

Second and third order nonlinear optical properties of C₆₀ based composites and multilayered structures with TPP and TPN are studied by transverse optical second and third harmonic generation, respectively. The results are compared with those obtained from pristine, photolyzed in vacuum and in oxygen atmosphere C₆₀ thin films. Second harmonic generation is observed from structures containing C₆₀ molecules. An enhancement of the quadratic susceptibility is observed from the multilayered structures. The third harmonic generation experiments show an enhancement of the cubic susceptibility from photolyzed C₆₀ thin films. No increase of $\chi^{(3)}$ in the multilayered structures or composites is observed. A slightly larger response is obtained with the multilayered thin films as compared to the composite material.

Application of J-aggregates as materials for optical switching

K.-H. Feller¹, R. Gadonas², E. Gaižauskas², H. Glaeske¹, A. Pugžlys²

¹Technical University Jena,
Faculty of Physics and Medical Engineering,
Tatzendpromenade 1b, 07745 Jena, Germany

²Vilnius University, Laser Research Center,
Sauletekio al.10, 2054 Vilnius, Lithuania

ABSTRACT

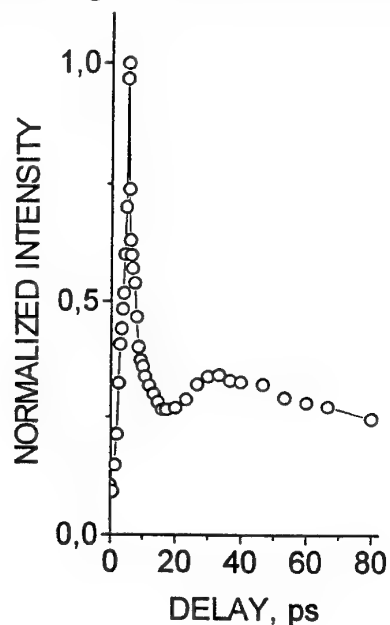
Recently, macromolecular organic materials, such as J-aggregates have shown to be promising candidates for applications in photonics for fast optical switching. The main advantage of such organic materials is the combination of large nonlinear susceptibilities of third order with fast response times (sub-ps to fs range) with respect to the incoming signal. Due to competing processes, such as saturation and exciton-exciton-annihilation, the mechanism of the governing NLO-processes are intensity-dependent themselves. This makes possible short switching times for processing of signals at moderate intensities due to high nonlinear efficiency, and the intensity can be used as an additional degree of freedom.

Therefore the studies of ultrashort near-resonant NLO-processes in J-aggregates, in solution as well as in Langmuir-Blodgett (LB)-layers, are of great importance. We report about results on time-dependent degenerate four-wave mixing (DFWM)- and transient absorption spectroscopy of PIC-J-aggregates in the near-resonant regime.

The most important features for an application for optical switches are an anomalous wavelength dependence of the power index of the DFWM-intensity on the reference intensity[1], which scales down from 3 in the off-resonant regime to about 1 in resonance, and the non-exponential and ultra-fast decay of the resonant DFWM-signal (see Figure).

The fast optical response, which can be due to either interfering or non-Markovian effects has to be explained to optimize this feature for application as materials for optical switching. Efforts have made to develop a model, which includes exciton-exciton-annihilation (enabling high energy exchange in four-wave interactions), two-photon resonances to higher excitonic energy levels (explaining the power index wavelength dependence)[2], and electron-vibrational coupling (inverse Raman process)[3]. The model is based on a nonperturbative analysis on the foundation of a three-level scheme by direct numerical integration of the density matrix equations of motion.

On the basis of our investigations we propose a nonlinear optical directional coupler based on an waveguide implemented LB-multilayer structure of PIC-J-aggregates.



References

- [1] R. Gadonas, K.-H. Feller, A. Pugžlys, G. Jonušauskas, J. Oberlé, C. Rullière, J. Chem. Phys., in press
- [2] E. Gaižauskas, K.-H. Feller, Photochemistry and Photobiology, in press
- [3] E. Gaižauskas, H. Glaeske, K.-H. Feller, Opt. Commun., in preparation

Aminovinylidicyanopyrazines as New NLO Chromophores
with Large β Values and Their Self-assembling

K. Shirai,* M. Matsuoka,* J. Y. Jaung** and K. Fukunishi**

* Kyoto Women's University, Imakumano, Higashiyama, Kyoto 605, Japan.

** Kyoto Institute of Technology, Matsugasaki, Sakyo-ku, Kyoto 606, Japan.

Dye Chromophores for 2nd order NLO materials have been studied extensively and intramolecular charge-transfer system was found to be the most effective chromophores which showed large β value. But, they have large dipole moment even in the ground state and usually cancelled their dipole moment in crystal level by the electrostatic interactions. And then, molecular stacking to keep their dipole moment was the most important methodology for 2nd order NLO materials. We found that amino-vinylidicyanopyrazine chromophores have large calculated β values. They were synthesized by the reaction of dicyanopyrazine with enamines such as Fischer's base (dyes **1** - **3**) and by the condensation of methylidicyanopyrazine with arylaldehyde (dye **4**). Their β values were calculated by the PPP MO method and the values were correlated with their chemical structures. The optimization of dye structures were performed by MOPAC PM3 method and their hydroxylpyrazine-pyrazinone tautomerism was discussed from their spectral properties. The calculated parameters for pyrazine dyes **1** - **4** were summarized in the Table. Dye **1a** and **1b** have similar β values but the pyrazinone tautomer **1c** has larger β value (2.6 times of **1b**). They have similar ΔE_i , $\Delta\mu$ and f values but their differences caused to big difference in β value. Dyes **2** and **3** are the structural isomer but dye **3** has bigger β value (3.2 times of dye **2**) which mainly caused to the big difference in $\Delta\mu$ value. Dye **4c** is the pyrazinone tautomer of **4b**, and again **4c** has the biggest β value (5.6 times of **4b**). It is very interest that tautomerism of dye chromophore affects very much on their β value. Anyway, these dyes have quite large β value in molecular level and effective molecular stacking to get large $\chi^{(2)}$ value were conducted. The solid state absorption spectra of dyes **1** - **3** were very much affected by the length of alkyl substituents. In general, the λ_{\max} value of

vapor deposited thin film shifted to longer wavelength according with the length of alkyl group, and showed very sharp absorption spectra with small half band width, usually observed in J-aggregate of cyanine dyes. The strictly oriented molecular stacking caused by hydrophobic interactions of the alkyl group together with intermolecular π - π interactions was proposed on solid state. The characterization of vapor deposited thin film of these dyes were under investigation.

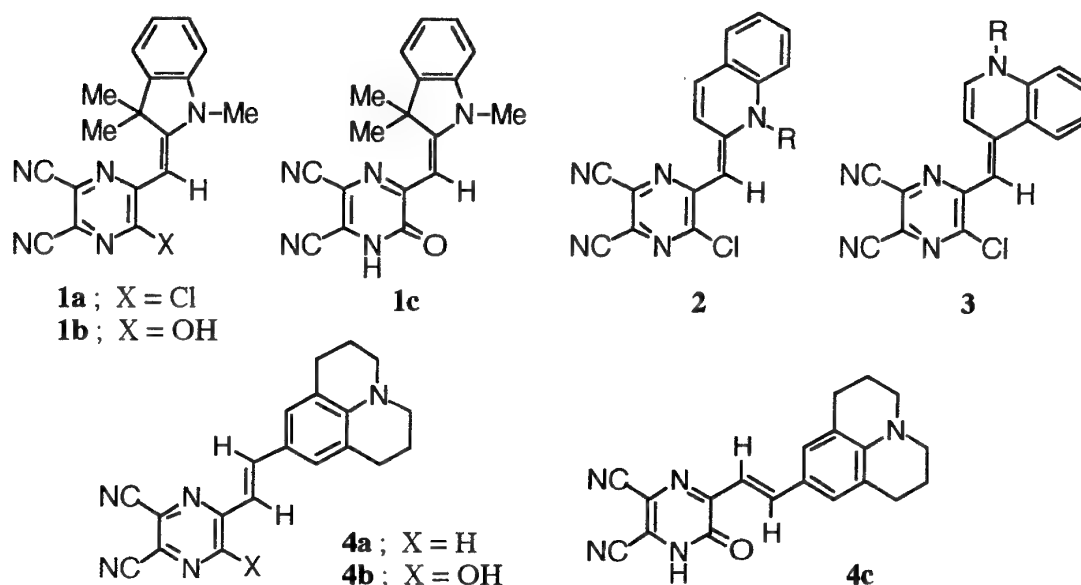


Table Calculated parameters for pyrazine dyes 1 - 4

Dye No.	β ($\times 10^{-30}$ esu)	ΔE_1 (eV)	$\Delta\mu$ (Debye)	f
1a	398	2.67	15.9	0.89
1b	444	2.66	15.2	1.09
1c	1147	2.51	14.8	1.25
2	251	2.57	5.1	1.12
3	801	2.45	9.0	0.95
4a	2031	2.48	24.9	1.09
4b	1686	2.53	23.2	1.36
4c	9434	2.29	20.5	1.44

Pyrazinophthalocyanines as New NLO Chromophores and Their Molecular Stacking

M. Matsuoka,* J. Y. Jaung** and K. Fukunishi**

* Kyoto Women's University, Imakumano, Higashiyama, Kyoto 605, Japan.

** Kyoto Institute of Technology, Matsugasaki, Sakyo-ku, Kyoto 606, Japan.

Phthalocyanine chromophores have been studied in details as 3rd order NLO material. They have large π -conjugation system, absorbed at 700 - 800 nm in the visible region, and have superior physical properties for device technology which are very important factors for organic NLO materials. We have been studied many dye chromophores as 2nd and 3rd order NLO materials from the points of molecular stacking caused by intermolecular π - π interactions. Dicyanopyrazine, synthesized from diaminomaleonitrile and 1,2-diketones, cyclized to give the corresponding pyrazinophthalocyanines (1) and their annelated analogues. Introduction of substituents on the pyrazine ring and/or annelation to heteroaromatics were very easy and variations of pyrazinophthalocyanines and pyrazinonaphthalocyanines could be synthesized. Long alkylphenyl substituent can also be introduced to the pyrazinophthalocyanine nucleus. The intermediate, such as 4-*n*-octylphenyldicyanopyrazine, showed phase transfer depending on the temperature caused by the hydrophobic interactions between the alkyl chains. The pyrazinophthalocyanine having long alkyl phenyl substituents also showed crystal morphology. They were soluble in most organic solvent and showed sharp absorption band at around 640 - 650 nm with strong red fluorescence in case of aluminium complex. It is very strange that they showed very small Stokes' shift of 5 nm which indicated that they are no energy loss in the excited state and may have high fluorescence quantum yield. Anyway, their NLO properties connected with their characters in the excited state are very interest.

On the other hand, dicyanopyrazinoindoles (2), as a precursor of annelated pyrazinophthalocyanine, also showed interesting phase-transfer in cases of their long alkyl derivatives. Dye 3 absorbed at around 710 nm cause to an enlargement of π -conjugation compared with dye 1. Dye 3 with long alkyl substituent at x-, y- and z-

positions of dye **2** were synthesized and their spectral properties, crystal morphology and performance of the vapor deposited their film were studied. They will be the candidates for new 3rd order NLO chromophores.

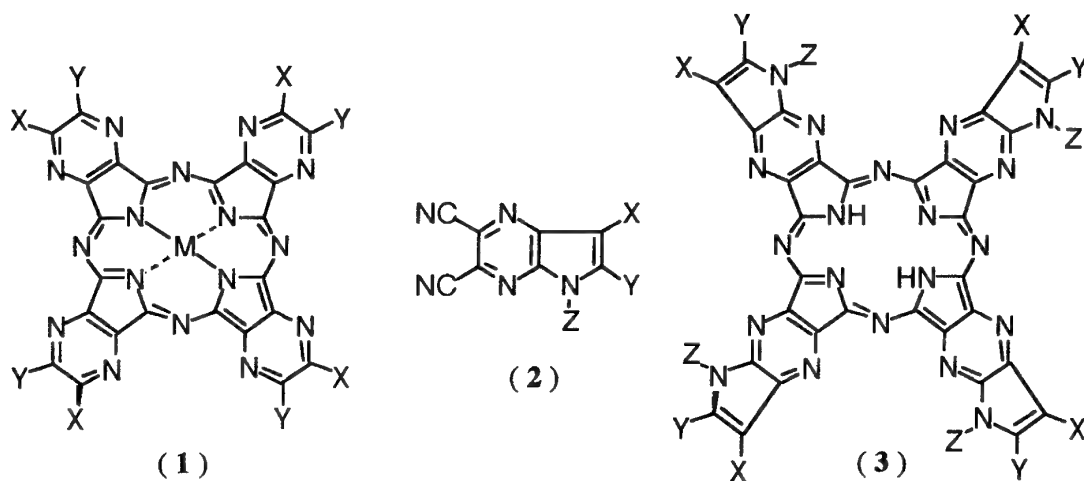


Table 1. Structure and spectral properties of dye 1

Compd.	X	Y	M	λ_{\max} (nm)	F_{\max} (nm)	SS
1a	Et	Et	Al(OH)	636	638	2
1b	4- <i>n</i> -ocrylphenyl	H	Al(OH)	651	656	5
1c	4- <i>n</i> -dodecylphenyl	H	Al(OH)	651	656	5
1d	4- <i>n</i> -hexadecylphenyl	H	Al(OH)	650	654	4

Table 2. Structure and spectral properties of dye 3

Compd.	X	Y	Z	λ_{\max} (nm)
3a	-C ₁₀ H ₂₀ -		-C ₁₂ H ₂₅	712
3b	-C ₁₃ H ₂₆ -		-C ₈ H ₁₇	712
3c	<i>n</i> -C ₁₄ H ₂₉	<i>n</i> -C ₁₅ H ₃₁	-C ₁₂ H ₂₅	713
3d	<i>n</i> -C ₁₄ H ₂₉	<i>n</i> -C ₁₅ H ₃₁	-C ₁₆ H ₃₃	714

Photoinduced Infrared Absorption Spectra of Conducting Polymers

E. Mulazzi

Dipartimento di Fisica and INFN, Università di Milano - Via Celoria 16 - Milano 20133 Italy

We present a theoretical analysis of the Photoinduced Infrared Absorption (PIA) spectra of polyacetylene (PA), triblock polyacetylene - polynorbornene - polyacetylene (PA) (PN) (PA) and diblock (PA) (PN) copolymers. The most striking feature in the PIA spectra of all these polymers is that the photoinduced vibrational broad band (in the frequency range $500\text{-}1000\text{ cm}^{-1}$) has a structured shape which changes in a dramatic way with the sample preparation and conditions. On the contrary the peak positions and the shape of the two other photoinduced vibrational bands do not show a similar behavior (see Refs. (1), (2) and (3)). We calculate the structured band shapes in the different polymers by following the model introduced in Ref (1). The evaluation of the band shapes are performed by calculating the lattice dynamics of the different conjugated segments, perturbed by the trapped electrons on different defect sites, together with the transition dipole moments and the segment distribution in the polymeric chains. Very good agreement is found between the experimental data (see Refs. (1), (2), (3)) and the evaluated band shapes, by using distributions of segments which are close to those found in the calculation of the Optical Absorption (UV -vis) and the resonant Raman Scattering band shapes in the same samples (Refs (4) and (5)). Within the same model we analyze also the photoinduced electronic band (peak position $\sim 0.5\text{ eV}$) and we can account for its peak position changes reported for the different samples.

In addition we present the calculated shape of the vibrational band ($500 - 1000\text{ cm}^{-1}$) observed in the doping induced infrared spectra of various doped PA (Ref. 6) and a comparison is made between these results and those obtained for the photoinduced bands.

Finally the PIA spectra of these polyacetylene - type polymers are analyzed also in comparison with the PIA spectra of PPV and PPP - type polymers as given in literature (Ref.7).

1. E. Mulazzi, A. Ripamonti, T. Verdon and S. Lefrant, Phys. Rev. 45, 9439 (1992).
2. E. Mulazzi, A. Ripamonti, C. Godon and S. Lefrant to be published in Synt. Metals 1997.
3. M. Mauri, W. Graupner, G. Leising Synth. Met. 69, 73 (1995).
4. Brivio and E. Mulazzi, Phys. Rev. B 30, 876 (1984).
5. E. Mulazzi, A. Ripamonti, C. Godon and S. Lefrant, Synth. Met. 69, 671 (1995).
6. S. Piaggio, G. Dellepiane, E. Mulazzi, R. Tubino, Polymers 28, 563 (1987).
7. See for instance the related papers in Synt. Met. 69, 1-3, 1995. See also the proceedings of ICSM96 in Synth. Met. (1997).

THERMAL STABILITY OF ANIZOTROPIC LC POLYMER NETWORKS

- THE ROLE OF MOLECULAR RELAXATIONS

P. Wojciechowski and J. Ulanski

Division of Polymer Physics, Institute of Polymers, Technical University of Lodz
ul. Zeromskiego 116, 90-924 Lodz, Poland

Liquid-crystalline (LC) polymers can easily develop an optical anisotropy subsequent to unidirectional drawing or shearing. Such materials may be interesting for optical applications, e.g. as polarizers or as matrices inducing orientation of incorporated chromophore molecules. On the other hand the anisotropy in LC polymers is unstable. After cessation of draw or shear, the induced internal stresses or, in general, the stored energy leads to reordering *via* molecular relaxations. Typically, the global molecular alignment first relaxes partially to form periodic zig-zag type supermolecular structure. This is seen in a polarizing microscope as banded texture with periodic dark bands lying perpendicular to the shear direction. The band periodicity reaches its minimum at some time depending on the polymer type, temperature and shearing condition; then the periodicity starts to increase and eventually the system recovers global isotropy. The processes of band formation and further molecular alignment relaxations are very sensitive to temperature.

Three different LC cellulose derivatives (LC-CD) were examined in order to correlate the chemical structure and the rate of band texture formation after cessation of shear: (hexanoyloxypropyl)cellulose, (propionyloxypropyl)cellulose and (cyanoethylpropyl)cellulose. The increase of the length and polarity of the side chains slow down the molecular relaxations increasing the stability of the anisotropy. The thermal stability of the anisotropy increases with increasing temperature of molecular α -relaxation. However, even for the most stable material, (cyanoethylpropyl)cellulose, an increase of the temperature to about 70° C leads to quick, spontaneous recover of isotropy.

The mesomorphic order of the oriented LC-CD can be stabilized *via in situ* photopolymerization of monomers able to form lyotropic solutions with the LC-CD.

Acrylic acid, methacrylic acid, and multifunctional monomer 1,4-butanediol dimethacrylate were chosen as polymerizable lyotropic solvents. The lyotropic solutions of the investigated LC-CD were oriented by shearing and then photopolymerized using mercury lamp (365 nm). The relaxation of the molecular orientation of the LC-CD is strongly affected by the polymer network originated from photopolymerization of the liquid monomer. The birefringence of the anisotropic polymer networks (APN) is stable to much higher temperatures compared to pure LC-CD. What more, the birefringence of the APN recovers upon cooling even if the sample was overheated above the isotropization temperature. The stabilization ability of the polymer networks is correlated with the molecular α -relaxation and T_g of the polymer obtained by photopolymerization and depends on interchain interactions with the LC-CD macromolecules. Strong interactions, like hydrogen bonds or dipole-dipole interactions, suppress the molecular relaxations of LC-CD macromolecules and results in highly stable birefringent, colorless and transparent polymeric materials.

This work was supported by the KBN project 1361/T09/95/08

Quadratic hyperpolarizability of donor-acceptor polyenes: a theoretical and experimental investigation.

M. Barzoukas¹, J. Muller¹, A. Fort¹, V. Alain², M. Blanchard-Desce²

¹ *Institut de Physique et Chimie des Matériaux de Strasbourg, Groupe d'Optique Nonlinéaire et d'Optoélectronique, UMR 046, 23 rue du Loess, 67037 Strasbourg, France*

² *Département de Chimie, Ecole Normale Supérieure, URA 1679 CNRS, 24 rue Lhomond, 75231 Paris Cedex 05, France*

Donor-Acceptor polyenes are model compounds for long distance intramolecular charge transfer between the end groups: they can present huge off-resonance quadratic hyperpolarizabilities $\beta(0)$. In this work, we have synthesized several series of polyenes of various lengths and bearing aromatic donors combined with potent heterocyclic acceptors. For each of these molecules, we have measured in solution the ground-state dipole and the quadratic hyperpolarizability $\beta(0)$.

We discuss the experimental results using a two-form two-state model we have developed recently. The correlation between hyperpolarizabilities and mixing in the ground state between the two limiting-resonance forms can help understand experimental trends. Thus, we show how upon charge separation the loss in aromaticity of the donor counterbalanced by the gain in aromaticity of the acceptor can lead to optimum mixing yielding maximum quadratic hyperpolarizability $\beta_{max}(0)$. Finally, we analyse the dependence of the quadratic hyperpolarizability $\beta(0)$ on the polyenic chain length. We show how this behavior is dominated by the way both $\beta_{max}(0)$ and the mixing are affected by the chain length.

A waveguide electro-optic modulator based on a DCANP Langmuir-Blodgett film

S. Sottini, D. Grando, L. Palchetti, E. Giorgetti

Istituto di Ricerca sulle Onde Elettromagnetiche "Nello Carrara", Consiglio Nazionale delle

Ricerche, Via Panciatichi, 64 I-50127 Firenze, Italy

Tel.: +39-55-42351, Fax: +39-55-410893, Telex 570231 IROE

E-mail: sottini@iroe.iroefi.cnr.it

R. Ricceri, G. Gabrielli

Dipartimento di Chimica, Università di Firenze, Italy

The interest in organic optical waveguides dates back to the very beginning of Integrated Optics (IO). At present, besides plastic optical fibers (POF), a complete organic IO Technology is available, that is a variety of devices, including amplifiers, modulators and switches which have been demonstrated by introducing suitable functional groups into polymer structures. The ability to engineer organic materials is perhaps their most attractive feature. Other advantages are expected as well, such as low material cost, cheap and mass production technologies, etc.

Focusing on organic waveguides for second order nonlinear optics, they require the fabrication of homogeneous and oriented thin films. Poled polymers including donor and acceptor groups have been widely investigated in the past years [1]. Alternatively the Langmuir-Blodgett technique (LB) is quite attractive to get oriented films because it requires a relatively cheap equipment and, at least in principle, it allows a fine control on the film thickness and refractive index. Unfortunately, LB films show some drawbacks as high propagation losses due to scattering and a thickness, which is usually not sufficient to achieve the waveguiding. These problems can be partially overcome by using an auxiliary guide, for example a graded index glass guide (GRIN) obtained by ion exchange in a soda-lime glass substrate [2]: in the resulting four layer guide (FLG), only a predetermined percentage of the guided light actually propagates in the organic film, thus reducing the total losses.

Here a waveguide electro-optic modulator based on a DCANP (2-docosylamino-5-nitropiridine) Langmuir-Blodgett film is described. The LB film (Fig.1) was transferred on a pyrex substrate,

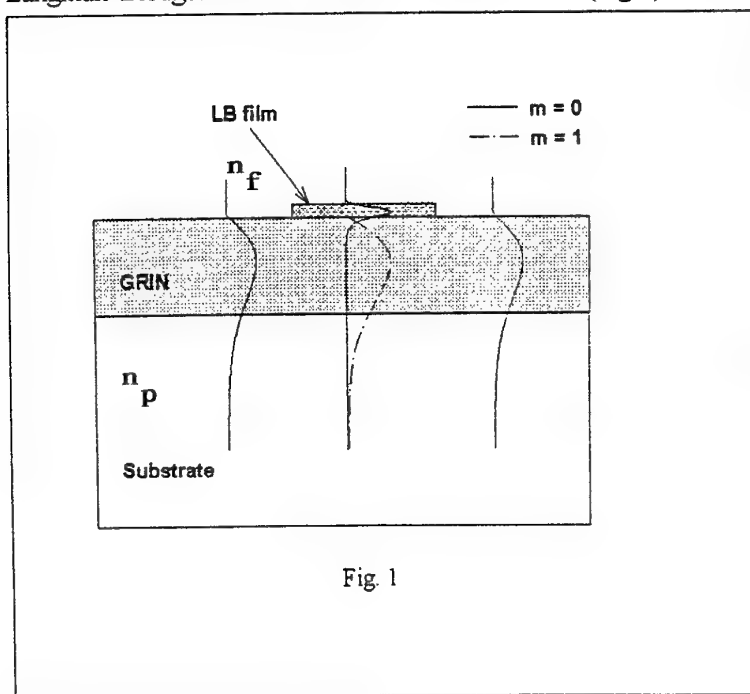


Fig. 1

which already included a channel GRIN, realized by K^+-Na^+ ion-exchange with a $3.6 \mu m$ wide mask. Pyrex was chosen just because n_p is much smaller than the refractive index of the DCANP film ($n_f=1.58$ at $\lambda = 850 \text{ nm}$). This condition is necessary to increase the percentage of guided power in the LB film. The obtained multilayer structure is a loaded FLG, where the light is confined in two dimensions not only in the GRIN channel but also in the DCANP film.

DCANP monolayers and LB films were described in a previous work [3]. In particular, 136 layer films of

DCANP were realized with the dipping direction perpendicular to the light propagation direction, so that the dipole orientation matches that of the TE guided field; the thickness of such multilayers was 0.30056 μm (the thickness of each transferred monolayer was 22.1 \AA).

As shown in Fig. 1, with our fabrication parameters and at $\lambda = 849 \text{ nm}$, the propagation is single mode in the channel GRIN, while a second mode is supported by the FLG, where the GRIN is loaded with the DCANP film. Consequently, at the input edge of the DCANP film, the light energy from the GRIN is splitted into the two modes pertaining to the FLG. The reverse process happens at the output edge of the FLG. In the case of a DCANP film having sharp edges, it was evaluated that only 17% of the energy in the $m=0$ mode of the GRIN is coupled into the $m=0$ mode of the FLG while the remaining 83% mainly goes into the $m=1$ one. However, the losses due to the mismatch between the $m=0$ modes at the transition between GRIN and FLG can be reduced up to 10% by tapering the edges of the DCANP film. The field distributions pertaining to the guided modes supported by the FLG were calculated: it was estimated that 25% of the energy propagating in the $m=0$ mode actually travels in the organic film whose losses, measured from the scattering data, turned out to be about 34 dB/cm.

Electro-optic tests and a measure of the related electrooptic coefficient r_{22} were performed on a sample analogous to that sketched in Fig 1 but with the addition of two Al electrodes, which were deposited on the pyrex substrate before the transfer of the LB film. The length of the FLG was 2.6 mm, a bit shorter than the electrodes.

By applying a voltage V at the electrodes, the refractive index n_f of the LB film is expected to vary according to the relation:

$$(1) \quad \Delta n_f = \frac{1}{2} \Gamma n_f^3 r_{22} \frac{V}{g}$$

Where g is the distance between the electrodes, and Γ is the overlap integral between the external electric field E_{ext} and the guided one E . TE propagation is supposed.

As already noticed, part of the light in the $m=0$ mode travels in the DCANP film and is affected by the Pockel's effect, while the $m=1$ mode is not perturbed because only 1% of its energy is confined in the organic film. Therefore, at the FLG output, when the two modes merge into the single mode of the GRIN, a strong attenuation of the $m=0$ mode and a modulation of its phase -dependent on the applied voltage V - are expected. On the contrary, $m=1$ acts as a reference. In particular, in the case of a sinusoidal voltage $V = V_0 \sin \Omega t$, an analogous modulation of the output field from the GRIN is expected. Our results, although very preliminary, confirm this expectation. From these data, it was possible to get a rough evaluation of r_{22} which turned out to be 4 pm/V. This value is certainly smaller than expected and the reasons, at the moment, are not clear. However, a Pockel's coefficient which is greater than 1/10 of LiNbO_3 coefficient r_{33} clearly confirms that the LB film of DCANP was properly oriented. Moreover, the propagation characteristics of the FLG were in good agreement with the calculations: this assures that the phase modulation affects only the $m=0$ mode and confirms that the film thickness and refractive index were as expected.

References

- [1] P.Pantelis and J.R.Hill: *Guest-host polymer systems for second order optical nonlinearities* in Polymer for lightwave and Integrated Optics, L.A.Hornak ed, Marcel Dekker Inc,1992
- [2] S.Sottini et alii: *Characterization of a Langmuir-Blodgett film waveguide by a four layer structure*, Proc. ECIO89, SPIE vol.1141,p.37,1989
- [3] R.Ricceri et alii, Langmuir,1996,in press

NONLINEAR IMAGE PROCESSOR FOR THIRD ORDER SUSCEPTIBILITY MEASUREMENTS AND CONTRAST INCREASING IN THE IMAGE PLANE

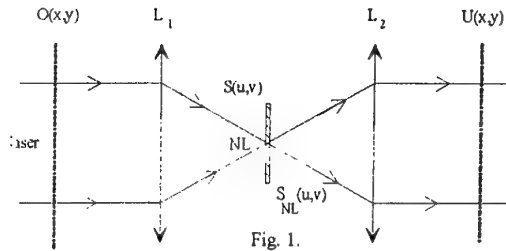
G. BOUDEBS *, M. CHIS, A. MONTEIL.

LABORATOIRE DES PROPRIETES OPTIQUES DES MATERIAUX ET APPLICATIONS. EP CNRS 130
Université d'Angers. 2, boulevard Lavoisier. 49045 ANGERS cedex 01. FRANCE.

* Corresponding author. Phone:(33) 2. 41.73.54.26. Fax:(33) 2. 41.73.53.52. E-mail: Boudebs@univ-angers.fr

Abstract

It has been shown that the use of a non linear material as a Fourier filter in the common focus of two lenses in a 4-f system allows all optical image processing (Fig. 1)^[1,2]. The measurement of the nonlinear changes undergone by the image of an object in this setup can be used to characterize the nonlinear response of the Fourier filter.



The method has been developed to measure the real and imaginary parts of χ^3 under picosecond excitation in various materials (liquids and crystals). It can be summarized as follows : for an object $O(x,y)$, the experimental image $I_e(x,y)$ is recorded on a calibrated CCD camera and compared with the calculated image $I_c(x,y)$. The calculation of $I_c(x,y) = |U(x,y)|^2$ is made numerically according to the choice of the object using the following scheme :

$$O(x,y) \xrightarrow{TF} S(u,v) \xrightarrow{T(u,v)} S_{NL}(u,v) \xrightarrow{H(u,v)} S'(u,v) \xrightarrow{TF^{-1}} U(x,y)$$

where TF and TF^{-1} are direct and inverse two-dimensional Fourier transforms. The involved parameters of the optical system are defined in $H(u,v)$ which is the classical optical transfer function : $H(u,v) = \text{circ}\left(\frac{\sqrt{u^2 + v^2} \cdot \lambda G}{ON}\right)$ where ON represents the numerical aperture, G the magnification and λ the wavelength. $T(u,v)$ characterizes the nonlinear medium. For a medium with a complex χ^3 , we write^[3] :

$$T(u,v) = \frac{\exp(-\alpha L)}{\left[1 + \beta \frac{1 - \exp(-2\alpha L)}{\alpha} |S(u,v)|^2\right]^{1/2}} \times \exp\left\{j \frac{\gamma}{2\beta} \ln\left[1 + \beta \frac{1 - \exp(-2\alpha L)}{\alpha} |S(u,v)|^2\right]\right\},$$

where L is the nonlinear material thickness (chosen smaller than the Fresnel length), linear and nonlinear absorption are characterized by coefficients α and β respectively, while γ is connected to nonlinear changes of the refractive index Δn (if $\alpha = 0$ and $\beta = 0$ then $\Delta n(u,v) = \frac{\lambda}{2\pi} \gamma |S(u,v)|^2$). Thus, the transmittance $T(u,v)$ is a function not only of the

medium parameters α , β , γ but also of the intensity $I(u,v) = 2\epsilon_0 n c |S(u,v)|^2$ (n is the refractive index) entering the sample in the Fourier plane.

The calculated intensity in the image plane is given by :

$$I_c(x,y) = |U(x,y)|^2 = \left[TF^{-1} \{S(u,v) \cdot T(u,v) \cdot H(u,v)\}\right]^2$$

Values of β and γ are obtained by fitting the experimental image with the calculated one. This method, tested with reference materials (CS_2), gives good results in agreement with other measurements made by other authors. The value obtained for the

constant n_2 defined by $\Delta n(u,v) = n_2 I(u,v)$, is $2,45 \cdot 10^{-18} \text{ m}^2/\text{W}$ deduced from the slope of the linear regression line represented in Fig. 2. Here we can see the evolution of the refractive-index change in the center of the Fourier spectrum in a 1-mm-long cell of CS_2 versus corresponding input intensity. The excitation is provided by a Nd:YAG laser delivering a 25 ps single pulse, linearly polarized, at $\lambda = 532 \text{ nm}$. This technique has been tested here with a Young's two-slit object.

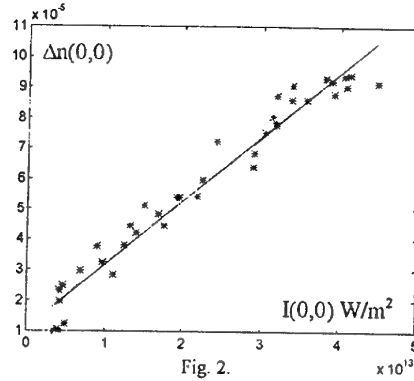


Fig. 2.

Compared to other methods, the nonlinear imaging method presents several advantages. Alignments are simpler than those necessary in wave mixings, no displacement of the sample is needed and one laser shot is sufficient to estimate non linear parameters.

The second part of this study deals with the simulation of the image formation involved by using our nonlinear processor with other different objects. We consider objects whose index and transmittance profiles presents a rectangular shape. These objects are described by^[4]:

$$O(x,y) = 1 + (\sqrt{T}e^{j\varphi} - 1) \text{rect}\left(\frac{x}{L_x}\right) \text{rect}\left(\frac{y}{L_y}\right), \text{ where } T \text{ represents the transmittance, } \varphi \text{ the}$$

phase difference and L_x (L_y) the width of the object. The simulated images through the system are given for increasing nonlinearities $\Delta n(u,v)_{\text{Max}}$. We note an increasing contrast in the image plane with increasing $\Delta n(u,v)_{\text{Max}}$. For a pure phase object ($T = 1$, $\varphi = 50^\circ$), practically invisible in the image plane (visibility $V \approx 0.15$) without nonlinearities, the visibility reach 0,65 if we remain limited to $\Delta n(u,v)_{\text{Max}} = 10^{-4}$. This limit expresses the fact that our simple model (based on linear system theory) is no longer valid when nonlinear effects are important. The simulation illustrated in Fig. 3 is given for α and $\beta = 0$.

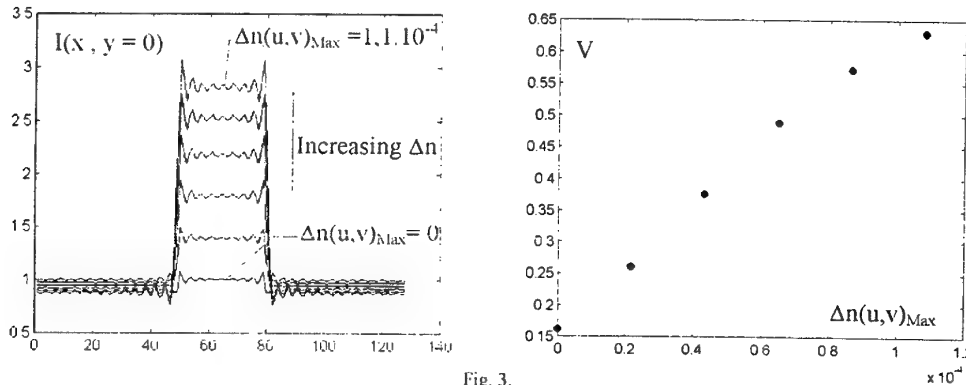


Fig. 3.

References

- [1] L. Pichon et al., Opt. Com., 36, 4, 277-280, (1981).
- [2] N. Phu Xuan et al., Opt. Com., 68, 4, 244-250, (1990)
- [3] G. Boudebs et al., J. Opt. Soc. Am. B, 13, 7, 1450-1456, (1996).
- [4] D. Courjon et al., J. Opt. Soc. Am., 5, 7, 1066-1072, (1988).

Second harmonic generation from Azobenzene derivatives in acrylic polymeric matrices

Enzo Campani, Giampaolo Gorini, Michele Nencioli

Dipartimento di Fisica, Università di Pisa, P.zza Torricelli 2, 56126 Pisa (Italy)

Giorgio Masetti

Istituto di Biofisica, Consiglio Nazionale delle Ricerche, via S.Lorenzo 26, 56127 Pisa (Italy)

ABSTRACT

Recent results of second harmonic generation (SHG) measurements from a newly synthesised organic polymer are presented and discussed. The new material was obtained by copolymerisation of methyl acrylate with the acrylic ester of Disperse Red 1 and it was investigated at room temperature as a thin film stuck through the spin coating technique onto an ITO coated slide. Azobenzene derivatives present as side chain groups in the copolymer were responsible for the observed non linear effect. In order to guarantee some degree of orientation in the polymer bulk an intense, static electrical field was applied across the film either above the glass transition temperature T_g (thermal orientation) or at room temperature in presence of 488 nm radiation from an Ar⁺ laser (photoinduced orientation).

An excimer laser pumped dye laser was used as primary source to induce frequency doubling from the film. Its wavelength was properly chosen at 710 nm in order to obtain an SHG signal at 355 nm, within a transmission window of the sample. Part of the light emitted by the film and colinear with the incident beam was filtered by a double monochromator and its intensity was measured by means of a photomultiplier and a gated detection system.

As regards the frequency doubling efficiency the best results were obtained with the photoinduction process wherein the radiation at 488 nm, resonant with the p-p* electronic transition of the azoderivative chromophore, should favour its mobility through a trans-cis-trans isomerisation mechanism. By so doing one could also monitor in real time during the experiment the re-alignment of the chromophores along the direction of the electric field.

The main results of this work are summarised as follows:

i) The intensity of the SHG signal was strongly dependent on the incidence angle of the exciting beam, its maximum being observed at 500, ii) lack of any observation of Maker fringes when varying the incidence angle assured us that the light coherence length within the film is longer than its thickness, iii) accordingly with the theory and with the assumed structure for the first hyperpolarisability tensor the doubling frequency efficiency significantly depends on the polarisation of the impinging beam and reaches its maximum value for polarisation parallel to the incidence plane.

As regards the effects induced by the 488 nm radiation we noted that no SHG signals could be detected when the electric field and the Ar⁺ laser are both on. On the contrary, high duplication conversions were obtained with the electric field alone provided the film had been previously irradiated for few seconds at 488 nm. Under these conditions the rise times of the signal decreased from 1030 to 200 s and its intensity increased by a factor 5 with respect to the use of the electric field alone.

Similar experiments were also performed on a mechanical dispersion of the same Disperse Red 1 in polymethylmetacrylate. Differently from what happens with the copolymer, when the electric field is on the Ar⁺ laser improves the orientation of the film, decreases the rise times and increases the maximum value of the SHG signal.

Moreover, with the mixture rather different results were found by us with respect to the previously ones reported by other authors which have been imputed to the different wavelength used to excite the same material.

Third order nonlinear optical properties of various families of tetrathiafulvalene derivatives

B. Sahraoui^(1,3), G. Rivoire⁽¹⁾, M. Sallé⁽²⁾ and A. Gorgues⁽²⁾

⁽¹⁾Laboratoire POMA, Equipe Photonique de Puissance, EP CNRS 130

Université d'Angers. 2, Boulevard Lavoisier, 49045 Angers, France.

⁽²⁾Laboratoire d'Ingénierie Moléculaire Matériaux Organiques, UMR CNRS 6501

Université d'Angers. 2, Boulevard Lavoisier, 49045 Angers, France.

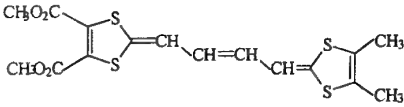
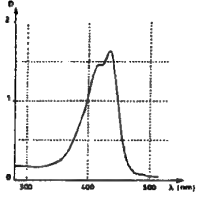
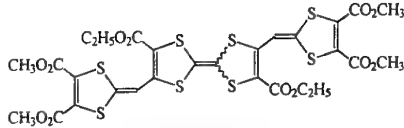
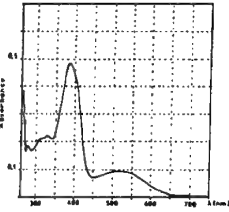
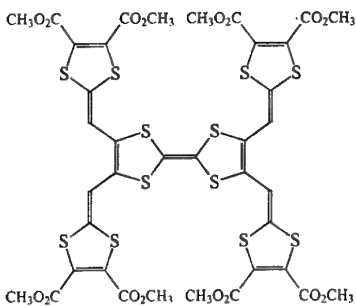
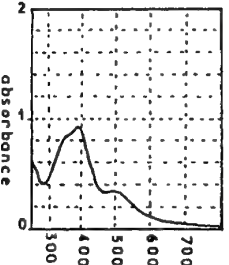
e-mail : sahraoui@univ-angers.fr

Tel : (33) (2) 41.73.54.24 Fax: (33) (2) 41.73.53.30

⁽³⁾ Also in Instytut Fizyki, Uniwersytet M. Kopernika 87-100 Torun, Poland

The investigations concerning the relationships between the molecular structure and nonlinear optical properties of organic compounds have been the subject of intense study[1-5]. These investigations serve to guide the development of new materials and devices.

In this work we present an analysis of the third order nonlinearities of three families of new tetrathiafulvalene (TTF) derivatives : ethylenic, bis(dithiafulvenyl)- and tetrakis(dithiafulvenyl)-substituted TTF analogues. We have determined the third order susceptibilities of TTF analogues using degenerate four wave mixing experiment (DFWM). From these results the values of second order hyperpolarisabilities γ are deduced. They are competitive with those of the other organic materials studied until then [1,6]. The most representative compounds of each family in term of γ , are presented in the Table. We have observed that an increase of the number of sulphur heterocycles in a molecule induces an increase of third order nonlinearities, but at the same time it induces an increase of absorption coefficients. The molecules of ethylenic and bis-dithiafulvenyl substituted TTF derivatives expose linear absorption, whereas the transmission study at 532 nm of tetrakis-dithiafulvenyl TTF analogues reveals the presence of a saturable absorption which is described by four levels energy model [7]. In the Table the corresponding linear absorption coefficients and the absorption coefficient at the ground state of a tetrakis-dithiafulvenyl TTF analogue are presented .

Molecules studied at 532 nm	Spectra of TTF derivatives	α [cm ⁻¹]	α/C [l/g.cm]	$ \chi_{xxxx} $ ·10 ⁻¹² [esu]	γ_{xxxx} ·10 ⁴⁵ [m ⁵ V ⁻²]
Ethylenic TTF derivative 		14	4.6	6	4.61
Bis-dithiafulvenyl substituted TTF derivative 		20.4	40.8	10	59
Tetrakis-dithiafulvenyl TTF derivative 		63.2	79	26	210
Polydiacetylenes [6]	DFWM	6.9	-	7	-

Acknowledgment

One of the authors (B.S) would like to thank the Polish Committee for Scientific Research for the grant KBN 2 PO3B 138 12 which supports partly this work.

References

- [1] J. Zyss, ed., *Molecular Nonlinear Optics : Materials, Physics and Devices*, (Acad., Boston, 1994)
- [2] I. Ledoux, *L'Onde Electrique*, vol.74, 6, 5 Novembre -Decembre (1994)
- [3] F. Kajzar, C. Taliani, R. Zamboni, S. Rossini, R. Danieli, *Synthetic Metals* 77, 257-263, (1996)
- [4] K. Kamada, M. Ueda, T. Sakaguchi, K. Ohta, T. Fukumi., *Chem. Lett.* 263, 215-222 (1996)
- [5] B. Sahraoui, M. Sylla, J. P. Bourdin, G. Rivoire, J. Zaremba, T.T. Nguyen and M. Sallé, *J. of Modern Optics*, vol 42, N° 10, 2095-2107 (1995)
- [6] J. M. Nunzi and D. Grec *J. Appl. Phys.* 62, 6 (1987)
- [7] B. Sahraoui, R. Chevalier, G. Rivoire, J. Zaremba and M. Sallé, *Optics Communications*, 135, 109-115 (1997)

OBTAINING A COMPROMISE BETWEEN HIGH RESOLUTION, SENSITIVITY AND SPEED IN THE LIQUID-CRYSTAL SPATIAL LIGHT MODULATOR WITH A POLYIMIDE PHOTOSENSITIVE LAYER

N.V.Kamanina† and N.A.Vasilenko‡

†Vavilov State Optical Institute, 12, Birzhevaya, St.Petersburg, 199034 Russia

‡Karpov Research Physical-Chemical Institute, 10, Vorontsovo Pole, Moscow 103064, Russia

Obtaining a compromise between high resolution, sensitivity and speed in light-addressed structures is the topical problem of lasers, correlators and other applications of non-linear media and devices. The liquid-crystal spatial light modulator (LC-SLM) with the photoconductor based on polyimide offers the most promise for attacking this problem. LC-SLM with the polyimide photosensitive layer shows a high resolution (more than 200 mm^{-1} at a level of 0.5 MTF and 1000 mm^{-1} at a level of 0.1 MTF) and a high sensitivity of $10^{-6} - 10^{-8} \text{ J cm}^{-2}$. These characteristics allowed LC-SLM to be applied to a correction of phase aberrations, decreasing a beam divergence from 20 mrad down to 0.15 mrad [1].

However, the temporal characteristics of LC-SLM with the polyimide photosensitive layer are worse than those of LC-SLM with other photosensitive layers. Therefore, a search for lines of attack on the problem of an enhancement of the temporal characteristics while retaining the high sensitivity and resolution is important for extending the applications of LC-SLM with the polyimide photosensitive layer.

In the present paper the possibilities for reaching the high speed while retaining the high sensitivity and resolution of LC-SLM with the polyimide photosensitive layer have been investigated by both changing the operating conditions and varying the conditions at the interface between the photoconductor and the liquid crystal.

The sinusoidal holographic grating was recorded by a second harmonic of the pulsed Nd-laser irradiation with a pulse width of 20 ps over a wide range of spatial frequencies ($50\text{-}800 \text{ mm}^{-1}$). The write energy density was $100\text{-}1000 \mu\text{J cm}^{-2}$. The grating was read out with a cw He-Ne-laser at the power density of $100 \mu\text{W cm}^{-2}$. The pulsed supply voltage was applied to LC-SLM. The dependence of a diffraction efficiency (η) on a delay (D) between a write pulse and a supply voltage pulse showed that η peaked at $D = 0.5 \text{ ms}$.

The interface conditions were varied by using different alignment films (AF): SiO , SiO_2 , GeO , CeO_2 , polyvinyl alcohol, and $\alpha\text{-C}_6\text{H}_6$. LC-SLM with polymer AF was found to exhibit shorter switching times than LC-SLM with oxide AF. Typical switch-on time (t_{on}) and switch-off time (t_{off}) were tens and hundreds of milliseconds, respectively, for LC-SLM with oxide AF. Minimum t_{on} (1-3 ms) and t_{off} (10-30 ms) were obtained in LC-SLM with polymer AF. However, the less was the switching time, the worse was a sensitivity. This fact was not in contradiction with the model of the internal *pin*-diode [2].

The optimal characteristics of LC-SLM with the polyimide photosensitive layer were found to be obtained by using polymer AF. They were: a resolution of 210 mm^{-1} and 760 mm^{-1} at a level of 0.5 MTF and 0.1 MTF, respectively; the maximum diffraction efficiency of $5 \times 10^{-7} \text{ J cm}^{-2}$ at $\eta = 1\%$; a speed of 7 Hz and more than 10 Hz on application of the unipolar and bipolar pulsed supply voltage, respectively.

[1] N.V.Kamanina, L.N.Soms, A.A.Tarasov. *Opt. Spectrosc.* (1990) **68**, 691.

[2] N.V.Kamanina, N.A.Vasilenko. *Proceed. SPIE* (1995) **2731**, 220.

Influence of Conjugation Length Expansion and Substitution on the Second-Order Hyperpolarizability γ of Oligotriacetylenes

Ulrich Gubler^a, Rainer E. Martin^b, Christian Bosshard^a, Rik. R. Tykwinski^b, Peter Günter^a, François Diederich^b

^aNonlinear Optics Laboratory, Institute of Quantum Electronics, ETH Hönggerberg, CH-8093 Zürich, Switzerland, ^bLaboratory of Organic Chemistry, ETH Zürich, CH-8092 Zürich, Switzerland.

The expansion of the conjugation length and the substitution by electron donating and accepting endgroups is a well known path to obtain larger second-order hyperpolarizabilities γ of organic molecules. Only few experimental datas are published of subsequently longer oligomer chains, because of the cumbersome synthesis of oligomers with well defined length.

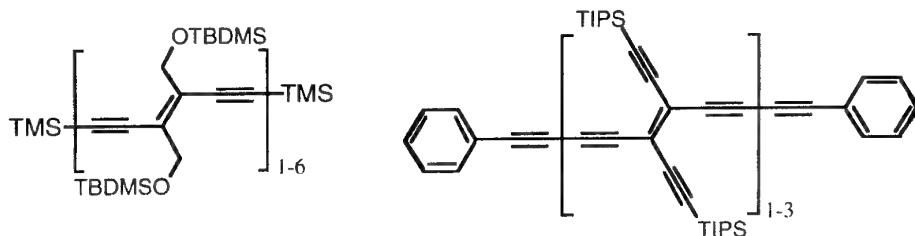


Fig.1 Unsubstituted oligotriacetylenes and tetraethynylethenes for measurements of the second-order hyperpolarizability γ by third harmonic generation (THG) in solution.

To investigate the conjugation length dependence of unsubstituted oligotriacetylenes, we measured samples of 1 to 6 monomer units and polydisperse polymer samples by third harmonic generation (THG) in solution ($\lambda=1907$ nm). The experiment revealed a power law dependence for the hyperpolarizability $\gamma \sim n^a$ on the conjugation length n . The exponent $a=2.5 \pm 0.1$ is in the range of what other groups measured on different molecular systems by the same technique, but is significantly lower than the values predicted by quantum chemical calculations. The polymer samples indicate a saturation of the power law in the range of 10 monomer units and a only linear increase in γ for longer polymer chains.

To estimate the impact of a second conjugation path perpendicular and in interaction with the main backbone, we measured unsubstituted oligotetraethynylethene samples too. Samples of 1 to 3 monomer units all showed a rise in γ of about one order of magnitude,

in contrast to other molecular system, which revealed a decrease by going from a one-dimensional to a two-dimensional system.

Substitution of the endgroups of the triacetylenes with electron-donating ($-\text{N}(\text{CH}_3)_2$) and electron-accepting groups ($-\text{NO}_2$) was performed for the mono- and the dimer in all possible combinations. Substitution of the longer oligomers was difficult because of a lack in chemical stability. The substitution increased the second-order hyperpolarizability γ by about two order of magnitudes, clearly favoring the asymmetric solution.

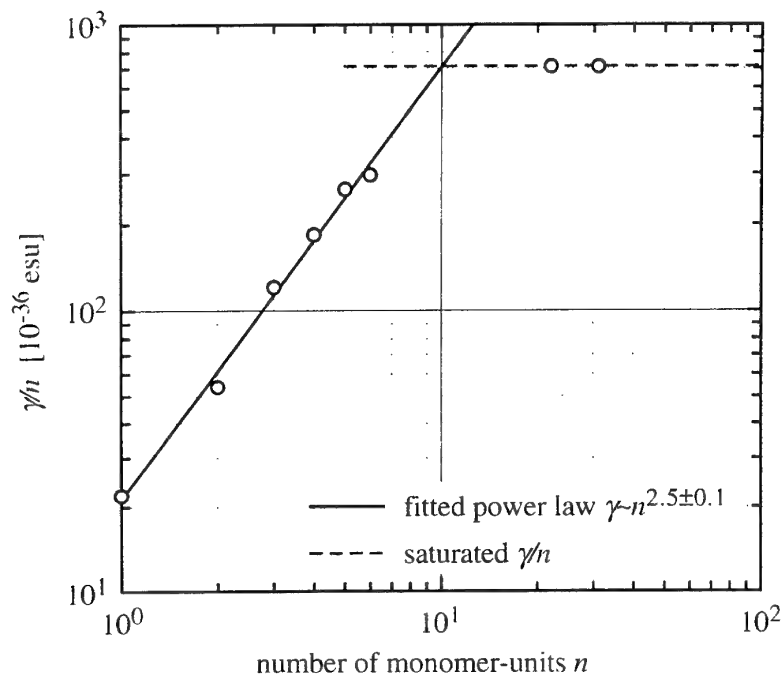


Fig. 2 The conjugation length dependence of the second-order hyperpolarizability γ of oligotriacetylenes yielded a power law, which saturates for 10 monomer units.

References:

- [1] R. E. Martin, U. Gubler, C. Boudon, V. Gramlich, C. Bosshard, J.-P. Gisselbrecht, P. Günter, M. Gross, F. Diederich, *Adv. Mater.* (submitted)

Novel Zwitterionic Chromophores for Electro-Optic Polymers

Ilias Liakatas, Man Shing Wong, Christian Bosshard, Martin Bösch
and Peter Günter

Nonlinear Optics Laboratory, Institute of Quantum Electronics, ETH-Hönggerberg,
CH-8093, Zürich, Switzerland

Potential applications in ultra-fast electro-optic modulation for applications in telecommunication have made organic nonlinear optical materials attract much attention during the last few years.[1] Electro-optic poled polymers have gained considerable interest as they can be easily processed for the fabrication of thin-film waveguiding structures. [2] Optimization of the electro-optic polymers focuses on the increase of the molecular nonlinearity and the better alignment of the molecules in the polymer matrix which leads to higher macroscopic nonlinearities. However, the acentric structure of the chromophores in a polymer induced by electric field poling is subject to thermodynamic relaxation. Recently, high glass transition polymers, e.g. polyimides, [3] have been used as a host matrix improving considerably the relaxation time of the acentric alignment of the chromophores. At the same time, the requirements for thermally stable molecules for a high temperature poling process have also increased.

We have recently synthesized stilbazolium based zwitterionic chromophores for electro-optic polymers.[4] Calculations have shown that their two counter ions can give rise to a large ground state dipole moment. We have shown experimentally that these chromophores have dipole moments up to $\mu = 13 \times 10^{-29}$ Cm implying a tendency for a high degree of orientation when poled. They also exhibited good thermal stability for high temperature poling.

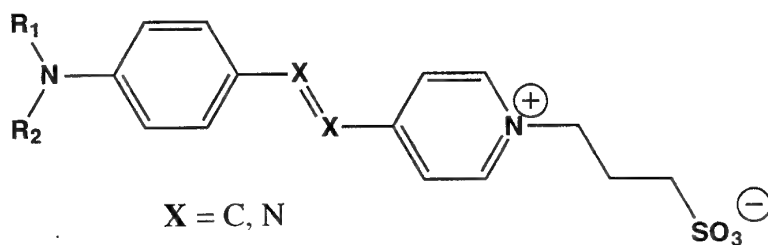


Fig.1 An example of zwitterionic chromophores.

Polyquinoline is a thermally stable and high glass transition temperature polymer.[5] We have used polyquinoline as a host matrix for the incorporation of azo based

zwitterionic chromophores because it is expected to sufficiently prevent the relaxation of the chromophores.

We will present experimental results on the molecular hyperpolarizability (up to $\beta = 90 \cdot 10^{-40} \text{ m}^4\text{V}^{-1}$) of our zwitterionic chromophores as well as on their solvatochromic behaviour. Strong fluorescence, formation of aggregation and an unusual increase of the absorption peak of the charge transfer band were observed for solutions in chlorinated solvents. Results on the macroscopic nonlinearity and thermal stability of guest-host systems using polycarbonate and of side-chain polyquinolines will be also reported. Guest-host systems of molecular concentration $N = 5 \cdot 10^{19} \text{ m}^{-3}$ in polycarbonate ($T_g = 150^\circ\text{C}$) were spin-coated and corona-poled. Nonlinear optical coefficients up to $d_{31} = 0.7 \text{ pm/V}$ were measured (reference: $d_{11}^{\text{Quartz}} = 0.3 \text{ pm/V}$)[6] which are comparable to that of Disperse Red 1 in the same host and their temperature limit of thermal stability was found to be around 200°C .

Acknowledgments: We acknowledge the ETH Council and the Swiss priority program Optique II for financial support.

References:

- [1] C. Bosshard, K. Sutter, P. Prêtre, J. Hulliger, M. Flörsheimer, P. Kaatz, and P. Günter, *Organic Nonlinear Optical Materials*, vol. 1. Amsterdam: Gordon and Breach Science Publishers, 1995.
- [2] R. Dagani, "Devices Based on Electro-optic Polymers Begin to Enter Marketplace," in *(C&EN) Chemical and Engineering News*, 1996, pp. 22.
- [3] P. Prêtre, "Modified Polyimide Side-Chain Polymers for Electrooptics," *Macromolecules*, vol. 27, pp. 5476, 1994.
- [4] I. Liakatas, M. S. Wong, C. Bosshard, M. Ehrensperger, and P. Günter, "Stilbazolium Based Zwitterionic Chromophores for Electro-optic Polymers," *Ferroelectrics*, 1996, in print.
- [5] Y. M. Cai and A. K.-Y. Jen, "Thermally stable poled polyquinoline thin film with very large electro-optic response," *Appl. Phys. Lett.*, vol. 67, pp. 299, 1995.
- [6] D. A. Roberts, "Simplified Characterization of Uniaxial and Biaxial Nonlinear Optical Crystals: A Plea for Standardization of Nomenclature and Conventions," *IEEE J. Quantum Electron.*, vol. 28, pp. 2057-2074, 1992.

INVESTIGATIONS OF AN OPTICAL ANALOG OF THE BORRMANN EFFECT IN RESONANT LIQUID-CRYSTAL MEDIA

V.V.Danilov and N.V.Kamanina

Vavilov State Optical Institute, 12, Birzhevaya, St.Petersburg, 199034 Russia

Diffraction suppression of absorption, that is analogous to the Borrmann effect observed for X-rays [1] and neutrons [2], is exhibited in nonlinear optical systems based on nemato-chiral liquid crystal mixture and a dye under a nanosecond pulsed laser irradiation. The suppression is generally observed when a laser wavelength falls within the overlapping region of the selective reflectance band of the nemato-chiral compound with the absorption band of the dye.

When the laser irradiation interacts with a matter, the created polarization grating is superimposed on the plane chiral structure forming deformation areas and resulting in the respective modulation of refractive index; in so doing a phase grating is formed. For these systems, the short switching time of 10 ns was observed at a relative low write energy of 10 μ J [3].

In the present paper the processes going on in the resonant liquid crystal (LC) medium have been investigated. The nemato-chiral mixture doped with ketocyanine (1%) was used as the resonant medium.

The grating was recorded by a dynamic holographic technique in the self-diffraction mode in the range of spatial frequencies of 200-300 mm^{-1} and at the write energy of 0.05-1.2 mJ. The writing and the readout were performed by a second harmonic (533 nm) of the pulsed $\text{KGd}(\text{WO}_4)_2$ -laser irradiation with a pulse width of 15 ns. The response was recorded in the first diffraction order. The nonlinear light-induced addition to refractive index of the LC medium was calculated to be 0.01, more considerable than the thermal-induced nonlinearities (10^{-5}).

A relaxation of the holographic grating was also investigated in the doped nemato-chiral LC compound. In this case, the grating was read out with a cw He-Ne-laser (630 nm). Multiple regions were identified in the time dependence of diffraction efficiency. The regions corresponded to successive turning on at least three mechanisms of the grating relaxation, each characterized by its own time constant.

The first mechanism was due to the Borrmann effect. The second was defined by a deformation of the nemato-chiral LC compound, resulting in a change in a helix pitch. The third was related to a formation of areas with the smectic order.

[1] G.Borrmann. *Z. Phys.* (1950) **127**, 297.

[2] Yu.Kagan, A.M.Afanas'ev. *Sov. Phys.-JETP.* (1966) **22**, 327.

[3] L.Zagainova, G.Klimusheva, L.Yatsenko, V.Danilov. *Mol. Cryst. Liq. Cryst.* (1990) **192**, 279.

POLYMERIC NONLINEAR OPTICAL WAVEGUIDES FOR ALL-OPTICAL SWITCHING AT TELECOMMUNICATION WAVELENGTHS

Adrian Boyle and Werner J. Blau

Physics Department, Trinity College Dublin, Dublin 2, Ireland

The construction and characterisation of a nonlinear fibre loop mirror of ultrafast all-optical switching and demultiplexing is described. The difficulties presented with using optical fibre as the active nonlinear element are discussed and the potential advantages of using polymer waveguides are presented. A complete characterisation of the nonlinear optical properties of a representative polymer channel waveguide is established in the near infrared at 1.3 μm and 1.55 μm . Nonlinear absorption results in a decrease of the propagating light intensity and its magnitude and potential influence on all optical switching is discussed. The nonlinear refractive index coefficient is measured by spectral broadening due to self - phase modulation and by pulse modulated Mach - Zehnder interferometry. The nonlinear refractive index coefficients are found to be $1.9 \cdot 10^{-17} \text{ m}^2/\text{W}$ at 1.32 μm and $1.0 \cdot 10^{-17} \text{ m}^2/\text{W}$ at 1.55 μm . A balanced evaluation of linear and nonlinear losses and nonlinear refraction concludes with the need to improve the polymer material and waveguide quality, but a clear demonstration of the excellent application potential of this material class.

POLY(ARYLENE ETHYNYLENE) COPOLYMERS: A MODEL STUDY IN MOLECULAR ENGINEERING FOR PHOTONIC DEVICES

Andrew Davey, Orla O'Connor, Emmanuel Bourdin and Werner J. Blau
Physics Department, Trinity College Dublin, Dublin 2, Ireland

It is established that polydiacetylenes possess some of the largest optical nonlinearities observed in conjugated polymers. Similarly, it is well known from the example of the PPV polymer family that the inclusion of arylene moieties into the polymer backbone can yield highly fluorescent materials. We have therefore decided to combine these two properties and to develop a family of poly(arylene ethynylene) copolymers whose fluorescence properties may be tuned by the appropriate choice of an arylene moiety and who also will possess a large nonlinearity, in particular a large multi-photon absorption. Starting from semi-empirical quantum chemical geometry optimisation models we determined the relevant optical properties of the molecules by configuration interaction. Subsequently a number of members of this copolymer family were synthesised with emissions ranging from blue to red, and whose fluorescence quantum yield is above 50% in some cases. Light emitting diodes were fabricated with efficiencies similar to those of simple PPV devices. Similarly, laser action was observed under ultraviolet laser pumping. The sign and magnitude of the second order hyperpolarisability was determined at 1064 nm and 532 nm. At 532 nm, a strong two photon resonance enhanced response is observed with values of the hyperpolarisability of 2×10^{-32} esu, mainly real negative. Intense fluorescence was stimulated by three photon absorption at 1064 nm which indicated a good potential to use such polymers for frequency up-conversion of near infrared laser pulses.

SECOND HARMONIC GENERATION FROM SUBPHTHALOCYANINES FILMS.

G. Rojo and F. Agulló-Lopez, Dept. Física de Materiales, C-IV

B.del Rey and T.Torres, Dept. Química Organica, C-I

Universidad Autonoma de Madrid.

Second Harmonic Generation (SHG) from $\lambda = 1.064 \mu\text{m}$ fundamental light have been measured for Subphthalocyanine films, by rotating the samples with regard to an axis contained in the film plane and perpendicular to the propagation direction. Two orthogonal linear polarizations of the incident light were used to calculate the three independent components of the $\chi^{(2)}$ tensor corresponding our films, having C_{ov} symmetry. The polarization of the second harmonic light was parallel to the incident plane (perpendicular to the rotation axis).

Partially ordered films were prepared by two different methods: spin-coating and evaporation. In the first case a corona poling technique was used to achieve the non-centrosymmetric ordering.

Optical absorption spectra showed a decrease in the Q band peak with increasing poling voltage. This effect allows us to calculate the electric field applied to the films during the the poling process.

The $\chi^{(2)}$ values have been determined by comparison with an X-cut LiNbO_3 plate, which was used as a reference ($\chi_{33}^{(2)}(\text{LiNbO}_3) = 1.97 \cdot 10^{-7} \text{ esu}$).

For spin-coating films with a poling field of $9 \cdot 10^5 \text{ V/m}$ were:

$$\chi_{13}^{(2)} = 8.1 \cdot 10^{-10} \text{ esu}, \quad \chi_{15}^{(2)} = -3.1 \cdot 10^{-10} \text{ esu}, \quad \chi_{33}^{(2)} = 1.2 \cdot 10^{-10} \text{ esu}.$$

indicating that the Kleinmann symmetry ($\chi_{13} = \chi_{15}$) is not obeyed.

The components of the molecular β tensor have been then calculated, yielding:

$$\beta_{13} = 180 \cdot 10^{-30} \text{ esu}, \quad \beta_{15} = -30 \cdot 10^{-30} \text{ esu}, \quad \beta_{33} = -32 \cdot 10^{-30} \text{ esu}.$$

PECULIARITIES OF THE INTERACTION BETWEEN HUMAN ERYTHROCYTES AND LIQUID CRYSTAL MATRIX IN THEIR MIXTURE

N.V.Kamanina† and V.N.Kidalov‡

†Vavilov State Optical Institute, 12, Birzhevaya, St.Petersburg, 199034 Russia

‡Pavlov St.Petersburg State Medical University, 6/8, L'va Tolstogo st., St.Petersburg, 197022 Russia

Nonlinear liquid crystal (LC) media are extensively used in the optical processing [1] and in the composite materials [2]. Recently the LC medium was proposed to use as a matrix for purposes of visualization, fixing and alignment of human erythrocytes [3].

In the present paper, the interaction between the erythrocytes and the LC matrix has been investigated at a various content of the red blood cells with the discoidal shape (discocytes) in the initial blood specimen.

The liquid crystal ZhK-1289 with positive dielectric anisotropy was used as the LC medium. A mixture of LC with the erythrocytes was introduced into the glass sandwich unit a clearance of 10 μm . (An erythrocyte size is 5-7 μm). The alignment film based on a solution of polychlorotrifluoroethylene in a mixture of acetone and toluene was deposited on the glass substrates of the unit. The microscopic investigations were carried out in the polarized light locating the unit at an angle of 45° to a plane of the input polarizer.

The prevailing alignment of the discocytes was found in comparison to the erythrocytes with the complicated shape (echino-, stomato-, poikilocytes, etc.). The erythrocyte alignment effect in LC was interpreted by the interaction between the red blood cells and dipole moment of valence oscillations of the $C \equiv N$ bond in the LC molecule. The dipole moment was created by rubbing of the alignment film.

It should be noticed that these investigations are of scientific and practical interest because, on the one hand, they are related to a study of the interaction of the LC molecules with a biological system, and on the other hand, they are able to be applied to diagnostics of the blood cell configuration.

[1] A.A.Vasil'ev, D.Casasent, I.N.Kompanets A.V.Parfenov. *Spatial Light Modulators*. Moscow: Radio i Svyaz' (1987) 320 p. [in Russian]

[2] G.M.Zharkova and A.S.Sonin. *Liquid Crystal Compositions*. Novosibirsk: VO Nauka (1994) 214 p. [in Russian]

[3] N.V.Kamanina, V.N.Kidalov. *Tech. Phys. Lett.* (1996) **22**, 571.

A new interferometric technique for the characterisation of optical nonlinearities in nematic liquid crystals

D. De Feo, S. De Nicola*, P. Ferraro†, A. Finizio*, P. Maddalena, G. Pierattini*

INFM, Dipartimento di Scienze Fisiche, Università di Napoli "Federico II"

Pad. 20, Mostra d'Oltremare, 80125, Napoli, Italy

Tel.: +39-81-7253354

Fax: +39-81-2394508

E-mail: pasmad@na.infn.it

**Istituto di Cibernetica del CNR, Via Toiano 6, 80072 Arco Felice (NA), Italy*

†Istituto Professionale di Stato per l'Industria e l'Artigianato: "G.L. Bernini"

Via Arco Mirelli 19/A, 80122 Napoli-Italy

Abstract

In this communication we present a new interferometric technique to measure the elastic constants of nematic liquid crystals. It is well known that a continuous wave laser beam impinging on a nematic liquid crystal film can induce a change in the orientation of the molecular director. In the case of homeotropic alignment and oblique incidence, the reorientation process has no threshold and the sample exhibits a giant optical nonlinearity due to the laser-induced change in the refractive index of the medium. In the small distortion approximation the whole problem is linear so that a powerful numerical technique such as Fast Fourier Transform (FFT) could be used to integrate the partial derivative differential equation describing the effect. The laser-induced change in the refractive index extends to a larger area than the irradiated one as consequence of the elastic coupling among the liquid crystal molecules. The measure of the spatial decay of the change of the refractive index in the liquid crystal film, which can be obtained putting the sample in the arm of an interferometer, gives in a direct way an estimate of the elastic anisotropy.

To this aim we have used a new type of an interferometer suitable for measuring the refractive index of microscopic transparent samples. This interferometer employs a mirror and a reflective type diffraction grating to recombine the object and reference beams. The mirror

and the grating are mounted on a compact and adjustable base plate. This interferometer works with expanded beams so that free access to the measuring arrangement system is allowed. The measurement procedure is completely automatic so that the system shows a good insensitivity to mechanical vibrations and air turbulence.

When no reorientation is induced, the interference pattern consists of a vertical equally spaced fringes whose spacing can be varied by slightly tilting the mirror with respect to the grating. The change in the refractive index of the liquid crystal sample, due to reorientation, produces a local shift of the interference fringes which can be measured by means a CCD camera. A demodulating algorithm based on a *Fast Fourier Transform* method of fringe pattern analysis is used to determine the unwrapped values of the bidimensional distribution of the phase. By a fit procedure of the experimental data to the theoretical model we measure the elastic anisotropy of a nematic liquid crystal film as given by the ratios between the Frank's elastic constants. These elastic constants describe the basic deformations of splay k_{11} , twist k_{22} and bend k_{33} respectively. The results are in good agreement with the measures obtained by other techniques.

Beside the sensitivity of the method, the main advantage of this technique is represented by the fact that just one bidimensional image of the interference fringe pattern is needed so that the measurement is performed in a direct manner. Furthermore the three elastic constants are all measured at the same point in the sample, with a high spatial resolution, and in the same environmental conditions.

Iron-based thin films and nanoparticles produced by laser-induced CVD

Rodica Alexandrescu, Ion Morjan, Ion Voicu

National Institute for Lasers, Plasma and Radiation Physics

P.O. Box MG-36, Bucharest, Romania

Friedrich Huisken

Max-Planck Institut für Stromungsforschung, Bunsenstrasse 10

D-37073 Göttingen, Germany

The researches devoted to iron-based materials have revealed the strong influence of the different processing techniques and conditions on the electronic, optical and magnetic properties. Either in the form of thin films or fine powders, the chemical composition and crystallographic structure (crystallite dimension and orientation, crystallographic phases) of iron-based particles are difficult to control using conventional processing techniques. As an alternative, the techniques employing laser induced chemical vapour deposition (CVD) from the gas phase allow for the production of particles in the nanometer size range, with better homogeneity and controlled composition. Starting from the absorption of energy quanta from the laser radiation, the basic mechanisms leading to solid particle nucleation may include:

- a) photolytic processes, when the UV radiation energy exceeds the dissociation energy of the precursor
- b) laser excitation in "hot" vibrational systems, when chemical reactions are driven by the IR radiation at high pressures and on a time scale $< \text{ms}$
- c) thermal driven reactions at an interface, following the laser heating of an absorbing substrate.

In this paper we illustrate the first two mechanisms described above by the laser stimulated deposition from iron pentacarbonyl (vapours) for producing iron thin films and iron-oxide-based ultrafine powders. $\text{Fe}(\text{CO})_5$ was chosen because it meets the prerequisites for CVD processes, i.e. stability and an appropriate vapour pressure at room temperature. It presents a first bond energy $\Delta H = 41.5 \text{ kcal/mole}$ and a high UV absorption cross section ($\sigma_{(248 \text{ nm})} = 2.7 \times 10^{-17} \text{ cm}^2$). In the dissociation process of $\text{Fe}(\text{CO})_5$, a disadvantage could be the contamination of the final product, due to incomplete elimination of the organic ligands.

In case of iron thin films, the irradiation of $\text{Fe}(\text{CO})_5$ vapours ($p = 0.3$ to 8 torr) was conducted at room temperature and in the static pressure mode. The radiation of the KrF excimer laser (30 mJ/pulse , 1 Hz repetition frequency) was directed perpendicular to the quartz substrate. The dynamics of the growing film composition

was investigated using X-ray photoelectron spectroscopy (XPS) techniques; with increasing number N of laser pulses ($N = 15$ to 2000), the surface carbon incorporation (mainly in carbidic forms) was found to decrease, while there is a simultaneous development of surface oxidized phases. A deposition mechanism accounting for these findings should consider the subsequent photolysis of photofragments brought onto to surface and the interference of enhanced heating effects on a nascent Fe surface.

The iron-based powders were produced by the CO_2 laser sensitized pyrolysis of iron pentacarbonyl. The IR radiation was used "to heat" a strong absorbing gas (SF_6), which then collisionally transfers its energy to $\text{Fe}(\text{CO})_5$ molecules, to make them decompose. The flow-reactor technique used for powder synthesis combines very sharp temperature gradients in the gas phase with reactions conducted in a wall-less environment. A pulsed TEA CO_2 laser (50 mJ energy/pulse, 20 Hz repetition rate) and a cross flow configuration was used. The pressure inside the reactor was kept at 300 torr. Vapours of $\text{Fe}(\text{CO})_5$ were injected inside the reaction cell by bubbling SF_6 ($\phi=20\text{sccm}$) through the liquid carbonyl container. The synthesized particles were characterized by X-ray diffraction (XRD), transmission electron microscopy (TEM) and XPS. The average diameter of the obtained particles was 20 nm. X-ray and electron diffraction techniques identified a majoritary $\beta\text{-Fe}_2\text{O}_3\cdot\text{H}_2\text{O}$ phase in the aged powder and low carbon contamination. The experimental evidence suggests that iron oxides were primary formed in the as-synthesized powders which further underwent conversion by the slow hydrolysis in the ambient. The relevant possibilities for this reaction route are discussed.

INTERCONNECTION BETWEEN ELECTRONICS AND PHOTONICS BY THE APPLICATION OF BISTABILITY IN LUMINESCENCE IN THIN CdS AND ZnSe FILMS

A.Kazlauskas¹⁾, B.Ullrich²⁾ and T.Kobayashi²⁾

¹⁾Inst. of Material Science and Applied Research, Vilnius University, Naugarduko 24, LT-2006 Vilnius, LITHUANIA; tel.: (+370-2) 636023; fax.: (+370-2) 263417; e-mail: arunas.kazlauskas@FF.VU.LT

²⁾Department of Physics, University of Tokyo

The requirement of cost effective technologies to create quite new electro-optical devices becomes more and more urgent since every foreseeable communication system will contain - besides electronics - sophisticated optical components. Thus, from the technical viewpoint, a compatibility of existing technologies of electronics with optical bistable (all-OB) devices is highly justified. This our work presents a new way of optical interfaced electronics by the application of all-OB in luminescence of II-VI wide-band-gap semiconducting thin films.

The excitation of thin CdS (ZnSe) films with the 514.5 nm (488 nm) Argon laser line causes well-known all-OBs in transmission. However, the nonlinear behavior of the thin CdS (ZnSe) films lets to expect more unusual features of the interacting light. It was found that the bistable switching occurs also in the emission line in IR region of the spectrum [1]. In fact, thin CdS (ZnSe) films exhibit all-OB in luminescence (all-OBL) which penetrates forbidden energy gap of GaAs.

This "penetrating feature" of GaAs by all-OBLs can be used to devise new optical interfaced electronic devices. The GaAs host material can act simply as a substrate for the thin bistable film and the optical switches can be treated by fibers at the rear of the GaAs structure or integrated GaAs photodiodes can treat the optical bistable signals. Thus, all three dimensions are available for data processing due to the different operation directions of electronics (horizontal) and optics (vertical). Beyond that, all-OBL can be used for new contact-free optical techniques as measurements of carrier concentrations in semiconducting materials. Additionally, we demonstrate that all-OBL is applicable for contact-free all-optical ammeters or temperature sensors. The discussed fusion between electronics and optics by all-OBL is not limited to electronics made of GaAs but can be used for all semiconductors which have the gap in the luminescent emission range of II-VI compounds.

1. B.Ullrich, A.Kazlauskas, S.Zerlauth, H.Nguyen Cong, and P.Chartier. First observation of bistability in luminescence. Extended Abstracts of the 1993 International Conference on Solid State Devices and Materials, Makuhari, Japan (1993) 669-672.

Nonlinear Phenomena in Interferometry on the Basis of the Optical Berry-Phases

Erna Frins (a. b.), Heidruna Schmitzer (a.), Wolfgang Dultz (c.)
a.) Universität Frankfurt (Main); b.) Universidad Montevideo, Uruguay;
c.) Deutsche Telekom AG Darmstadt, Germany

The physical characteristics of an optical device can depend in a very nonlinear way on the variation of system parameters, even in vacuum without any nonlinear material present and at very low light intensities. As in the case of nonlinear optics the characteristic quantity depending nonlinearly on the wavelength, amplitude or the phase of light, often is the intensity or the phase of an interference pattern. Well known examples are the Airy-type transmission characteristics of a Fabry-Perot interferometer or the fluctuating stray light speckles from a moving diffusing screen.

A very fruitful new source of nonlinear phenomena in linear optics are the optical Berry phases or topological (geometric) phases. Their unique properties like achromatism, unboundedness and additivity to the usual dynamical phase can be transferred to new optical devices for information processing and measurement. Especially Pancharatnam's phase in polarization optics generates extremely fast achromatic phase shifts and allows very sensitive phase measurements in interferometry. S. Pancharatnam had shown in 1956 that an analyzer P introduces a phase difference γ between two coherent light beams of different polarization P_1P_2 , which is proportional to the spherical excess of the triangle P_1P_2P on the Poincaré sphere. By moving the analyzer P on the Poincaré sphere the interferometer can be tuned, in certain circumstances in a very nonlinear way. Since Pancharatnam's phase depends only on polarizations, it can be made chromatic in a way we like, without taking special material properties into considerations.

We describe the origin of nonlinear effects in linear optics and introduce new applications of the topological phases. Dispersion compensated interferometers and speed enhanced optical switches are promising devices which use optical linear nonlinearities for information processing and telecommunication.

ROLE OF INTRINSIC AND EXTRINSIC DEFECTS ON ELECTRO- OPTIC PROPERTIES OF LiNbO_3

Marc Fontana, Michel Aillerie, Farid Abdi, and Karima Chah,

Laboratoire Matériaux Optiques à Propriétés Spécifiques, CLOES, Université de Metz et Supélec - 2, rue E. Belin 57078 METZ Cedex 3 - France

Although lithium niobate has been widely studied and used for its electro-optical and non linear optical properties, only a few investigations have concerned the role of defects on these properties. This is particularly important for dopings which lead to damage-resistant LiNbO_3 crystals.

It is however known that some of linear optical properties are strongly dependent on the intrinsic defects related to the non-stoichiometry and on the doping.

We have investigated the electro-optic properties of lithium niobate crystals with different compositions and various natures and concentrations of defects.

The dependence of the coefficients r_c and r_{22} on the concentration of intrinsic defects provides information on the origin of the electro-optic properties of lithium niobate. The influence of Mg and Cr on the coefficients r_c and r_{22} is discussed, in view of the structure of intrinsic and extrinsic defects.

Nonlinear Optical Properties of Mercury-(I)-Chloride

Heidruna Schmitzer, Wolfgang Dultz
Universität Regensburg, Telekom Darmstadt

Calomel (Hg_2Cl_2) belongs to the extraordinary class of Mercury-(I)-Halogenides with highly anisotropic physical optical properties. Mercury-(I)-Halogenides like Hg_2Cl_2 , Hg_2Br_2 , Hg_2I_2 are positiv uniaxial crystals (class 4/mmm) with inversion symmetry. Due to their chain like crystal structure they are highly birefringent and have sucessfully been used as monolithic polarisers. Together with its high transmission range from the Far Infrared light to the Ultraviolet spectral region (20 μm - 380 nm) this anisotropic property makes especially Hg_2Cl_2 perfectly apt for nonlinear optical processes in the whole spectral region: Materials for all optical switches in optical telecommunication must have a high intensity dependent index of refraction, which is given by the nonlinear third order susceptibility $\chi^{(3)}$. By phasematched Third Harmonic Generation we could measure the effective nonlinear susceptibilities of Typ-I and Typ-II phasematching in Hg_2Cl_2 to be $|\chi_{\text{eff,Typ-I}}^{(3)}| = 3.4 \times 10^{-22} \text{ m}^{-2} \text{ V}^{-2}$ and $|\chi_{\text{eff,Typ-II}}^{(3)}| = 7.4 \times 10^{-22} \text{ m}^{-2} \text{ V}^{-2}$. The Typ-III phasematching uses the same tensor components as Typ-(I) and was therefore deduced to be $|\chi_{\text{eff,Typ-III}}^{(3)}| \cong 1.1 \times 10^{-22} \text{ m}^{-2} \text{ V}^{-2}$. The effective third order susceptibilities of Hg_2Cl_2 are two orders of magnitude higher than those of CaCO_3 and the tensor components $\chi_{11} - 3\chi_{18}$ seem to exceed the components of ADP by a factor of 5. These measurements show that Calomel might be a promising material to be used in nonlinear optical switches.

CHARACTERIZATION OF BUNDLES OF SINGLE-WALLED CARBON NANOTUBES PRODUCED BY THE ELECTRIC ARC TECHNIQUE

M. Lamy de la Chapelle^{a)}, S. Lefrant^{a)}, C. Journet^{b)}, W. Maser^{b)}, P. Bernier^{b)}, A. Loiseau^{c)}

^{a)} IMN-Univ.Nantes, BP32229, 44322 Nantes cedex 3, Nantes

^{b)} GDPC-Univ.Montpellier II, 34095 Montpellier cedex 5, France

^{c)} Lab. Phys. Solide, ONERA, BP 72, 92322 Chatillon cedex, France

Extensive studies have been carried out recently to produce single-walled carbon nanotubes for both fundamental science and future technical applications. In fact, single-walled nanotubes present specific electronic properties which strongly depend on their diameter and on the presence of structural defects. In order to achieve the production of nanotubes with controlled properties, it is of prior importance to use spectroscopic techniques efficient for their characterization in a non-destructive way. Second, an important aspect is the ability of preparing such compounds in significant quantities. In order to do so, the electric arc-discharge method has been recently used with success (1). Electrodes are made of graphite, the anode being charged with metallic catalysts, such as Ni, Co, Y. Depending on the synthesis conditions and on the location where the sample is taken in the synthesis chamber, single-walled or multi-walled nanotubes can be produced. In addition, the co-evaporation of metals during the discharge leads to the formation of other compounds such as metal carbon composites nanostructures, in general embedded in glassy carbon. This is put in evidence by HRTEM observations by also X-ray diffraction experiments. Also, SQUID measurements have revealed particles which exhibit superconducting phases presumably in the form of $\text{YNi}_2\text{B}_2\text{C}$ or $\text{YNi}_4\text{Bi}_4\text{C}$ compounds, since transition temperatures have been measured to be 15 or 16K. Such particles have diameters between 2 and 10 nm (2).

All these results have been confirmed by Raman experiments. In agreement with HRTEM observations, three types of Raman spectra have been observed (Fig.1). One corresponds to glassy carbon with the characteristic bands at 1340 and 1580 cm^{-1} (Fig.1a). Another spectrum is typical of graphitic nanoparticules and multi-walled nanotubes, composed of a main « graphitic » band at 1580 cm^{-1} and also a weak band at 1340 cm^{-1} (Fig.1b). Spectrum 3 is the signature of single-walled nanotubes (Fig.1c). It is composed of a double peak at 1533 and 1582 cm^{-1} which does not depend on the area investigated.

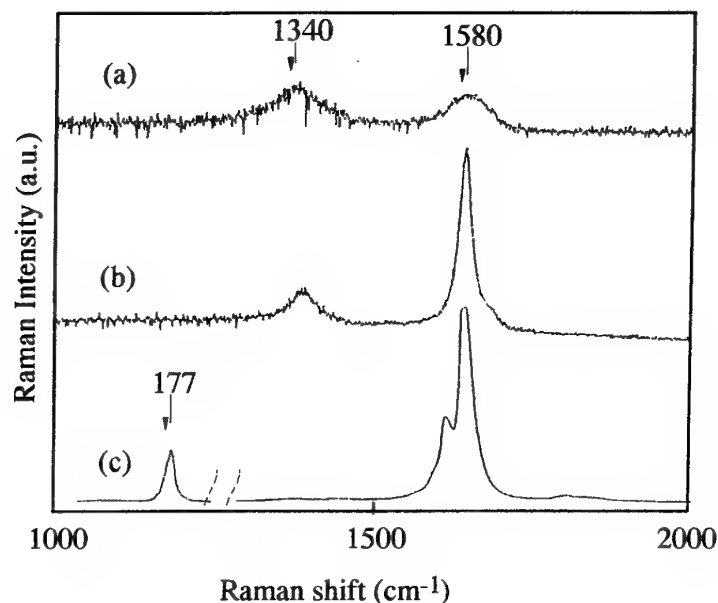


Fig. 1: Raman spectra of carbon nanotubes and nanoparticles

From a detailed analysis and in particular in improving the spectrometer resolution, we showed for the first time that a low frequency band observed in spectrum 3 at $\approx 180 \text{ cm}^{-1}$ can be resolved in several components, each being associated with a single-walled nanotube of a typical diameter. In fact, we can suggest that each area studied is characterized by a distribution of diameters for the SWNT's. These results are in rather good agreement with recent calculations performed by Rao et al.(3). In this paper, we will review the most recent results obtained on these carbon samples and stress out the ability of the Raman Scattering technique to characterize such compounds in a non-destructive way.

References:

1. M. Lamy de la Chapelle, S. Lefrant, Ph. Molinié, C. Godon, W. Maser, P. Bernier and P.M. Ajayan, Proceedings SPIE, Fullerenes and Photonics, 1996.
- 2 W. Maser, I. Luk'yanchuk, P. Bernier, Ph. Molinié, S. Lefrant, Ph. Redlich and P.M. Ajayan, Accepted in Advanced Materials, 1997.
3. A.M. Rao et al., Science 275, 1997

**Fabrication and properties of materials for Er^{3+} doped Yb^{3+} sensitized
high - power lasers**

Ivan Kašík, Vlastimil Matějec, Jiří Kaňka, Daniela Berková

Institute of Radio Engineering and Electronics, Academy of Sciences of the Czech Republic, Chaberská 57,
182 51 - Praha 8

Abstract

In the paper, results on preparation and properties of materials for the development of high-power fiber lasers are presented in the paper with the aim to show a complex relation between the chemical composition of materials, their implementation into a waveguiding structure using two methods of preparation and generation of the amplified stimulated emission (ASE) in the structure. The attention is given to Er^{3+} doped, Yb^{3+} sensitized fiber lasers emitting at $1.55 \mu\text{m}$ when pumped at $1.064 \mu\text{m}$ by a Nd:YAG laser. The UV curable acrylate coated fibers for the development of the lasers have been drawn from preforms which are composite silica glass structures with a central circular core, an optical cladding and silica buffer. Silica glasses doped with Al_2O_3 and P_2O_5 have been studied as suitable matrices for entrapping rare-earth elements in the fiber core. The optical cladding has been fabricated from silica doped with P_2O_5 and with fluorine. The optical fiber core and cladding have been fabricated by the MCVD method combined with the solution doping technique or with the sol-gel method.

The part dealing with preparation is concentrated on the process of fabrication of a thin layer ($0.5\text{--}15 \mu\text{m}$) of $\text{Er}^{3+}\text{--Yb}^{3+}\text{--Al}_2\text{O}_3\text{--P}_2\text{O}_5\text{--SiO}_2$ glass on the inner wall of the substrate silica tube. For the both methods of preparation, the MCVD method and the sol-gel method, this process consists of coating of a porous layer on the wall and its sintering. While with the MCVD method the porous layer of silica or P_2O_5 doped silica was coated and then soaked with a solution of raw materials AlCl_3 , ErCl_3 and YbCl_3 , in the sol-gel method the porous layer was fabricated by coating the sol layer on the wall and its gelling. The details on the preparation of raw solutions and sols, fabrication of the porous layers and their sintering are given. In the experiments, materials were prepared with a maximum Al_2O_3 , P_2O_5 , Yb^{3+} , Er^{3+} contents of 10 mol. %, 18 mol. %, 5 mol. % and 0.3 mol. %, respectively. On the basis of the experiments the methods of preparation are compared from the point of view of achieving the desired dopant concentration profiles in the layer and the possibility

axial as well as angular variations of the layer dimensions showing thus the advantages and disadvantages of the both methods.

The influence of properties of the deposited glass layer on the process of formation of the fiber core during the viscous collapse of the composite tube on the preform for drawing fibers is discussed from the point of view of reaching the desired refractive-index profile in the core and controlling the geometrical and stress birefringence in the core.

The spectral attenuation measurements on the fabricated fibers have shown the effect of the dopant concentration and refractive-index profile on the absorption spectra of the Er^{3+} ions. The amplified spontaneous emission of the fibers around $1.55\ \mu\text{m}$ induced by pumping the fibers at $1.064\ \mu\text{m}$ has been observed.

For measuring ASE and testing lasing properties of the fabricated fibers, a fiber ring laser set up has been built. This set up, consisting of a Nd:YAG pumping laser, the measured fiber, WDM couplers, optical isolator and optical couplers has enabled us to couple the pump power of up to about 1.3 W into the measured fiber and to monitor the unabsorbed pump power and laser output. The ring laser operated in the free-running regime at wavelengths depending on the length of the measured fiber and the output coupling ratio.

Several crucial material parameters have been identified on the basis of the measurement of the lasing properties. The ratio of Er^{3+} and Yb^{3+} ions has been determined to have to be higher than 1:6 for obtaining the lasing effect. The high concentration of Yb^{3+} ions has been observed to induce the lasing effect of Yb^{3+} at $1.09\ \mu\text{m}$ decreasing thus the power conversion efficiency of Er^{3+} around $1.55\ \mu\text{m}$. The relation between the profiles of the dopant concentration, refractive-index profile of the fiber and the slope efficiency has been observed. This relation has also been theoretically explained.

Using the experimental fiber ring cavity with a fiber of the average Er^{3+} and Yb^{3+} concentrations of 800 and 9600 ppm, respectively, the fiber provided at its output an intercavity signal power of hundreds mw (over 600 mW) with a power conversion efficiency of about 25% when pumped by about 1.3 W at $1.064\ \mu\text{m}$. On the basis of the measured average signal powers one can conclude that the fiber will make it possible to generate high energy soliton pulses with a high repetition rate if the laser is passively mode-locked. These experiments are started now.

TITLE OF THE PAPER: INFRARED REFLECTANCE INVESTIGATION
OF $x\text{Sb}_2\text{S}_3 \cdot (1-x)\text{As}_2\text{S}_3$ GLASSES

AUTHOR OF THE PAPER: J. A. KAPOUTSIS^a

AUTHOR'S AFFILIATION: ^aTheoretical and Physical Chemistry Institute,
National Hellenic Research Foundation,
48 Vass. Constantinou Ave., Athens 116 35, Greece

^bCentre of Optoelectronics of the Institute of
Applied Physics
No.1, Academiei Str. Chisinau, MD-2028,
Republic of Moldova

CO-AUTHORS: E. I. KAMITSOS^a, I. P. CULEAC^b, M. S. IOVU^b

KEY WORDS

Chalcogenide glasses/ $\text{As}_2\text{S}_3\text{-Sb}_2\text{S}_3$ / infrared reflectance/ glass structure/ mixed bridges

ABSTRACT

Infrared reflectance spectra of chalcogenide glasses in the system $x\text{Sb}_2\text{S}_3 \cdot (1-x)\text{As}_2\text{S}_3$ have been measured and analysed to investigate the glass structure as a function of antimony sulfide content. The infrared spectra of such glasses can be understood on the basis of vibrations of trigonal pyramidal AsS_3 and SbS_3 units, which retained their structure and exhibit considerable mixing through As-S-Sb bridges.

Crystal growth of NLO borates

Andrzej Majchrowski

Institute of Applied Physics WAT 01-489 Warsaw Kaliskiego 2 Poland

Borate crystals exist in many structural types due to three-fold (trigonal) or four-fold (tetrahedral) coordination of boron atoms in boron-oxide compounds. Various borate anionic groups as basic structural units cause the existence of different structures of borate crystals what gives the possibility of selecting appropriate materials for chosen applications. According to Chen et al.[1] the following anionic groups as basic structural units in borate crystals are of practical interest: $(\text{BO}_3)^{3-}$, $(\text{BO}_4)^{5-}$, $(\text{B}_2\text{O}_5)^{4-}$, $(\text{B}_2\text{O}_7)^{8-}$, $(\text{B}_3\text{O}_6)^{3-}$, $(\text{B}_3\text{O}_7)^{5-}$, $(\text{B}_3\text{O}_8)^{7-}$, $(\text{B}_3\text{O}_9)^{9-}$, $(\text{B}_4\text{O}_9)^{6-}$ and $(\text{B}_5\text{O}_{10})^{5-}$. Generally borate crystals have high optical quality, a high damage threshold for laser radiation, transparency far into the ultraviolet and good chemical stability.

First crystal from the borate series found to be a very good piezoelectric material for surface acoustic wave (SAW) devices was lithium tetraborate $\text{Li}_2\text{B}_4\text{O}_7$ [2]. It has properties which are the mixture of lithium niobate and quartz properties. However the most interesting features of borate crystals are their NLO properties. Powerful tunable ultraviolet sources, required for many spectroscopic applications, rely on frequency-doubling of lasers working in the visible range. The discovery of $\beta\text{-BaB}_2\text{O}_4$ (BBO) [3] triggered intensive researches in the area of non-linear borates. As a result a group of promising NLO materials has been found, among which the most interesting are: LiB_3O_5 (LBO) [4], CsB_3O_5 (CBO) [5], $\text{CsLiB}_6\text{O}_{10}$ (CLBO) [6], $\text{KBe}_2\text{BO}_3\text{F}_2$ (KBBF) [7], and $\text{Sr}_2\text{Be}_2\text{B}_2\text{O}_7$ (SBBO) [8]. They can find applications in second harmonic generation, sum or difference frequency mixing and optical parametric oscillators.

Borates are also very attractive as host materials, due to possibility of substitution of some ions in host lattices by, for example neodymium or chromium ions. The substitution forms lasing materials with non-linear behaviour, what gives as a result self-frequency doubling materials. The most promising of these materials are: $\text{Nd}_x\text{Y}_{1-x}\text{Al}_3(\text{BO}_3)_4$ (NYAB) [9], $\text{YAl}_3(\text{BO}_3)_4\text{:Cr}$ (YAB:Cr) [10], $\text{GdAl}_3(\text{BO}_3)_4\text{:Cr}$ (GAB:Cr) [11] with huntite structure and $\text{Ca}_4\text{GdO}(\text{BO}_3)_3\text{:Nd}$ (GdCOB:Nd) [12] from oxoborates family. Y and Gd do not show absorption in the wavelength range interesting for NLO applications and can be easily substituted by Nd or Cr, in some cases up to 15% without modification of the noncentric host lattice. The crystals are presently intensively investigated as candidates for self-frequency doubling laser crystals. Moreover, chromium doped borates may be used in lasers with tunability.

Some of borates melt congruently, what allows to obtain their crystals using standard methods like Czochralski or Kyropoulos techniques. However most of the discussed materials melt incongruently or there are phase transitions which influence the quality of as grown crystals. Solution growth enables to overcome incongruent melting, and in case of unwanted phase transitions the temperature of crystallisation is lowered below the temperature of phase transitions.

Both Czochralski technique and top seeded solution growth (TSSG) have been used to obtain borate crystals. The former one has been used in case of lithium tetraborate. Typical resistance furnace with construction allowing to obtain high temperature gradients in the vicinity of the interface has been built. The construction enabled to diminish viscosity of the melt due to its overheating. High viscosity of molten borates was the most serious problem encountered during the investigations. Since too fast rotation of growing crystal caused unstable flows in the viscous melt, small rotation rate melt had to be applied. As a result the interface was strongly

convex towards the melt. It caused non-uniform distribution of temperature gradients on the melt-crystal interface. In the central part of the crystal the gradient was small enough to start unstable growth due to constitutional supercooling [13]. Also pulling rate had to be small enough to prevent the formation of inhomogeneities in the crystal. Among other borates CLBO and GdCBO can be grown by the Czochralski method. GdCBO melts in 1480°C and viscosity, to my knowledge, do not influence the process of crystal growth. In case of CLBO the viscosity of the melt is very high what in connection with low temperature of melting (845°C) causes similar problems as in case of lithium tetraborate. To avoid these problems TSSG technique has been used to obtain CLBO crystals.

CLBO crystals have been grown in a three-zone resistance furnace which allowed to shape temperature gradients over and inside the melt in wide range. Precise temperature control and regulation set has been built using 906 Eurotherm programmers. It allowed to change the temperature inside the furnace linearly at 0.01°C/h. Platinum crucible has been used. The melt was enriched in caesium and lithium oxide to diminish its viscosity. Crystals were not pulled up during the growth. The temperature gradient over the melt was established in such way that crystals could grow inside the melt. The typical process lasted two or three days and then the crystal was pulled from the melt and cooled at 10°C/h. As grown crystals were colourless, totally transparent and did not include any macroscopic defects. They were confined by flat faces. Preliminary investigations of β -BBO and NYAB crystal growth have shown that the temperature regulation set enables to obtain good quality BBO crystals from the flux, too.

REFERENCES

1. C.Chen, Y.Wu and R.Li, "The development of new NLO crystals in the borate series", *J. Cryst. Growth*, 99,(1990), 790-798
2. T.Łukasiewicz and A.Majchrowski, "Czochralski growth of lithium tetraborate single crystals", *Materials Letters* 11,(1991),281-283
3. L. K. Cheng, W. Bosenberg, C.L. Tang, "Growth and characterization of low temperature phase barium metaborate crystals", *J. Crystal Growth*, 89 (1988), 553-559
4. C.T. Chen, Y. Wu, A. Jiang, B. Wu, G. You, R. Li, S. Lin, "New nonlinear-optical crystal LiB_3O_5 ", *J. Opt. Soc. Am.*, B6, (1989), 616-621
5. Y.Wu, T. Sasaki, S. Nakai, A. Yokotani, H. Tang, C. Cheng, " CsB_3O_5 : a new nonlinear optical crystal", *Appl. Phys. Lett.* 62 (1993), 2614-2615
6. Y. Mori, I. Kuroda, T. Sasaki, S. Nakai, "Nonlinear optical properties of cesium lithium borate", *Jpn. J. Appl. Phys.*, vol.34 (1995), L296-L298
7. L. Mei, Y. Wang, C. Chen, B. Wu, "Nonlinear optical materials based on $\text{MB}_2\text{BO}_3\text{F}_2$ (M=Na, K)", *J. Appl. Phys.*, 74 (1993), 7014-7015
8. C.L. Hill and X. Zhang, "Design and synthesis of an ultraviolet-transparent nonlinear optical crystal $\text{Sr}_2\text{Be}_2\text{B}_2\text{O}_7$ ", *Nature*, vol. 373, (1995), 322-324
9. S. T. Jung, J. T. Yoon, S. J. Chung, "Phase transition of neodymium yttrium aluminium borate with composition" *Mat. Res. Bull.*, 31(1996), 1021-1027
10. G. F. Wang, T. Han, H. G. Gallagher, B. Henderson, "Novel laser gain media based on Cr^{+3} - doped mixed borates $\text{RX}_3(\text{BO}_3)_4$ ", *Appl. Phys. Lett.*, 67:26(Dec 1995), 3906-3908
11. M. Iwai, Y. Mori, T. Sasaki, S. Nakai, N. Sarakura, Z. Liu, Y. Segawa, "Growth and optical characterization of Cr:YAB and Cr:YGAB crystal for new tunable and self-frequency doubling laser", *Jpn J. Appl. Phys.*, 34(1995),2338-2343
12. G. Aka et al., Laboratoire de Chimie Appliquee de l'Etat Solide ENSCP, Paris, France, private information
13. A. A.Majchrowski, J. Mija "Czochralski growth of oxide single crystals under conditions of forced convection in the melt", *Materials Science and Engineering A* 173, (1993) 19-22

BISTABLE OPTICAL EXCITATION OF $F_A(Li)$ CENTERS IN CUBIC CRYSTALS OF ALKALI HALIDES

A. Scacco

Dipartimento di Fisica, Università *La Sapienza*

P.le A. Moro 2, 00185 Roma, Italy

U.M. Grassano

Dipartimento di Fisica, Università di Roma Tor Vergata

Via della Ricerca Scientifica 1, 00133 Roma, Italy

G. Baldacchini, R.M. Montereali

ENEA, Dip. INN, Settore Fisica Applicata, Centro Ricerche Frascati

C.P. 65, 00044 Frascati, Italy

S. Boiko, G. Tarasov

Institute of Semiconductor Physics, Academy of Sciences of Ukraine

Prospect Nauki 45, 252650 Kiev, Ukraine

Optically non-linear cubic crystals exhibit a number of particular effects connected with their symmetry properties. Among them there are interesting effects of polarization self-action, resulting in the self-induced change of polarization state for an intense electromagnetic wave travelling through the crystal. The physical reason for the polarization change is the anisotropy of the non-linear susceptibility, whose real part gives the birefringence whereas the imaginary part causes the dichroic non-linear absorption. Such a non-linearity makes the directions of symmetry (crystal axes) not equivalent with respect to the polarization plane orientations. Some of such directions become stable and the polarization plane tends to rotate towards them, while others are instable and the polarization plane rotates away from them. The occurrence of instable directions allows to

obtain polarization optical bistability inserting the non-linear crystal into a cavity.

There exist different mechanisms of optical non-linearity in cubic crystals containing impurities or radiation induced defects. Those controlled by fast electronic processes need strong electro-magnetic fields, whose electric component should have intensity comparable with that of the intra-atomic field. Those connected with saturation or bleaching of the optical absorption are developed under resonant excitation and their magnitude is strongly dependent on the ratio between the characteristic relaxation times of the excited and ground electronic states of the defects. If such a ratio is large enough, then non-linear optical effects can be observed even in a weak electromagnetic field.

Due to the relaxation, rearrangements of the atomic or electronic configuration occur resulting in the change of the excitation conditions. This leads to optically induced anisotropy of the crystal, because the electronic configurations which either do not or weakly interact with the light are predominantly generated. The dipole moments involved in the actual transition, initially equally distributed in the plane perpendicular to the direction of the polarized light propagation, can be redistributed because of the relaxation among the various symmetry directions. Alkali halides containing F_A centers are typical systems showing such a behavior under illumination with polarized light.

Starting from the above described mechanisms of optical non-linearity and optically induced anisotropy, in this work is reported the possibility of polarization induced optical bistability in cubic crystals of alkali halides with reorienting defects lying along the symmetry axes, such as the $F_A(\text{Li})$ centers. Furthermore, the possible changes in the luminescence yield, caused by such a bistability, are described.

Design, Evaluation and Optimization of MQW Binary-Phase Modulators

E. Serrano*, M.P.Y. Desmulliez[†], H. Inbar*, B.S. Wherrett*

*Department of Physics, Heriot-Watt University, Edinburgh EH14 4AS, Scotland, UK.

Tel : 44 131 451 332 Fax : 44 131 451 3136. Email : E.Serrano@hw.ac.uk

[†] Department of Computing & Electrical Engineering

Over the last fifteen years, various types of semiconductor electro-absorption modulators have been fabricated and analyzed. The potential use of such devices in photonic switching fabrics and inter-chip interconnections has provoked numerous studies of their performance capabilities and design trade-offs [1,2]. Recently, Trezza and coworkers reported a π -phase change in a reflection-mode vertical cavity asymmetric multiple quantum well [3], in which the absorption variation induced by an external applied field causes a change in the dominant role played by one of the cavity mirrors. Moreover, the device is designed so that no change in throughput is induced by the bias voltage. The π phase change at constant reflectivity requires a careful cavity design and the precise determination of the operating wavelength and voltage swing. A systematic study demands the implementation of a tolerance methodology. Results, based on such a methodology, will be presented that analyze which parameters are in achieving the best overall device performance, the optimum operating conditions and the higher degree of robustness (the tolerance) to the variations in device characteristics.

In Figure 1 the device structure and its equivalent representation have been displayed. The method used in tolerance analysis is the same as that which was implemented successfully with the SEEDs arrays [4]. The model is simple enough to enable tolerance analysis to be carried out without great computational demands, while being sufficiently realistic to show good agreements with existing experimental data.

The model uses the method of the effective interfaces [5] combined with the Babic-Corzine analytical expression of the penetration depth and reflection delay introduced by the mirrors [6] as shown in figure 1. Assuming that the gratings are made of low absorption materials at the operating wavelength, the complex amplitude r , of the overall reflectivity can be expressed as :

$$r = \frac{r_I + r_{II} \exp(-i\phi) \exp(-\alpha L_{MQW})}{1 + r_I r_{II} \exp(-i\phi) \exp(-\alpha L_{MQW})}$$

where $\phi = 4\pi L_{MQW} n_{eff}/\lambda - 4\pi n(L_t + L_b)/\lambda_B + 4\pi n(L_{spacer} + L_t + L_b)/\lambda$ is the round trip phase; n_{eff} is the equivalent refractive index of the quantum well structure, n is the refractive index of the spacer and the mirrors, λ_B is the Bragg wavelength of the mirrors and α is the absorption spectrum. The reflectivity coefficients of the subsystems I and II (fig. 1) are r_I and r_{II} , respectively. The different lengths are explained in the caption of the figure 1. A semi-empirical model of the field dependence of the absorption spectrum of the MQW structure is also used with particular emphasis on the heavy-hole excitonic resonance. We use a model based on experimental data and full k-p based theoretical treatment that have been shown to match. The resulting variations of the absorption and refractive index, derived through the Kramers-Kronig relation, are presented in figure 2. At point A (850 nm), there is no index change for a voltage swing of 4 Volts. These would be the operational conditions for the device exemplified. The optical responses of the resulting phase modulator are shown in figures 3 and 4. For the example given, at 850 nm, a π phase change is obtained for a voltage swing of 4 Volts with no change in reflectivity. Of primary importance is the study of the robustness of these optical responses with variations of voltage, wavelength, cavity thickness, top-mirror

reflectivity and temperature. Inserting the microscopic model for Δn and $\Delta \alpha$ into the macroscopic expressions allows us to determine the tolerance of the phase modulator to the variations of these device parameters. The phase modulation versus the operating wavelength and the cavity thickness have been displayed in figures 4 and 5 respectively. Results will be presented.

Bibliography

- [1] R.H. Yan, R.J. Simes, and L.A. Coldren, IEEE J. Quantum Electron. **25**, p. 2272, (1989).
- [2] P. Zouganeli, P.J. Stevens, D. Atkinson, and G. Parry, IEEE J. Quantum Electron. **31**, p. 927, (1995).
- [3] J.A. Trezza, and J.S. Harris Jr., J. Appl. Phys., **75**, p. 4878, (1994).
- [4] M.P.Y. Desmulliez, B.S. Wherrett, and J.F. Snowdon, Appl. Opt. **33**, p. 1368, (1994).
- [5] S.D. Smith J. Opt. Soc. Am. **48**, p. 43 (1958).
- [6] D.I. Babic, and S.W. Corzine, IEEE J. Quantum Electron. **QE-28**, p. 514 (1992).

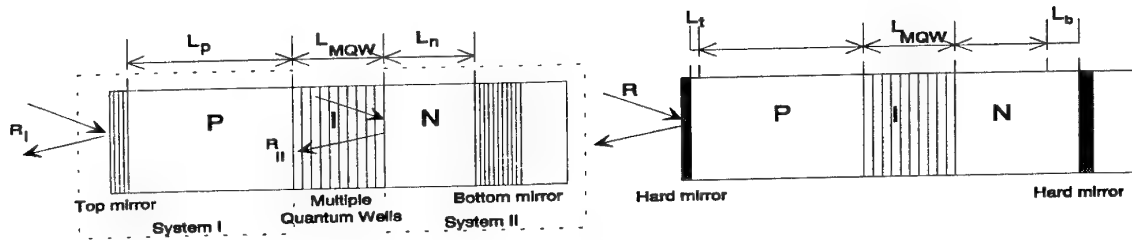


Figure 1 : Schematic of the Asymmetric Fabry-Perot modulator and its equivalent representation. The thickness of the spacer is $L_n + L_p$. Using the Babic-Corzine theory, L_t and L_b account for the phase changes at the mirrors, for a wavelength within the stop band of the mirrors

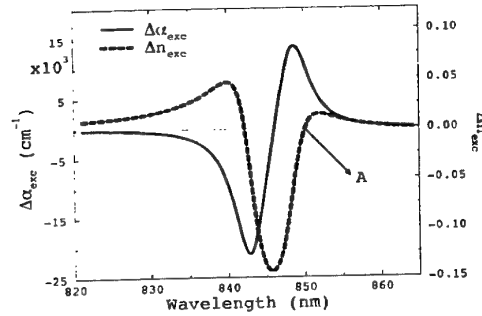


Figure 2.

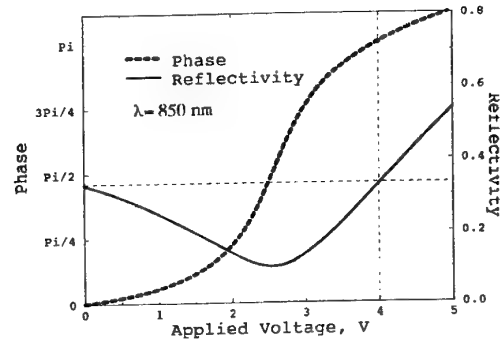


Figure 3.

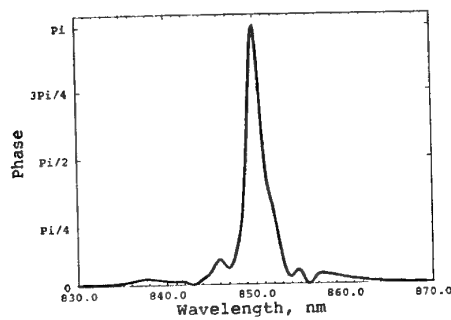


Figure 4.

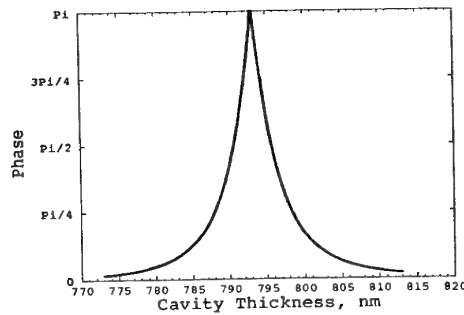


Figure 5.

Nonlinear refractive index modifications in dielectric waveguides

S. Monneret, F. Flory

Laboratoire d'Optique des Surfaces et des Couches Minces - Unité associée au CNRS - Ecole Nationale Supérieure de Physique de Marseille - Domaine universitaire de Saint-Jérôme - 13397 Marseille Cedex 20- France Phone (33) 91 28 80 52 Fax (33) 91 28 80 67

Most of dielectric thin films can be used as planar waveguides, and then support a discrete number of TE and TM guided modes. A laser beam incident on a totally reflecting prism tightened against a guide can excite resonances of the electromagnetic field corresponding to the guided modes. These resonances are associated with dark lines generally called m-lines in the reflected spot. The theory of this Totally Reflecting Prism Coupler (TRPC) has been described by several authors.¹

The work presented here, which is based on a pump-and-probe TRPC², is devoted to study light-induced thermal refractive index modifications in dielectric thin films. Such a two-beam setup permits us to estimate rise and relaxation times, as well as the amplitude Δn of the thin film refractive index variations.³ Results concerning different waveguide materials are presented.

A first beam (pump), which can be chopped at different frequencies, comes from a cw Ar⁺ laser of power up to 1.5 W, emitting at 514.5 nm. A second beam (probe) comes from a cw low power He-Ne laser emitting at 632.8 nm. Both these beams are focalized at the same place on the prism base. Each beam is coupled to the waveguide and excites a resonance. A light detector is located in the reflected probe beam behind a slit and connected to an oscilloscope. It is used to record the change in light intensity due to the pump-induced displacement of the probe m-line.

First of all we need to modelize the prism coupling to know the coupling efficiency.^{3,4} The modeling takes into account the two lateral dimensions of the pump Gaussian beam, in order to calculate the power distribution in the system prism/air/waveguide/substrate. But the coupling efficiency strongly depends on the thickness t_a of the air layer that lies between the prism and the waveguide. The experimental determination of t_a results from the recording of one of the pump or probe near field intensity distribution. We are thus able to determine the intensity distribution of the pump beam and its maximum value I_{\max} in the waveguide.

The lateral shift Δs of the probe m-line is measured with the photodetector. By choosing a pump beam waist much larger than the probe one, we can assume to have a uniform change in refractive index in the probed zone of the guide. Then the modeling of the TRPC allows us to determine Δn from Δs .

With a pump beam of a few hundreds of milliwatts, we can measure values of Δn as low as 1×10^{-6} . Figure 1 gives an example of the experimental dependence of Δn versus I_{\max} . It clearly demonstrates a linear relationship between Δn and I_{\max} , which can be written $\Delta n = \alpha I_{\max}$, where α is a thermal nonlinear coefficient. The relaxation times we measure are typically of a few milliseconds, which confirm effectively the thermal origin of the measured nonlinearities.

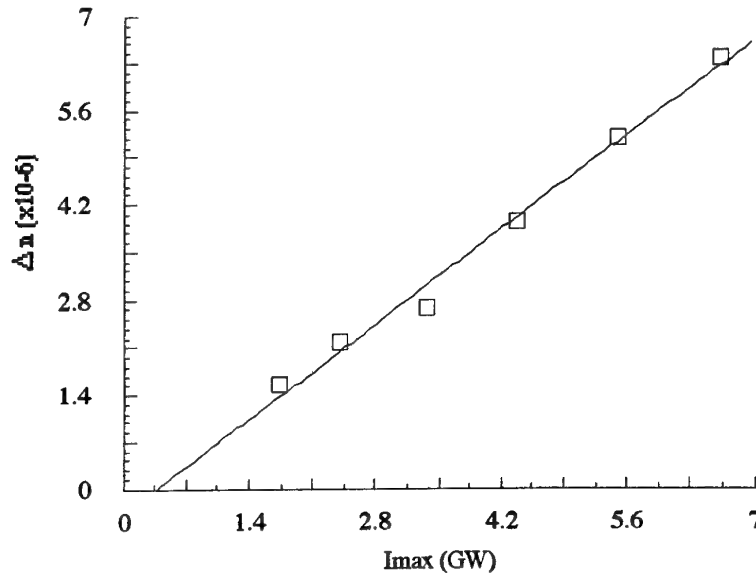


Fig. 1 : Experimental results giving Δn versus I_{\max} for a Ta_2O_5 thin film obtained by the use of a plasma-assisted evaporation technique. The corresponding pump laser powers vary about from 100 mW to 450 mW. Chopper frequency = 200 Hz. Here $\alpha = 1 \times 10^{-15} \text{ m}^2/\text{W}$.

Significative experimental values of α will be given, concerning different dielectric materials (Ta_2O_5 , SiO_2 , ...), and different deposition techniques (electron beam, ion-assisted and plasma-assisted deposition techniques). The study of the spatial extension of the thermal light-induced phenomena, as well as their dependence with modal characteristics, will be reported. It will also be shown that this method can be easily extended to picoseconds light pulses sources, in order to study electronic non linearities in thin films.

References:

1. P. K. Tien and R. Ulrich, "Theory of prism-film coupler and thin-film light guides", J. Opt. Soc. Am. **60**, 1325-1337 (1970).
2. M. Bertolotti, E. Fazio, A. Ferrari, F. Michelotti, G.C. Righini, C. Sibilìa, "Nonlinear coupling in a planar waveguide", Opt. Lett. **15**, 425-427 (1990).
3. S. Monneret, S. Tisserand, F. Flory, and H. Rigneault, "Light-induced refractive index modifications in dielectric thin films: experimental determination of relaxation time and amplitude", Appl. Opt. **34**, 4358-4368 (1995).
4. H. Rigneault, F. Flory, and S. Monneret, "Nonlinear totally reflecting prism coupler : thermomechanic effects and intensity-dependent refractive index of thin films", Appl. Opt. **34**, 4358-4368 (1995).

TITLE OF THE PAPER: STRUCTURE OF POTASSIUM GERMANATE
GLASSES BY VIBRATIONAL SPECTROSCOPY

AUTHOR OF THE PAPER: Y. D. YIANNOPOULOS^a

AUTHOR'S AFFILIATION: ^aTheoretical and Physical Chemistry Institute,
National Hellenic Research Foundation,
48 Vass. Constantinou Ave., Athens 116 35, Greece

^bDepartment of Materials Science and Engineering,
Lehigh University, Bethlehem, PA 18015, USA

CO-AUTHORS: E. I. KAMITSOS^a and H. JAIN^b

KEY WORDS

germanate anomaly/ potassium germanate glasses/ infrared reflectance/ Raman/
germanium coordination

ABSTRACT

Germanate glasses exhibit extrema in the composition dependence of their physical properties; a behaviour known as the "germanate anomaly effect". An infrared reflectance and Raman study of potassium germanate glasses spanning the entire glass forming region is presented in order to investigate the composition dependence of the structural modification mechanism. To assist spectral interpretation, corresponding crystalline germanate compounds were prepared and studied. Analysis of data that at low alkali oxide content, small ring arrangements are favoured, while further alkali oxide addition triggers the germanate tetrahedra to octahedra transformation mechanism. High potassium contents favour the formation of non-bridging oxygen containing germanate tetrahedra. This mechanism induces the progressive depolymerization of the germanate glass network.

SOL-GEL PREPARATION AND CHARACTERIZATION OF α -Fe₂O₃ FILMS

C. Baratto ^(a), P.P. Lottici ^(a), G. Antonioli ^(a), G. Gnappi ^(b),
A. Montenero ^(c), M. Guarneri ^(c), T. Besagni ^(d)

(a) INFN and Dipartimento di Fisica, Università, Viale delle Scienze, PARMA

(b) CORIVE, Viale delle Scienze, PARMA

(c) Dipartimento di Chimica Generale ed Inorganica, Chimica Analitica, Chimica Fisica,
Università, Viale delle Scienze, PARMA

(d) MASPEC-CNR Institute, Via Chiavari 18
43100 PARMA - Italy

The third-order non-linear optical susceptibility $\chi^{(3)}$ of thin films of α -Fe₂O₃ has been recently reported as the highest among the inorganic oxides [1]. Its value, 5.8×10^{-11} esu, measured by the third harmonic generation method, exceeds that of SiO₂ glass by about three orders of magnitude. The sol-gel technique is particularly suitable to prepare thin films of α -Fe₂O₃ through a simple deposition by dip-coating, which ensures a good homogeneity of the samples. In this work we report on the characterization by XRD, AFM (Atomic Force Microscopy) and Raman spectroscopy of films of α -Fe₂O₃ obtained by two different sol-gel procedures. In the first preparation (A) the starting solution is given by iron nitrate enneahydrate Fe(NO₃)₃·9H₂O in a mixture of 2-methoxyethanol (CH₃OCH₂CH₂OH) and 2,4 pentanedione (CH₃COCH₂COCH₃), whereas in the second preparation (B) the iron oxide is obtained by hydrolysis of FeCl₃·6H₂O at pH=9.

The films were obtained by multiple (>10) dipping on silica and glass substrates: their crystallization by heating up to 500 °C was checked by XRD and Raman spectroscopy. The XRD spectra show the α -Fe₂O₃ hematite structure for both preparations, and no evidence of different oxide phases. Raman data are reported in the literature only on α -Fe₂O₃ as single crystals or powders [2,3]. We obtained Raman spectra on the films in the Brewster configuration: all seven phonon peaks ($2A_{1g}+5E_g$) of rhombohedral α -Fe₂O₃ are observed for both preparations, when heated at 500 °C. The Raman spectra reveal that the films are polycrystalline in nature and the frequencies of the modes are the same as the powder material. Confinement effects due to nanocrystals are therefore ruled out.

The morphology of the films was investigated by AFM. The samples (A) heated at 500 °C show three dimensional structures having an average height of 10 nm and an average base radius of about 100 nm. In the (B) samples, at the same temperature, larger (~ 1-2 μ m) structures of irregular shape are present, and the measured roughness is about 50 nm.

[1] T. Hashimoto, T. Yamada, T. Yoko, J. Appl. Phys. **80**, 3184 (1996)

[2] R. Beattie, T.R. Gilson, J. Chem. Soc. A5, 980 (1970)

[3] R.J. Thibau, C.W. Brown, R.H. Heidersbach, Appl. Spectr. **32**, 532 (1978)

EFFECT OF EXCITON DEPHASING IN A SEMICONDUCTOR MICROCAVITY

E. Brambilla, F. Castelli, L.A. Lugiato,
*Istituto Nazionale di Fisica della Materia,
Dipartimento di Fisica dell' Università,
via Celoria 16, 20133 Milano, Italy*

and I. Abram
*CNET, Laboratoire de Bagnex,
19996 Avenue Henri Ravera, 92220 Bagnex, France*

Abstract

We consider a planar MQW semiconductor microcavity delimited by Bragg mirrors, in which delocalized Wannier excitons interact with the radiation field. In the low excitation regime one can describe the interaction as occurring between an excitonic mode and a near longitudinal cavity mode, both corresponding to harmonic oscillators; this leads to the onset of two composite modes which are called upper and lower cavity-exciton polaritons. Even in the resonant case in which the exciton and the cavity mode have the same frequency, the two polariton modes have different frequencies; this frequency splitting, which is called vacuum field Rabi splitting, has been experimentally observed in semiconductors in the early nineties [1].

If one neglects the damping processes which arise, on the one hand, from the coupling of the exciton mode with other spontaneous emission radiation modes and, on the other, from the coupling of the relevant cavity mode with outside the cavity, the picture which emerges is that of a mutual and periodic exchange of energy between the exciton mode and the cavity mode, and when the cavity mode is initially empty of photons, this exchange occurs with the vacuum field Rabi frequency. Thus, in this framework spontaneous emission becomes a reversible precess, characterized by Rabi oscillations.

Taking the damping processes into account, the coupling between the two modes offers an important possibility for engineering spontaneous emission; as observed experimentally, this allows for a drastic enhancement of the spontaneous emission coupling efficiency and the possibility to approach thresholdless laser emission [2].

In particular, when the coupling constant is substantially larger than the decay rates of both modes (strong coupling regime), the dynamics is governed by the two polariton modes, which decay independently of each other. For example, in the resonant case the two polaritons decay with the same rate, equal to the average of the decay rates of the two bare modes. Because in microcavities the cavity decay rate is much larger than the spontaneous emission rate of the bare excitons, this implies that the polariton decay is much faster than the bare exciton decay, i.e. spontaneous emission has been accelerated and this is an important benefit in the case of microcavities operating in such a strong coupling regime [3].

On the other hand elastic and incoherent processes, like scattering with phonons, lead to dephasing of the exciton mode, and can be detrimental to the benefits created by strong

coupling [2]. We have studied the influence of exciton dephasing over the spontaneous emission efficiency, by adding to the simple master equation model, which describes the two coupled and damped oscillators, the appropriate term which takes exciton dephasing into account.

The complex dynamics of the exciton decay is governed by the following relevant parameters : the free exciton spontaneous emission rate γ_{ex} , the damping rate of the cavity mode k_{ph} , and the dephasing coefficient γ_ϕ , describing exciton phase destroying processes. The dephasing coefficient is strongly affected by temperatures changes, while γ_{ex} and k_{ph} are nearly constant. In fact, at room temperatures γ_ϕ can be even larger than the coupling constant g , and this means that the polariton lifetime becomes very short, and no Rabi doublet can be experimentally observed.

We are however interested in studying the radiative decay rate; In absence of dephasing and under strong coupling conditions ($g \gg \gamma_{ex}, k_{ph}$) an excited polariton state decay directly on the ground state with the rate constant $\gamma_{ex} + k_{ph}$, that is much larger than the bare exciton decay rate $2\gamma_{ex}$ because in a microcavity one has usually $\gamma_{ex} \ll k_{ph}$. When the presence of dephasing is considered, there is a phenomenon of admixture of the two polaritons, and the dynamics can be clearly distinguish in two stages. In the first stage the dephasing gives rise to a redistribution of the populations of the the two polariton states, over a time scale of the order of γ_ϕ^{-1} ; in the second stage the polaritons simultaneously decay to the ground state, with a decay rate that remains of the same order of $\gamma_{ex} + k_{ph}$. This happens even in conditions of very strong dephasing, *i.e.* when γ_ϕ is larger than g , k_{ph} and γ_{ex} , and the separation between the two stages of the dynamics becomes clearest. These results can be carried out analytically in the regime in which the dephasing rate is smaller than the coupling, as it happens in the experiment performed at CNET [4].

Therefore, even if the two polaritons have mixed each other during the short time stage of the evolution, the decay to the ground state occurs according to the dressed state decay rate. In other words, the benefit of having an accelerated spontaneous emission persists even in the presence of dephasing, showing that the spontaneous emission acceleration under strong coupling condition is robust with respect to dephasing.

Acknowledgements

Work in the framework of the ESPRIT Long Term Research Project ACQUIRE (Advanced Quantum Information Researches)

References

- [1] C. Weisbuch, M. Nishioka, A. Ishikawa, and Y. Arakawa, *Phys. Rev. Lett.* **69**, 3314 (1992).
- [2] H. Cao, J. Jacobson, G. Bjork, S. Pau, and Y. Yamamoto, *Appl. Phys. Lett.* **66**, 1107 (1995).
- [3] I. Abram and J.L. Oudar, *Phys. Rev.* **51**, 4116 (1995).
- [4] I. Abram, B. Sermage, S. Long, J. Bloch, R. Planel, and V. Thierry-Mieg, in *Microcavities and Photonic Bandgaps: Physics and Applications*, ed. by J. Rarity and C. Weisbuch, Kluwer Acad. Publ., 1996, p.69.

Picosecond relaxation dynamics of localized excitons in ZnSe/ZnS_xSe_{1-x} strained-layer superlattices

M.C.Netti ^a, R.Tommasi ^{a,b}, M.Lepore ^c, I.M.Catalano ^a, A.Vinattieri ^d, M.Colocci ^d and I.Suemune ^e

a) Dipartimento di Fisica - INFN, Università degli Studi di Bari, via E.Orabona,4 - 70126 Bari - ITALY

b) Istituto di Fisica Medica - Università degli Studi di Bari, via E.Orabona 4 - 70126 Bari - ITALY

c) Dipartimento di Fisica - INFN - Università "Federico II" - Napoli - ITALY

d) LENS - European Laboratory for Non Linear Spectroscopy, Largo E.Fermi, 2 - 50125 Firenze - ITALY

e) Research Institute for Electronic Science -Hokkaido University- Sapporo JAPAN

The localization effects due to interface roughness caused by unavoidable well width fluctuations or compositional disorder are a crucial aspect in II-VI quantum well systems. Several authors have reported that optical gain in ZnSe/ZnS_xSe and ZnCdSe/ZnSe arises from recombination via localized states [1][2][3]. The excitonic character of laser action due to the modified stability of the excitonic particle is further enhanced by exciton localization to the local inhomogeneities within the well.

We report here a detailed study of the relaxation dynamics of localized excitons in a set of symmetric ZnSe/ZnS_{0.18}Se_{0.82} strained-layer superlattices (SLSs). The main peculiarity of these samples is their quasi-3D character given by the 10:90 offset distribution between the conduction and valence band, that make these SLSs of a shallow type-I. The conduction and valence band offsets are about 10 meV and 150 meV, respectively for all the samples.

We performed time-resolved photoluminescence (TR-PL) measurements on five samples with well width $L_w=20$ Å, 40 Å, 50 Å, 83 Å and 94 Å at 10 K using a Nd:YAG pumped dye laser (5 ps pulse, 800-900 nm, 76 MHz repetition rate). The PL were dispersed by a 0.22 double monochromator (energy resolution 1 meV) and detected by a synchroscan streak camera with an overall resolution of 20 ps. TR-PL experiments were performed at very low density of injected carriers (10^{-6} - 10^{-7} cm⁻²) and at different exciting energies ($\hbar\omega_{exc} > E_{gap}^{barrier}$, $\hbar\omega_{exc} \cong E_{bup}^{barrier}$, $\hbar\omega_{exc} < E_{gap}^{barrier}$) to better discriminate the exciton formation, migration and relaxation mechanisms.

Typical TR-PL profiles are shown in Fig.1 for the 83 Å sample obtained at 10 K and with the excitation energy set in the continuum of states ($\hbar\omega_{exc} = 3.065$ eV). The experimental TR-PL (symbols) were recorded at different detection energies of the PL inhomogeneously broadened line reported in Fig.2. Similar results have been obtained for the other samples. The main characteristic of these TR-PL curves is the decay that changes from mono-exponential to bi-exponential depending mainly on the detection energy and the ratio between exciton radius (a_0) and the well width (L_w). In particular, a mono-exponential decay at lower detection energies turns into a bi-exponential one at higher detection energies for all the sample except for the 40 Å one. This

peculiar decay behavior is strictly related to the different contributions of free and localised exciton to the luminescence. Due to the difficulty of elaborating a complete model of population dynamics of localized and free excitons for a quantitative analysis, we attempted to fit our results with a simple bi-exponential function. The results of the fit are reported on Fig.1 (solid lines curves) and the rise and decay times reported on Fig.2 (symbols). The rise times, related to the formation of the excitons, decrease by increasing the detection energy for all the samples with $L_W < a_0$. Conversely, for the samples with $L_W > a_0$ they increase and afterwards decrease with increasing the detection energy. This anomalous trend of the rise times in thicker wells may be the evidence of the hopping among localization sites before recombination. This effect could be due to the lower density of injected carriers (10^6 - 10^7 cm $^{-2}$) with respect to the density of localization sites (typically 10^{10} - 10^{11} cm $^{-2}$).

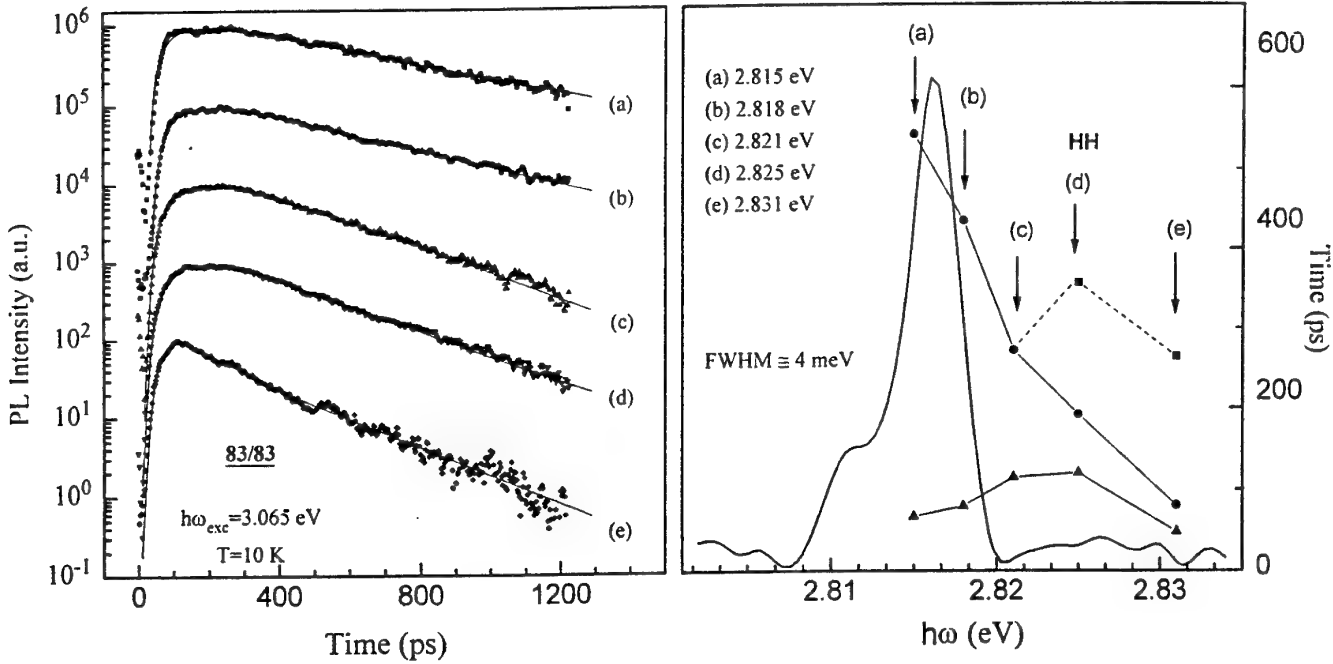


Fig.1 - TR-PL curves (symbols) obtained at different detection energies ((a)-(e) reported in Fig.2) at 10 K and $\hbar\omega_{exc} = 3.065$ eV for the 83 Å sample. Solid lines are the results of the fit with a simple biexponential function.

Fig. 2 - Rise times (triangles) and decay times (squares and circles) obtained by the fit superimposed to the inhomogeneously broadened PL line.

References

- [1] J.Ding et al. Phys.Rev.B **47**, 10528 (1993); J.Ding et al. Phys.Rev.Lett. **69**, 1710 (1992)
- [2] Y.Kuroda et al. Appl.Phys.Lett. **61**, 1182 (1992)
- [3] R.Cingolani et al. J.Opt.Soc.Am. **B 13**, 1268 (1996)

Nonlinear refractive index measurement of dispersion shifted fibres from the maximum frequency extent of SPM spectra

Riccardo CALVANI, Renato CAPONI, Diego ROCCATO
CSELT - Centro Studi e Laboratori Telecomunicazioni - S.p.A.
Via G. Reiss Romoli, 274 - 10148 Torino - Italy
Tel.: +39.11-228-56.70 - Fax.: +39.11-228-50.85

The measurement of the nonlinear refractive index n_2 in optical fibres is assuming an increasing interest for the realization of aggregate transmission flows at very high bit rates (~ 40 Gbit/s) in telecommunications. The recent importance of n_2 in this area is due to both the potentially negative impact of related phenomena, like the FWM or modulational instability, on conventional (optically linear) systems, and to the opposite possibility of improving their performance through the exploitation of different n_2 -dependent nonlinearities, as in the well known example of soliton propagation - where the fibre dispersion is compensated for by the Kerr effect originating from the same propagating signal, or self-phase modulation (SPM).

Most of the published techniques for characterizing n_2 are based on SPM or XPM (cross-phase modulation), which are generated by intense pump pulses inducing nonlinear phase shifts in themselves (SPM) or on a different probe beam (XPM). The measurand is then obtained from an analysis of resulting intensity profiles in the time or frequency domain [1, 2].

In the present paper, a new technique relying on the evaluation of the spectral SPM width for pump pulses propagating over a short length z of dispersion shifted fibre (DSF) is proposed. This configuration is a typical case of pure SPM - which can be described by a well known analytical model [3] - as dispersion and absorption (and also polarization changes) becomes negligible for low values of the coordinate z . In particular, the maximum extent of the instantaneous frequency shift, or chirp, due to SPM is given by:

$$\Delta\omega_{\max} = \frac{\pi n_2 z}{\lambda A_{\text{eff}}} \cdot \left[\left(\frac{dF^2}{d\tau} \right)_{\tau=\tau_1} - \left(\frac{dF^2}{d\tau} \right)_{\tau=\tau_2} \right] \cdot P_{\text{peak}} \quad (1)$$

where λ is the pump wavelength, τ is the proper time of the pulse (referred to its maximum), τ_1 and τ_2 are the inflection points of its (normalized) intensity envelope $F^2(\tau)$, A_{eff} is the effective area of the fibre and P_{peak} is the peak power.

Using equation (1), n_2 can be easily determined from the knowledge of the other parameters involved, as well as of the pulse profile $F(\tau)$. Unfortunately $\Delta\omega_{\max}$ is not directly related to any parameter of the SPM spectrum, so that it provides only an approximate estimate of the corresponding frequency width, at least for modest values of P_{peak} . Conversely, the precision of this evaluation improves with the increase of the pump power, because $\Delta\omega_{\max}$ can be demonstrated to approach the real spectral extent asymptotically (for $P_{\text{peak}} \rightarrow +\infty$). Numerical simulations are then required - and will be briefly illustrated in the following - for studying the possible implications of the above limit in order to derive n_2 with sufficient precision from the measurement of the SPM spectrum at reasonable pump levels through eqn. (1).

It is noteworthy that the proposed technique offers the advantage of a continuous power scanning, contrary to previous frequency- and time-resolved methods [1, 2], where discrete values (integer multiples of $\pi/2$ and π respectively) of the nonlinear phase shift as a function of the variable P_{peak} are needed [4].

To evaluate the correspondence of the spectral FWHM with $\Delta\omega_{\max}$ in practical cases, numerical simulations of pure SPM spectra were performed through the FFT algorithm for a 0.56 km long DSF, with zero dispersion wavelength at 1568.5 nm and $A_{\text{eff}} = 43 \mu\text{m}^2$, using hyperbolic

secant pulses - that is assuming $F(\tau) = \text{sech}(\tau)$ - at 1549.5 nm. In Fig. 1 the frequency extent of computed output spectra versus P_{peak} is described by curve (b), which closely approximates the slope of the straight line (a) - corresponding to eqn. (1) - at least for $P_{peak} \geq 8W$. This result demonstrates the feasibility of the proposed n_2 measurement in a range of pump powers easily attainable with laboratory sources, such as a color center laser (FCL).

An experiment with a DSF (having the same parameters as in the simulations) was performed using transform-limited pump pulses of 6 ps FWHM and $\Delta\tau \cdot \Delta\nu = 0.32$ (very close to the ideal value for the sech profile) from an FCL laser operating at 1549.5 nm, with a mode-locking frequency of 76.3 MHz. The FWHM values of the SPM spectra versus P_{peak} are shown in Fig. 2, together with the linear best fit of the experimental points. The corresponding slope is very close to the coefficient calculated for line (b) of Fig. 1. Finally, by introducing this figure into eqn. (1), $n_2 = 2.6 \cdot 10^{-20} \text{ m}^2 / \text{W}$ is obtained, in good agreement with recent data.

References

- [1] K. S. Kim, R. H. Stolen, W. A. Reed, K. W. Quoi, Opt. Lett., **19**, 257 (1994).
- [2] C. Naddeo, M. Artiglia, R. Caponi, F. Cisternino, D. Roccatto, ECOC'94, Italy, p. 327.
- [3] R. R. Alfano, "The supercontinuum laser source", Springer-Verlag, New York, (1993).
- [4] R. Calvani, R. Caponi, C. Naddeo, D. Roccatto, patent pending.

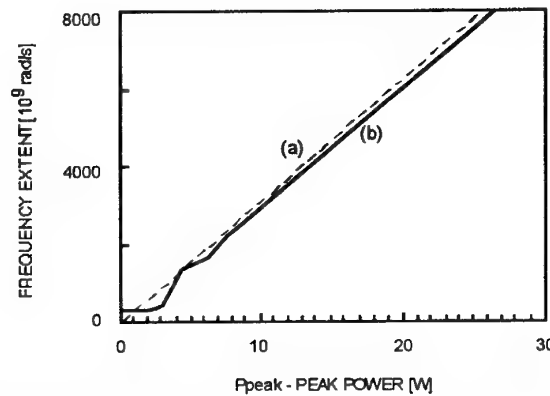


Fig. 1 - Calculated curves for a 0.56 km DSF with pump pulses of hyperbolic secant profile:

(a) the straight line of equation (1), (b) FWHM of the simulated SPM spectra versus P_{peak} .

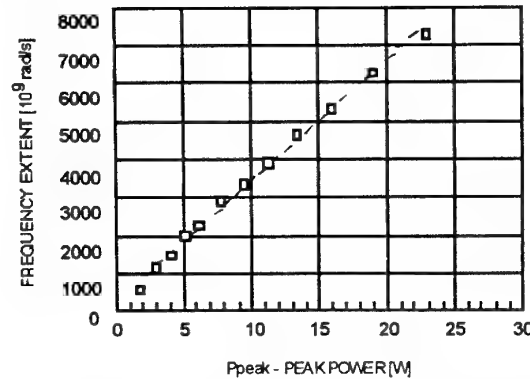


Fig. 2 - Experimental behaviour of the SPM frequency extent versus P_{peak} for the DSF of Fig. 1, with pulses having $\Delta\tau \cdot \Delta\nu = 0.32$ (very close to the ideal value of the sech envelope): () FWHM data, measured from SPM spectra, (---) linear best fit of the FWHM points.

SOLUTION GROWTH OF L-ALANINE AS A MATERIAL FOR NON-LINEAR OPTICAL APPLICATIONS

M.Zha, M.Ardoino, L.Zanotti

Ist. MASPEC-CNR, via Chiavari 18/A 43100 Parma (Italy)

In the field of organic materials for non linear optical applications, α -aminoacids present many interesting properties to be studied. Molecular chirality guarantees that the crystals will be acentric, the materials are colorless and do not contain strongly conjugated group, so that the crystals should have wide transparency in visible and UV region of the spectrum. Further, the zwitterionic structure of these molecules, which behaves like dipolar ions, assure for the crystal lattices a stronger mechanical hardness in respect of other organic materials usually bounded by weaker interaction. Moreover, they can be considered the starting point for syntetising and processing more complex organic - inorganic structures, which can be possible candidates for application as L-arginine phosphate.

The simplest member of the family of α -aminoacids is the L-alanine ($\text{CH}_3\text{CH}(\text{NH}_2)\text{COOH}$), which is known to crystallize in the orthorhombic space group $P2_12_12_1$.

Authors initiate a program for the growth of L-alanine single crystals, with the aim of obtaining specimens with chemical and optical perfection to allow a satisfactory assessment of the optical properties.

L-alanine is soluble in water and slightly soluble in alcohols. As growth solvent, pure water as well as water mixture with different percentage of methanol and ethanol have been tested. The addition of about 10 % of alcohol does not reduce the solubility of

alanine in water, but at the same time strongly stabilize the solution as it avoids the eventual formation of biological poisoning which might introduce scattered inclusions in the crystals. A larger percentage of alcohols as well as the pH of the solution can strongly affect growth behavior.

Growth experiments have been performed with different supersaturation conditions in completely free growth systems or, alternatively, by using appropriate seeds. From the point of view of crystal quality the best results have been achieved with seeded growth and large supersaturation: in these cases samples of the order of $10 \times 5 \times 5 \text{ mm}^3$ have been obtained. Practical experience has shown that when low supersaturation conditions are applied, seed defects cannot be recovered and the crystal quality tends to deteriorate, and this makes difficult to grow high quality large crystals.

Experimental observations pointed out the complex morphology of L-alanine crystals, with the appearance of at least four families of faces, and the close relationship between surface imperfections and crystal morphology. For this reason, investigation on growth morphology in connection with crystal structure has been carried out.

These studies have stressed the correlation between the growth stability and the morphological importance of the various faces and have contributed to assess the growth process. Furthermore, these studies led us to formulate the hypothesis that the large steps parallel to c crystallographic axes which always appear on $\{110\}$ and $\{120\}$ faces might be attributed to the very similar morphological stability of these faces.

All these observations and crystal growth results are reported in this contribute and discussed.

STUDIES ON SOLUTION GROWTH OF LARGE MONOMETHYLUREA SINGLE CRYSTALS

M. Zha, M. Ardoino, L. Zanotti

Institute MASPEC-CNR, via Chiavari 18/A, 43100 Parma, Italy

Many efforts have been done in the recent years in the search of organic materials for nonlinear optical applications. A branch of this research is devoted to materials transparent in blue and UV region of the spectrum, suitable for applications such as high density data storage and parametric emission. Urea was one among the first materials exploited in this field and it is still of interest though difficult to be grown in high quality, large size crystals. As a development, a methyl derivative of urea, the monomethylurea (NMU, $\text{CH}_3\text{NHCONH}_2$), has been studied.

Here we report a systematic studies on NMU crystal growth from alcoholic solutions. Different growth conditions have been performed:

- a) completely unconstrained conditions (free growth);
- b) mechanical direction limitation method;
- c) top-seeded growth.

We have found that under the unconstrained growth condition NMU exhibits a rod-like habit, with four well developed lateral $\{011\}$ faces and two tilted wedge-like $\{110\}$ faces at each end. The morphological stability of both $\{011\}$ and $\{110\}$ faces can be deduced by Donnay-Harker (DH) theory (based on interplane distances) and can be further assessed by the evaluation of direction of intermolecular bond chains (Hartman- Perdok theory).

These points are confirmed by means of calculations based on attachment energy, performed by Sherwood and co-workers. Actually the same results can be obtained by an attachment energy calculation with a rough estimation of electric charge distribution.

From the results we conclude that $\{011\}$ are the most stable faces, and suitable growth condition can be achieved provided the growth of $\{110\}$ faces are stabilised.

For this reason have developed the so called mechanical direction limitation method to grow NMU crystals. By using this method, we have successfully grown

large NMU single crystals starting with long, thin seeds ($70 \times 2 \times 2 \text{ mm}^3$) capped along $\langle 100 \rangle$ direction so that only stable lateral $\{011\}$ faces development is allowed. The growth process is based on lowering temperature about $0.1^\circ\text{C}/\text{day}$. The obtained crystals display cross-section of around $25 \times 25 \text{ mm}^2$ - $30 \times 30 \text{ mm}^2$ with very high structural and optical quality.

The main advantages of this method is its stability. One can reproduce such high quality crystals by carefully preparing seed and control the temperature reduction rate. On the other hand, the presence of the seed along the axis of the crystals strongly reduce the available cross-section for optical applications. To increase the useful cross section, one might try to grow crystals with even larger cross section, or try to find an alternative growth method.

To release the cap constrain, one must stabilise $\{110\}$ faces by more precisely temperature control and much more careful preparation of starting material. In the alternative experiment, seeds were cut from previously grown crystal perpendicular to $\langle 100 \rangle$ direction. These square platelets ($8 \times 8 \text{ mm}^2$) of thickness of 2-3 mm are fixed on a Teflon holder.

All seeds grow in the same way: the growth starts with the formation of a rim on the platelet, and crystallisation develops unconstrained from this rim originating $\{110\}$ faces which ultimately merge into a dihedron. Then crystal growth goes on perpendicular to $\{110\}$ faces.

In this case supersaturation must be kept extremely low, with a temperature reduction rate of the order of $0.03^\circ\text{C}/\text{per day}$, so that to keep $\{110\}$ faces stable. Our experiment shows that this method is useful to prepare high quality NMU crystals.

The high structural quality has been confirmed by x-ray examination. The optical assessment are presented elsewhere in this conference.

SPATIAL OPTICAL SOLITONS IN A BK7 GLASS PLANAR WAVEGUIDE

M. Bertolotti, E. Fazio, F. Garzia, G. Lanciani, C. Sibilio, M. Suriano, M. Zitelli

Dipartimento di Energetica, Università di Roma "La Sapienza"

INFM-GNEQP CNR

Via Scarpa 16 00161 Rome, Italy.

tel: +39-6-49.76.65.42

fax: +39-6-44.24.01.83

G.C.Righini

IROE CNR

Via Panciatichi 64 Florence, Italy

ABSTRACT: We report the observation of stable self-trapping of laser beams inside a nonlinear planar glass waveguide. We realized a high gain, low repetition rate pulse amplifying system in order to produce the required power to observe nonlinear Kerr effects without producing thermal nonlinearities. We also investigate theoretically and experimentally the collision between two quasi-solitons of parallel polarization.

SPATIAL SOLITON GENERATION, INTRODUCTION

Spatial optical solitons are light beams which propagate undiffracted in a nonlinear medium because of the balance between two competing effects: diffraction and autofocusing generated by the material electronic nonlinearity. In a three dimensional medium in which the light diffracts in two transverse directions, selftrapping is not stable and often leads to catastrophic self-focusing; thus, to generate a spatial soliton it is necessary to limit diffraction to only one transverse dimension, for instance using a planar waveguide.

Considering a light beam propagating in a planar waveguide, we assume that the change in the refractive index due to third order non-resonant electronic nonlinearity $n_2 |E|^2$ (n_2 is the nonlinear index coefficient, $|E|^2$ is the field intensity) is much smaller than the linear index difference between film and substrate $n_0 - n_s$, that the transverse mode size along the confinement axis w is much smaller than the beam width along the diffraction axis a_0 , and assume also the absence of losses and the paraxial approximation. It exists then a critical beam power where the beam tends to assume and maintain a hyperbolic secant transverse shape, and conserves its transverse width during propagation. The critical power is given by

$$P_s = \frac{2n_0 w}{n_2 a_0 k_0^2} \quad (1),$$

where k_0 is the vacuum wavenumber.

EXPERIMENTAL RESULTS

In Fig.1 we report the experimental setup and results for spatial soliton generation in a planar waveguide. The guide has a substrate of shott BK7 glass ($n_0 = 1.518$, $n_c = 1.511$, $n_2 = 3.2 \times 10^{-16} \text{ cm}^2/\text{W}$); the film has been obtained for $\text{K}^+ - \text{Na}^+$ ion-exchanging in thermal bath in KNO_3 , the refractive index profile has been measured by a double Lloyd's interferometric technique [W.A.Ramadan, E.Fazio, M.Bertolotti, Appl. Opt. 35, 6173 (1996)], the effective thickness is $1.5 \mu\text{m}$ and the guide is monomodal for both polarizations. We end fire coupled a high power pulsed beam generated by a previously realized amplifying system [M.Zitelli, E.Fazio, M.Bertolotti "On the design of multipass dye laser amplifiers", presented at IEEE J.of Quantum Electron.]. By measuring the transmission across a vertical aperture at the guide output we could analyze the self focusing and diffraction experienced by the beam. In the experiment the beam propagated in the guide for about 8 soliton periods (25 mm), which are sufficient for spatial soliton formation, and we expected a critical power $P_S = 115 \text{ kW}$, which must be

assumed as an average pulse power over the temporal width. We see that for average powers greater than 40 kW the transmission begins to raise almost linearly, due to self focusing, and for powers of 100-120 kW it becomes constant. We assume that at this power the beam has self trapped. For higher powers other nonlinear effects such as two photon absorption and higher order soliton generation could become important.

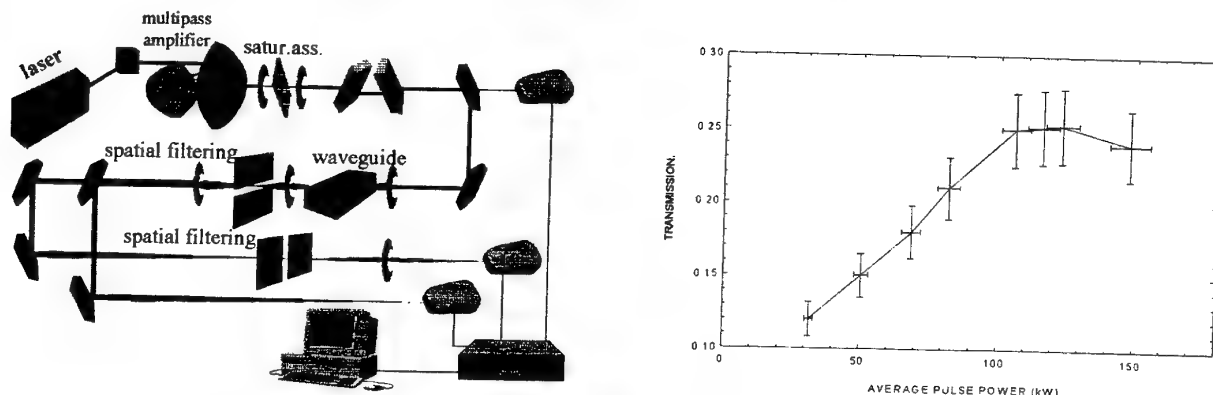


Fig.1 : Spatial soliton generation experimental setup and results.

COLLISION BETWEEN TWO QUASI SOLITON OF PARALLEL POLARIZATION

When two soliton beams propagate with a small angle between them and meet to a certain point inside the waveguide they are said to make a collision. At every guide transverse cross section the nonlinear index variation is given by

$$n_{nl} = n_2 (|E_1|^2 + |E_2|^2 + 2E_1E_2 \cos\phi) \quad (2)$$

and is proportional to the two beam intensities and to an interference term (for beams of parallel polarizations), which contains the relative phase ϕ between the two fields. The two beams tend to move towards the higher index regions and are thus deflected or shifted in their transverse position by the collision. Such interaction depends on the relative phase, the relative angle and initial distance of the beams. After collision the two solitons are able to conserve their shapes by virtue of the stability of such fields in a planar waveguide. We propagated two beams with power slightly smaller than the critical for soliton generation, and an angle of 5° . We observed a transfer of energy towards the higher power beam and a certain transverse shift of the two beams after collision (Fig.2), which was weakly dependant on the initial relative phase.

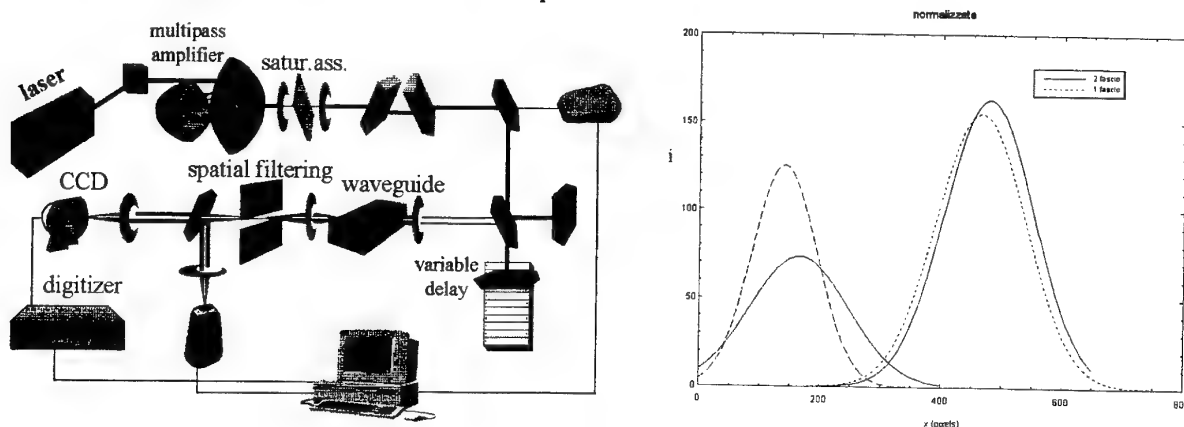


Fig.2 : Experimental setup and results for collision of two quasi solitons. The dotted lines are the transverse intensity profile fits for the non interacting beams at the guide output; the solid lines are the beams after collision.

ELECTROOPTICAL PROPERTIES OF HYDROGEN-BONDED SELENATES

L. Guilbert, J.P. Salvestrini and M.D. Fontana

Laboratoire Matériaux Optiques à Propriétés Spécifiques

C.L.O.E.S., Université de Metz-Supelec

2, rue E. Belin 57078 Metz Cedex 3, France

The hydrogen bonded selenate family exhibits interesting properties^{1,2} for electrooptic and non linear optics. In the present work, the electrooptical coefficients and dielectric permittivity of Rubidium Hydrogen Selenate (RHSe) and Ammonium Hydrogen Selenate (AHSe) are compared in the low frequency range 0 - 1 MHz.

For both compounds the major terms of the Pockels tensor, r_{42} , mainly comes from the piezo-optic contribution $p_{44} d_{42}$. For paraelectric AHSe this indirect Pockels coefficient is high (about 200 pm/V) relatively flat up to 100 kHz, whereas for ferroelectric RHSe a giant contribution arising from domain dynamics appears below 1 kHz. This latter effect is explained³ and calculated in terms of ellipsoid-tilting caused by the switching of ferroelastic domains.

Références :

1 - "*New crystal with strong electrooptic effect : Rubidium hydrogen selenate*", J.P. Salvestrini, M.D. Fontana, M.Aillerie, Z. Czapla, Applied Physics Letters, 64, 1420(1994)

2 - « *Electrooptical properties of hydrogen selenates* », European Optical Society Topical Meeting, », J.P. Salvestrini, L. Guilbert, M.D. Fontana et Z. Czapla, VAL THORENS (1996)

3 - « *Electrooptical properties of rubidium hydrogen selenate : Influence of the DC electric field and origin of the large electrooptic coefficient* », J.P. Salvestrini, L. Guilbert, M.D. Fontana and Z. Czapla, soumis à J.O.S.A. B, (1997)

Third order nonlinear optical properties of $\text{Zn}_{1-x}\text{Mg}_x\text{Se}$ crystals

B. Sahraoui

Laboratoire des Propriétés Optiques des Matériaux et Applications (POMA).

Université d'Angers. 2, Boulevard Lavoisier

49045 Angers cedex 01 (France).

e-mail : sahraoui@univ-angers.fr

Tel: 41.73.54.24 Fax: 41.73.53.30

W. Bala, G. Glowacki

Institute of Physics, N. Copernicus University, Grudziadzka 5, 87-100 Torun, Poland

Tel. (48 56) 210 65, Fax (48 56) 253 97

e-mail : wbala@158.75.5.35

The mixed crystals and quantum well structures of wide-bandgap $\text{A}^{\text{II}}\text{B}^{\text{VI}}$ compounds are an important class of materials with a variety of potential applications in optoelectronics and nonlinear optical devices for optical signal processing and optical computing. Wide-bandgap ternary $\text{Zn}_{1-x}\text{Mg}_x\text{Se}$ compounds are particularly attractive for optoelectronics applications, especially for light-emitting devices that operate in the blue-green region of the spectrum, and nonlinear optical devices. Knowledge of the absorption coefficients and refractive indexes of the ternary crystals under high excitation is especially important in the design and analysis of laser structures and wave-guiding devices utilizing these semiconductors in the ultraviolet, visible and infra-red range. Although the optical properties of $\text{Zn}_{1-x}\text{Mg}_x\text{Se}$ compounds have been well established recently, little is known about their nonlinear properties versus Mg content.

In this work, the dependence of absorption and third order susceptibilities of $\text{Zn}_{1-x}\text{Mg}_x\text{Se}$ crystals on Mg content are investigated using picosecond pulses from a mode-locked Q-switched Nd: YAG laser operating at 532 nm.

The measurements of the resistivity, Hall mobility and carrier concentration were performed by the Van der Pauw method using indium dots as contacts. The absorption is characterized by the transmission of $\text{Zn}_{1-x}\text{Mg}_x\text{Se}$ crystals as a function of Mg content. In these crystals, two-

photon absorption is observed at 532 nm as the incident photon energy is less than direct band gap energy E_g but greater than $E_g/2$ [2] The linear absorption is due, among other reasons, to the impurity levels in the band gap. Transmission of the $Zn_{1-x}Mg_xSe$ crystals were studied versus input beam. We observe that the transmission increases with the increasing Mg content in the crystal, which is caused by the increase of the energy band gap and lattice constant. From nonlinear transmittance at 532nm, we have evaluated two photon absorption and calculated imaginary part of the third order susceptibility $\chi^{(3)}$. It is found that the magnitude of the nonlinear absorption decreases with an increase of Mg content in $Zn_{1-x}Mg_xSe$ crystals. For the crystals with relatively small nonlinear absorption coefficient, we estimated the real part of $\chi^{(3)}$ using the degenerate four wave mixing method. The magnitude of real part of $\chi^{(3)}$ for the crystals studied increases lightly with an increase of free electron concentration.

Moreover, doping and thermal treatment, which change the contamination of native defects, are important parameters to determine the third order susceptibilities of $Zn_{1-x}Mg_xSe$ crystals. They allow a simultaneous increase of the refractive index change and decrease of the absorption.

References

- [1] R. A. Fisher Optical phase conjugation, Academic Press, Inc., London, (1983)
- [2] J. H. Bechtel and W. Smith, Phys. Rev. B, Vol. 13, N°8, 3515-3522, 15 (1976)
- [3] G. G. Gurzadyan and R. K. Ispiryan, Appl. Phys. Lett. Vol. 59, N°6, 630-631, 5, (1992)
- [4] M. Sheik-Bahae, J. Wang, R. DeSalvo D. J. Hagan, E. W. Van Stryland, Opt.Lett. Vol. 17, N°4, 15 (1992)
- [5]- B. Sahraoui, R. Chevalier, X. Nguyen Phu, and G. Rivoire, J. Appl. Phys., 80 (9) 4854-4858, (1996)

FREE- ELECTRON MODEL FOR THE POLARIZABILITIES OF NANOSYSTEMS

D. Truchado, G. Rojo and F. Agulló-López

Dept. Física de Materiales, C-IV. Universidad Autónoma de Madrid,
Cantoblanco, 28049 Madrid

Rigorous calculations of the linear and nonlinear polarizabilities are difficult and cumbersome. Therefore, in many cases is preferable to use simple phenomenological approaches, easy to handle, and having a direct physical meaning. Moreover, they are particularly adapted to provide some general guidelines on the role of the different physical parameters on the nonlinear response. One such approach is the free electron model by Rustagi and Ducuing¹ (RD) for linear molecules, e.g. polyenes. It yields closed analytical expressions for the linear α and the third-order γ polarizabilities. The RD model has been recently extended² by us to 2 and 3 dimensions. This allows to deal with planar systems, as phthalocyanines, or volume systems as metal nanoparticles in a glassy host. Here, we focus on the three-dimensional case and investigate the effect of the shape of the nanosystem on the polarizabilities. One starts from a cubic box, containing the electrons, and having infinitely high potential barriers. It has been shown that α and γ grow with the electron population N (for a fixed box side $2L$) and with the box side $2L$ (for fixed N). The sign of α is positive (for $N > 6$ and any L) and that of γ is generally negative, except for particular values of N . Then, one reduces one dimension, e.g. $2L_z$, of the box to convert it into a thin plate. α_{zz} and γ_{zzz} decrease with L whereas α_{xx} (or α_{yy}) and γ_{xxx} (or γ_{yyy}) correspondingly increase. On the other hand, the sign of α_{zz} (α_{xx}) keeps positive during box compression but that of γ_{zzz} (and γ_{xxx}) changes from negative to positive. Similar results are observed during additional compression into a thin strip by reducing the $2L_y$ dimension of the thin plate. Finally, the results for the two limit cases (thin plate and thin strip) have been compared to those obtained through pure one- and two-dimensional approaches. Good coincidence is only observed for a low enough electron population N .

REFERENCES

1. K.C. Rustagi and J. Ducuing, *Optics Commun.* **10**, 258 (1974).
2. D. Truchado, A. Hierro, M.A. Diaz-Garcia and F. Agulló-López, *J. Mod. Optics* **44**, 179 (1997).

Linear Electro-Optic measurements in Nd:MgO:LiNbO₃ and LiNbO₃ single crystals.

MEFLEH A., BRUNET S., BENET S.
C.N.R.S. - I.M.P. UPR 8521.
Groupe Physique des Matériaux - Métrologie
Université de Perpignan
52, Avenue de Villeneuve, 66860 Perpignan, FRANCE
Tél : +33-4-68.66.20.64 , Fax : +33-4-68.66.22.87
E-mail : mefleh@univ-perp.fr , Benet@univ-perp.fr

I. INTRODUCTION.

This paper presents a short description of an apparatus recently developed in our laboratory to measure Linear Electro-optic Coefficients of crystals. We have determined the reliability of the set-up using a standard LiNbO₃ crystal, and then we put it into practice with the recently developed Nd:MgO:LiNbO₃ crystal which is characterised by : High damage threshold, noncritical phase matching (NCPM) at room temperature.

II. EXPERIMENTAL APPARATUS.

The scheme of the experimental set-up is shown in Fig.1. This apparatus is composed of two parts : the optical system and the electronic system.

The optical system is formed by He-Ne laser, an attenuating filter, a polarizer is rotated 45° from x to y principal dielectric axes of the crystal, a collimator lens, a Pockels cell, a quarter-wave plate and an analyzer crossed to the polarizer.

The Pockels cell is formed by a support and an enclosure. The support including the crystal and the two wires connections, is mounted on a three axes rotator. The wall makes the circulation of water possible controlling the temperature of the cell by a regulator with an accuracy of 0.1%.

The electronic system is formed by high voltage power supply, photomultiplier, Lock-in amplifier equipped with a mechanical optical chopper working at the optimum frequency of 20 Hz. An oscilloscope allows to control the amplitude and phase of the signal fed into the Lock-in amplifier.

III. ELECTRO-OPTIC MEASUREMENTS.

LiNbO₃ is an electro-optic, acousto-optic and non-linear crystal with numerous applications in bulk and waveguide components. Doping LiNbO₃ with 5% MgO and 0,23% Nd permitted the development [1] of self-frequency-doubled and self-modulated lasers.

Furthermore, Zhong et al [2] have shown that photorefractive damage in LiNbO₃ can be greatly reduced by doping it with approximately 5% or more of MgO. Therefore, Nd:MgO:LiNbO₃ appears to be a potentially high damage threshold laser material.

The Nd:MgO:LiNbO₃ is an uniaxial crystal and has a trigonal structure (point group symmetry 3m). The electro-optic properties can be described by the coefficients r_{22} , r_{13} , r_{33} , r_{51} of the electro-optic tensor. We have used a 5×5×20 mm³ (x,y,z) crystal cut normal to the principal dielectric axes. The z-faces were optically polished and gold electrodes were coated on the x-faces. In this configuration, the phase shift between the two beam polarisation components along x and y axes is given by :

$$\Gamma(E) = -\frac{2\pi}{\lambda} L n_o^3 r_{22} E$$

Where λ is the laser wavelength, L the crystal length along z axis, and n_o the ordinary index in the absence of electric field E along the y axis.

To determine electro-optic coefficient we have measured $\Gamma(E)$ which is induced by the application of a dc electric field, or dc associated with ac electric field with a frequency $f = 15$ kHz.

Our technique consists of using the Senarmont set-up [3-4], allowing to measure the angle θ of the analyzer corresponding to a minimal transmission of the output optical signal. This angle yields the half of the $\Gamma(E)$. This method provides a very good accuracy ($\approx 5\%$) in the determination of the E/O coefficients. The variation of the angle θ as a function of the applied dc voltage at temperature ($T = 22^\circ\text{C}$) is shown in Fig.2. Results show a linear dependence of the electric field phase retardation, indicating that only the linear Electro-optic effect was thus detected. The slope $\delta\theta/\delta V$ allows to calculate the E/O coefficient $r_{22} = (6 \pm 0.3) 10^{-12} \text{ m/V}$.

We found that the electro-optic coefficient r_{22} is independent of around room temperature. This feature is one of the criteria to be checked for modulators.

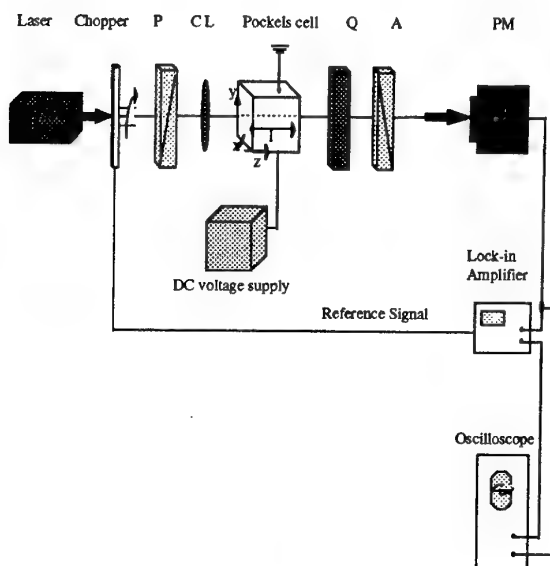


Fig.1. Experimental set-up for measurement of electrooptic coefficients.

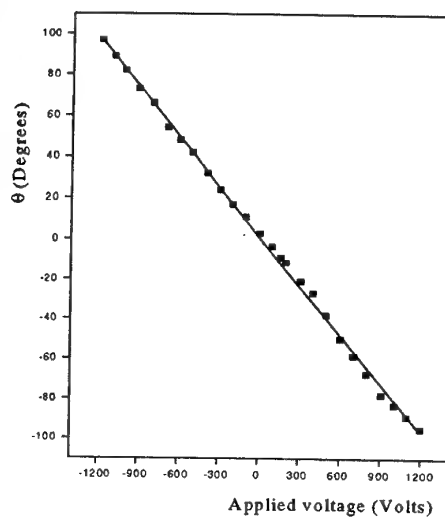


Fig.2. Variation of the applied voltage induced phase shift related to the r_{22}

We have measured the effective electro-optic coefficient $r_e = r_{33} - \left(\frac{n_o}{n_e}\right)^3 r_{13} = 17 \pm 0.3 10^{-12} \text{ m/V}$ in a LiNbO_3 crystal, and we have determined its dependence on temperature.

When compared to the coefficient of LiNbO_3 ($r_{22} = 6.8 10^{12} \text{ m/V}$) at low frequency reported by YARIV [5], we notice a negligible difference.

The findings indicate that Nd:MgO:LiNbO_3 is a very promising crystal for designing miniature green lasers, self-modulated and self Q-switch lasers, and waveguide devices.

REFERENCES

- [1] B. Herreros, G.Lifante, F. Cusso, J. Phys. D: Appl. Phys. **28** (1995).
- [2] G. Zhong, J. Jian and Z. Wu, 11th int. Quantum Electronics Conf. New York (1980).
- [3] M.D. Fontana, F. Abdi, J. Appl.Phys. **77**, 5 (1995).
- [4] M.Aillerie, M.D. Fontana, J. Appl.Phys. **65**, 6 (1989).
- [5] Yariv, Optical Electronics, 4d ed. Sanders college Publishing (1991).

Analytical modeling of the transient effects during two-wave mixing in thin photorefractive crystals

Qin ZOU

Institut National des Télécommunications, 9 rue Charles Fourier, 91011 Evry cedex, France

Abstract

It is known that in two-wave mixing photorefractive crystals the time-dependent recording beams can exhibit, during transients, an oscillatory behavior [1-7]. This effect can be significant if the beam ratio is large and the recording angle is small. A number of numerical models have been developed and verified experimentally for different crystals. Here we present our theoretical investigations in the modeling of the phenomena involved in the transient state within the limits that the fringe modulation is small and allowed to be constant.

We have firstly investigated in the transient solution of the space-charge field. By using Kukhtarev's electron transport equations, for a standard two-wave mixing configuration, the transient space-charge field can be described by the following equation:

$$E_s(x, t) = E_o + m \beta f(t) \cos[Kx + \psi(t)] \quad (1)$$

where the time-dependent amplitude and phase mismatch can be written as:

$$f(t) = \sqrt{1 - 2 \exp(-at) \cos(bt) + \exp(-2at)}$$

$$\operatorname{tg} \psi(t) = \frac{1 - \sqrt{1 + \alpha^2} \exp(-at) \cos\left(bt + \arccos \frac{1}{\sqrt{1 + \alpha^2}}\right)}{\alpha - \sqrt{1 + \alpha^2} \exp(-at) \cos\left(bt - \arccos \frac{\alpha}{\sqrt{1 + \alpha^2}}\right)} \quad (2)$$

All symbols are defined conventionally. We note that in the absence of the applied field, α and b are equal to zero. Some effects, which can be predicted from the above equations, have been discussed, such as the time retardation between the amplitude and phase fringes and the initial spatial phase shift between the induced index grating and the interference pattern at the beginning of the interaction.

The dependence of the rates of intensity change on the recording angle and that on the applied field have been derived respectively. It follows that the maximum oscillatory rate can be obtained when the ratio between the oscillation frequency b and the inverse time constant a becomes maximum, which corresponds to an optimum recording angle and an optimum applied field. Their numerical values calculated for BSO crystals are found to be in good agreement with those observed in experiments [4].

We attempt to show that the fringe bending can be also characterized by the tangent angle in the equal index plans, which oscillates during the formation of the index grating and tends

to zero when saturation is reached. An example is shown in Figure 1, in which the optimized values of the material parameters are used in order to obtain the maximum rate of intensity change. It can be seen that for the diffusion limit in particular ($\psi = \pi / 2$), the contour lines of the tangent angle surface remain curved but the fringes become unslanted.

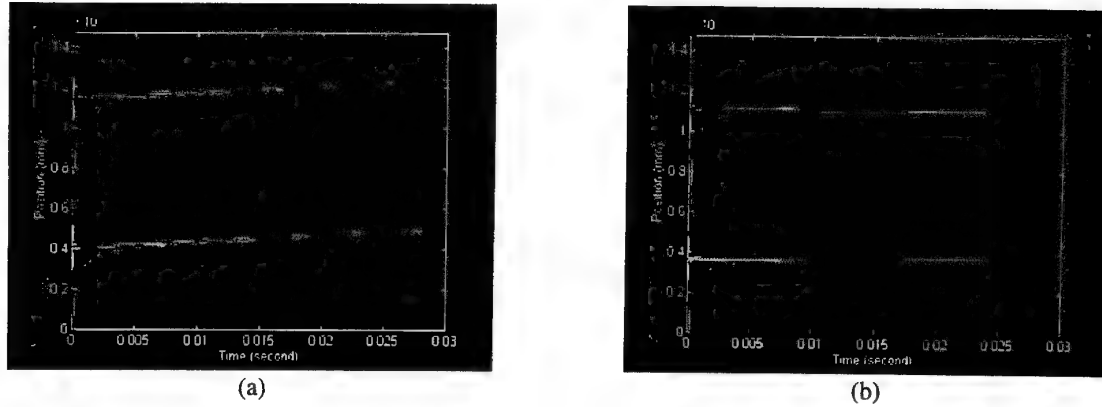


Figure 1. Contour plots of the transient angle surface for BSO thin crystals for $\lambda = 0.5145 \mu\text{m}$, $K = 0.426 \times 10^6$ (1/m) and $m = 0.01$. (a) $E_0 = 10 \text{ kV/cm}$, $\alpha = 5.7$ and $b/a \approx 3$; (b) $E_0 = 0$, $\alpha = 0$ and $b = 0$.

The two time-dependent coupled-wave equations have been solved with the transient solution of the space-charge field obtained previously, using the usual assumptions. The analytic solution of these equations can be written in terms of intensity ratio:

$$\frac{I_S(t)}{I_R(t)} = \frac{I_S(0)}{I_R(0)} \exp[\alpha(t)] \quad (3)$$

where $\alpha(t)$ is the straightforward integration of the imaginary part of the space-charge field:

$$\alpha(t) = r\omega n_o^2 E \left[t - \frac{\alpha a + b}{a^2 + b^2} \exp(-at) \sin(bt) + \frac{a - \alpha b}{a^2 + b^2} \exp(-at) \cos(bt) + \frac{\alpha b - a}{a^2 + b^2} \right] \quad (4)$$

Note that the intensity gain factor can be defined as $\alpha(t)/t$. The temporal variations of the two recording intensities have been analyzed and compared with those of the space-charge field for BSO crystals, which indicated that both the amplitude and the phase of the space-charge field oscillate more strongly than the two recording intensities. This is the predicted result since $\alpha(t)$ is the time average of the imaginary part of the space-charge field.

References

- [1] N.V. Kukhtarev, V.B. Markov, and S.G. Odulov, *Opt. Commun.*, 23, p.338, (1977).
- [2] P.N. Günter, *Phys. Rep.*, 93, p.199, (1982).
- [3] H. Rajbenbach, J.P. Huignard, and B. Loiseaux, *Opt. Commun.*, 48, p.247, (1983).
- [4] J.M. Heaton and L. Solymar, *IEEE, J. of quantum electronics*, 24, No.3, p.558, (1988).
- [5] J.M. Heaton and L. Solymar, *Optica Acta*, 32, No.4, p.397, (1985).
- [6] E.S. Maniloff, K.M. Johnson, and K. Wagner, *JOSA B*, 9, No.9, p.1673, (1992).
- [7] A. Abdelghani-Idrissi, C. Ozkul, N. Wolffer, P. Gravey, and G. Picoli, *Opt. Commun.*, 86, p.317, (1991).

High index jump proton exchanged waveguides in z-cut LiNbO₃ with undegraded nonlinear optical coefficients

J. Rams, J. Olivares^{a)} and J.M. Cabrera

Universidad Autónoma de Madrid, Depto. Física de Materiales C-IV
Canto Blanco, E - 28049 Madrid, Spain

Proton-lithium exchange (PE) of LiNbO₃ substrates produces high index jump ($\Delta n_e > 0.1$), almost step profile optical waveguides very appropriated for the tight light confinement. The exchange rate x must be within the $0.5 < x < 0.8$ range and the so-called β -phase material is obtained. However, these β -phase guides suffer from high optical losses and degraded nonlinear optical coefficients which make them useless for most applications (see for example reference [1]). Here we report a different exchange procedure which uses benzoic acid vapor and gives rise to stable, high quality β -phase guides exhibiting very low losses and almost undegraded d_{33} nonlinear optical coefficient. The method proposed here makes use of the sealed-ampoule set-up introduced by Li *et al* [2], in order to subject the substrate to the action of benzoic acid vapor. After the process, the substrate shows a strong increase of the OH⁻ absorption band, and a waveguide appears supporting modes on the extraordinary refractive index only.

The effective index (n_{eff}) of Z-cut LiNbO₃ wafers was used for characterizing the evolution of the exchanged layer in the whole time range, as shown in Figure 1A. The figure shows two regions, a first one for short exchange times in which $\Delta n_{eff} = n_{eff} - n_e$ keeps quite low, and a second one for long exchange times in which Δn_{eff} saturates at a high value. The measured values of Δn_{eff} at saturation are 0.1325, 0.0984 and 0.084 respectively for 457 nm, 632.8 nm and 1047 nm. This behavior suggests a growing α -phase layer in the short time region, and the emergence of a β -phase material in the long time region. When the exchange temperature is 300°C, the same behavior is observed but the transition between the two regions appears later. The above considerations are further confirmed by comparing Figure 1A with the time evolution of the OH⁻ infrared absorption band. The OH⁻ absorption band has been fitted to two gaussian components peaking at the α - (3482 cm⁻¹) and β - (3510 cm⁻¹) phase positions respectively and have been plotted in Figure 1B.

The quality of the *vapor-guides* was ascertained by the measurement of two key parameters: the optical losses and the d_{33} nonlinear optical coefficient. Optical losses were measured with a digitizing video camera by taking the image of the light scattered out of the waveguide along the beam path. With our set-up the detection limit is 0.35 dB/cm, and neither α -phase nor β -phase guides did show any decrease of the scattered light, indicating that actual losses are below this value (among the best reported in the literature for PE-guides)

The nonlinear optical coefficient d_{33} of our guides was compared to that of the virgin substrate by measuring the second harmonic (266 nm) generated from a 532 nm pulsed beam coming from a doubled Nd:YAG laser (1.06 μ m). Since the wavelength of the second harmonic is strongly absorbed by the LiNbO₃ lattice (absorption edge at 330 nm), only the

^{a)} Present address: Chemistry Physics and Environmental Sciences School, Sussex University, Falmer
BN1 QH9, Brighton, UK

harmonic generated in the last ~40 nm goes out of the sample. Therefore only the outer layer of the sample, fully corresponding to the exchanged material, is actually measured. The second harmonic power measured for α - and β -phase guides respectively was 80% and 70% of that measured for the virgin substrate, the scattering of the data being within the 10%. The power measured in our set-up is proportional to $(d_{33}/\alpha)^2$, α being the absorption coefficient at 266 nm which is a 10% higher in the β -phase layer than in the substrate or in the α -phase layer. Then, our results indicate that the d_{33} value in both type of guides is 90% of the substrate value. Although APE-guides do exhibit partially recovered nonlinear optical capabilities, to the best of our knowledge, this is the first report on high index, sharp profile (β -phase) PE-guides showing excellent SHG capabilities. Since these β -phase guides allow much tighter confinement and higher mode overlap than APE-guides, our finding appears very promising for increasing the SHG efficiency on Z-cut substrates which previously have been periodically poled to achieve the quasi phase matching condition.

Acknowledgments

We are gratefully acknowledged to J.A. Muñoz for useful help with the SHG measurements. J. Olivares is indebted to the European Union for a postdoc grant. The work has been supported by the Spanish Comisión Interministerial para Ciencia y Tecnología under Grant TIC96-0668.

REFERENCES

- [1] J.M. Cabrera, J. Olivares, M. Carrascosa, J. Rams, R. Müller, E. Diéguez, *Advances in Physics* **45**(5), 349 (1996).
- [2] M.J. Li, M. De Micheli, D.B. Osirowsky, M. Papuchon, *Annales des Télécommunications* **43**(1-2), 73 (1988).

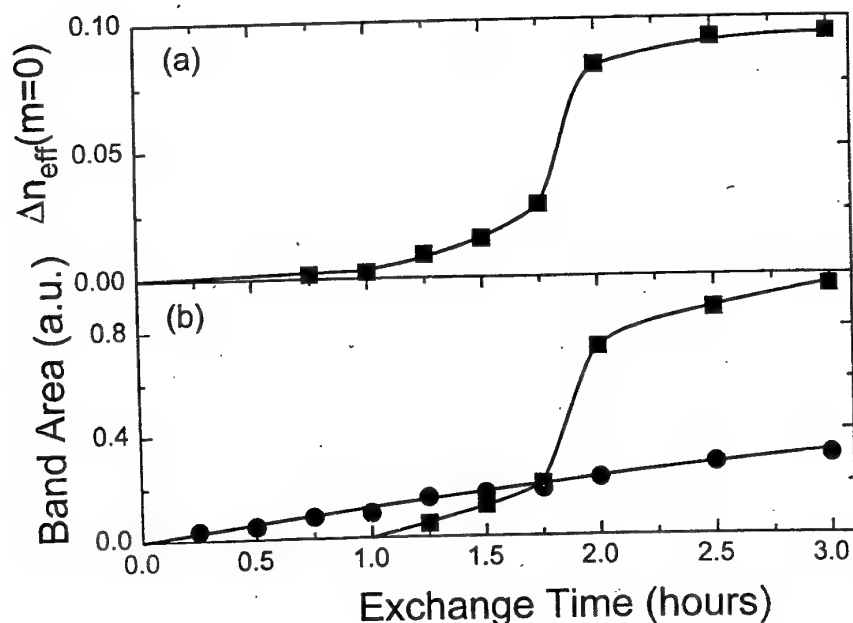


Figure 1

A) Effective index of the fundamental mode as a function of the exchange time, for a temperature of 350°C. B) Area under the α -phase (circles) and β -phase (square) components of the OH^- absorption spectrum as a function of the exchange time.

Nonlinearity of lithium fluoride crystals with F_2^- color centers

Petr G. Zverev

General Physics Institute

Vavilov str., 38, Moscow 117942 Russia

Phone (7-095) 135-03-18

E-mail: zverev@ftt.gpi.ru

Lithium fluoride crystal with F_2^- color centers (CC) is known to be a reliable saturable absorber for neodymium lasers [1]. Our recent preliminary investigation of $LiF:F_2^-$ CC crystal nonlinearity have been done using degenerate four wave mixing technique [2]. In this report it is investigated using Z-scan technique under irradiation with nano and picosecond YAG:Nd laser pulses. The Z-scan technique is known to provide precise measurements of the magnitude and the sign of third order nonlinear susceptibility [3]. It consists in the scanning of a sample through the focus of the Gaussian pump beam. As it was shown before the "open aperture" Z-scan is sensitive only to nonlinear losses such as saturation of absorption or two-photon absorption. The "closed aperture" Z-scan data provides the measurement of a nonlinear refraction simultaneously with nonlinear losses. The division of the "closed" by the "open aperture" data extracts results that depend only on the nonlinear refractive index.

Z-scan measurements in $LiF:F_2^-$ CC crystal were done with pico and nanosecond laser pulses. Electro-optically Q-switched and passively mode locked YAG:Nd laser (1064 nm) with pulse duration 35 ps and 10 Hz repetition rate was used as a light source in picosecond Z-scan experiments. The spatial profile of the laser output in the far field was controlled to be almost Gaussian. The lens with 80 cm focal length focused the beam into $LiF:F_2^-$ CC crystal 20 mm long. The result of the division of the "closed" by the "open aperture" data for CC crystal with initial transmission 40% at 1064 nm wavelength (absorption coefficient $\alpha_{1064} = 0.48 \text{ cm}^{-1}$) and pump pulse energy 5.5 μJ is shown in Fig. 1. It exhibits behavior typical to nonlinear medium with a positive third order nonlinearity, resulting in self focusing. The energy dependence of nonlinear refractive coefficient exhibited linear behavior at low energy level with the saturation at pump energy above 50 μJ that corresponded to the pump intensity of more than 10 GW/cm^2 at the focal point. The value of the real part of nonlinear susceptibility

obtained from unsaturated data was $\chi_{\text{real}}^{(3)} = 1.6 \times 10^{-11}$ esu in the above crystal. It was found that this value linearly depends on the concentration of F_2^- CC and remains 10-20 times higher than that in pure LiF host material.

The similar Z-scan dependencies were obtained under irradiating LiF:F_2^- CC crystal with a Q-switched YAG:Nd laser that provided nanosecond pulses with duration 12-15 ns and 10 Hz repetition rate. The accumulation of nonlinearity in irradiating area that was observed at high pump energy can be attributed to the two photon destruction of color centers. The positive nonlinear susceptibility discovered in LiF:F_2^- CC crystal is described due to CC nonlinearity.

1. T. T. Basiev, S. B. Mirov, and V. V. Osiko, IEEE J. of Quantum Electr., **QE-24**, 1052 (1988).
2. T. T. Basiev, P. G. Zverev, S. B. Mirov, and S. Pal, SPIE **1500**, '65 (1991).
3. M. Sheik-Bahae, A. A. Said, T. H. Wei, D. J. Hagan, and E. V. Van Stryland, IEEE J. Quantum. Electron., **QE-26**, 760 (1990).

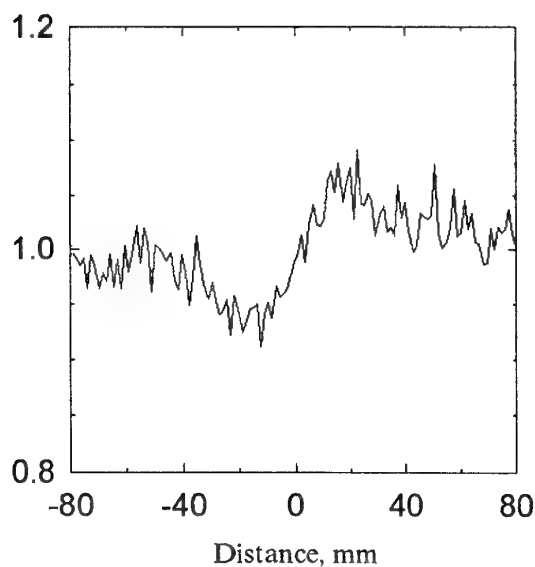


Fig. 1. The result of division of the "closed" by the "open aperture" Z-scan data sets in LiF:F_2^- CC crystal with 40% initial transmission. It exhibits positive nonlinearity typical for self-focusing materials.

Stimulated Raman Scattering in Solid State Materials

Petr G. Zverev and Tasoltan T. Basiev

General Physics Institute

Vavilov str., 38, Moscow 117942 Russia

Phone (7-095) 135-03-18

E-mail: zverev@ftt.gpi.ru

Stimulated Raman Scattering (SRS) can be used to shift laser frequency to different spectral regions. SRS has been demonstrated in various gas, liquid and solid state media. In this report the results on investigation of SRS in crystalline Raman materials are presented. The advantage of solid state Raman material is high concentration of Raman active centers and their favorable thermal and mechanical properties. There is a limited number of solids that have been identified to possess the narrow, isolated and intense Raman active vibronic modes necessary for efficient SRS scattering. In solids there are intense modes that can be attributed to internal symmetrical vibrations within molecular ionic complexes, such as $(\text{CO}_3)^{2-}$, $(\text{NO}_3)^{-}$, $(\text{SO}_4)^{2-}$, $(\text{WO}_4)^{2-}$ and $(\text{MoO}_4)^{2-}$. It was shown before that the efficient SRS frequency conversion of YAG:Nd³⁺ laser radiation to the oscillation with the wavelength at 1.5 μm and longer can be perspective for developing laser sources for eye safe spectral region [1,2].

In this report we discuss Raman features of solid state media that can predict its SRS properties. In station case the gain of the SRS process is determined by the peak cross section of the SRS active mode and is inversely proportional to the spectral linewidth. Internal vibrations in molecular ionic crystals are strongly localized at molecular ion and well isolated from lattice vibrations. By investigating the linewidth broadening with crystal temperature it is possible to predict the dominant relaxation mechanism for high frequency Raman phonons.

The high resolution measurement of ^{frequency} linewidth broadening and shift with temperature were done in $\text{Ba}(\text{NO}_3)_2$ crystal and especially its SRS active A_g mode ($\Omega=1047 \text{ cm}^{-1}$), corresponding to symmetrical stretching of three oxygen atoms in $(\text{NO}_3)^{-}$ molecular ion. The analysis of relaxation mechanisms have shown that its unique feature is the absence of three phonon splitting process due to energy conservation law. This leads to low probability of its relaxation and, correspondingly, small linewidth value that was measured to be 0.56 cm^{-1} at room temperature [3]. As a result $\text{Ba}(\text{NO}_3)_2$ crystal has high SRS gain coefficient that is approximately twice higher than that in calcite crystal and is very attractive for developing Raman lasers. The investigated frequency shift of internal phonons was found to be mostly due to internal modes interaction and proves low

phonon-lattice coupling. The observed frequency shift of A_g mode in $Ba(NO_3)_2$ crystal is important to predict exact value of shifted laser radiation for developing Raman lasers.

SRS as a threshold process require a high pump intensity to obtain significant conversion efficiency. It can be accompanied by other nonlinear processes [4]. The investigation of nonlinearity with picosecond laser pulses using Z-scan technique allows us to observe self focusing in barium nitrate crystal and determine nonlinear susceptibility in it. It was found that the self focusing accompanies SRS mostly with picosecond pump pulses when SRS exhibit a transient behavior and its threshold is increased. The comparison with other Raman crystal will be presented.

Higher order Stokes and Anti-Stokes components oscillation, as well as stimulated Brillouin scattering can accompany SRS in a single-pass Raman cell and can strictly restrict conversion efficiency at high pump intensities. External and intracavity schemes of Raman shifters pumped with neodymium and tunable color center lasers were investigated. Raman shifters with external cavity or intracavity configuration has high discrimination against parasitic nonlinear processes. Such kind of Raman shifter can give a significant increase of conversion efficiency and intensity of Raman scattering with respect to single pass cell. By using special dichroic mirrors with optimal reflectivity it is possible to increase the intensity at the first Stokes wavelength and practically delete the oscillation at the second one. Another ^{set of} mirrors with high reflectivity for the first Stokes component and optimal for the second one provides Raman laser output only at the second Stokes wavelength. Another qualitative difference of the Raman shifter with external cavity or intracavity configuration is the possibility to concentrate Raman scattering in the narrow spatial angle close to the diffraction limited one. It is important to note that such effect can work also with a multimode pump laser that has high divergence. That's why such Raman shifter can sufficiently increase the brightness of the laser beam.

The results on SRS in barium nitrate Raman laser crystal of nano and picosecond laser pulses are presented. Our experiments have shown that barium nitrate Raman laser in external cavity configuration can provide laser oscillation either at the first, or second, or third Stokes components with efficiency up to 73, 53 and 25%, respectively.

1. T.T. Basiev, V.N. Voitsekhovskii, P.G. Zverev and oth., Sov. J. of Quantum Electron., 17, 1560 (1987).
2. P.G. Zverev and T.T. Basiev, OSA Proceedings on the Advanced Solid State Lasers, (OSA, Washington, DC), 24, 288 (1995).
3. P. G. Zverev, W. Jia, H. Liu, and T. T. Basiev, Optics Lets. 20, 2378 (1995).
4. P.G. Zverev, J.T. Murray, R.C. Powell, R.J. Reeves, and T.T. Basiev, Opt. Commun., 97, 59 (1993).

SINGLE ATOM MANIPULATION OF LOCALIZED ELECTROMAGNETIC MODES IN ONE-DIMENSIONAL PHOTONIC CRYSTALS

A. Napoli

INFM, Istituto di Fisica dell'Università di Palermo, via Archirafi 36, 90123
Palermo, Italy

A one dimensional photonic crystal consists of alternating layers of material with different dielectric constants. This arrangement is periodic in one dimension (say z) and homogeneous in the x - y plane. It is well known that such multilayered films can act as a perfect mirror for light with a frequency within a sharply-defined gap. When however a defect is introduced in this structure, that is the translational symmetry is broken, localized modes can arise with a frequency isolated inside a photonic band gap. Suppose for instance that the defect consists of an air-interface between two equal parallel perfectly multilayered films with a marked dielectric contrast [1]. Then an existing electromagnetic mode in the photonic gap propagating along the z axis sees the two sides of the defect as frequency-specific mirrors. Thus the arrangement bears a strong resemblance with the behaviour of a metallic cavity and moreover the localized modes must be quantum-mechanically treated. Assume that only one frequency is allowed in the photonic band gap. For symmetry two independent modes with orthogonal polarization in the x - y plane and equal frequency exist. In this paper we propose the possibility of manipulating the populations of these modes by sending through the air interface-defect appropriate excited Rydberg atoms with a prefixed velocity. A new effective exactly solvable Hamiltonian model of such atom-cavity system is given. The single atom manipulation of the localized and isolated defect mode proposed in this paper mimics a typical experiment realized in the context of the micromaser theory [2].

References:

- [1]C.M. Soukoulis, Photonic band gaps and localization, N.Y. Plenum press 1993, NATO ASI Series B.
- [2]S. Haroche, Fundamental Systems in Quantum Optics, Les Houches Session LIII, (North-Holland, Amsterdam, 1992).

Cubic nonlinear optical response in a substance: dispersion and achievable values of parameters.

V.I.Kovalev.

Lebedev Physics Institute of Russian Academy of Sciences

The retrospective of the problem of search for nonlinear optical materials for different purposes from the outset till the present shows the huge variety of suggested and researched materials (including exotic). At first glance the process looks to be an infinite due to infinite number of usable materials in nature, and to some extent irregular and accidental due to a lot of approaches for evaluation and calculation nonlinear response parameters of materials for different mechanisms of nonlinearity. In this work the attempt is done to treat and systemise the most widely known mechanisms of cubic nonlinear response (CNR) of matter (see first column in Table) in frames of models of an anharmonic oscillator or of coupled oscillators [1].

Despite the relative simplicity of the used approach it provides good agreement with experimental data on third order susceptibility $\chi^{(3)}$ (it varies in the range of 15 orders of value in dependence on both material and CNR mechanism and in the range of many orders of value in frames of the any particular mechanism, and the ranges for different mechanisms are overlapped) and with other models.

No less important parameter of CNR is its decay time τ , which varies in more wider range ($<10^{-15}$ -100 s). It's shown that for almost all mechanisms of CNR (only exception is the nonlinearity due to anharmonicity of bound electrons) in steady state $\chi^{(3)}$ is proportional to τ and coupling coefficients - CNR figures of merit $\chi^{(3)}/\tau$ - appears to be the characteristic parameter of correspondent mechanism. Their value varies only slightly from one material to another and demonstrates specific dependence on radiation frequency ω for a given CNR mechanism.

Some of measured absolute values of $\chi^{(3)}$ and the correspondent values of τ as well as $\chi^{(3)}/\tau$ at 10 μm for each of the listed mechanisms are presented in the Table. It's seen that two types of CNRs, namely nonresonant orientational and resonant due to transition saturation in semiconductors, are the leaders in absolute value of $\chi^{(3)}$ (~ 0.1 -1 esu). However, if one compares these CNRs from the standpoint of $\chi^{(3)}/\tau$, this parameter for the strictional and thermal CNRs appears to be the most inefficient ($\sim 10^{-2}$ - 10^{-5} esu/s) compared to the most efficient ones - "electronic" - ($\sim 10^4$ - 10^5 esu/s).

The scaling $\chi^{(3)}(\omega)$ for CNRs under test are presented at the fifth column of Table. The characteristic property of "Rayleigh" CNRs is the absence of direct ω dependence for $\chi^{(3)}$, what is the result of "huge" (compared to electron) mass of substance which is the involved to the CNR process. The same reason, that is the inertia, but of electron due to its terminal mass, is the reason of strong dependence of $\chi^{(3)}$ on ω ($\sim \omega^{-3,4}$) for electronic CNRs. The ω dependence of $\chi^{(3)}$ for strictional and thermal CNRs ($\chi^{(3)} \sim \omega^{-2}$) is the result of correspondent dependence of τ due to "gradient" nature of CNR.

The obtained results stimulated the question: how big may be $\chi^{(3)}/\tau$ in a substance? It looks to be very actual because *in situ* $\chi^{(3)}/\tau$ (pract. dim. cm^2/J), is the major parameter for the applicability and competitiveness of a set of nonlinear optical devices including phase conjugate mirrors, bistable elements, optical transistors etc.

The known absolute leader in experimentally achieved value of $\chi^{(3)}/\tau$ is CNR due to the saturation of the excitonic transition in GaAs for $\lambda \cong 0.82 \mu\text{m}$ at $T = 10\text{K}$ there have been achieved $\chi^{(3)}/\tau \cong 10^8 \text{ esu/s} / 2 / \approx 10^5 \text{ cm}^2/\text{J}$.

Basing on the presented above results (/1/) it may be shown that the highest $\chi^{(3)}/\tau$ are achievable only for electronic CNRs in materials where the "optical" electron is coupled to the atomic rest as weak as possible. The appropriate analysis was done for CNRs due to anharmonicity of bound electrons, saturation of resonant transitions, free electron generation, as well as for CNR of free electrons due to conduction band nonparabolicity. It's shown that $\chi^{(3)}/\tau$ may be gained by a factor of 10^3 - 10^4 compared to one obtained in /2/. The materials were and conditions how to achieve such values are discussed.

1. V.I.Kovalev. Izv. of the Russian Acad. Nauk, ser. Phys., v.60, N6, p.75, 1996.
2. H.M.Gibbs. Optical bistability: Controlling light with light. Academic Press, Inc., 1985.

Table

MECHANISM	$\chi^{(3)}, \text{esu}$	τ, s	$\chi^{(3)}/(\tau)$	$\chi^{(3)}(\omega)$
NONRESONANT				
Bound electr. anharmonicity	$\sim 1.5 \cdot 10^{-10}$	$2 \cdot 10^{-15}$	$7.5 \cdot 10^4$	$3 \cdot 10^{-11} E_g^{-4}$ $E_g \gg \hbar\omega$
Rayleigh anh.				
-orientational	$\sim 10^{-1}$	$\sim 10^{-1}$	~ 1	const.
-strictional	$\sim 10^{-7}$	$\sim 10^{-1}$	$\sim 10^{-6}$	$\sim \omega^{-2}$
-thermal	$\sim 2.5 \cdot 10^{-5} \beta$	$\sim 2.5 \cdot 10^{-3}$	$\sim 10^{-2} \beta$	$\sim \omega^{-2}$
Free electron CNRs				
-2-photon free el. generation	$\sim 10^{-5}$	$10^{-8} - 10^{-9}$	$\sim 10^4$	$\sim \omega^{-3}$
-conduc. band nonparabol.	$\sim 10^{-7}$	$\sim 10^{-11}$	$\sim 10^4$	$\sim \omega^{-4}$
RESONANT				
Raman type - SBS	$10^{-10} - 10^{-9}$	$10^{-8} - 10^{-7}$	$\sim 10^{-2}$	$\sim \omega^{-1}$
Transition saturation				
-atomic and molecular	$\sim 10^{-3}$	$\sim 10^{-4}$	~ 10	$\sim \omega^{-2}$
-interband in semiconds	$\sim 10^{-1}$	$\sim 10^{-6}$	$\sim 10^5$	$\sim \omega^{-3}$

Frequency stability and selection in semiconductor lasers by phase-conjugate optical feedback

O.Kh.Khasanov, T.V.Smirnova, O.M. Fedotova

Solid State & Semiconductor Physics Institute

17 Brovki str., 220072, Minsk Belarus

External cavity effects on injection semiconductor laser (SL) dynamics is of considerable interest. This is due to the practical importance of this system, especially of external cavities with phase conjugate mirrors. Phase conjugate feedback has only recently been investigated and therefore up to now its influence on SL dynamics is not clarified yet.

In this report the dynamics of the injection SL with external optical phase-conjugate feedback (EPCF) is considered. The feedback is formed via four-wave mixing in Cs vapour. The EPCF-effect on the laser output parameters is known to depend on its level. For weak EPCF the SL have demonstrated, for example, linewidth narrowing, frequency selection, etc. When the EPCF signal intensity increases its influence can be ambiguous and various generation regimes can be realized.

Analyzed mathematical model is based on the rate equations for the slowly varying envelope of the complex electric field within the laser, $E(t)$, and the carrier density $N(t)$. Unlike other authors we consider the effect of bimolecular recombination of carriers and noise. The conditions of the frequency stability on selection as well as coherence collapse are studied.

Note, the external cavity acts like a ring cavity with a holographic reflection grating as one of the reflectors as long as the four-wave mixing phase matching conditions are satisfied. Single round trip approximation is considered.

As analysis shows, the laser frequency can lock to ω_D , where ω_D is the D_2 -line frequency of Cs, provided $\Delta\omega = |\omega_D - \omega| \leq k_m(1 + \alpha^2)$. Here ω is the lasing frequency in absence of the feedback, k_m is the feedback rate, α is the linewidth enhancement parameter. If the feedback is too weak for locking the laser output oscillates at twice the difference frequency $\Delta\omega$. These oscillations can efficiently couple to the relaxation oscillation, providing a mechanism for unstable chaotic behavior.

Multiple photon echo generation in optically dense crystals

O.K.Khasanov, T.V.Smirnova, O.M.Fedotova

Solid State & Semiconductor Physics Institute

17 Brovki str., 220072, Minsk Belarus

Photon echo (PE) phenomenon is successfully applied to dynamics holography, creation of optical memory and information processing systems. It is one of the methods of nonstationary laser spectroscopy. Last time the reports about its application to biologic objects have been appeared. As a rule, the approximation of optically thin media is used when PE process is investigated. However, the exciting pulses wave lengths are much less than the real crystal sample sizes. Therefore it is necessary to take into account the resonance media back reaction on each exciting pulse from the sequence and in echo-responses.

In presented work the process of multiple photon echo (MPE) excitation by the sequence of N pulse pairs in optically dense media is investigated. The value of time delay between the pulse pairs T can be any large and comparable with the longitudinal relaxation time T_1 , and the time delay between the pulses in the pairs is satisfied to the condition: $\tau \ll T_2$, where T_2 is the transverse irreversible relaxation time. The non-linear evolution of each pulse in extended sample heeding the irreversible relaxation during the time of whole pulse sequence is analyzed. In the case of optically thin media with considering of the irreversible relaxation during the time of pulse action the results of the calculation of photon-echo intensity are essentially differ from ones in the work [1] where the analytical approach is used. In optically dense media this difference is more larger. In particular, we study the optimal conditions of MPE-generation. For initial areas of the exciting pulses in the pairs θ_1 and θ_2 there are: 0.5π and 0.7π . The dependence of MPE-intensity on whole pulse pairs number is investigated on the example of first order echo-response. It is shown to become weak beginning with $N=4-5$ pairs up to $N=20-30$ pairs which corresponds to so called "saturation" regime. We analyze the errors in estimation of times T_1 , T_2 which can be introduced by the neglecting of irreversible relaxation and of the propagation effects.

Reference

- [1]. Yashin A.N. , Kuz'min V.S. "*Optika i spektroskopiya*" **64** (1989) p.866